Development of Improved Galvanic Anodes for the Protection of Steel in Concrete

by

Alexei Bogdanovic

A Thesis submitted to the Faculty of Graduate Studies of

The University of Manitoba

In partial fulfillment of the requirements of the degree of

MASTER OF SCIENCE

Department of Civil Engineering

University of Manitoba

Winnipeg

THE UNIVERSITY OF MANITOBA

FACULTY OF GRADUATE STUDIES

*****

COPYRIGHT PERMISSION

Development of Improved Galvanic Anodes for the Protection of Steel in Concrete

BY

Alexei Bogdanovic

A Thesis/Practicum submitted to the Faculty of Graduate Studies of The University of Manitoba in partial fulfillment of the requirement of the degree

Of

MASTER OF SCIENCE

ABSTRACT

Corrosion in reinforced concrete is a major problem affecting modern infrastructure. If left untreated, severe damage may occur, rendering the structure aesthetically unpleasing and structurally deficient. It is estimated that nearly 15% of all bridges in the U.S. are deemed to be structurally inadequate and are in dire need for major repairs. The toll of corrosion on the economy can be enormous; in a recent study it was estimated that the indirect cost of corrosion is equivalent to 6% of the U.S. Gross Domestic Product. It is therefore imperative that new and improved remedial measures be developed. In Canada, the problem is equally dire; it is estimated corrosion affecting Canadian reinforced concrete infrastructure will cost approximately $30 billion annually.

Corrosion of steel reinforcement in concrete is an electro-chemical process. The harmful by-product of oxidizing iron is known as rust. This rust is several times larger in volume than steel and results in the deterioration of concrete due to extreme tensile pressures. Chloride induced corrosion is very common in coastal regions or areas where de-icing salts are used. Once the chlorides have penetrated to the steel reinforcement surface, the chlorides enter into a chemical reaction in which the natural passive film encasing the steel reinforcement is broken down. Without the passive film the rebar is free to corrode.

There exist many alternatives in corrosion remedial measures, some of which are undesired and costly. Depending on the circumstance, the degree of corrosion and the importance of the structure, some remedial measures may be preferable to others. However, the cost and effectiveness of the remedial work do not always reach the desired level of protection. In fact, one of the most common remedial practices is known as concrete patch repair and it often accelerates corrosion activity in adjacent non-treated concrete. This phenomenon is known as 'ring anode' effect. The cause of corrosion acceleration is due to electrochemical incompatibilities between the repaired concrete and existing concrete.

Discrete sacrificial anodes are designed to prevent or reduce the corrosion caused by the ring anode effect. Sacrificial anodes function by attaching a more susceptible metal (typically zinc) to the steel reinforcement, which in theory should render the steel into a cathode, thus protecting it from corrosion. Sacrificial anodes are an attractive remedial alternative primarily due to their low maintenance, low cost, and long life expectancy.

Sacrificial Anode A is a new generation protocol discrete anode, intended to provide maximum protection to nearby steel. Presently, sacrificial anodes that are commercially available only provide corrosion prevention or low corrosion control. The maximum protection as deemed by National Association of Corrosion Engineers (NACE)

International is cathodic protection and it occurs once the steel has been polarized to levels above 100 mV. At this level, corrosion is virtually, if not completely, halted.

The primary objective of this research is to test the performance of the new Sacrificial Anode A and compare its performance to sacrificial anodes already available on the market. Reinforced concrete slab specimens, were equipped with the different sacrificial anodes and were then exposed to various environmental and chloride conditions. The specimens were monitored for half-cell potentials, current density output, and potential decay. After several months exposed to these conditions, results show Sacrificial Anode A, was able to consistently out-perform the other sacrificial anodes. Cathodic levels were reached on several occasions with polarization of the steel reaching well above 100 mV. Results also indicated that Sacrificial Anode A was able to generate current densities well into the 2 to 20 mA/m^2 range required for maximum protection.

ACKNOWLEDGEMENTS

This research project was joint collaboration between the University of Manitoba, Vector Construction, and NSERC. The author wishes to give his gratitude to his advisors Dr. Mufti, Dr. El-Salakawy, and Dr. Thompson. Special thanks to Vector Construction, and in particular: David Whitmore, vice-president of Vector Construction, Martin Beaudette, Jason and Andre. The project could not have been realized without their infinite knowledge and guidance, the unlimited access to their facility and equipment, and their generous financial support.

Special thanks also to Dr. Darshan Sidhu, and Nancy Fehr for all their help in contributing to the theoretical and grammatical expertise, respectively.

Appreciation is also extended to Dr. Svecova for the use of the environmental chamber, and the technical assistance of Mr. Moray McVey, Grant Whiteside and Chad Klowak, for their assistance, as well as the whole ISIS staff.

Finally, special thanks to Connie Wenzoski and Kathie Anderson for their help and assistance throughout my undergraduate and graduate career.

TABLE OF CONTENTS

LIST OF FIGURES

LIST OF TABLES

1.0 INTRODUCTION

1.1 PROBLEM

Corrosion of modern infrastructure is a severe problem faced by engineers, governments, and stakeholders alike. Its impact on society affects everything from the general safety of the public to the economy of country. A 2002 study headed by the U.S. Federal Highway Administration (FHWA) revealed that the annual direct cost of corrosion is estimated to be $276 billion. This figure represents 3.1% of the U.S. Gross Domestic Product (GDP). This figure reaches as high as $552 billion or 6% of the GDP, if the indirect cost relating to corrosion is analyzed. It is estimated that of this cost, 30% is related directly to corrosion in steel reinforced concrete structures [1].

There are approximately 583,000 bridges in the United States according to the National Bridge Inventory Database of which, approximately 235,000 of those are constructed using conventional steel reinforced concrete, and 108,000 are constructed using prestressed concrete. Significant portions of these bridges (approximately 15%) are deemed to be structurally deficient due to corroded steel reinforcement. In other words, these structurally deficient bridges can no longer sustain the intended load for which they were designed. The direct cost alone to tackle the problem of these structurally deficient bridges is estimated to be approximately $8.3 billion annually. This includes $3.8 billion in replacement of the bridges and $2 billion each for maintenance and capital costs for concrete bridge decks and concrete substructures, respectively [2].

Canada's infrastructure is also deteriorating at an alarming rate. Due to a lack of general maintenance it is estimated the overall cost or rehabilitation to Canada's infrastructure is approximately $125 billion annually, of which $30 billion is directly related to corrosion in steel reinforced concrete structures [3].

Besides the monetary impact corrosion has on the economy, the safety risk to the public is also a cause for great concern. Corrosion if left untreated can severely weaken a structure to the point that failure may occur. Corrosion will continue to degrade our infrastructures if no action in prevention and/or restoration is taken. There exist several mitigation techniques that combat corrosion either by preventing or reducing the rate of corrosion. Many of these techniques, however, are costly and impractical. Despite these techniques there is no perfect solution and thus corrosion continues to remain a major problem. Therefore, it is imperative to continue research and investigate new techniques to discover better, more practical, and cost-effective mitigation measures against steel corrosion in concrete structures.

1.2 OBJECTIVE

The primary focus of the research involves the testing and evaluation of a higher output galvanic anode system (sacrificial anode) designed for cathodic protection of steel reinforced concrete. The new system known, as sacrificial anode "A" is an enhancement of previous galvanic puck-shaped systems designed for discrete protection, which are presently available on the market. These older systems produce a lower level of current output, often resulting in polarization of the steel that is well below cathodic protection. Existing sacrificial anodes often provide minimal protection to the steel reinforcement against corrosion. Cathodic protection is deemed to be the highest level of protection, able to virtually stop all ongoing corrosion activity. The degree of protection depends on several factors such as: current output, exposure conditions, concrete resistivity, and distance of anode to bars, among others. Important findings that this project will reveal include:

- Current output limits
- Range of area protected
- Degree of protection
- Comparison to currently available galvanic anodes

The secondary focus of this project is to test a new form of galvanic anodes. Unlike the puck shape anodes, these groups of anodes are much larger in size and their main objective is to provide protection on a global scale. Therefore, these anodes are designed to provide high levels of protection (cathodic protection) spread over a wider area.

Data collected from this research project will greatly assist engineers in addressing the crucial corrosion dilemma that is constantly plaguing our infrastructure systems. Therefore, it is imperative to understand the effect that this newly developed system has on reinforced concrete in order to mitigate corrosion activity.

1.3 SCOPE

In order to fully comprehend the objective of this research project, it is first important to have a good understanding of the fundamentals of the corrosion process. Therefore section 2, discusses in details the electro-chemical corrosion process. The section also briefly discusses the most common corrosion detection techniques as well as different remedial techniques used in reinforced concrete.

Section 3 deals with the experimental portion of the research project. A complete description of the test specimens (including geometry, constituents, bars etc) is discussed. Next, a general explanation of sacrificial anodes is presented along with a description of the anodes to be used in the research project. Section 3 also discusses several key factors

influencing corrosion rate in reinforced concrete and how they are related to the research. These factors include: chloride content, resistivity and environmental conditions. Testing methods and procedures used are discussed next, followed by a description of the control specimens and a tabulated test matrix summary.

Section 4 reviews the theoretical analysis related to the research. Based on past literature, an in-depth discussion covering the effects of polarization is presented. It is important to understand the theory behind galvanic protection so that proper analysis of the results can be determined.

The test results and discussion are presented next in section 5. Tables and graphs are used to present the results in a clear manner so that proper comparisons can be made. A brief discussion on results obtained for chloride content and pH levels extracted from test specimens "A" and the control specimens. A subsection of visual observations also provide pictures of the specimens at the end of testing period.

Finally, the conclusions and summary of the findings are recapped in section 6. Recommendations on future research are also presented along with some final remarks regarding the importance of continuing research in the field of corrosion in reinforced concrete.

2.0 BACKGROUND

2.1 CORROSION PROCESS

Corrosion in steel reinforced concrete is an electrochemical process that is initiated by the break down of the natural passive film layer (ferric oxides), which encases the steel rebar. The passive layer is produced by the high alkalinity levels in the concrete pores (pH > 12) and functions as a self-sustaining, self-repairing film, which protects against corrosion. Therefore, as long as the passive film is intact, in theory, there should be no corrosion activity occurring. The two main factors known to break down the protective film are chlorides (Cl) attributed to deicing salts or marine environments and carbon dioxide (CO_2) attacks, which generally occur in industrial zones. The full or partial break down of this film is known as depassivation. Other factors that may influence depassivation are the physical and chemical properties of concrete, the chemical composition of steel and continual mechanical stresses [4, 5]. Although, corrosion can be initiated by carbonation attack, this research only focuses on chloride attack.

In order for the corrosion process to occur, the following conditions must exist: [4]

- Electrolyte – a medium in which the flow of current can be conducted (concrete)
- Metallic path – steel bars
- Anodic site – location where electrons are released
- Cathodic site – location where electrons are received

The corrosion process begins when iron dissolves in concrete pore water, releasing electrons from the anodic site of the steel. The following reactions are produced:

[1] $Fe \rightarrow Fe^{2+} + 2e^-$

[2] $Fe^{2+} + 2Cl^- \rightarrow FeCl_2$

Following the initial reaction, electrons are dispersed along the anodic site, resulting in an increase in electric potential. The electrons then flow to the site of lower potential known as the cathode. Balance is maintained at the cathode where the electrons are consumed by oxygen reduction. The cathodic reaction is described below.

[3] $1/2 \cdot O_2 + H_2O + 2e^- \rightarrow 2OH^-$

The negative hydroxide ($2OH^-$) ions produced at the cathode and iron chloride ($FeCl_2$) produced from the anode migrate towards one another and combine to form ferrous hydroxide, $Fe(OH)_2$, as shown by the following reaction:

[4] $FeCl_2 + 2OH^- \rightarrow Fe(OH)_2 + 2Cl^-$

The ferrous hydroxide compound will react further to form the chemical by-product known as "rust". The reaction is shown below.

[5] $2Fe(OH)_2 + 1/2 \cdot O_2 \rightarrow Fe_2O_3 + 2H_2O$

The by-product Fe_2O_3, or red rust, has the same mass of steel but may have a volume upwards of four times that of steel. This increase in volume causes a tremendous increase in internal stress, eventually resulting in cracking, spalling and delamination of the surrounding concrete. Therefore, corrosion affects the integrity of steel reinforced concrete in two primary ways: first, the corrosion process eats away at the steel cross-section reducing its strength; and second, the by-product rust leads to concrete deterioration. It is important to realize that the above reactions are not the only reactions capable of causing corrosion. It is also worth noting that oxygen and water are crucial ingredients for the development of corrosion as shown schematically in Figure 1 [6, 7]. Finally, it is also worth mentioning that "pitting" corrosion is simply a corrosion cell that forms in a localized area of the steel. As the number of "pits" increase, they combine together to create general corrosion. "Pitting" corrosion is usually generalized by an accelerated rate of corrosion due to a lack of oxygen present in the anodic pit [8].

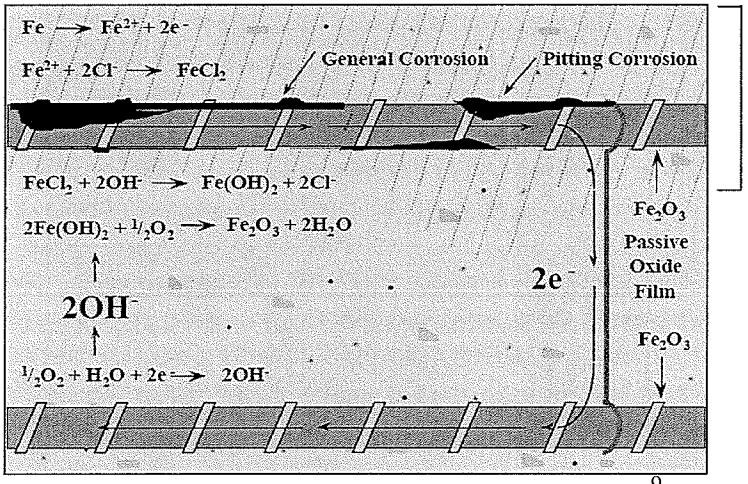

Figure 2-1: Typical corrosion macro-cell process [9]

2.2 CORROSION DETECTION

Detecting and measuring the degree of corrosion in steel reinforced concrete before further problems develop is crucial to maintain or extend the intended service life of the structure. If corrosion is left unchecked, severe cracking or spalling may occur, affecting the integrity of a structure. It is difficult, however, to detect corrosion immediately since the steel reinforcement is embedded in the concrete. Apart from physically removing the steel under investigation, which of course would be impractical and costly in most cases, other means of detection are required. This is why most detection methods do not directly monitor the degree of corrosion but rather the symptoms caused by corrosion. One symptom in particular that often indicates the presence of corrosion is delamination. Delamination refers to the gap that occurs after the de-bonding of the steel and concrete

interface. This de-bonding is often a result of the expansion tensile forces of rust against the concrete, which causes the loss in bond strength. As a result, a gap is often formed. There exist several corrosion detection techniques used by engineers to aid in the detection of corrosion in steel reinforced concrete. It is important to realize most of these systems are based on empirical or interpretational results. Techniques that rely on detecting symptoms associated with corrosion can also be misleading since many of these symptoms can be the result of other factors. For instance, delamination can also be the result of freeze and thaw action. Bearing this in mind, a list of the most common techniques along with the advantages and disadvantages of each will be discussed next [10].

2.2.1 Traditional Chain-Drag Test

This technique involves listening to the acoustic response of a chain being dragged across the concrete area under investigation. The response for intact concrete will be a clear ringing noise. Delamination will return a hollow or dull sound. The test has been standardized by ASTM D 4580. This method is popular with technicians and engineers since it is relatively simple and inexpensive when considering a small scale area.

However, when used on a larger scale, such as a bridge deck, the traditional chain-drag test is often not feasible. The reason being, the cost of diverting traffic often outweighs the simplicity of the system. Another shortcoming is that background noise (such as traffic) could severely jeopardize the interpretation of the acoustic response. Also, this technique does not have any modern data collection system; and therefore, it could be tedious and frustrating marking all the areas of interest [10].

2.2.2 Automated Chain-Drag System

The automated chain-drag system follows the same principal as the traditional chain-drag test, but instead the chains are mounted to an automated cart. High-tech microphones, a data-acquisition system, and an onboard computer provide a real-time map of the concrete area under investigation. The system is capable of locating and storing data from the problem areas where delamination is detected. As with the traditional test, the automated chain-drag system may also be influenced by external noise [10].

2.2.3 Electro-Mechanical Sounding System

This technique also focuses on detecting delaminations and follows the same principles as the two previous systems. This system is automated but instead of chains it uses two rigid metallic wheels that tap the concrete surface 33 times per second. Sonic receivers are used to capture the acoustic sounds. Although this system is a recent edition of ASTM D 4580-02 Standard not much has been published on the performance history. However, ASTM does state that this technique is less accurate than the traditional chain-drag test [10].

2.2.4 Impact-Echo Method

This technique was pioneered in the 1980s and relies on interpreting mechanically induced energy introduced to the concrete, in the form of stress waves. These stress waves are created by a steel impactor located on the surface. The stress waves pass through the entire thickness of the concrete unless a flaw or irregularity in the concrete is encountered, in which case, the stress waves are reflected back to the surface. A transducer at the surface collects the reflected waves and an algorithm analyzes the data to determine the location and depth of the flaw. The flaw may be the result of a range of factors, including: failed overlay, improper consolidation of concrete, or delamination [10].

2.2.5 Infared Thermography

Infrared thermography uses the principal of diffusion rate to detect irregularities or flaws in concrete. Passing a thermal front through concrete, irregularities will diffuse at a different rate than the remainder of the concrete. This difference in diffusion causes discontinuities in temperature and can be recorded with the use of an infrared camera. Careful interpretation of the infrared images are required to properly determine information relating to the defect encountered. Delaminations can be detected but this system still requires improvement for it to be an efficient tool for corrosion detection. A major shortcoming is that the system is extremely sensitive to surface debris, such as oil drippings and lane markings. Debris will generate a different temperature than the surrounding concrete making it difficult to interpret the difference between actual flaws in the concrete and the surface debris. Therefore, to obtain accurate readings, often the impractical measures must be taken before testing. For instance, in bridge inspections, the road will need to be closed for cleaning of the deck to eliminate any debris. Despite the drawbacks, infrared thermography is standardized in ASTM D 4788 [10].

2.2.6 Ground-Penetrating Radar

Ground-penetrating radar (GPR) uses electromagnetic energy emitted into the concrete to determine the presence of different materials. A portion of the electromagnetic energy will be reflected back when encountering materials with different electromagnetic properties. A radar antenna intercepts the reflected energy and the properties are determined using electromagnetic energy and wave theory. Unlike the other systems discussed thus far, GPR is capable of detecting various layers of flaws within the concrete. This is of importance especially when dealing with multiple reinforcement layers. Other systems simply detect the closest flaw to the surface and are unable to detect any flaws underneath the first layer. GPR systems are also available on mounted vehicles so that inspections can be done more efficiently. One major drawback of GPR is the difficulty in interpreting the data and, the associated requirement for highly specialized personnel [10].

2.2.7 Half-Cell Test

Unlike the other techniques viewed thus far, the half-cell potential test does not detect flaws or the symptoms of corrosion in the concrete; instead it measures the probability or risk of active corrosion activity. The technique requires the use of a reference electrode (typically silver/silver chloride or copper/copper sulphate), which is simply metal submerged in its own ions. The reference electrode has a known, stable potential and when connected to the steel in concrete, the difference in potential is recorded. Based on empirical observations of the potential recorded, the probability of corrosion in steel is determined. A half-cell test can be deceptive however, since the potential is not solely a function of corrosion conditions. Factors such as moisture and oxygen availability can drastically misrepresent the empirical interpretations. It is important to keep in mind that the half-cell test does not measure corrosion rate but simply the probability of corrosion activity [8].

2.2.8 Optimal Technique

There is no single technique that is optimal for detecting corrosion in reinforced concrete structures. Detection methods should be based on simplicity, efficiency and cost [6]. Conditions and the desired level of detection accuracy may also vary and therefore certain techniques may be beneficial for the particular task in hand. It is important to realize that corrosion detection is not an exact science since the steel is generally embedded in concrete, thus eliminating direct contact. Steel extraction for physical examination would determine the presence of corrosion but generally would not be an economical option.

2.3 REMEDIAL MEASURES

With the continued use of deicing salts and the ever-increasing number of structures built in coastal regions, engineers are constantly looking for improved techniques to prevent and rehabilitate reinforced concrete structures subjected to corrosion. Many engineers today have been leaning towards the use of higher quality materials such as high performance concrete and corrosion-resistant reinforcement to help prevent the initiation of corrosion. Despite the attempts to prevent new corrosion activity, there still exist thousands of structures that are in desperate need of repair and rehabilitation. Every corrosion-based problem encountered in reinforced concrete structures is unique in its own right and, hence, it is imperative that engineers treat it as such. There are several factors that must be taken into consideration to determine the optimal solution for the problem. The most frequently used repair options are briefly listed next. Many of these repair methods can be used singly or in combination with others.

2.3.1 "Do Nothing" Approach

Often the most economical and beneficial solution when faced with concrete structures subjected to corrosion is to do nothing at all. This approach is favourable when the structure in question has a limited design life, aesthetic issues are not of importance and the levels of corrosion present are not critical. If this approach is taken, it is often necessary to continuously monitor the rate of corrosion for potential safety concerns relating to the integrity of the structure.[11]

2.3.2 Surface Barriers

This method involves the application of an overlay or coating at the surface level of the structure to prevent the further ingress of chlorides. This method is often used when the chloride levels in contact with the reinforcement are still relatively low. Thus, by reducing or stopping excess chloride penetration, the passive film does not deteriorate [11].

2.3.3 Patch Repair

This is perhaps the most common repair solution practiced in the field. The method entails the removal of the chloride-contaminated concrete around the corroding reinforcing bars, followed by cleaning of the corroded bars, and then re-application of fresh uncontaminated concrete or mortar. The patch repair method is often used in combination with the surface barrier method. Caution should be taken however with the patch repair method as it often leads to corrosion in the area adjacent to the initial repair site [11]. This is commonly known as ring-anode corrosion and will be discussed in further detail below.

2.3.4 Electrochemical Techniques

Electrochemical protection was first used by Sir Humphrey Davy in 1824, when he halted the decay of copper sheathing in wooden warship hulls by attaching it to small buttons of zinc. The basic concept behind electrochemical treatment functions under the same principles of the corrosion process. By connecting the steel under consideration to a foreign anode, a current is passed to the steel and the corrosion process is reversed. In essence, the foreign anode will convert the steel into the cathode. Recall from above, the cathode is where the electrons are received and in theory, the cathode is corrosion free. Electrochemical techniques have been used for many years on ship hulls, oilrigs, and gas pipelines [8, 12]. It was not until 1973 that electrochemistry protection was used in reinforced concrete when it was applied to a bridge deck [4]. Electrochemical chloride extraction, impressed current and galvanic protection are three electrochemical techniques often used in the repair of reinforced concrete. It is important to note that impressed current and galvanic protection techniques are often referred to in literature and papers as cathodic protection. However, according to NACE International, cathodic

protection is defined as the level of maximum protection against corrosion and is met only when a minimum of 100 mV polarization of the steel is achieved. For the remainder of this thesis, cathodic protection will be referred to only as the term put forth by NACE Standards.

2.3.4.1 Electrochemical Chloride Extraction

The electrochemical chloride extraction method is relatively new, and functions on much of the same principals as the impressed current method. The main difference is that a much higher current intensity is passed through the reinforcement, for a relatively short period of time, causing the extraction of the chlorides present. This enables the passive layer to reform protecting it from further corrosion. The method has been unsuccessful in tidal structures when submerged, since it has been found that the current "leaks away" [11].

2.3.4.2 Impressed Current Protection

By applying an external source of current to the steel, impressed current protects the steel reinforcement by converting the steel into the cathode. This method is often used in harbor structures and requires complete monitoring to verify its effectiveness. The use of impressed current often delivers complete protection and reduces the need for patch repair [11].

2.3.4.3 Galvanic Protection

Galvanic protection uses sacrificial anodes attached to the steel reinforcement to provide protection for the structure. The sacrificial anodes take advantage of the difference in potentials between metals to create a natural low current to protect the steel. Unlike, the current impressed system, there is no need for an external source of power and thus no monitoring is required. Galvanic protection may come in the form of installed (discrete) cast anodes or sacrificial coating that is sprayed onto atmospherically exposed concrete [4]. The basics of this method will be discussed in further detail in a later section.

2.3.5 Replacement

Often viewed as the last resort, this option is by far the most costly. Generally, this option will be required if the corrosion problem is irreparable or the extent of the damage is such that repairing the structure would not be beneficial. Also, replacement of a structure can greatly impact the service demands expected by the public. The benefit to replacement of a structure is that the entire corrosion problem is eliminated and the option for the use of corrosion resistant materials can be implemented in the new design. Depending on the situation, full or partial replacement of a damaged structure may be needed [11]. Figure 2-2, depicts partial replacement of a bridge due to corrosion damage.

Figure 2-2: Partial replacement of chloride-contaminated concrete [13]

2.3.6 Repair Cost

As already mentioned, the cost due to corrosion each year reaches billions of dollars in the U.S. alone. With a high percentage of the existing infrastructure in need of repair, and the continual use of deicing salts (chloride) on highways, the cost will surely increase. It is crucial repairs to many of these infrastructures be dealt with as soon as possible to avoid further corrosion damage and increase repair costs. Table 2-1, summarizes the average cost and cost range for different repair techniques described earlier for bridges. It also summarizes the average life expectancy of each repair technique along with the range of life expectancy. From Table 2-1, Portland cement concrete patch repair is the most expensive repair option and has an average repair life expectancy of seven years. The patch repair option using bituminous concrete is the least expensive but also only has an average life expectancy of one year. These repair options also give a potential to further corrosion possibilities due to the ring-anode effect. When dealing with electrochemical repair options, it is clear that the uses of sacrificial anodes are the least expensive. It also provides an average of 15-year protection. Of course different repair options have different benefits under different circumstances. Therefore, the least expensive option isn't always the superior choice. Table 2-2 gives the unit cost for replacing bridges from 1995 to 1999. The costs are based on the mean costs for all states in the U.S. for each year. The trend in unit costs of replacement of bridges increases every year from 1995. The difference in unit cost between 1995 and 1999 is

$90. It is apparent that the cost of replacement is much greater than the cost of repairing. Therefore, it is imperative to deal with the corrosion problem affecting modern infrastructure as quickly and efficiently as possible in order to minimize the economical impact. If corrosion is not treated, concrete may be damaged beyond the point of repair and replacement of partial or the entire structure may be the only alternative.

Table 2-1: Summary of cost and life expectancy for different repair options for chloride removal in bridges [14]

Type of maintenance	Average cost, $/m^2	Range of costs, $/m^2	Average expected life, years	Range of expected life, years
Portland cement concrete patch	$395	$322 to 469	7	4 to 10
Bituminous concrete patch	$90	$39 to 141	1	1 to 3
Impressed-current CP (substructure)	$143	$76 to 211	20	5 to 35
Sacrificial anode CP (substructure)	$118	$108 to 129	15	10 to 20
Electrochemical removal (substructure)	$161	$107 to 215	15	10 to 20

Table 2-2: Unit costs for highway bridge replacement [14]

	1995	1996	1997	1998	1999
Unit costs, $/m^2	$768	$771	$836	$855	$858

3.0 EXPERIMENTAL PROGRAM

3.1 TEST SPECIMENS

Identical rectangular concrete slab specimens with embedded reinforcements were used to evaluate the performance of the different galvanic anode systems. The dimensions of the slab specimens were 540 x 330 x 100 mm. Plastic containers were chosen as the optimal formwork for casting the concrete specimens. The containers could be purchased meaning no construction for the formwork was required; also, the plastic container allowed for easy drilling and placement of the steel rebars. The concrete mixture was designed for 28-day strength of 30 MPa and was common to all specimens. The calculations for the concrete design is presented in Appendix A and are based on the design methods provided by the Cement Association of Canada [15]. The concrete constituents are shown in Table 3-1.

Table 3-1: Concrete constituents.

Constituents	Quantity
Water-cement ratio	0.48
Type 10 cement (kg/m^3)	331
20 mm coarse aggregate (kg/m^3)	1012
Fine aggregate, natural sand (kg/ m^3)	824
Water (kg/ m^3)	103
Air content (%)	5 - 7
Slump (mm)	75 ± 20
Air-entraining admixture (kg/ m^3)	0.166
Target f'_c @ 28 days (MPa)	30

The slab specimens were reinforced with four 20-M bars spaced symmetrically at 145 mm o.c. Providing four 20-M bars coincided with the accepted 2.24% ratio of steel reinforcement to concrete volume that is typically used in the flexural design of bridge decks [16]. A 530 x 320 mm steel mesh was also installed below the reinforcing bars in each specimen to simulate a slab with multiple reinforcement layers. A 20 mm cover was provided for both the reinforcing bars and the steel mesh below. One galvanic anode system was placed in each specimen midway between the first two reinforcing bars as shown in Figure 3-1. The galvanic anode was placed at the same level of the reinforcing bars so that maximum current efficiency could be transmitted to each bar, as shown in Figure 3-2. The galvanic anode was strategically placed for two reasons: first, an accurate measurement of the effectiveness of the galvanic system could be viewed by taking the average current readings from the two nearest bars; second, the decrease in protection for the reinforcing bars with increasing distance could be assessed. Connections from the anode to the steel reinforcement were connected by use of exteriorly plastic-protected

wires. The wires were connected to an "on-off" switch so that the current output to the bars and mesh could be interrupted. The two closest bars to the sacrificial anode system, labeled Bar 1 and Bar 2, were connected together and controlled by one switch. One average current reading was recorded for the two closest bars. A current reading was also taken for Bar 3, Bar 4 and for the mesh. Figure 3-3, shows the slab specimens on the day of casting.

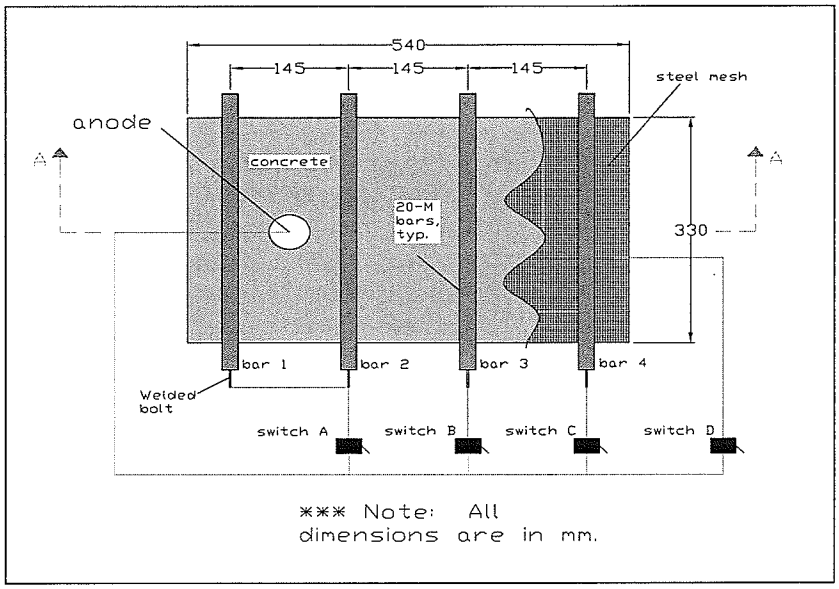

Figure 3-1: Plan view of typical reinforced concrete slab specimen with embedded galvanic anode system

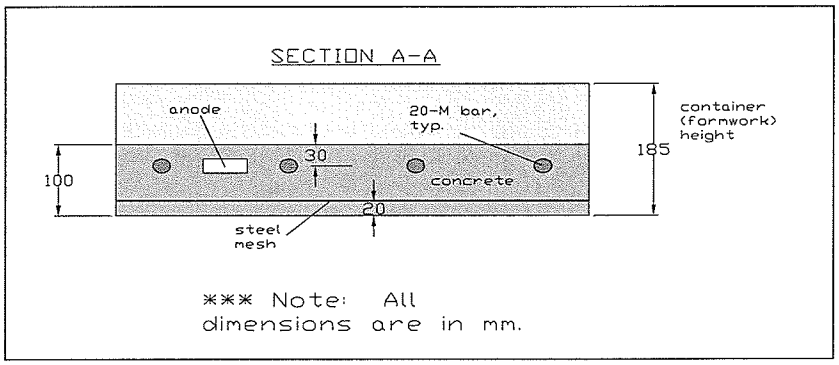

Figure 3-2: Cross-section of typical reinforced concrete slab specimen with embedded galvanic anode system

Figure 3-3: Photo of concrete slab specimens on day of casting

3.2 SACRIFICIAL ANODES

Sacrificial anodes represent a form of electrochemical treatment aimed at protecting the reinforcing steel against corrosion. Sacrificial anodes take advantage of the natural difference in potential between dissimilar metals. When coupled together in the presence of an electrolyte, the two dissimilar metals form an electrochemical cell. Therefore, the metal with the greater potential will liberate electrons (current) to the metal with the lower potential. In essence, the metal with the greater potential becomes the anode whereas the metal with the least potential becomes the cathode. In theory, the cathode is where the reduction process occurs, and thus, cannot corrode. By coupling a sacrificial anode to steel in concrete, the steel will become the cathode and thus should be protected against corrosion. The sacrificial anode however, will corrode and eventually be consumed. Sacrificial anodes are generally composed of zinc, magnesium or aluminum due to their relatively high galvanic potential in comparison to iron (steel) [4, 11]. Unlike iron, these metals do not create the harmful by-product rust. Table 3-2, depicts the galvanic potential of various metals in the electromotive series. A mortar enriched in alkaline electrolytes typically encapsulates sacrificial metal in order to improve the overall effectiveness of the anode. This promotes and sustains anodic dissolution of the metal at an adequate rate in order to ensure continual galvanic protection[17].

Table 3-2: Electromotive series [17]

Metals	State	Standard Potential, Volts
Potassium	Active End	-2.922
Magnesium		-2.340
Aluminum		-1.670
Zinc		-0.762
Iron		-0.440
Hydrogen		0.000
Copper		+0.345
Silver		+0.800
Platinum	Passive End	+1.200

The main focus of this project deals with 'puck' sacrificial anodes that are generally used for discrete protection. However, new 'strip' sacrificial anodes were also tested to analyze its effectiveness in a global setting. A brief description of each anode and its intended application will be discussed in the next subsections.

3.2.1 Puck Anodes

Up to date, sacrificial anodes have been almost exclusively used for corrosion protection or corrosion control of a localized area. More specifically, they are often used in conjunction with patch repair of deteriorated concrete sites caused by corrosion. By installing the sacrificial anodes around the new patch, protection against ring-anode effect is provided. This phenomenon is discussed in the upcoming subsection. Sacrificial puck anode is an economical solution to extend the service life of the repaired concrete. Since there are no external power sources or monitoring equipment, the process is virtually maintenance free. Its major drawback is generally due to its relatively low current output and small effectiveness range. Therefore, it is often not convenient to use if a high degree of protection such as cathodic protection is required.

The 'puck' sacrificial anodes refer to its shape resembling a hockey puck, as shown in figure 3-4. They are typically only a few inches in diameter and approximately one inch in height. As previously mentioned, the core of the sacrificial anodes are comprised of a higher potential metal, typically zinc alloy, which favors corroding over a less noble metal (i.e. steel). These anodes are almost always encapsulated with a specially devised cementitious mortar that aids in activation process. The mortar prevents the formation of an interfering passive layer and thus facilitates zinc dissolution [18].

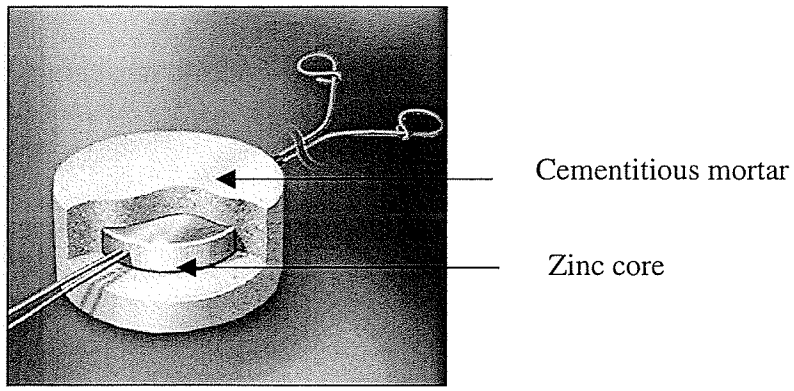

Figure 3-4: Typical puck anode

All puck anodes tested in this program are commercially available products with the exception of Sacrificial Anode "A", which is a new product. They all have the same geometry but vary in chemical make-up properties of the mortar, and/or metallic core. For privacy purposes, the actual make-up of the anodes cannot be revealed.

3.2.1.1.Ring anode effect

The ring anode effect or patch accelerated corrosion is a phenomenon that is caused by concrete patch repair. Concrete patch repair is perhaps the most common and simple method in dealing with localized corrosion. The method involves removing the contaminated concrete where corrosion has initiated, cleaning the bars, and replacing the contaminated concrete with repair mortar. Although this method has great effect in reducing the corrosion within the repair site, it has the reverse effect for the surrounding concrete. Prior to the repair, the area of contaminated concrete act as the anode and therefore protected the surrounding concrete from corrosion. By removing this concrete and replacing it with fresh mortar, a difference in potentials between the existing concrete and the newly replace mortar has developed. Often, the surrounding concrete is itself slightly contaminated with chlorides and corrosion can rapidly initiate. Therefore, action must be taken quickly to the surrounding concrete before deterioration occurs. In many instances corrosion can be chased around the entire structure, turning a relatively small, local problem into a much greater and costlier problem [18].

By applying sacrificial anodes connected to the steel in conjunction with the patch repair, the ring anode effect may be prevented, as the sacrificial anodes will corrode preferably to the steel reinforcement. The spacing of the sacrificial anodes depends on its current throwing power and on the desirable level of protection. Special attention must be made to the environment in which the sacrificial anode is to be used. Figure 3-5, shows an example of the installation of puck sacrificial anodes with concrete patch repair.

Figure 3-5: Patch repair in conjunction with sacrificial anodes

3.2.2 Strip Anodes

Sacrificial strip anodes are a prototype galvanic system, which functions on the same principals as the puck anodes. The intent of the sacrificial strip anodes is to generate a high level of current output that can protect further distance than its puck counterpart. In essence it is intended for protection on a global scale. The hope is to achieve not only corrosion control but also possibly cathodic protection. This could be used in applications for global implications where methods such as impressed current are not warranted. The strip anodes tested in this project are not commercially available and are each designed with different compositions. These anodes are rectangular in shape and are approximately couple inches in depth and width, and are several inches in length. Among other features, they are equipped with more zinc (proportionally to their size) than a traditional puck sacrificial anode. Figure 3-6, shows a typical strip anode.

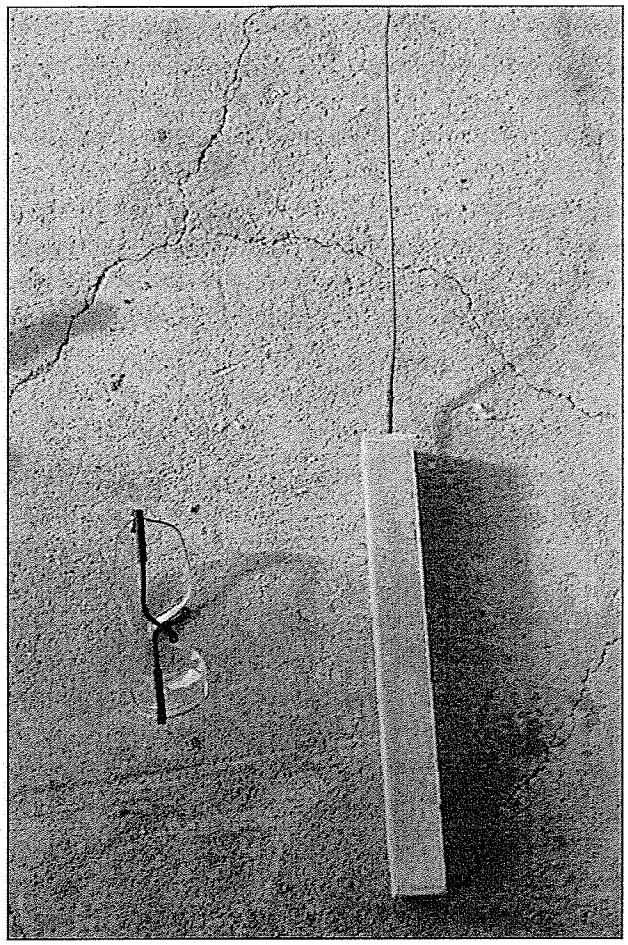

Figure 3-6: Typical strip anode

3.3 CHLORIDE CONTENT

It is well documented that chlorides can induce corrosion activity in reinforced concrete. These chlorides generally originate from three conditions: deicing salts, coastal environments and or, the presence of chlorides in the initial concrete mix (for example with the use of calcium chloride dihydrate) [19]. However, an ongoing source of debate among investigators is the chloride threshold level required to commence the corrosion process in reinforced concrete. For corrosion to initiate, chlorides must first reach the level of the reinforcing steel. However, concrete, or more specifically the hydration products of cement, has the capability to bind with the free chlorides ions. This leads to the formation of calcium chloroaluminate, otherwise known as Friedel's salt, which immobilizes the chlorides and prevents further penetration. When chloride concentration surpasses the concrete's capability to bind, the excess chlorides are free to initiate the corrosion process. The capability of concrete to bind to chlorides can be viewed as a sponge soaking up water; the maximum amount of water the sponge can absorb is its threshold. Therefore, the threshold level is the amount of chlorides that can be

"absorbed" without initiating corrosion. The chloride threshold is situated at the steel-concrete interface [20].

Many factors influence the value of chloride threshold levels such as:

- water-cement ratio;
- cement type content and admixtures;
- pore solution pH;
- capillary structure;
- rebar composition and surface conditions;
- curing period and curing temperature;
- exposure temperature and relative humidity;
- oxygen availability at rebar surface; and
- rebar polarization potential [20].

Due to the numerous factors affecting the chloride threshold, there has been much debate on a single 'universal' value. As a result, different authors and investigators have presented a wide range of chloride threshold levels. Glass et al. have concluded that the chloride threshold levels may vary between 0.17-2.5% of total chlorides (bond plus free chlorides) by relative weight of cement [20, 21]. In contrast, Alonso et al. argue that chloride threshold varies between 1.24-3.08% of total chlorides by weight of cement. This translates to 0.39-1.16% free chlorides by weight of cement [21].

In a paper published by Morris et al. [21] an empirical relationship between chloride threshold content and concrete resistivity (which represents the quality of concrete) was put forth. The authors derived the following empirical formula for chloride threshold content expressed by relative weight of cement:

$$Cl_{TH}\ (\%) = 0.019\rho + 0.401 \qquad (1)$$

The formula is a function of concrete resistivity, ρ (kΩ cm) as shown in Equation 1. The formula suggest that resistivity of concrete is associated with concrete quality and thus, an increase in resistivity is associated with increase in chloride threshold. Equation (1) was derived by testing various concrete mix specimens, either partially immersed in a saline solution of 3.5% chlorides by weight of cement or exposed to seashore conditions. The equation is only valid for standard concrete mixed with Type I Portland cement [21].

In the present research project, it was decided that two levels of chloride contamination would be used in the testing of the galvanic systems. One level would simulate conditions just above the threshold levels (low contamination), whereas the other level would be more representative of an aggressive environment, such as structures located near coastal regions (high contamination). The different levels of chloride contamination enabled the analysis of the performance of the galvanic systems with respect to different corrosion rates. The chloride levels used were as follows:

- low contamination – 1.2% free chlorides by relative weight of cement; and
- high contamination – 3.9% free chorides by relative weight of cement.

A conservative approach was taken towards the chloride threshold level in an attempt to guarantee corrosion activity. The chloride threshold was deemed to take place at 1.16% free chlorides by weight of cement, as per Alfonso et al. To accelerate the corrosion process, chlorides in the form of NaCl (common table salt) were mixed with the concrete constituents at the time of casting. This also allowed for a uniform distribution of chlorides throughout the concrete specimen.

3.4 EXPOSURE CONDITIONS

Environmental conditions such as temperature and relative humidity (i.e. moisture content) have a tremendous influence on the corrosion process of reinforced concrete. In most instances, the corrosion rate will generally increase with an increase in temperature and/or relative humidity. As is the case for all chemical reactions, ambient temperature is an influential factor in the rate at which the chemical reaction is realized. The rate of the cathodic and anodic chemical reactions is dependent on temperature, among several other factors. This phenomenon is explained by the Arrhenius equation:

$$k = A \cdot e^{(-E/RT)} \qquad (2)$$

where k, is the constant rate of the chemical reaction; T, is temperature in Kelvin; E, is the activation energy; A, is the pre-exponential factor; and R, is the gas constant [22]. A general rule of thumb is that an increase of temperature of 10 °C can double the corrosion rate. This rule of thumb is dependent, however, on the interaction with several other factors that affect the corrosion rate, such as oxygen diffusion and relative humidity [23]. Figure 3-7, shows the general relationship between temperature and corrosion rate [24].

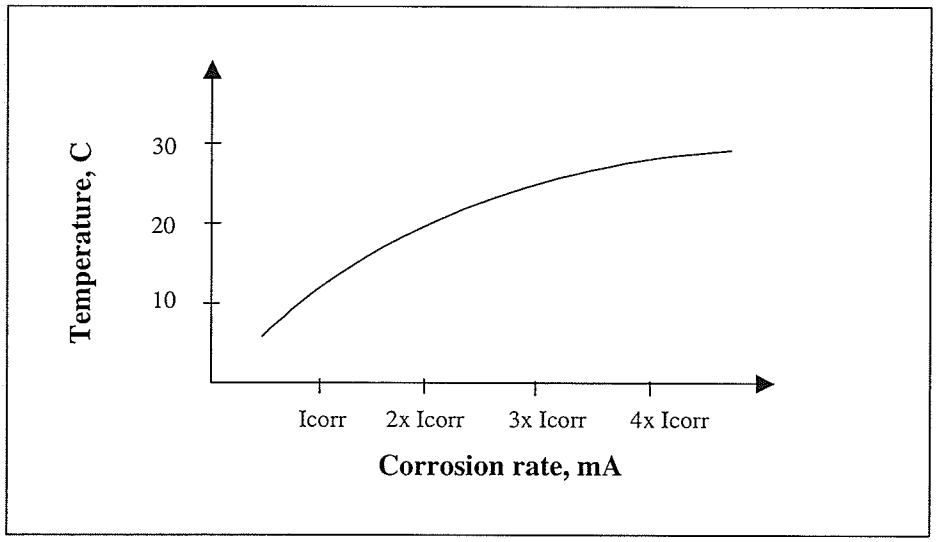

Figure 3-7: Relationship between temperature and corrosion rate [24]

Relative humidity is also a crucial factor affecting the rate of corrosion in reinforced concrete. In general, high relative humidity in atmospheric conditions will lead to high moisture content within the concrete. When conditions in the concrete are dry, corrosion rates decreases, and vice versa. The reason being that in dry concrete, the resistivity increases, hampering the flow of electrons, thus reducing the corrosion rate. Unlike the somewhat linear relationship between the temperature and corrosion rate seen in Figure 3-7, corrosion rates are nearly non-existent when relative humidity is less than 85% and increase drastically between 85-95% relative humidity, as shown by Figure 3-8. It is for these reasons regarding temperature and relative humidity that coastal regions, particularly of hot regions, are often considered to be the most detrimental to reinforced concrete.[24]

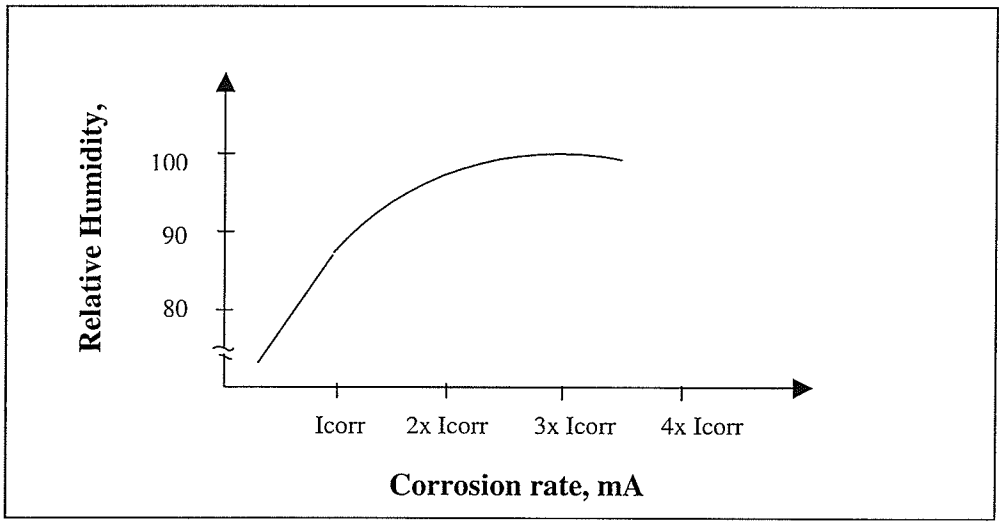

Figure 3-8: Relationship between relative humidity and corrosion rate [24]

Two exposure conditions were considered for this project. The first exposure condition simulated an aggressive environment via an environmental chamber at the University of Manitoba. The specimens sent to the environmental chamber underwent constant high temperature and relative humidity, 35 °C and 90 %, respectively, for a period of 172 days. The second exposure condition involved exposing the specimens to the somewhat unpredictable Winnipeg outdoor weather, throughout the months of April to October. Table 3-3, shows the mean maximum temperature; mean minimum temperature and the total precipitation for Winnipeg during the months of April to October. Natural ponding was achieved for the specimens exposed to outdoor conditions after periods of precipitation, by sealing around the edges of the concrete-plastic formwork interface.

It is important to note that the specimens were kept at room temperature (approximately 20 C and 50 % R.H.) for a period of eight months after casting of the slabs was completed. During this period, all the connections and wiring for the system were finalized. After the eight-month period, half of the specimens were sent outdoor for testing. The remaining slabs were kept at room temperature for additional two months, after which they were sent to the environmental chamber at the University of Manitoba for testing. All switches connecting the galvanic system to the bars and mesh were turned off from the time of casting until the time of the first test readings. This allowed corrosion activity to commence without the protecting influence offered by the galvanic systems.

Table 3-3: Monthly Winnipeg data report for 2006 during the testing period [25] *(Source: Environment Canada)*

	Mean Max Temperature, °C	Mean. Min Temperature, °C	Total precipitation, mm
April	15.8	2.4	16.5
May	18.5	5.4	44.5
June	25.2	11.1	29.0
July	29.8	13.2	10.5
August	27.0	12.5	52.0
September	20.7	6.3	41.5
October	8.7	-1.7	11.5

Winnipeg is located in southern Manitoba, in the center of Canada. It has a cold continental climate with temperatures reaching well below freezing during its winter months. Summers are short and very warm [26]. Table 3-4, shows the historical climate conditions in Winnipeg.

Table 3-4: Historical Winnipeg climate [26]

Month	Av. Daily Max. Temp. (^{o}C)	Av. Daily Min. Temp. (^{o}C)	Av. hours Sunshine (per day)	Av. Days with Rainfall	Av. Days with Snowfall	Av. Depth of Snow on Ground (cm)	Average Wind speed (km per hr)
Jan.	-13	-23	3.9	1	12	18	17
Feb.	-9	-19	4.9	1	8	20	17
Mar.	-1	-11	5.8	3	7	13	18
Apr.	10	-2	8.0	5	3	3	18
May	19	5	9.2	11	1	0	18
Jun.	23	11	9.4	13	0	0	16
Jul.	26	13	10.2	11	0	0	15
Aug.	25	12	9.0	10	0	0	15
Sep.	19	6	6.0	11	0	0	17
Oct.	11	0	4.7	8	2	0	18
Nov.	-1	-10	3.1	2	9	5	17
Dec.	-10	-19	3.2	1	11	10	17

3.5 TESTING METHODS

Testing consisted of a half-cell test for control specimens, and open-circuit potential, potential decay, and current output readings for the specimens embedded with the galvanic systems. On-going testing was conducted for a period of approximately 5 months for the specimens housed in the environmental chamber and outdoor conditions. A long-term reading was also taken on the specimens housed in the chamber after approximately 500 days. The different testing methods are discussed in more detail next.

3.5.1 Corrosion Potential: Half-Cell Test

Half-cell tests are perhaps the most commonly used non-destructive method in determining the probability of rebar corrosion in concrete due in large part to simplicity and cost-effectiveness. The basis behind this method, measures potential differences between a reference electrode with a known potential (datum) and the steel rebar under investigation. Generally, a copper/copper sulphate is used for the reference electrode. The method is standardized in ASTM C-876 and determines weather the rebar is in an active state or in a passive state [27, 28]. Rebar in the active state will have a potential

difference of -350 mV or less, whereas the rebar in the passive state will have a potential difference of -200 mV or greater. It is important to note that the half-cell method only determines the probability of corrosion activity present and does not measure the corrosion rate of the steel since no information regarding the kinetics is provided [28]. Table 3-5, shows the interpretation of half-cell potential readings for the copper/copper sulphate reference electrode.

The general rule of thumb is: the more negative the potential, the higher the risk of corrosion activity. This may not always be the case since many factors such as oxygen, chloride concentration, and concrete resistance can influence the potential readings. For instance, a decrease in oxygen at the steel-concrete interface can significantly affect the results of potential readings. This can occur in dense, low permeability concrete or in reinforced concrete submerged in water. It is also important to note, when taking half-cell readings of galvanically protected reinforced concrete, the current flow for should be interrupted for a minimum time period of 24 hours to allow the steel to fully depolarize [20, 29].

Table 3-5: Half-cell potential interpretations for a copper-copper sulphate reference electrode [29]

Potential range	Corrosion state	Probability of Corrosion
> -200 mV	Passive	10 % (low risk)
-200 to - 350 mV	Unknown	Intermediate risk
< -350 mV	Active	90 % (high risk)

Half-cell tests were conducted on the control specimens for both exposure conditions (outdoors and environmental chamber) to determine the probability of corrosion activity. A copper/copper sulphate ($Cu/CuSO_4$) reference electrode was used to conduct the half-cell and potential decay tests. For both types of tests, the readings were taken on the concrete surface directly overtop and to the center of each bar under investigation, as shown schematically in Figure 3-9. The reference electrode was connected to the positive terminal of the voltmeter and the steel was connected to the negative terminal. Mesh measurements for the half-cell and potential decay tests were taken at the center of the slab specimen. A wet sponge soaked in soapsuds was placed between the concrete surface and the reference electrode in order to decrease resistance. It is important to note that direct corrosion potential cannot be taken for specimens embedded with anodes since the steel is polarized due to continuous current being provided by the anodes. Therefore, half-cell tests conducted for specimens with anodes required a minimum of 24 hours of depolarization to record the native or open-circuit corrosion potentials. This procedure is further explained in section 3.5.3.

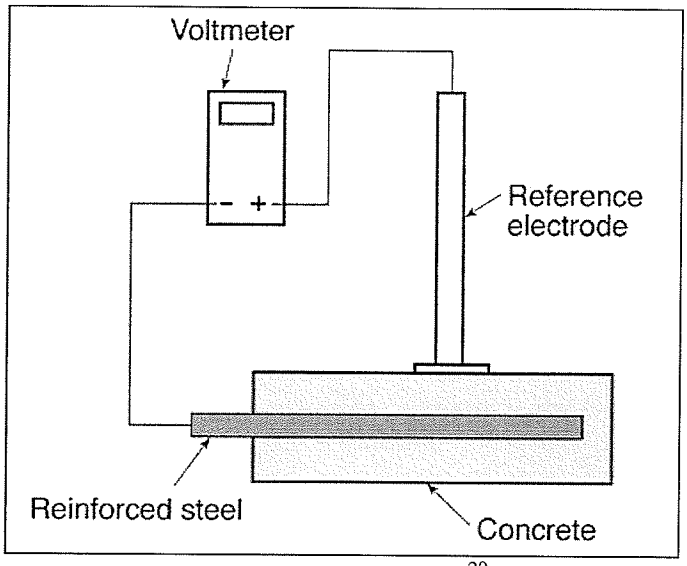

Figure 3-9: Half-cell testing setup [29]

3.5.2 Current Output

As previously mentioned, sacrificial anodes function on the principal of converting the steel into a cathode by connecting dissimilar metals in which the metal with the highest potential (typically zinc) will naturally corrode, thereby releasing electrons to the steel. This release in electron flow or current is in essence the protecting mechanism against corrosion. In a paper published by Whitmore[1], there exists a correlation between current density and three basic levels of protection against corrosion. The first level, corrosion prevention is defined as preventing the initiation of corrosion activity in contaminated reinforced concrete. This method is often helpful in preventing ring-anode effect in patch repairs of chloride-contaminated concrete. The amount of current density required to prevent corrosion from occurring generally ranges between 0.25 to 2 mA/m^2. The second level of corrosion protection is called corrosion control. Corrosion control is associated with the capability of significantly reducing the rate of corrosion activity in reinforced concrete. Corrosion control may not necessarily eliminate or stop all corrosion activity but it will slow down the process, thereby, prolonging the life expectancy of a structure. The current density required for corrosion control generally ranges between 1 to 7 mA/m^2. Although polarization of steel does occur within the current density range of corrosion control, it often falls significantly short of reaching the 100 mV criteria specified by NACE. The last level of protection is referred to as cathodic protection. Cathodic protection is deemed to be the upper level of protection against corrosion. At this stage, corrosion activity is completely or almost completely eliminated. Current density generally required to reach cathodic protection varies between 2 to 20 mA/m^2 [1]. Cathodic protection is associated with a minimum of 100 mV polarization of the steel in

the negative direction. Table 3-6, illustrates a summary of the three basic levels of protection against corrosion.

Table 3-6: Current density range for the three basic levels of protection against corrosion [1]

	Corrosion Prevention	Corrosion Control	Cathodic Protection
Objective	Prevention of corrosion activity	Significantly reducing on going corrosion activity	Stopping or virtually stopping all corrosion activity
Current required per steel surface area	0.25 to 2 mA/m2	1 to 7 mA/m2	2 to 20 mA/m2
Protection level	Good	Better	Best

A current reading was taken by attaching a multi-meter to the switch corresponding to the bar or mesh under investigation. The switch was turned off only for the bar in consideration once the multi-meter was connected and was immediately turned back on once the current reading was obtained. Bars 1 and 2 were connected to a single switch. This allowed the average current to be taken for these bars, which were spaced at equal distance to the anode. Bars 3, 4 and the mesh were each connected to an individual switch. Figure 3-10, illustrates the typical procedure to measure current output readings. Bar 4 was arbitrarily selected as depicted in Figure 3-10.

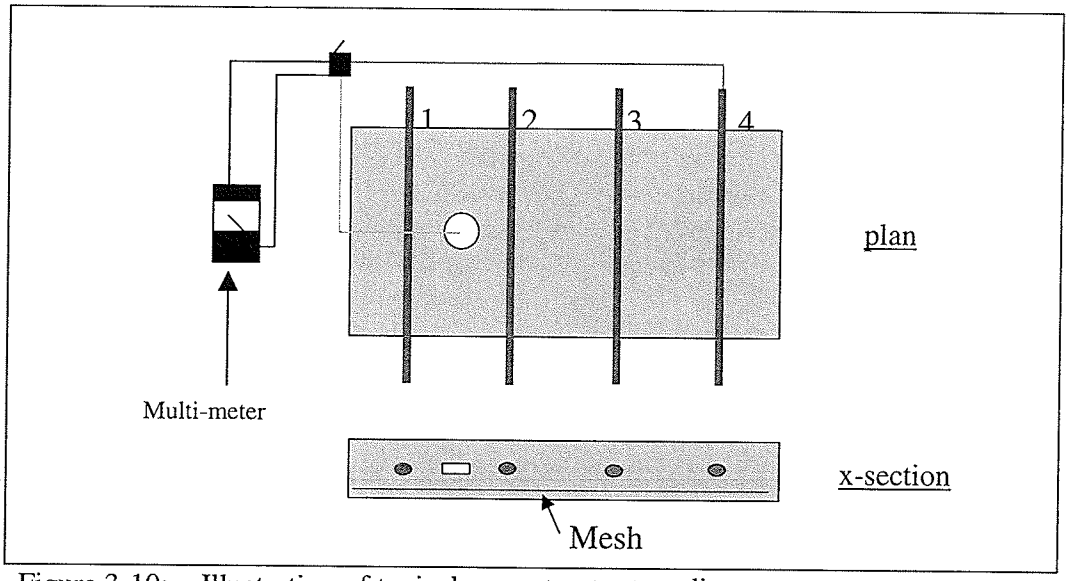

Figure 3-10: Illustration of typical current output reading

3.5.3 Potential Decay

According to NACE International, cathodic protection is the highest level of protection against corrosion in which virtually all corrosion activity is halted. When a current (i.e., the flow of electrons) is transmitted to the steel, the potential of the steel shifts negatively towards the potential of the connecting anode. A polarization shift of at least 100 mV is the most fundamentally sound criteria in confirming whether cathodic protection is reached. There are two methods, which can prove the 100 mV polarization criteria. The first method "formation" involves taking a "native" (i.e., initial or free-corroding) potential prior to any application of current to the steel. Potential readings thereafter are taken immediately after all current to the system is interrupted. This second readings is called "instant off", and the difference between the "instant off" and the native potential determines the amount of polarization that has occurred. For cathodic protection to have occurred, the difference must be greater than or equal to 100 mV [30, 31]. The second method "decay" requires the "instant off" reading to be measured first. The current is left off for a minimum period of 24 hours to allow the steel to depolarize. A second potential reading is then taken once the steel is completely depolarized in which case the potential will be stabilized as shown in Figure 3-11. The difference between the two readings determines the amount of polarization undergone by the steel due to the applied current. If the difference is greater than or equal to 100 mV the cathodic protection is achieved [30, 31]. The "decay" method enables readings of the corrosion potential of the steel at the time of testing. In other words, once completely depolarized, this represents the state of corrosion of the steel. Therefore, the second reading of the "decay" method is equivalent to the half-cell potential discussed previously. The "formation" method only uses the initial "native" potential as a reference point to the corrosion potential of the steel. Under perfect and homogenous conditions, in theory, the "native" potential should be equal to the corrosion potential (depolarized); however, the corrosion potential is influenced by several factors such as: temperature, relative humidity, and applied current.

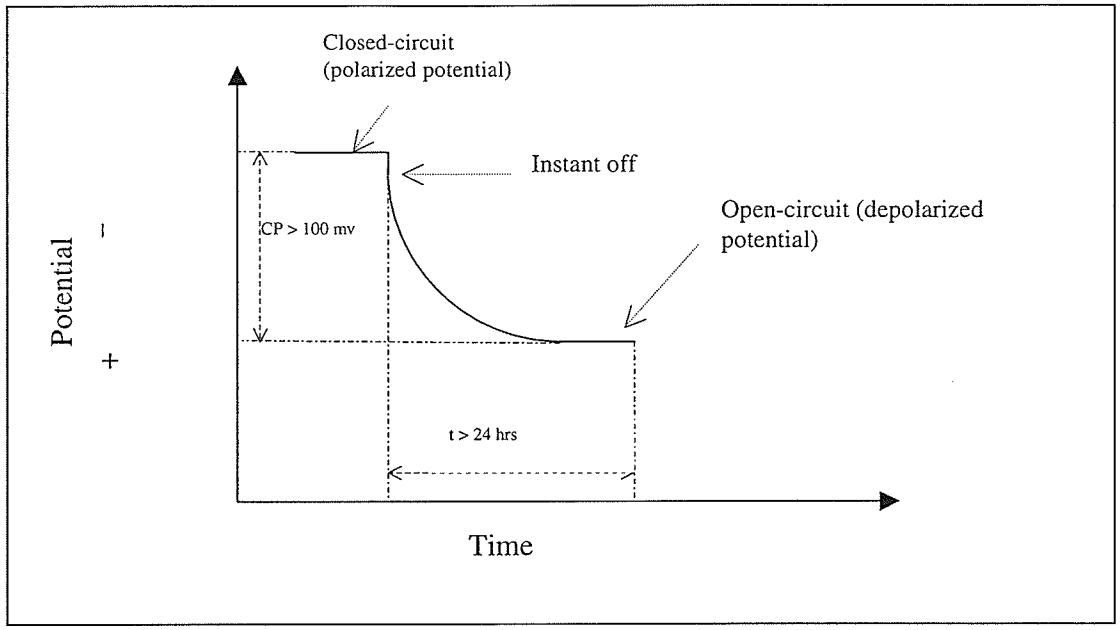

Figure 3-11: Cathodic protection based on the potential decay criterion [30]

Another criterion adopted by NACE International to determine the presence of cathodic protection is referred to simply as "instant off". This method simply requires the "instant off" reading to be equal to or more negative than -850 mV when using a $Cu/CuSO_4$ electrode. It is important to note that the "instant off" reading does not need to be equal to or more negative than -850 mV as long as the potential difference using the two previous methods are at least 100 mV [30].

Cathodic protection measured throughout this project was done by means of the "decay" criterion. The switches were left of for a minimum of 24 hours in order to allow the steel to depolarize. The potential readings were recorded with a $Cu/CuSO_4$ electrode and were conducted in accordance to the ASTM C-876 standard. The same procedure was used in the "decay" method that was used in the half-cell tests.

3.6 RESISTIVITY

It is well documented that a correlation exists between the rate of chloride ingress and the resistivity of concrete. Viewed with the naked eye, concrete seems to be an impermeable, solid material; however, viewed under a microscope, concrete is seen to be a web of interconnecting pores and capillaries, voids woven between the cement paste and the aggregates. The degree of permeability is dependant on the density and quality of concrete. It is due to the porosity of concrete that water and other contaminates such as chloride ions are able to penetrate into the concrete, eventually reaching the level of reinforcement. The rate of ingress of chloride ions is dependant on the chloride diffusion

coefficient and can be expressed by Fick's Law for a one-dimensional model. Fick's Law for a one-dimensional model is given by Eq. (3), and the Figure 3-12, gives an illustrated version of Fick's Law. Chloride diffusion coefficient is, in general, inversely proportional to the resistivity of concrete. Thus, concrete with low resistivity will translate into a higher chloride diffusion coefficient and therefore greater penetration. Studying Figure 3-12, it is apparent that chloride concentration is greatest at the surface and reduces with depth. However, with time the chloride concentration with depth will increase to the same level of concentration at the surface [9, 32]. In order to accelerate the corrosion process the diffusion was overlooked by adding chlorides in the form of table salt (NaCl) to the concrete constituents at the time of mixing.

$$C_{(x,\,t)} = C_o[1\text{-}erf(x/(2(D_c t)\text{^}0.5))] \qquad (3)$$

Where, $C_{(x,\,t)}$ = chloride concentration at time t and depth x
C_o = chloride concentration at surface (kg/m^3)
D_c = chloride diffusion coefficient (cm^2/yr)
erf = error function (standard mathematical tables)

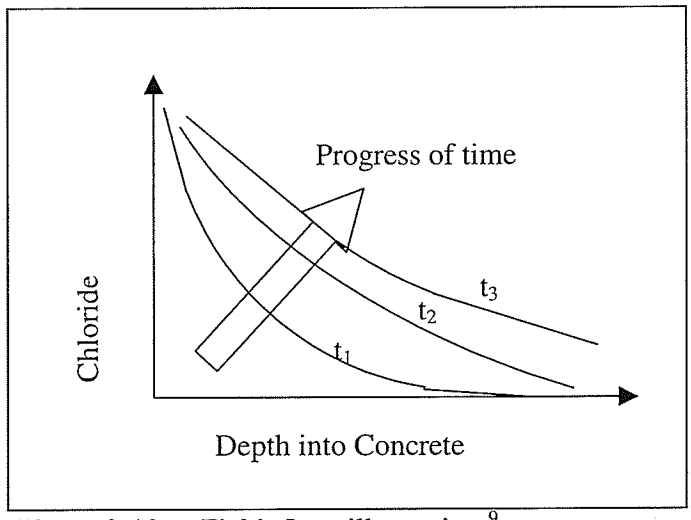

Figure 3-12: Fick's Law illustration [9]

Resistivity of concrete also directly affects the corrosion rate of steel reinforcements after depassivation has occurred. This is because the current is transported through the capillaries by the ions in the pore liquid. Thus, an increase in pore saturation and the number of larger capillaries will decrease the resistivity of concrete. In other terms, by increasing the water-cement ratio, electrons are more readily transported and therefore the corrosion rate is increased. Concrete resistivity ranges from the order of 10^1 to 10^5 Ωm depending on the quality concrete and moisture availability [33].

Resistivity can also affect the ability of the galvanic system to generate current to the corresponding steel reinforcement. Therefore, 10% of silica fume per weight of cement

was added to the same constituents as shown in Table 3-1, in order to increase the resistivity of the concrete. Test were taken to demonstrate the affects of resistivity on concrete and on the current distribution provided by the sacrificial anode.

3.7 CONTROL SPECIMEN

Four control specimens identical in geometry to the other specimens were cast using the same constituents as the original batch specified in Table 1. The control specimens did not have any anodes installed in them and the bars were not connected to one another. One control specimen was exposed to each condition. Therefore, two control specimens, containing 1.2% and 3.9% chloride by weight of cement, respectively, were exposed to the environmental chamber, whereas the other two were exposed to outdoor conditions.

3.8 TEST MATRIX

In total 76 concrete slab specimens were cast for this research project. A summary of the specimens is given in Table 3-7.

Table 3-7: Test matrix summary

<table>
<tr><th>Specimen</th><th>Duplicates</th><th>Exposure Conditions</th><th>Chloride Content</th><th>Summation of specimens</th></tr>
<tr><td>Puck anodes:
A, B, C, D, E</td><td>Yes
(x 2)</td><td rowspan="4">• Environmental chamber
(constant 35C and 90% humidity)

• Outdoor conditions
(Winnipeg's climate)</td><td rowspan="3">• High levels
(3.9% by weight of cement)

• Low levels
(1.2% by weight of cement)</td><td>5 x 2 x 2 x 2
= 40 specimens</td></tr>
<tr><td>Strip anodes:
S, M, L</td><td>Yes
(x 2)</td><td>3 x 2 x 2 x 2
= 24 specimens</td></tr>
<tr><td>Control</td><td>No</td><td>1 x 1 x 2 x 2
= 4 specimens</td></tr>
<tr><td>Resistivity:
Anode A</td><td>Yes
(x 2)</td><td>—</td><td>1 x 2 x 2 x 2
= 8 specimens</td></tr>
</table>

4.0 THEORETICAL ANALYSIS

4.1 BASIC PRINCIPLES

The corrosion process consists of two separate reactions (anodic and cathodic), which occur simultaneously. The anodic reaction, which measures the rate of oxidation, is represented by the curve A in the Evan's Diagram, shown below in Figures 4-1 a) and b). The anodic reaction can follow two distinct paths depending on the environment in which it is initiated. For corrosion initiated in soils or carbonated concrete, the anodic reaction behaves in the "active" form. This behavior is illustrated in Figure 4-1(a). The behavior of anodic reaction differs in alkaline environments such as concrete. Oxidation under these circumstances follows a more complex 'active-passive' behavior, as shown in figure 4-1(b). The anodic reaction in concrete very rarely enters into the trans-passive region. The cathodic reaction, which measures the rate of oxygen reduction, is represented by curve C. The corrosion rate (I_{corr}) and corrosion potential (E_{corr}) of the steel in question, is taken by the intercept of the anodic and cathodic reactions curves [32, 34].

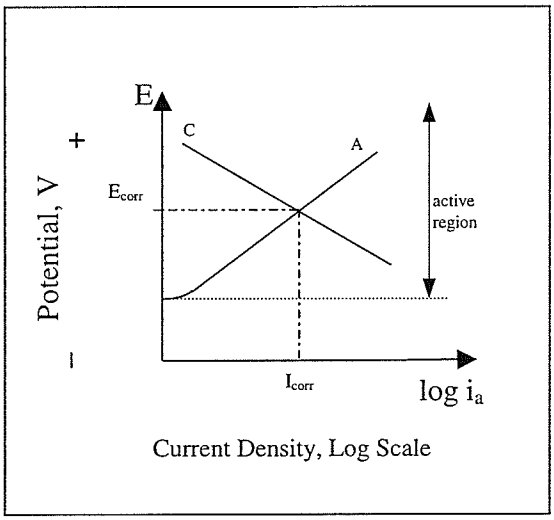

Figure 4-1(a): 'active' condition [32]

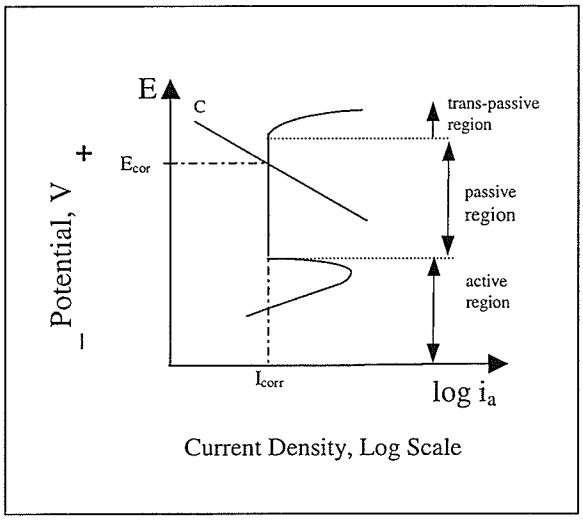

Figure 4-1(b): 'active-passive' condition [32,34]

In high alkaline concrete, oxidation of the steel creates a protective, dense, ferric oxide film, which drastically decreases the corrosion rate (I_{corr}). The passive region of the Evan's Diagram is where this protective film is known to exist. Generally, the anodic and cathodic reactions intercept in the passive zone, in which case the steel is stable. The corrosion rate is insignificant when the steel is in the passive state. As the corrosion potential (E) becomes increasingly negative, the intercepts will eventually exit the passive region and enter into the active region, in which point the passive film will deteriorate. A

break down in the passive film will lead to a substantial increase in corrosion rate, as illustrated by the log scale of Figure 4-1 (b) [32, 34].

4.2 EFFECTS OF OXYGEN AND CHLORIDE

Variations in the surrounding concrete environment may cause electrochemical potential imbalances between the adjacent zones (i.e. existing concrete versus repair substrate). The greater the electrochemical potential imbalance between adjacent zones the greater the driving force becomes. The driving force is simply the potential difference between the anodic and cathodic sites, and it is the measure of the tendency for each reaction to occur spontaneously. Electrochemical potential imbalances can stem from a wide range of factors such as the difference in the physical or chemical properties of the steel or the surrounding concrete itself. For instance, the difference in steel homogeneity at the surface, grain boundaries, difference in concrete density and permeability, can all lead to electrochemical imbalances.

To illustrate further, repair substrate can have a different degree of porosity and hence would contain a different amount of oxygen concentration. This can lead to establishment of an anodic site at the location of lower oxygen level. This phenomenon is known as differential aeration corrosion and can occur even in a chloride free environment. When oxygen levels diminish, the cathodic reaction also decreases, thereby lowering the tendency of the cathodic reaction to occur. As a result, the corrosion potential (E_{corr}) becomes increasingly negative. This process is demonstrated graphically by the Evan's diagram, shown below in Figure 4-2. The corrosion rate will not change substantially as long as the intercept of the two reactions is within the passive zone. If the difference in oxygen concentration between the anodic and cathodic sites is extreme, the corrosion potential (E_{corr}) will continue to increase negatively and the driving force will increase. The steel can than enter into the active region of the Evans Diagram, in which case corrosion rate will increase substantially. Curve Ca to Cd, in Figure 4-2, represents the decrease in cathodic reaction [32, 34, 35]. Therefore; a variance in oxygen levels between adjacent sites will affect the cathodic reaction. As long as oxygen is still readily available at the cathodic site corrosion can still take place.

Chlorides concentration alternatively, effects the anodic reaction. As chloride content increases, the passive film is consumed and a shift in the anodic reaction occurs. The greater the chloride content the smaller the passive region becomes. At high chloride concentrations the passive region disappears, thereby increasing the corrosion rate and decreasing the corrosion potential. The shift in anodic reaction is illustrated by the anodic curve A1 to A4, shown in Figure 4-3 [32, 34].

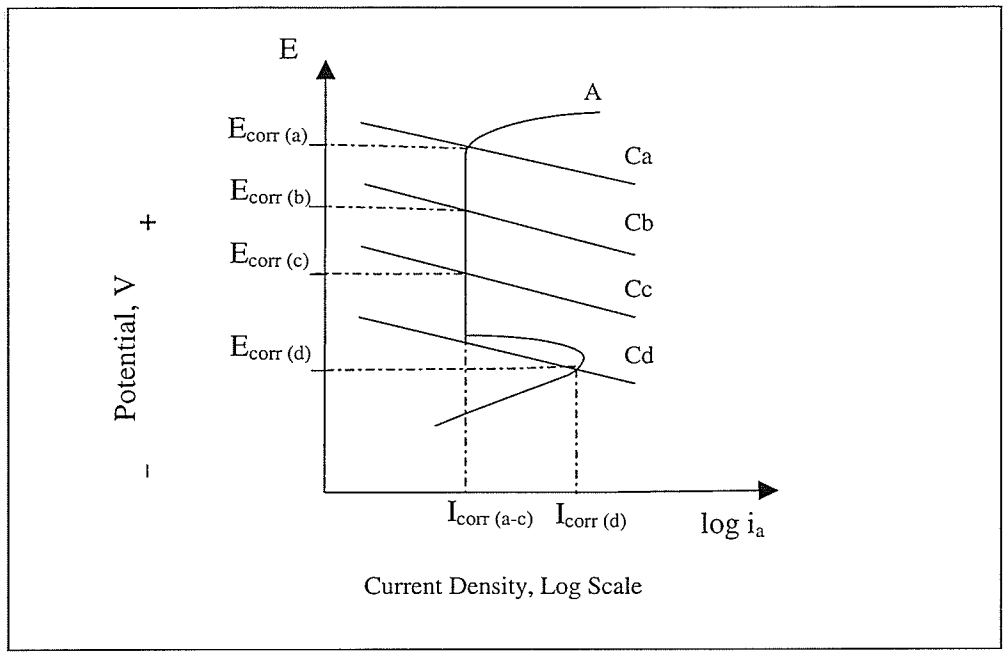

Figure 4-2: The effect of oxygen levels on steel corrosion rate in chloride-free concrete [34]

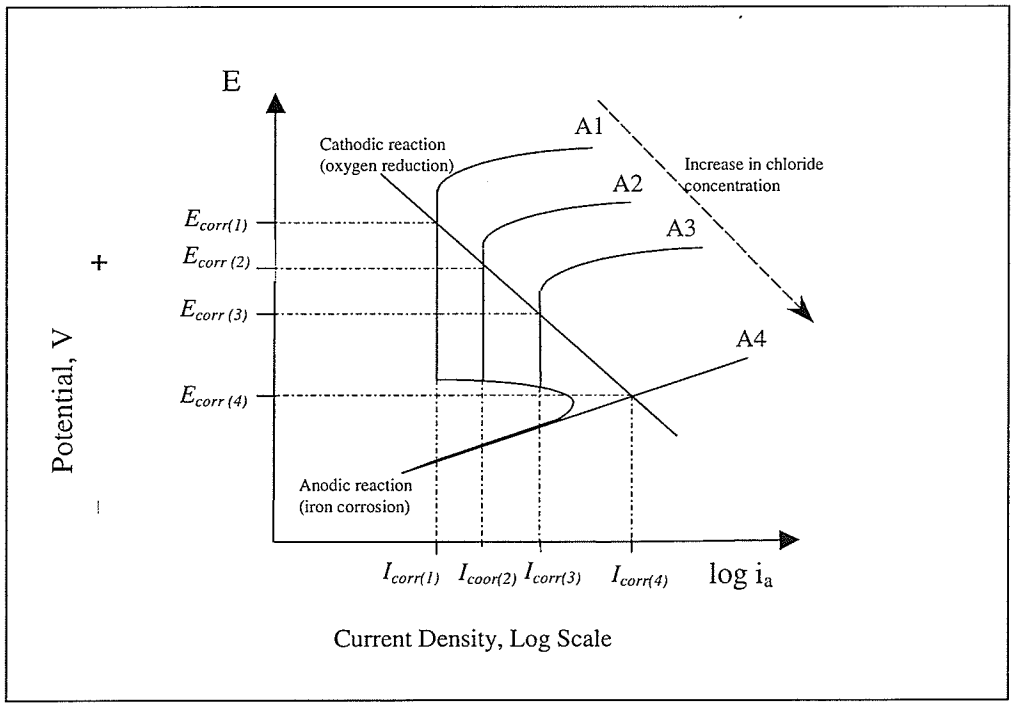

Figure 4-3: The effect of chloride levels on steel corrosion rate in concrete [34]

4.3 ELECTROCHEMICAL INCOMPATIBILITY IN PATCH REPAIR

Although extreme precaution is often taken in conducting patch repairs, such as the removal of neighboring contaminated concrete, it is difficult to completely eliminate the risk of ring anode effect. The reason being, electrochemical incompatibilities often develop between the existing and repaired areas. As mentioned previously, one such incompatibility is linked to the difference in porosity between the repair mortar and the concrete. For instance, if the existing concrete is of greater porosity than the repair mortar, a greater amount of oxygen will be present in the existing surrounding concrete area. Differences in porosity will lead to an uneven oxygen concentration distribution along the surface of the steel. This, in turn, causes a potential differences which leads to the formation of a macro-cell along the steel. In the regions of high oxygen (existing concrete) reduction will occur converting this region into the cathode. Oxidation occurs in the region of less oxygen. Therefore, the patch region develops into the anode. If the oxygen difference between the existing and patch region is small, the potential difference will also be small. In such a case, the intercept may lie within the passive range, in which case no increase in corrosion rate will occur. However if the difference in oxygen is great, the intercept may lie outside the passive range, and corrosion rate may increase. This process is shown by the Evan's diagram in Figure 4-4(a) and schematically in Figure 4-4(b). Curve C1 represents the cathodic reaction in the existing concrete area. The oxygen deficient region under the repair patch is shown by cathodic curves C2 and C3. Keep in mind; this potential difference due to oxygen can take place in chloride free environment [32, 34].

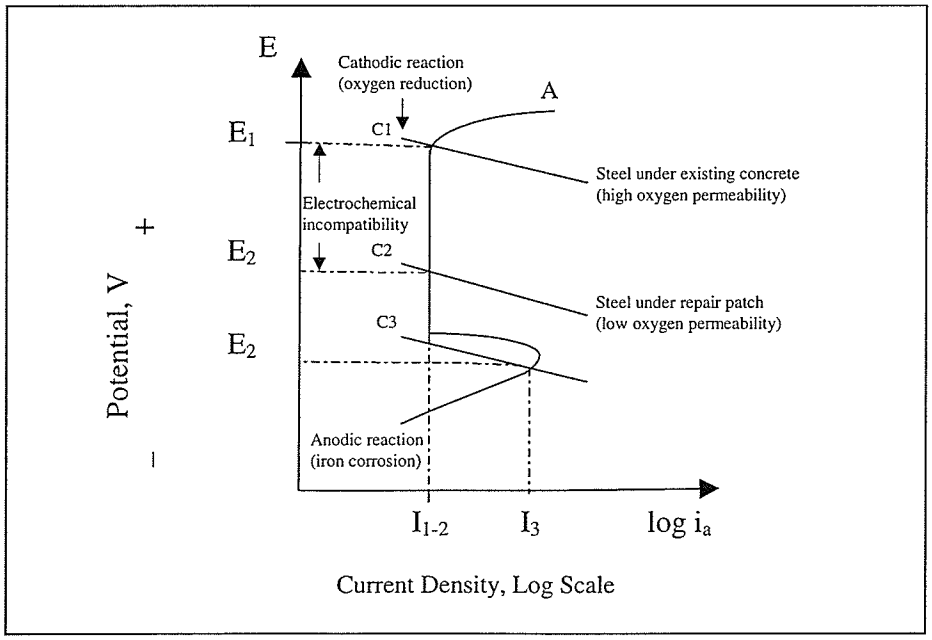

Figure 4-4(a): The effect of oxygen incompatibility on steel corrosion rate in concrete patch repair [34]

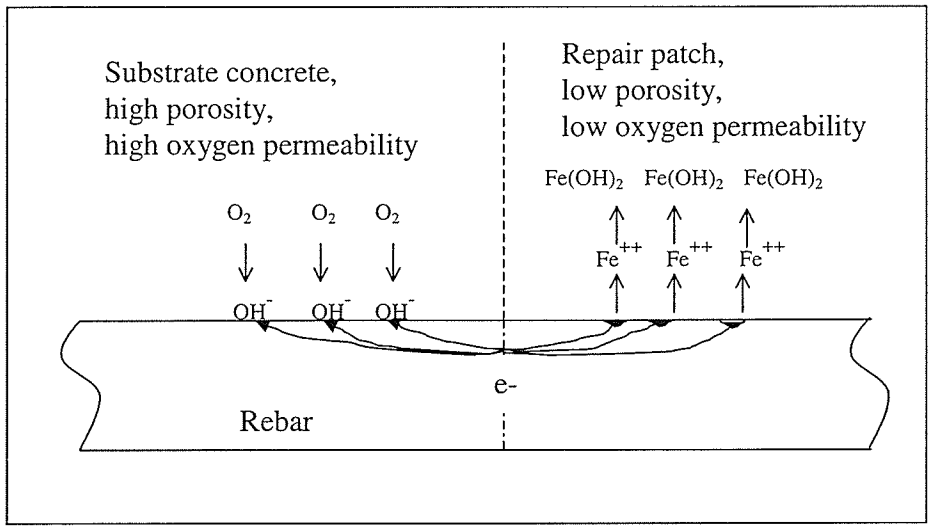

Figure 4-4(b): Illustration depicting oxygen incompatibility in patch repair concrete [34]

Another electrochemical incompatibility, which creates a potential difference in patch repair, is due to unbalanced amounts of chlorides. Generally, all contaminated chloride concrete is removed in patch repair, but chlorides often remain in the existing concrete. This creates a potential difference causes the formation of a chloride induced macro-cell. The process is described by the Evan's diagram in figure 4-5(a) and figure 4–5(b). If the existing concrete is contaminated even slightly with chlorides, the anodic reaction will be influenced. The greater the potential difference between the two regions, the greater the anodic shift and the smaller the passivity region becomes. This is shown by curves A1 and A2 in figure 4-5(a). It is important to point out that chloride induced corrosion is much more aggressive than oxygen induced corrosion. The reason being chloride macro-cell acts as an autocatalyst and therefore the corrosion rate is increased. This occurs because oxidation creates positive ferrous ions (Fe++). A build up of positive ions attract the negative chlorides ions, and thus chloride concentrations increase in the anodic region. In addition, the build up in chlorides lowers the pH of the concrete. Both of these actions further deteriorates the passive film, expanding the anodic region and increasing the corrosion rate [32, 34].

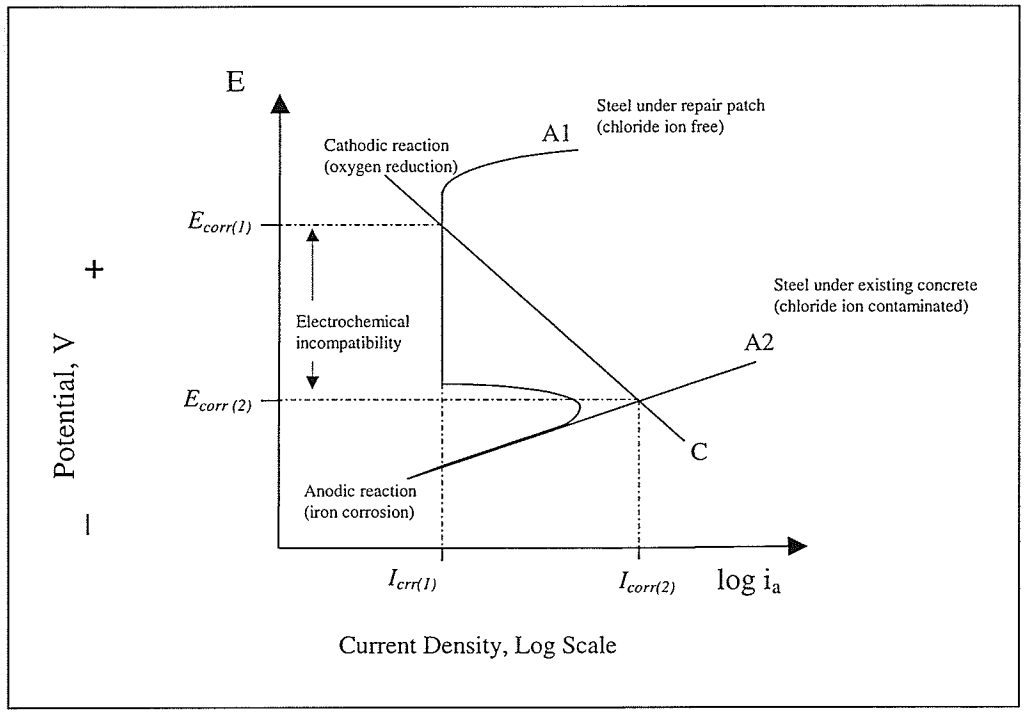

Figure 4-5(a): The effect of chloride content incompatibility on steel corrosion rate in concrete patch repair [34]

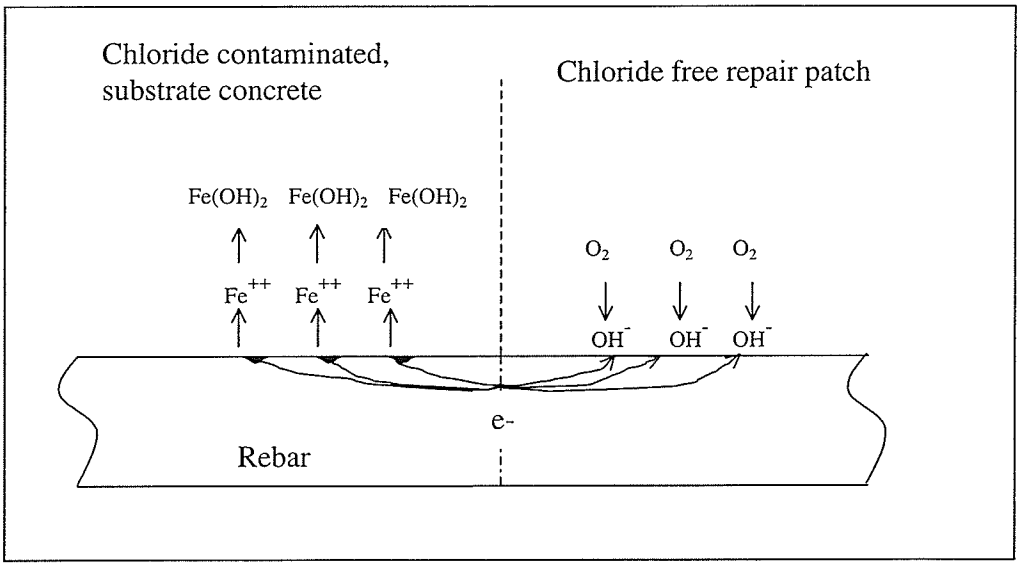

Figure 4-5(b): Illustration depicting chloride incompatibility in patch repair concrete[34]

4.4 EFFECTS OF POLARIZATION

Current applied to the steel reinforcement by sacrificial anodes (or other electrochemical methods) has two principal modes of protecting steel against corrosion. The first and most common understanding of how this is done is known as the *primary effect* or cathodic polarization. However, in certain instances, a *secondary effect* is achievable and it is often overlooked. The *secondary effect* or anodic polarization may be as important, if not more important than its counterpart. These two principals are discussed below. Negative effects of steel polarization will also be addressed [32].

4.4.1 Primary Effect

The driving force that causes the flow of electrons between the anode and the cathode are attributed the potential differences between these two regions. Potential is the measure of tendency for oxidation and reduction reactions to occur spontaneously. In essence, the driving force is simply the difference in the steel potential in an aggressive environment and the equilibrium potential. When the oxidation reaction takes place, the flow of current is opposed by anodic resistance and therefore the corrosion rate can be expressed as: $i_a = L / R$. The level of resistance is proportional to the amount of passive film encasing the steel. Therefore, if there is a substantial amount of passive film still intact around the rebar, the degree of resistance will be high.

The *primary effect*, which is thermodynamic in nature, is achieved by the potential shift of steel in the negative direction when current is applied. The tendency to oxidize the iron is reduced when the cathodic reaction is polarized. This negative potential shift reduces the driving force and corrosion rate. The greater the driving force is minimized the greater the level of protection the steel will receive. NACE has determined polarization of 100 mV will virtually stop the corrosion and is the basis for cathodic protection. Lower levels of polarization will provide corrosion control. Cathodic polarization also increases the chloride 'threshold'. In fact, even low levels of polarization associated with current in the range of 0.2-2 mA/m2, can increase the chloride 'threshold' by the order of one magnitude. This is the basis for corrosion prevention. It is important to note that the effects of cathodic polarization are immediate but cease once the protecting current has halted [32, 36].

4.4.2 Secondary Effect

Conventional understanding indicates that the principal protection against corrosion is due to the negative potential shift of the cathode (*primary effect*). This is the basis for the "instant off" criterion for determining cathodic protection, as discussed previously. However, in steel reinforced concrete environment, the cathodic kinetic reactions are weakly polarized. This indicates that the cathode is constantly resisting the negative potential shift. As chlorides breakdown the passive film layer, corrosion rate increases, as does the oxidation reaction. An increase in oxidized iron ions signifies a depolarization in anodic reaction. The *secondary effect* focuses on anodic polarization of

steel and the effect it has on the cathodic region. By introducing current, a positive shift in open circuit potential is associated with anodic polarization. The polarization of the anodic reaction results in the migration of chlorides away from the rebar and increase in pH in the surrounding concrete. This promotes the re-passivity of the film, creating a much less aggressive environment. When current is applied, the flow travels through the electrolyte by way of migrating ions. The flow is proportional to the mobility and magnitude of ion movement. Current flows in the same direction as positive ions (from anode to cathode). As current flows to the cathode, negative ions travel in the opposite direction towards the anode. Thus, current flow produces a migration of chloride ions (Cl^-) away from the cathode. Research shows that the open circuit potentials become more positive with the formation of the passive film. This reduces the tendency for steel oxidizing and therefore, reduces or eliminates the corrosion activity. The shift in open circuit potential also leads to a decrease in the amount of current required to maintain the same level of protection. Both the *primary* and *secondary effects* occur concurrently as a result of applied current, but the *secondary effect* is often overlooked.

The theory relating to the beneficial of effects of anodic polarization versus cathodic polarization is depicted using the Evans diagram, in research papers published by Glass et al. A specimen subjected to chloride contamination was initially corroding at 30 mA/m^2. By applying a current density to the specimen of 40 mA/m^2, and keeping the anodic and cathodic reaction kinetics unchanged, the corrosion rate decreased to 15 mA/m^2. This represents the effects of a negative potential shift. However, by allowing a positive increase of 200 mV in open circuit potential, a decrease in corrosion rate to 0.8 mA/m^2 was observed. This increase in positive potential is associated with the change in environment surrounding the concrete and perhaps the re-passivity of the film. In short, cathodic polarization is related to the negative polarization shift of the cathode, whereas the anodic polarization is related to the change in environment surrounding the rebar. Figure 4-6, illustrates the Evans diagram associated to these findings [32, 36].

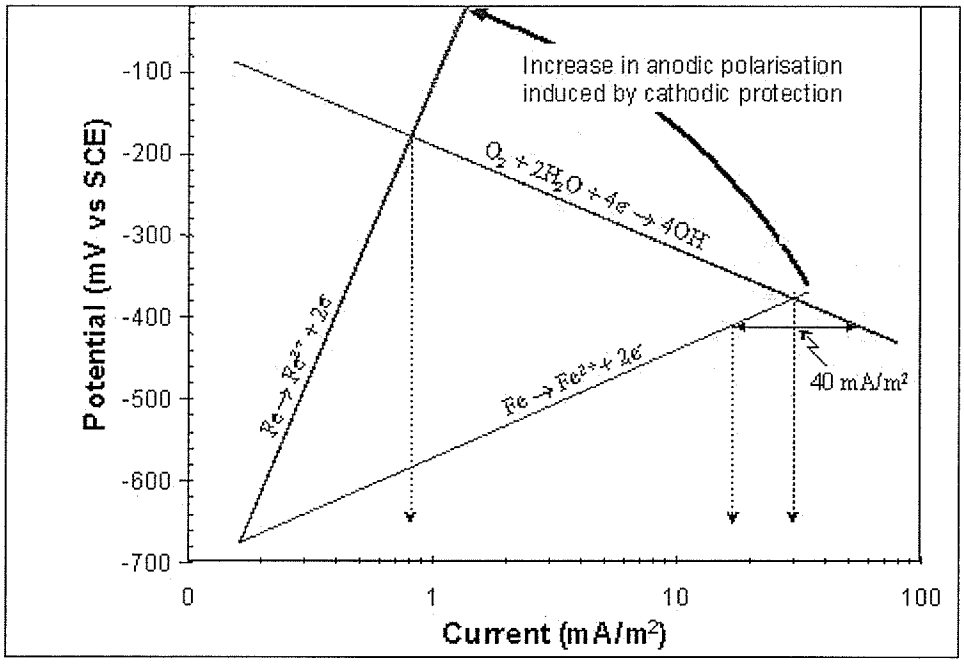

Figure 4-6: Effects of anodic polarization on corrosion rate in reinforced concrete [36]

4.4.3 Negative Effects

The old cliché: too much of something good is bad; is also applicable to the case of polarization of steel. At high levels of polarization, hydrogen evolution occurs in the cathodic areas. This can lead to hydrogen embrittlement of the reinforcing steel, and thus jeopardizing its strength capability. This is particularly true for applications using high strength steel (σ_R > 700 MPa). Hydrogen embrittlement cannot occur at potentials more negative than -900 mV, when exposed to alkaline environments (pH >12). This is true even for the most susceptible steel reinforcements, such as prestressed strands or quenched and tempered steel. For lower strength steel (σ_R < 700 MPa), hydrogen embrittlement is not an issue. [32]

Other negative factors associated with polarization of steel to very negative potentials include: adhesion loss and concrete degradation. The former, can occur at potentials reaching -1100 mV. Although not much is documented on the cause of this phenomenon, it generally occurs with ribbed steel reinforcement. The latter, is related to the increase in alkalinity surrounding the rebar. If alkali-reactive aggregates are present in the concrete there may be a risk of alkali-silica reaction, only if the current is excessively high in the short-term or moderately high (>10 mA/m^2) in the long-term applications. Alkali-silica reaction causes premature deterioration of concrete. [32]

5.0 RESULTS AND INTERPRETATION

5.1 SACRIFICIAL PUCK ANODE ANALYSIS

The results for the performance of the new galvanic system A and the other commercially available galvanic systems, which have been labeled: B, C, D, and E, are presented in this section. The results include half-cell tests (open circuit potential), current density output, and potential decays. These tests were conducted on a steel reinforced concrete slab specimens containing 1.2% and 3.9% chlorides by weight of cement. Half of these specimens were further subjected to continuous high temperature and high humidity (35 C, 90% R.H.) via an environmental chamber, or exposed to Winnipeg's outdoor conditions from the months of April to October. Duplicates of each slab specimens were also tested under the same conditions to achieve greater accuracy of the results (average of the two specimens). Control specimens containing no galvanic system were also subjected to the same conditions. No duplicates were tested for the control specimens. To compare the performance of the sacrificial anodes, the results were plotted for one particular bar (or the mesh) subjected to the same conditions. For instance, result from current output delivered to Bar 3 for the different specimens and subjected to the 1.2% chloride by weight cement in the environmental chamber were plotted together. This facilitated the comparison between the different galvanic systems. The plotted results were the average of the duplicates for each specimen, except for the controls.

5.1.1 Half-Cell Results: Environmental Chamber

Half-cell potential (open circuit) readings were conducted for both the control and galvanically protected specimens. All specimens (control and galvanic) were cast with the pre-determined amount of chloride content and were kept at room temperature and humidity for approximately a 10-month period. The specimens were then exposed to the environmental chamber 7 days before turning on the galvanic systems (i.e. the switch) and recording the initial reading (time zero days). Prior to this period, the circuit was disconnected and the sacrificial anodes bared no influence on the Bars and mesh. After the initial connection of the circuit, the sacrificial anodes were free to electro-chemically interact with the steel. In total, the environmental chamber was in-operation for a period of 172 days (not including the 7 day period prior to the initial reading). After this period, the specimens returned to room temperature and humidity, while the sacrificial system remained operational. A long-term reading was taken at 506 days to see how the specimens were behaving. The only period in which the sacrificial systems were disconnected throughout this period was during testing periods. Figures 5-1 to 5-5 show the half-cell potential results for the control and galvanically protected specimens, subjected to 3.9% chloride by weight of cement. Figures 5-6 to 5-10 show the half-cell potential results for the control and galvanically protected specimens, subjected to 1.2% chloride by weight of cement.

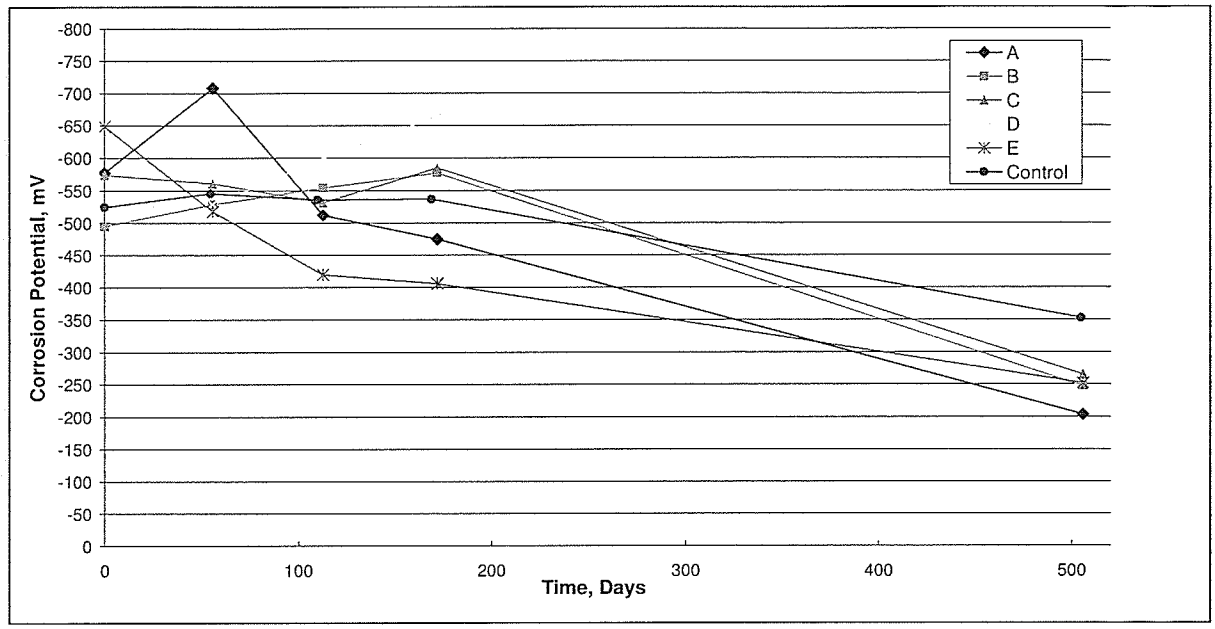

Figure 5-1: Half-cell potential of the different galvanic systems for Bar 1 subjected to 3.9% chloride by weight of cement and exposed to the environmental chamber

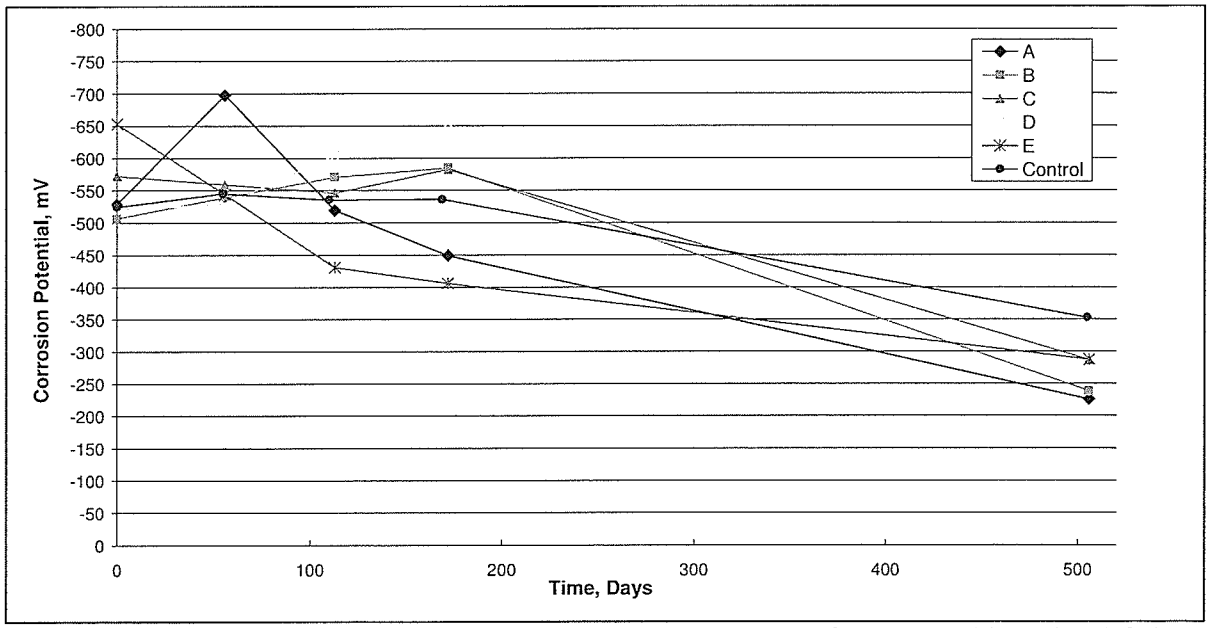

Figure 5-2: Half-cell potential of the different galvanic systems for Bar 2 subjected to 3.9% chloride by weight of cement and exposed to the environmental chamber

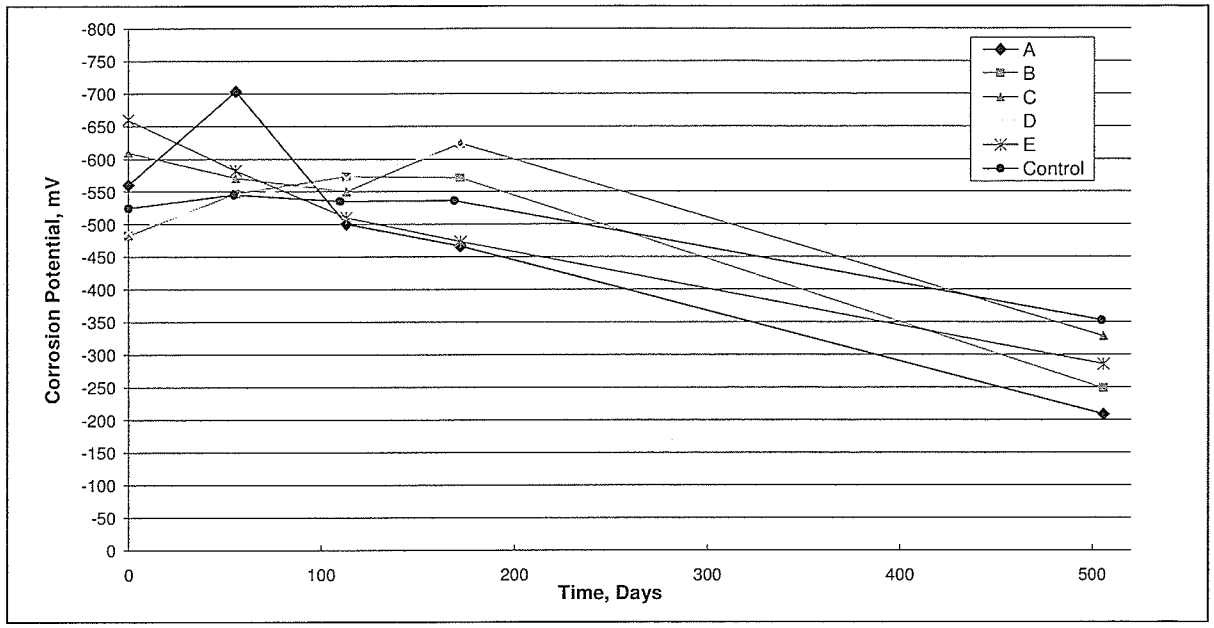

Figure 5-3: Half-cell potential of the different galvanic systems for Bar 3 subjected to 3.9% chloride by weight of cement and exposed to the environmental chamber

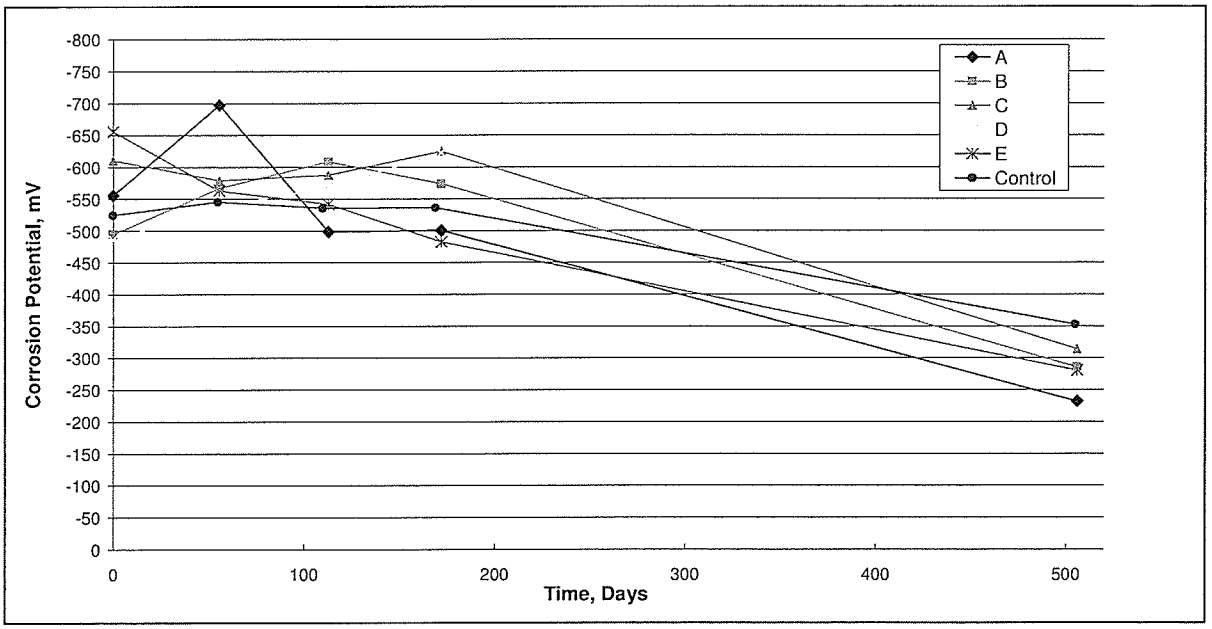

Figure 5-4: Half-cell potential of the different galvanic systems for Bar 4 subjected to 3.9% chloride by weight of cement and exposed to the environmental chamber

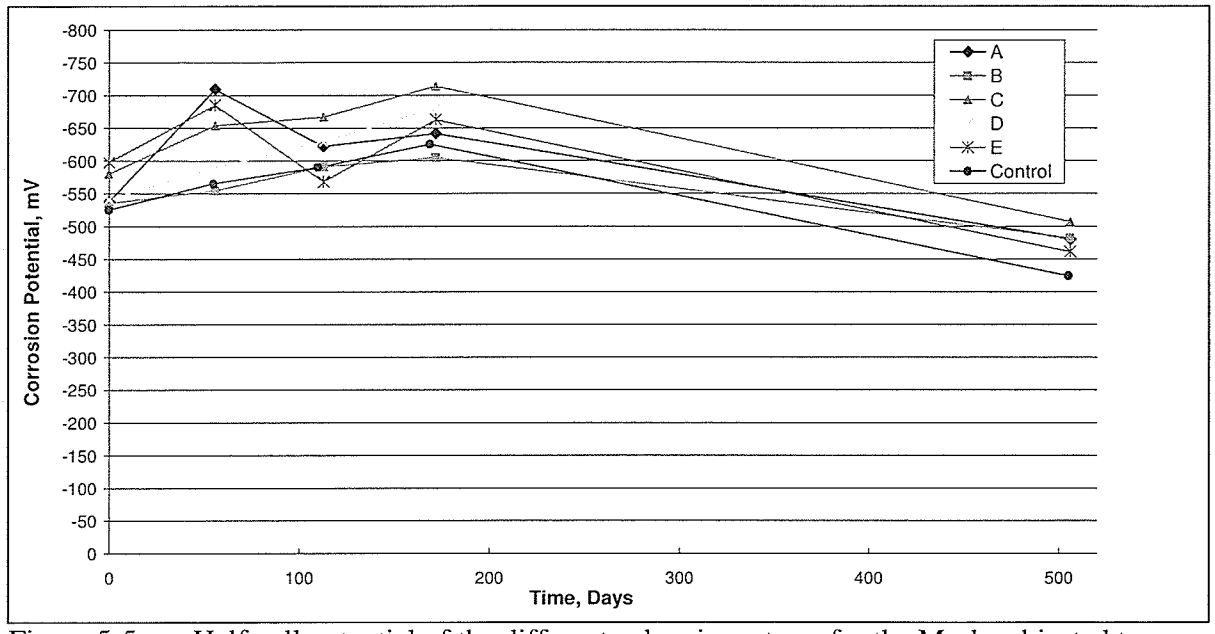

Figure 5-5: Half-cell potential of the different galvanic systems for the Mesh subjected to 3.9% chloride by weight of cement and exposed to the environmental chamber

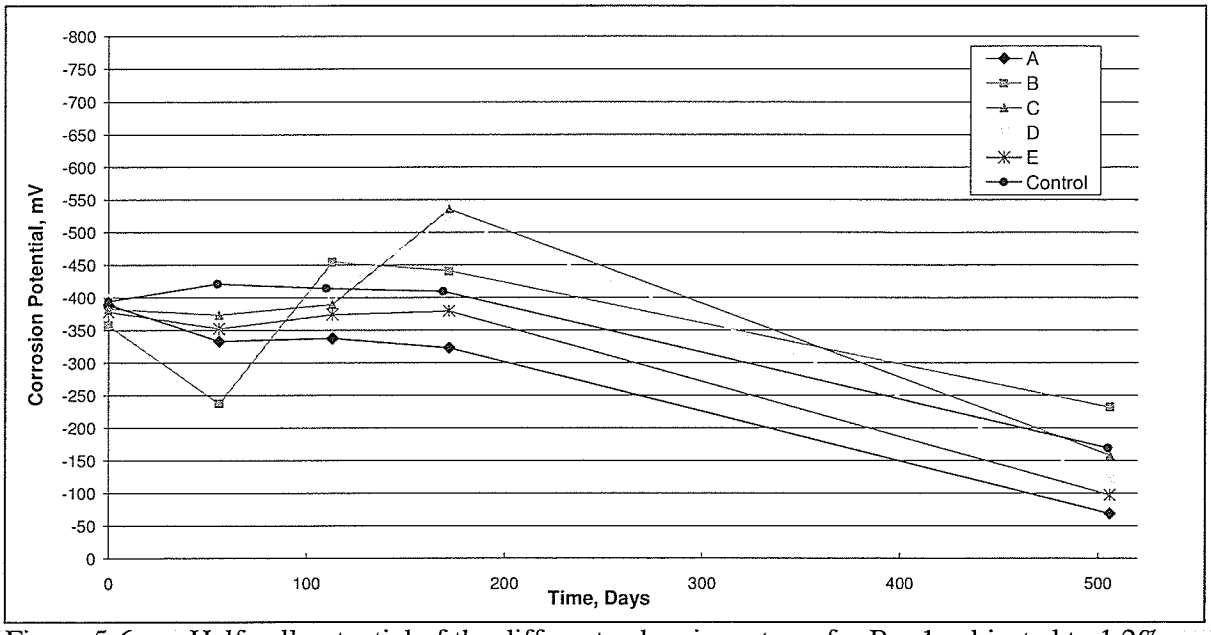

Figure 5-6: Half-cell potential of the different galvanic systems for Bar 1 subjected to 1.2% chloride by weight of cement and exposed to the environmental chamber

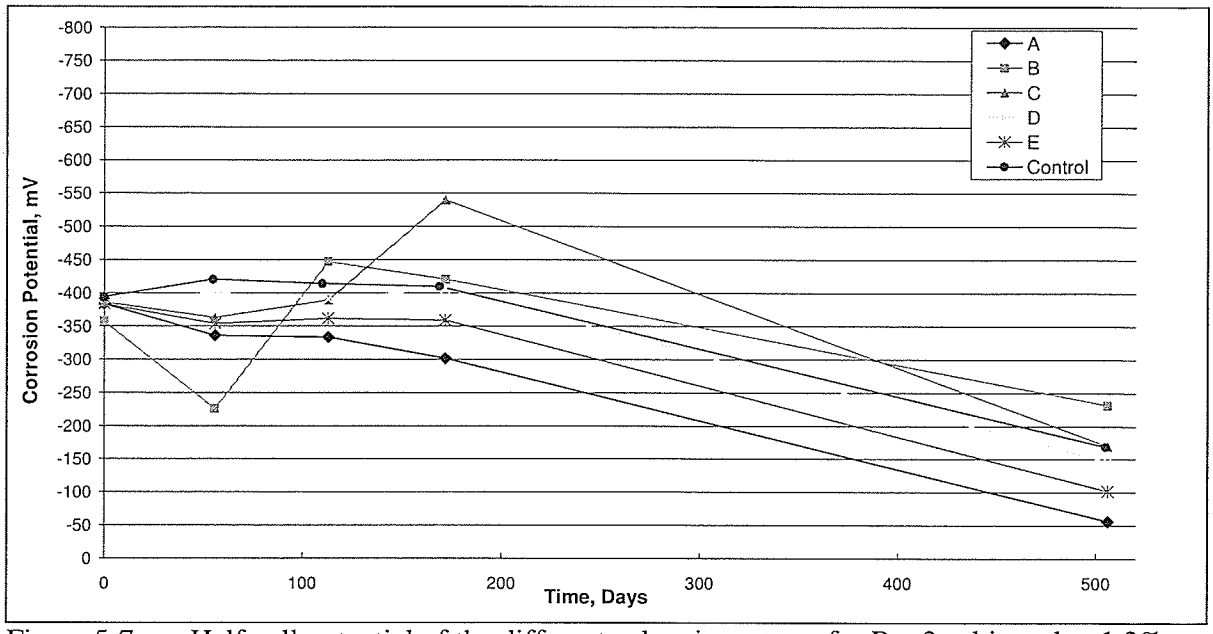

Figure 5-7: Half-cell potential of the different galvanic systems for Bar 2 subjected to 1.2% chloride by weight of cement and exposed to the environmental chamber

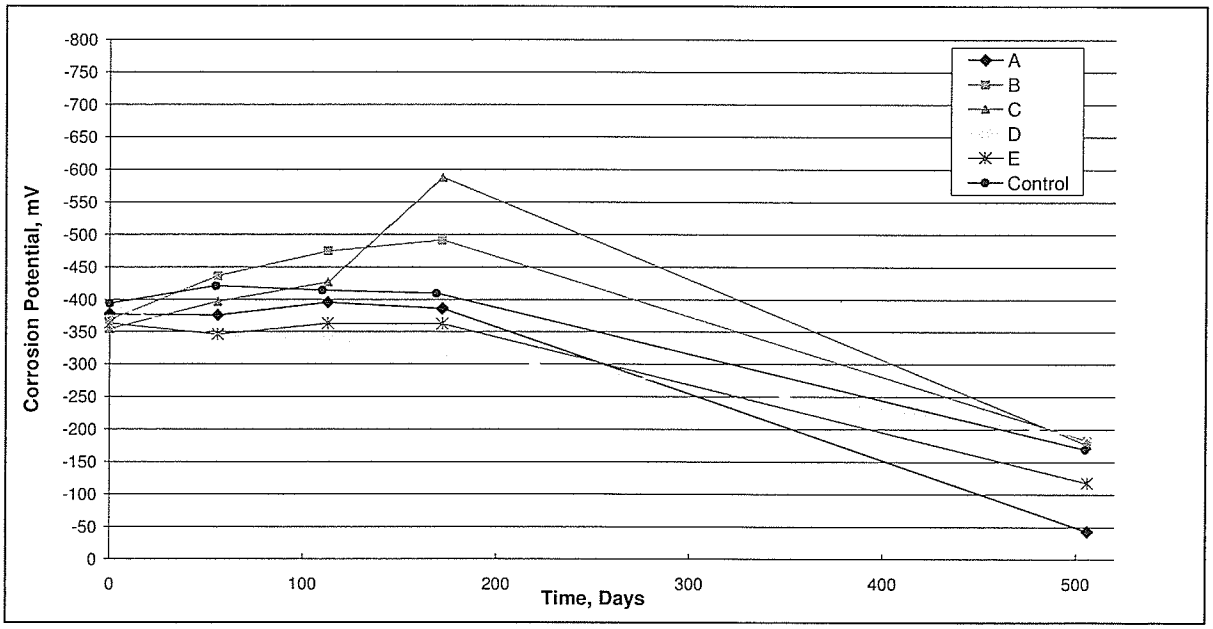

Figure 5-8: Half-cell potential of the different galvanic systems for Bar 3 subjected to 1.2% chloride by weight of cement and exposed to the environmental chamber

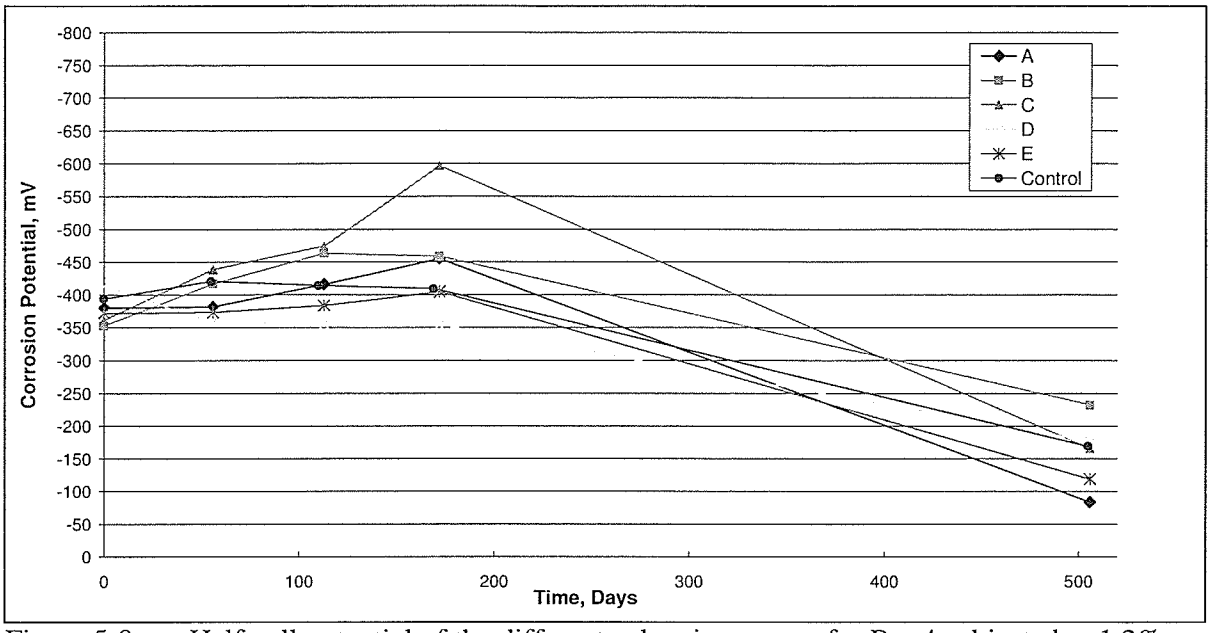

Figure 5-9: Half-cell potential of the different galvanic systems for Bar 4 subjected to 1.2% chloride by weight of cement and exposed to the environmental chamber

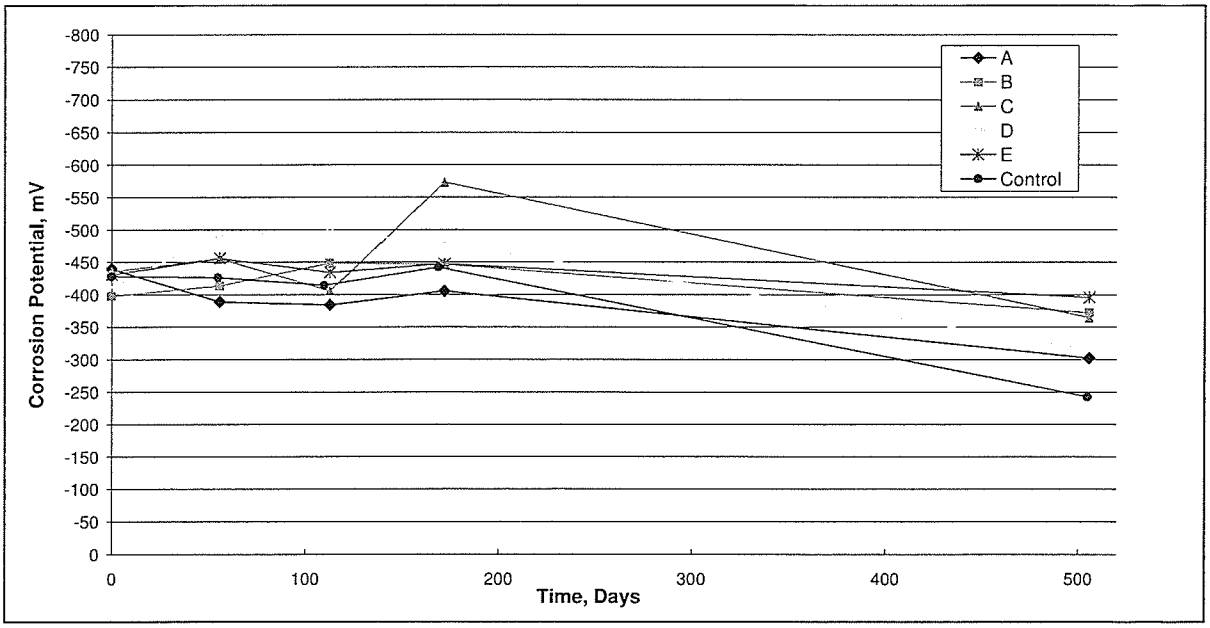

Figure 5-10: Half-cell potential of the different galvanic systems for the Mesh subjected to 1.2% chloride by weight of cement and exposed to the environmental chamber

Note that, at the moment of the long-term testing severe corrosion occurred on many of the wires and switches, causing a possible disconnection in the circuit. Unfortunately, for this reason, no

readings were available for both duplicates of Sacrificial Anode D subjected to high chlorides. It is important to also point out that the half-cell corrosion potential for the control specimen comprised of the average results taken from the four bars. Since the control bars were not subjected to any sacrificial anode system and since all other conditions are essentially the same (geometry, properties, chloride content, moisture, etc...) the half-cell potential readings in theory should also be similar. Thus, the average of the four bars was plotted for each control specimen so that an accurate datum point could be established. The control half-cell potential obtained for the mesh, which has a different geometry to the bars, was plotted separately. Control mesh results were compared to the other mesh potentials obtained by the different specimens.

It is difficult to see any clear trend in the half-cell results for the different systems when comparing them to one another. There is a lot of fluctuation and overlapping in the Figures 5-1 to 5-10. However, when analyzing the initial reading, half-cell potential for the specimens exposed to high chlorides ranged in the vicinity of -475 mV to -650 mV. Comparing these initial readings with the ASTM interpretations (Table 3-5), the potentials are much more negative than the -350 mV mark, indicating a probability of corrosion of at least 90%. This signifies that at the moment of time zero, corrosion has most likely initiated and the steel is in an active state. Specimens subjected to low chlorides, recorded an initial half-cell reading typically ranging from –350 mV to –450 mV. This was expected since it indicates a less aggressive environment for the specimens containing 1.2 % chlorides per weight of cement. Despite the less aggressive environment, the initial half-cell readings still indicate an active state where the probability of corrosion taking place is still high. These initial half-cell results coincide well with the proposed objective of testing the level of protection offered by the galvanic systems in a corroding environment (i.e., corrosion control and not corrosion prevention).

As expected, the initial potential readings were very similar for all bars subjected to same chloride levels, despite the difference in galvanic systems. Since the circuit was disconnected prior to the initial reading, no protecting current was present and therefore the galvanic systems had no effect on the steel. However, with continuous exposure to high temperature and relative humidity as well as the continual activation of the galvanic systems, the open circuit (half-cell) potential readings for the different specimens varied with time. Under ideal conditions, the following trends would be expected:

1. Open-circuit corrosion potential becomes more positive with time relative to the control half-cell potential due to the protection of the current;
2. The greater the amount of current supplied to the reinforcement the greater the open-circuit potential shift in the positive direction would become (i.e. open-circuit potential would vary with galvanic systems, distance to the sacrificial anode, and steel to sacrificial anode area ratio).

However, this was not always the case. Many galvanic systems showed corrosion potential more negative than the control corrosion potential. For instance, the open-circuit potential for Sacrificial Anode A, exposed to high chlorides for Bars 1 to 4 (Figure 5-1 and 5-4) behaved in an almost identical manner. The initial readings for the bars saw a half-cell reading slightly greater than the control. At a time of 56 days, the open-circuit potential peaked in the negative direction

reaching potential near –700 mV, roughly 150 mV more negative than the control potential. The open-circuit potential then became more positive than the control potential thereafter. Sacrificial Anode D on the other hand, started with an initial half-cell potential more positive than the control; it continuously recorded increasingly more negative potentials thereafter. Although more negative half-cell readings are associated with higher corrosion probability, it gives no indication on the corrosion rate. Therefore, despite the fact that corrosion potentials may indicate high corrosion probability, it is important to analyze all the various tests to conclude whether corrosion is taking place and to what extent.

The open-circuit potential for Sacrificial Anode A specimens containing low chloride levels behaved much more as expected. The initial half-cell readings were in proximity to the control potential, signifying an approximately equal risk of corrosion. After activation, the open-circuit potential for Sacrificial Anode A increasingly became more positive than the potential for the control specimens. This was the trend in particular for Bars 1 and 2 (Figures 5-6 and 5-7). As discussed in the theoretical analysis section, when current is supplied to the reinforcement, the surrounding within the concrete changes, thus rendering the environment less aggressive. This improvement in environment leads to a decrease in corrosion potential. Corrosion potential also appears to be increasing negatively with distance from the anode as seen in Sacrificial Anode A for Bars 3 and 4 (Figures 5-8 and 5-9). Recall, from Section 3.1., that Bars 1 and 2 are spaced at equal distance from the anode, whereas Bars 3 and 4 are increasingly further away in distance, respectively. In theory, relatively less current should be delivered to these further bars. The result for mesh open-circuit potential also shows more negative values. This is again expected since the steel mesh covers a much larger area.

When the environmental chamber was turned "off" after 172 days, the corrosion potential shifted significantly for each case towards the passive region. In fact, the half-cell readings at 506 days indicate corrosion potential typically between –100 mV to –300 mV for specimens exposed to low chlorides. Therefore, the corrosion potential shifted from active corrosion activity to a range of uncertain corrosion activity or passive activity (less than 10% probability of corrosion). This was expected since temperature and relative humidity greatly influence corrosion, as illustrated previously by Figures 3-7 and 3-8, in Section 3.4. Most galvanic system specimens exposed to high chloride levels also showed an open-circuit potential more positive than the control potential at readings at 506 days. Again, this is due to the environment becoming less aggressive, combined with the continual protection offered by the sacrificial throughout this period.

Since it is difficult to analyze the results because of the fluctuation and overlapping of the corrosion potential curves, a weighted-average of the potential was tabulated. This weighted-average is representative of the mean corrosion potential throughout the testing period. Table 5-1, shows the weighted-average of the half-cell readings for the galvanic systems exposed to high chlorides. In the interest of comparing the specimens exposed to high temperature and relative humidity (35 C and 90%, respectively), only the readings taken when the environmental chamber was functional (first 172 days) will be analyzed. Table 5-2, shows the weighted average of the half-cell readings for the galvanic system exposed to low chlorides. Again only the first 172 days were taken into consideration for this table.

Table 5-1: Average weighted corrosion potential for specimens subjected to 3.9% chlorides by weight of cement and exposed to 35 C and 90% relative humidity for 172 days.

Galvanic system	Average - weighted corrosion potential for Bar 1, mV	Average - weighted corrosion potential for Bar 2, mV	Average - weighted corrosion potential for Bar 3, mV	Average - weighted corrosion potential for Bar 4, mV	Average - weighted corrosion potential for Mesh, mV
A	-580	-567	-571	-573	-640
B	-539	-552	-549	-570	-572
C	-557	-561	-579	-594	-656
D	-574	-572	-555	-554	-610
E	-487	-500	-552	-557	-627
Control	-537	-537	-537	-537	-577

Table 5-2: Average weighted corrosion potential for specimens subjected to 1.2% chlorides by weight of cement and exposed to 35 C and 90% relative humidity for 172 days.

Galvanic system	Average weighted corrosion potential for Bar 1, mV	Average weighted corrosion potential for Bar 2, mV	Average weighted corrosion potential for Bar 3, mV	Average weighted corrosion potential for Bar 4, mV	Average weighted corrosion potential for Mesh, mV
A	-342	-337	-384	-405	-398
B	-365	-355	-447	-429	-428
C	-408	-406	-432	-465	-455
D	-431	-396	-345	-365	-478
E	-368	-362	-357	-382	-443
Control	-412	-412	-412	-412	-425

When comparing the two tables, it is easy to realize the specimens contaminated with higher chlorides (Table 5-1) are in fact exposed to a much more aggressive environment than their counterparts, as shown by the higher negative half-cell values. Sacrificial Anode B, C, and E have similar trends to what is expected, as shown in Table 5-1; the closer the bar is to the sacrificial anode the less negative (i.e. or more positive) the half-cell readings, thus signifying a less aggressive environment. The mesh readings in each of these cases also show a higher corrosion potential. This was expected since the steel surface area of the mesh is much greater than that of the bars. For the most part in Table 5-1, the corrosion potentials for the bars protected by the galvanic systems was more negative than the control specimens.
The specimens in Table 5-2 for the most part (except Sacrificial Anode D) behaved as expected. The half-cell potential increased negatively as distance from the anode increased. Mesh readings generally also indicated a more aggressive environment as compared to bars for a particular specimen. Corrosion potential readings for the bars relating to the galvanic systems were virtually all more positive than the bars in the control specimen indicating a less aggressive

environment when the current was being delivered to the reinforcement. However, almost the opposite effect was seen when comparing the mesh corrosion potential. By analysis of the half-cell readings only, this implies that the possibility for corrosion activity in the mesh is higher when it is galvanically protected under the present wiring system. The most logical explanation for this anomaly is the result of a macro-cell between the mesh and the Bars. This will be discussed in greater detail in the following sections.

In theory, it would be expected that the galvanic systems that generates a longer sustained current over a certain period of time would provide the most protection to the steel. It would render the environment within the concrete less aggressive, thus lowering the risk of corrosion and ultimately shifting the open-circuit potential by greater values towards the positive direction. So, a galvanic system with greater current capacity should in theory have values of open-circuit potential more positive than a galvanic system that produces less current. However, this is not always the case as many different factors affect the overall performance of a system. Assuming that all environmental conditions are the same for each slab under investigation (i.e. exact chlorides, resistance, moisture, etc...), it is still vital to consider the current distribution and potential decay or "instant off" readings, in order to make a educated conclusion of the results. In other words, corrosion potential can only tell you part of the story. Corrosion potential defines the risk (or tendency) of corrosion due to the state of the environment within concrete, but it does not necessarily give any information on the performance of a system (i.e., the decrease in corrosion rate). Therefore, it is important to analyze each of these conditions prior to making any conclusion about a particular sacrificial anode.

5.1.2 Half-Cell Results: Outdoor Conditions

Half-cell and open circuit results for the specimens exposed to outdoor conditions are shown in Tables 5-11 to 5-20. The outdoor specimens were cast with the same batch as the specimens exposed to the environmental chamber. The specimens were contaminated with the two levels of chlorides: 3.9% per weight of cement and 1.2% per weight of cement. The specimens were then kept in room conditions for approximately only 8-months, after which they were sent outdoors prior to initial testing. Half-cell (i.e. open circuit) results for the specimens exposed to outdoor conditions are shown for high chloride contaminate levels and low chloride contaminate levels, in Figures 5-11 to 5-15, and 5-16 to 5-20, respectively.

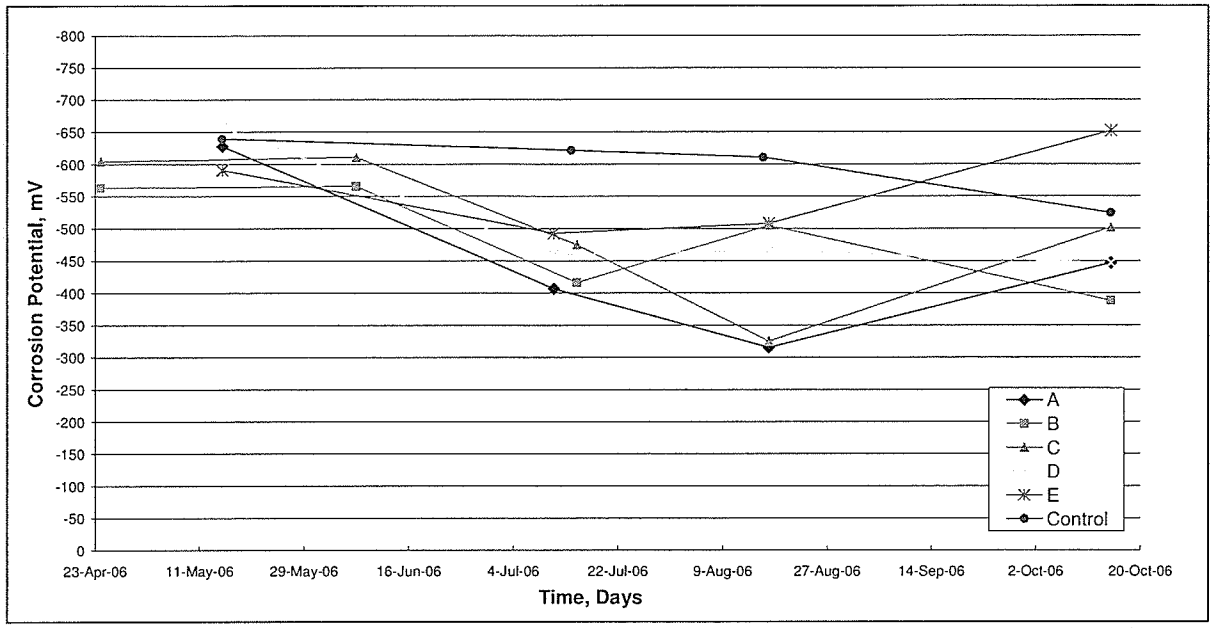

Figure 5-11: Half-cell potential of the different galvanic systems for Bar 1 subjected to 3.9% chloride by weight of cement and exposed to Winnipeg's climate

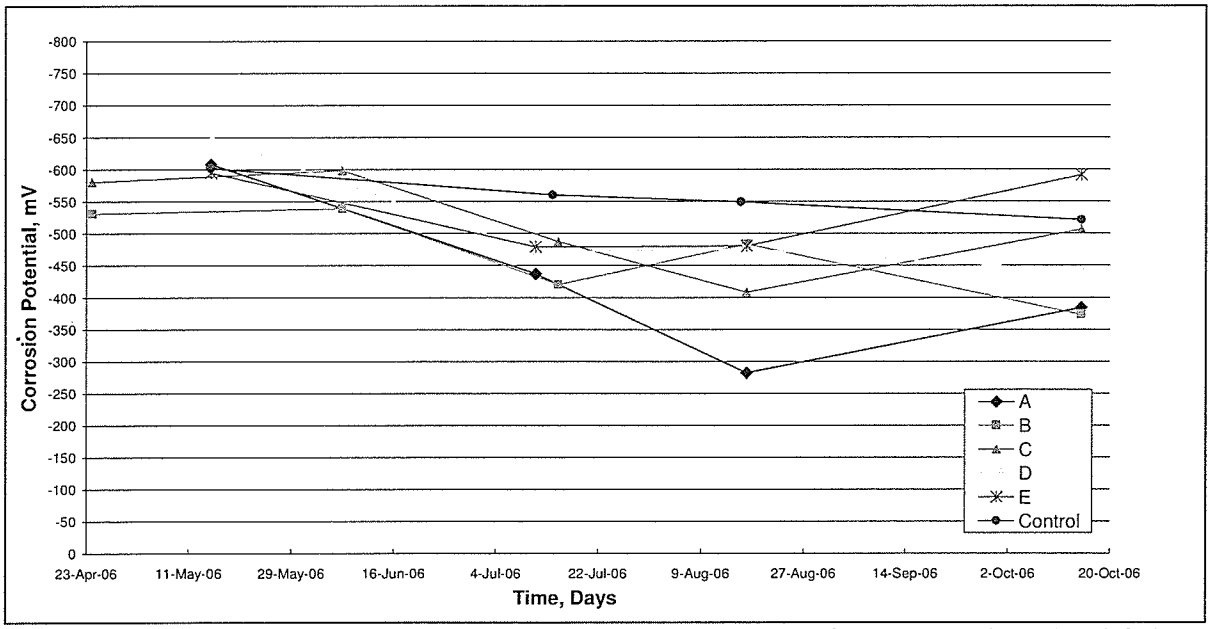

Figure 5-12: Half-cell potential of the different galvanic systems for Bar 2 subjected to 3.9% chloride by weight of cement and exposed to Winnipeg's climate

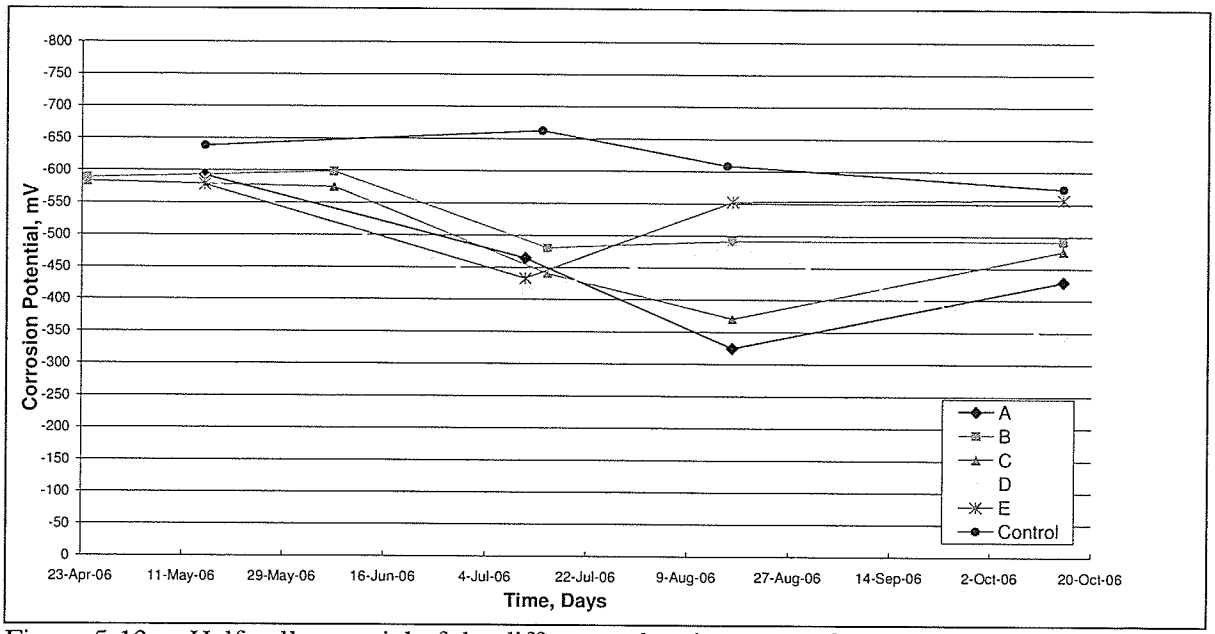

Figure 5-13: Half-cell potential of the different galvanic systems for Bar 3 subjected to 3.9% chloride by weight of cement and exposed to Winnipeg's climate

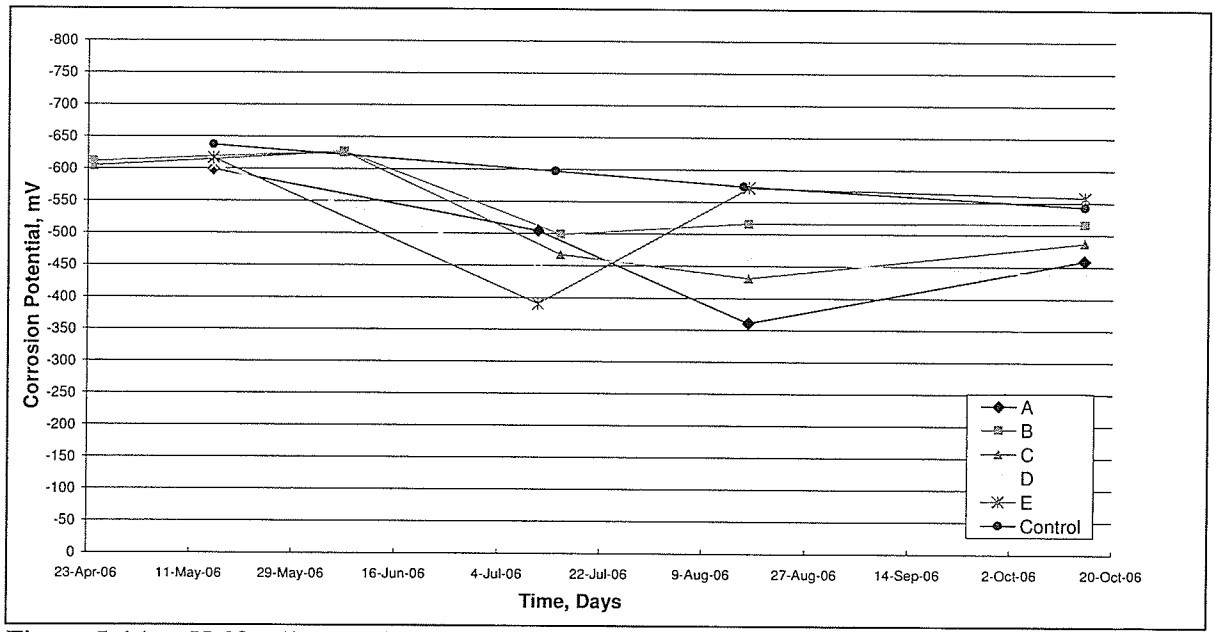

Figure 5-14: Half-cell potential of the different galvanic systems for Bar 4 subjected to 3.9% chloride by weight of cement and exposed to Winnipeg's climate

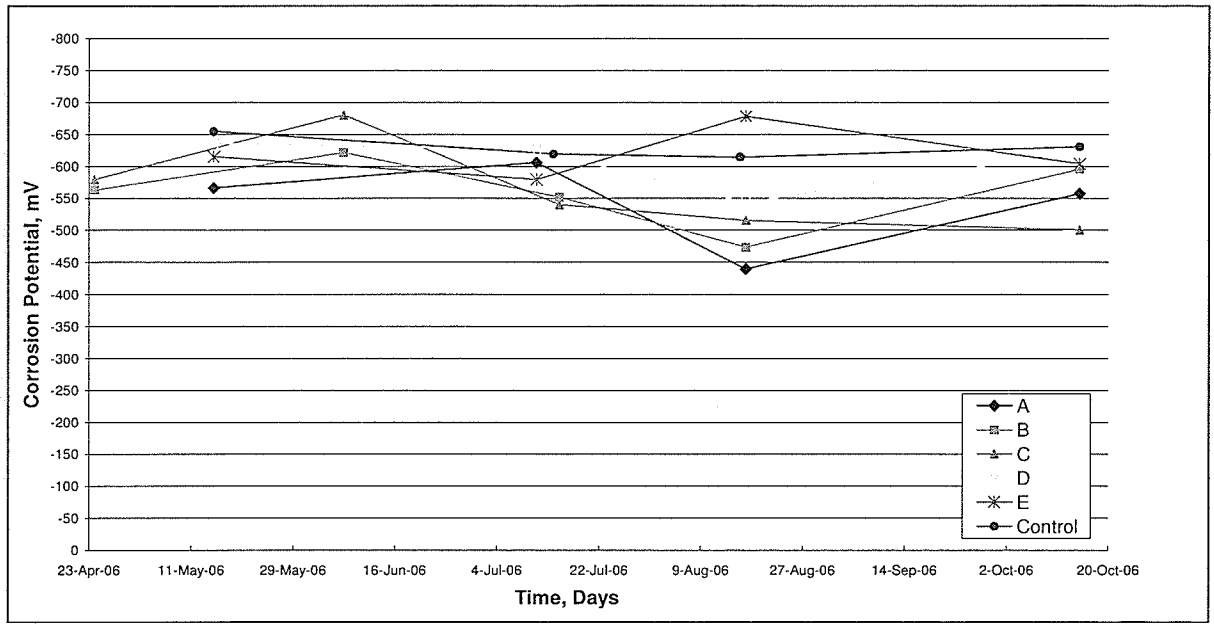

Figure 5-15: Half-cell potential of the different galvanic systems for the Mesh subjected to 3.9% chloride by weight of cement and exposed to Winnipeg's climate

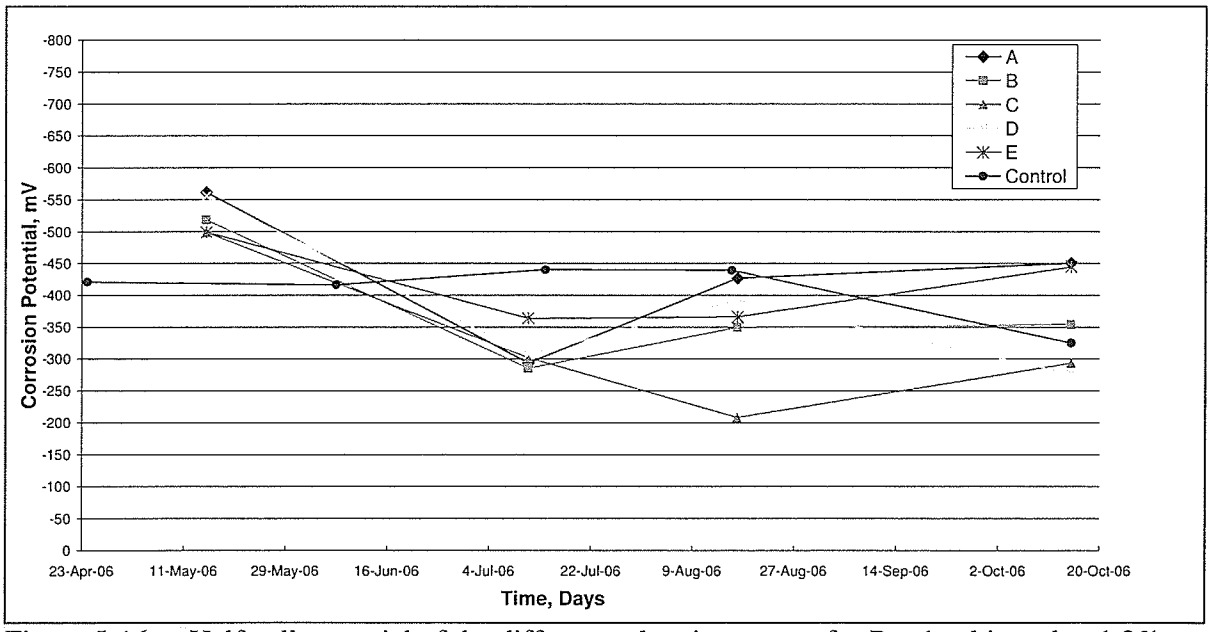

Figure 5-16: Half-cell potential of the different galvanic systems for Bar 1 subjected to 1.2% chloride by weight of cement and exposed to Winnipeg's climate

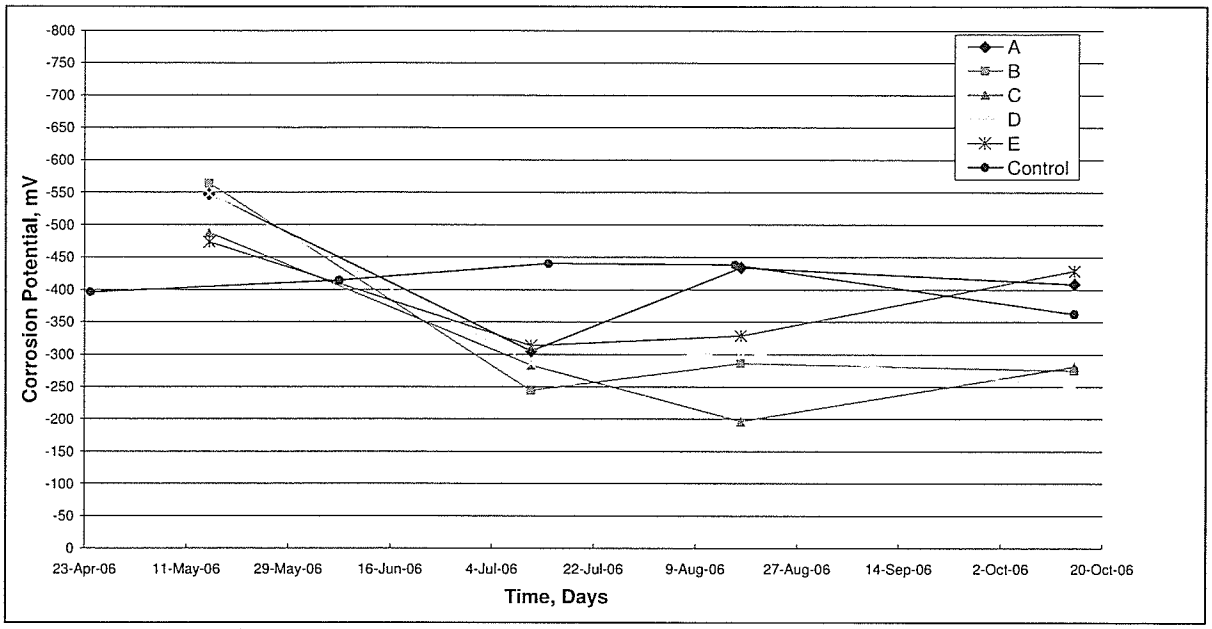

Figure 5-17: Half-cell potential of the different galvanic systems for Bar 2 subjected to 1.2% chloride by weight of cement and exposed to Winnipeg's climate

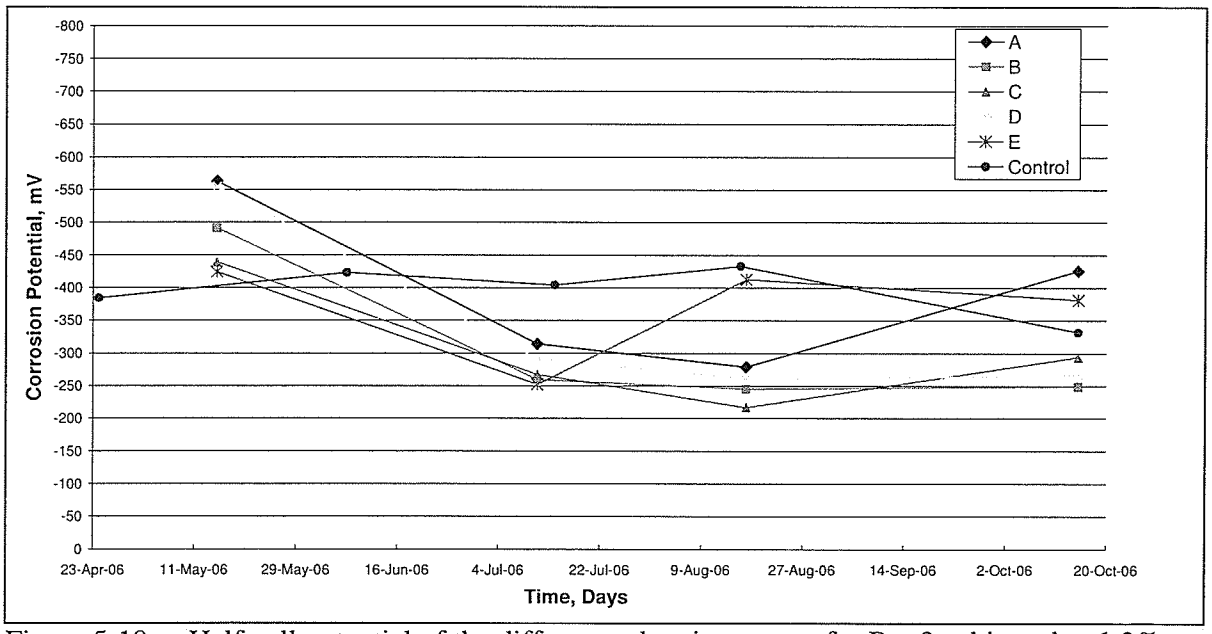

Figure 5-18: Half-cell potential of the different galvanic systems for Bar 3 subjected to 1.2% chloride by weight of cement and exposed to Winnipeg's climate

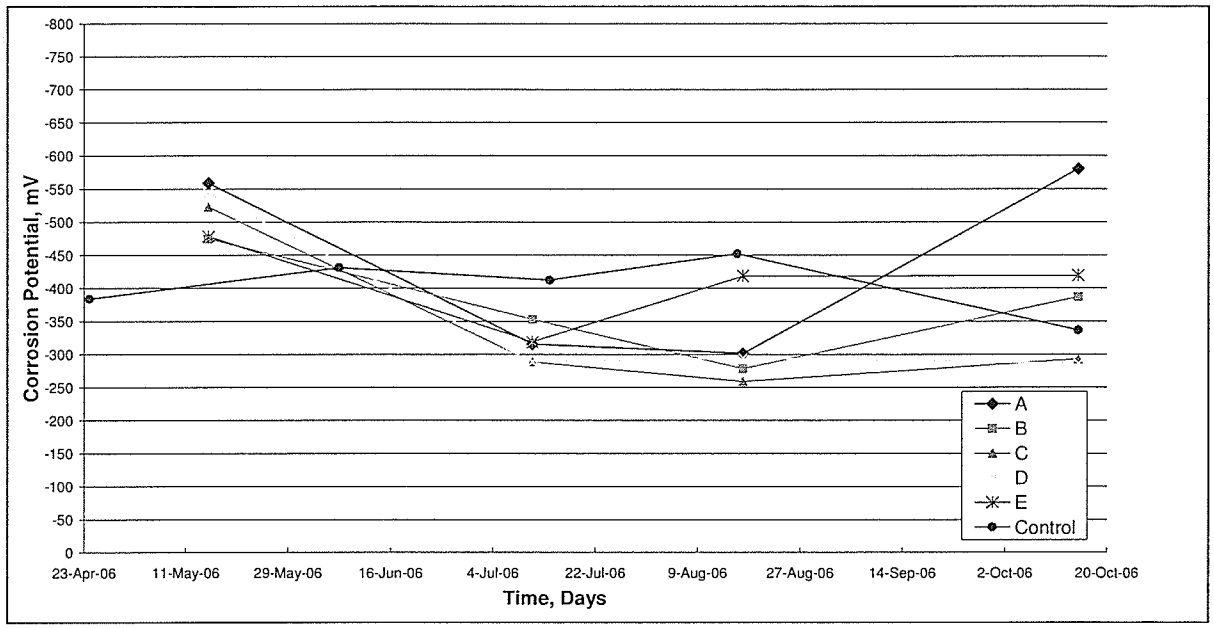

Figure 5-19: Half-cell potential of the different galvanic systems for Bar 4 subjected to 1.2% chloride by weight of cement and exposed to Winnipeg's climate

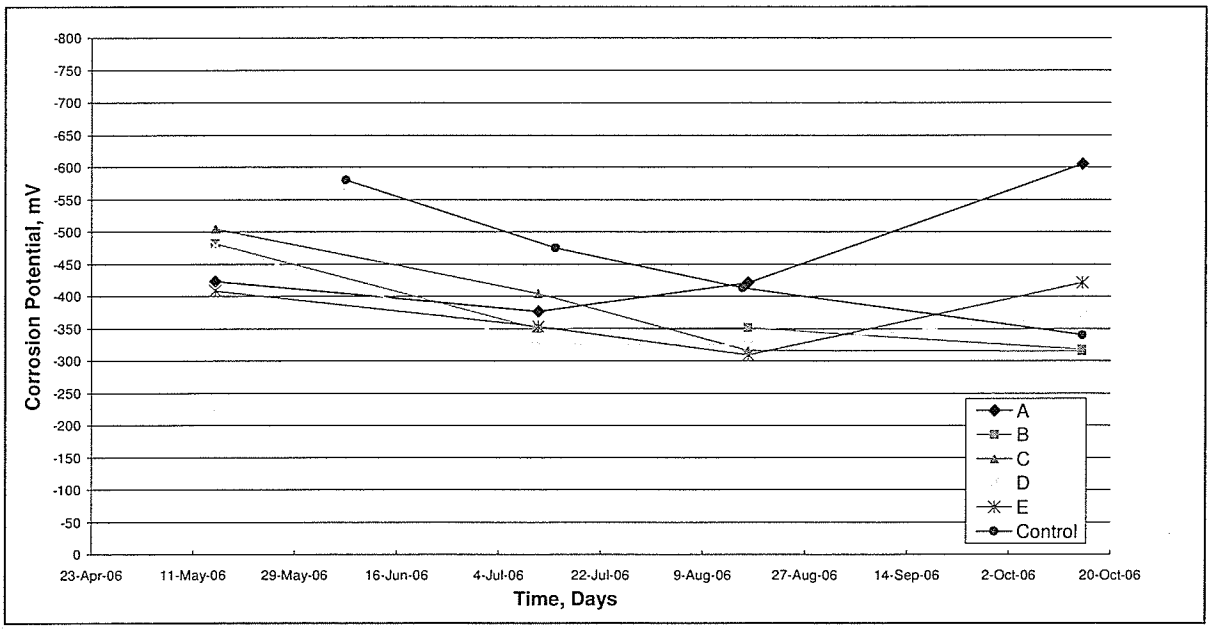

Figure 5-20: Half-cell potential of the different galvanic systems for the Mesh subjected to 1.2% chloride by weight of cement and exposed to Winnipeg's climate

Due to time constrictions and inexperience in taking initial half-cell readings, only Galvanic Systems B and C for high chloride contents and the control specimen contaminated with low

chlorides were tested first in late April 2006. The remainder of the specimens began its first round of testing in mid May 2006.

The general trends for the specimens containing galvanic systems for both cases of contaminate levels are similar. The initial half-cells reading are relatively very negative; after the activation of the galvanic anode, the open circuit potential begins shifting towards the positive direction; between early July and mid August there is a peak in potential in the positive direction; finally, the open circuit potential shifts towards the negative direction. The trend of the open circuit potential increasing positively with respect to the initial half-cell readings coincides well with the original presumptions. Prior to the initial reading, the specimens were contaminated with a designated amount of chloride and were subjected to no external current (i.e., switches were not turned "on"). After activation, the most simplistic assumption is that the open circuit potential will become increasingly positive due to the protecting current.

One major difference between the specimens housed in the environmental chamber as opposed to the specimens kept outdoors is that, unlike the chamber environment, the outdoor conditions are not constant. Temperature fluctuates outdoors on an almost hourly basis. The temperature between night and day, week-to-week, and month-to-month, all vary. Relative humidity also varies continuously, with precipitation occurring sporadically throughout the testing period months. A complete daily report of the Winnipeg's climate throughout the months under investigation is attached in Appendix B. Recalling Table 3-3, July was the hottest and driest month, averaging a mean high temperature of 29.8 C and total precipitation of 10.5 mm. Dry conditions result in an increase in concrete resistivity since the water particles used to conduct the flow of electrons across the electrolyte are scarce. Thus, corrosion activity is diminished. This explains the shift of potential in the positive direction seen in early July for almost every galvanic specimen. August on the other hand was a hot and humid month, with the average high temperature and total precipitation reaching 27 C and 52.0 mm, respectively. The end of the month of August saw the corrosion potential number of galvanic specimen shift back towards the negative direction, indicating a more aggressive environment. Other specimens had their potential continue to peak in the positive direction or simply remain the same. Basic theory would imply that, as temperature and relative humidity increase, so should the corrosion activity and thus the corrosion potential. However, as moisture increases, concrete resistivity drops; and the ability for the sacrificial anode to distribute current increases. There are several factors that may affect the overall performance of the sacrificial anode. It is also important to note that the outdoor specimens were kept in their plastic formwork to allow for natural ponding. The edge of the concrete-plastic interface was initially sealed with caulking so that ponding would only occur from the top surface of the slab. Unfortunately, the caulking deteriorated on many specimens allowing water to penetrate to the bottom of the formwork. Eventually all caulking was removed in an attempt to maintain equal conditions. Ponding in this case was still possible, but it would encase the entire slab. The plastic formwork also proved to be a nuisance in many instances because it was easily damaged. This allowed for water to drain out of some specimens whereas as others remained submerged. Repairs were attempted, but this proved to be an ongoing struggle.

Tables 5-3 and 5-4 show the average-weighted corrosion potential for the outdoor specimens containing 3.9% and 1.2% chloride by weight of cement, respectively.

Table 5-3: Average weighted corrosion potential for specimens subjected to 3.9% chlorides by weight of cement and exposed to Winnipeg's climate from the months of April to October, 2006

Galvanic system	Average - weighted corrosion potential for Bar 1, mV	Average - weighted corrosion potential for Bar 2, mV	Average - weighted corrosion potential for Bar 3, mV	Average - weighted corrosion potential for Bar 4, mV	Average - weighted corrosion potential for Mesh, mV
A	-427	-410	-437	-468	-537
B	-488	-471	-526	-551	-556
C	-488	-507	-477	-516	-565
D	-496	-500	-453	-480	-601
E	-546	-522	-521	-522	-621
Control	-611	-611	-611	-611	-630

Table 5-4: Average weighted corrosion potential for specimens subjected to 1.2% chlorides by weight of cement and exposed to Winnipeg's climate from the months of April to October, 2006

Galvanic system	Average - weighted corrosion potential for Bar 1, mV	Average - weighted corrosion potential for Bar 2, mV	Average - weighted corrosion potential for Bar 3, mV	Average - weighted corrosion potential for Bar 4, mV	Average - weighted corrosion potential for Mesh, mV
A	-415	-410	-371	-407	-443
B	-362	-323	-296	-358	-369
C	-307	-293	-288	-323	-378
D	-374	-333	-325	-337	-362
E	-405	-370	-359	-399	-363
Control	-418	-418	-418	-418	-479

Analyzing Table 5-3, the corrosion potential for each case indicates an active state with a probability of corrosion well above 90%. The control specimen subjected to high chloride levels shows an average corrosion potential of –611 mV for the bars and –630 mV for the mesh. From Table 5-3, it is clear that corrosion potential for the control is more negative than specimens. This indicates a higher probability of a more active corrosion activity within the control specimen. This is what is expected since the control specimen is not protected by any sacrificial anodes. Comparing the results from Table 5-3 to Table 5-1, the opposite trend takes place in many instances. In the environmental chamber, many specimens containing sacrificial anodes recorded a more negative corrosion potential than its control specimen counterpart. By analyzing

the half-cell potential results alone, this trend of specimens protected by sacrificial anodes recording more negative corrosion potential than the control (unprotected) specimen, is counter-intuitive. At this stage it is difficult to formulate any conclusive reason for this trend based solely on the results obtained from the half-cell tests. Further investigation based on the other results is needed to come up with an educated hypothesis.

Analyzing Table 5-4, the trends are similar to the trends seen for the outdoor specimens exposed to high chloride levels. Throughout the testing period, the average-weighted corrosion potential for the protected specimens are generally significantly more positive than the corrosion potential displayed by the corresponding control specimen. Again, this trend is opposite to the results from the specimens housed in the chamber (when active) subjected to the same chloride levels, and suggests that outdoor conditions are less aggressive. Comparing the corrosion potential between Tables 5-3 and 5-4, it is clear that Table 5-4 is the less aggressive environment. In fact, many specimens exhibit corrosion potential more positive than –350 mV. This correlates with a corrosion activity in the uncertain range, where the probability of corrosion is greater than 10% but less than 90%.

In terms of distance of bar from the anode, the trend for both Tables 5-3 and 5-4 are not always so clear. In theory, the bars located at a further distance from the anode should receive less current due to the increase in concrete resistivity. Consequently, the surrounding environment should be more aggressive at the further bars; and thus, a higher corrosion potential should be observed. This is not the case for a majority of the galvanic specimens subjected to the two levels of chloride contaminates exposed to outdoor conditions. Possible macro-cell corrosion between the mesh and the furthest bars is the most logical explanation, and this phenomenon will be discussed latter sections. Mesh corrosion potentials are generally expected to be more aggressive than the bars due to the larger surface area required to be protected. This was generally the trend in both conditions as shown in Tables 5-3 and 5-4.

5.1.3 Current Output: Environmental Chamber

The amount of current delivered to the reinforcement plays an important role in determining the level of protection offered by the galvanic system. The transfer of electrons from the higher potential sacrificial anode to the lower potential steel causes the protective current. The amount of current delivered is a function of the surrounding environment and the capacity of the sacrificial anode to deliver the current. Other factors include distance from anode and steel to anode surface area ratio. Current output was measured by connecting a multi-meter to the switch connecting the anode and reinforcement wires. Figures 5-21 to 5-24 and Figures 5-25 to 5-28 represent the current density for specimens exposed to the environmental chamber and subjected to 3.9% and 1.2% chlorides by weight of cement, respectively.

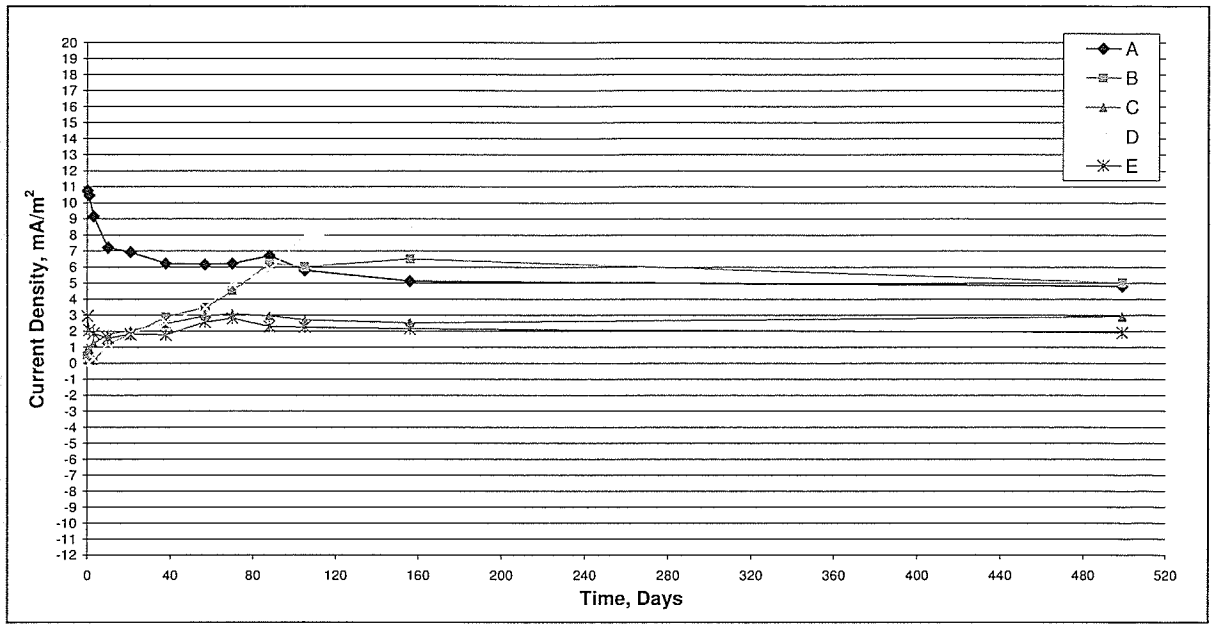

Figure 5-21: Average current density recorded for Bar 1 and Bar 2, subjected to 3.9% chloride by weight of cement and exposed to the environmental chamber

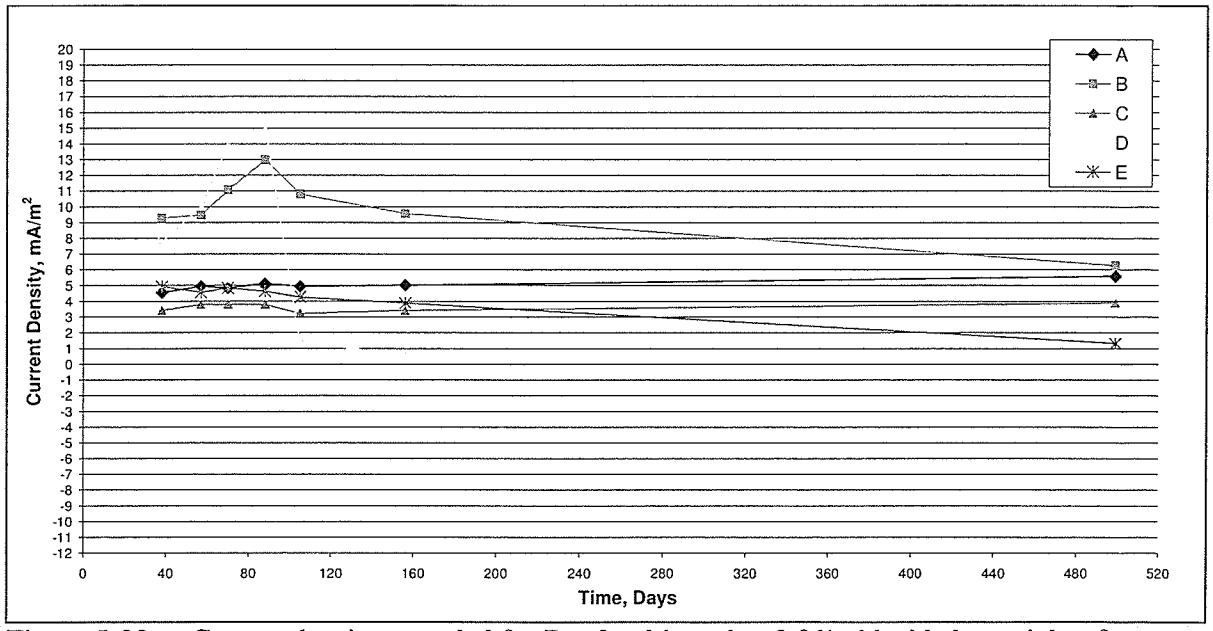

Figure 5-22: Current density recorded for Bar 3 subjected to 3.9% chloride by weight of cement and exposed to the environmental chamber

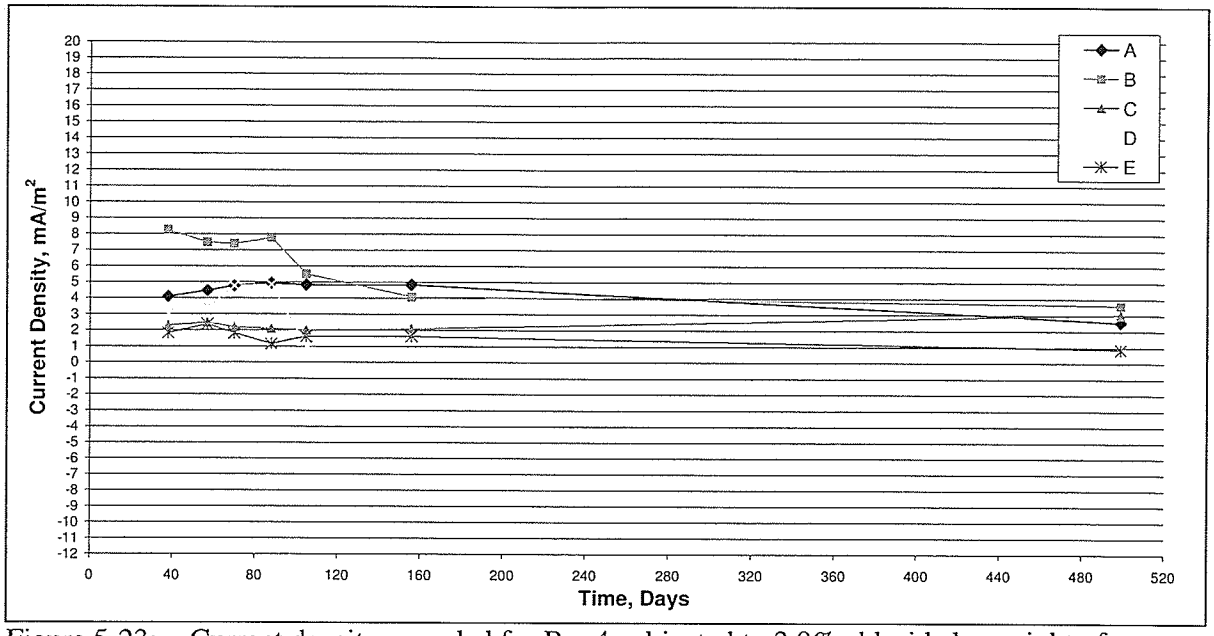

Figure 5-23: Current density recorded for Bar 4 subjected to 3.9% chloride by weight of cement and exposed to the environmental chamber

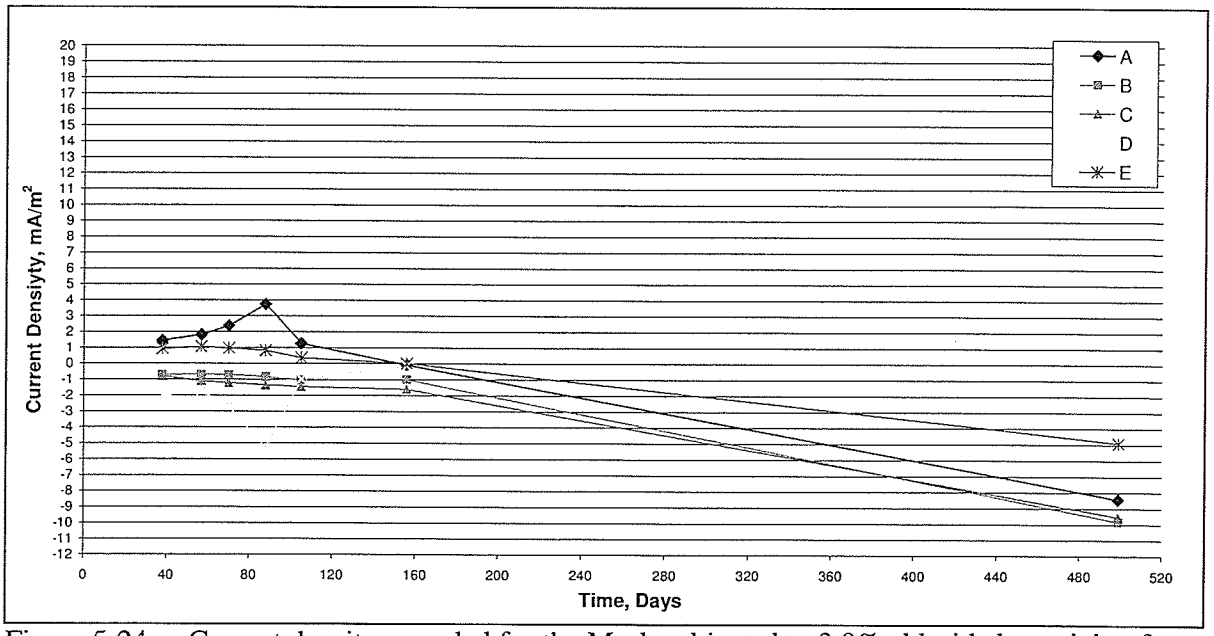

Figure 5-24: Current density recorded for the Mesh subjected to 3.9% chloride by weight of cement and exposed to the environmental chamber

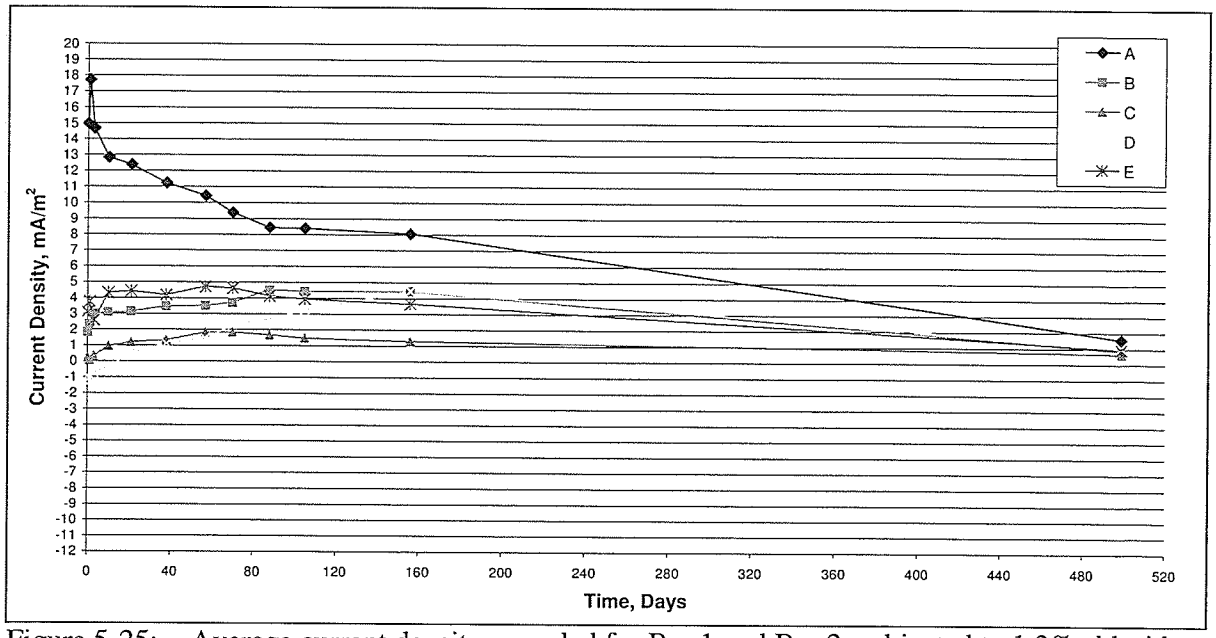

Figure 5-25: Average current density recorded for Bar 1 and Bar 2, subjected to 1.2% chloride by weight of cement and exposed to the environmental chamber

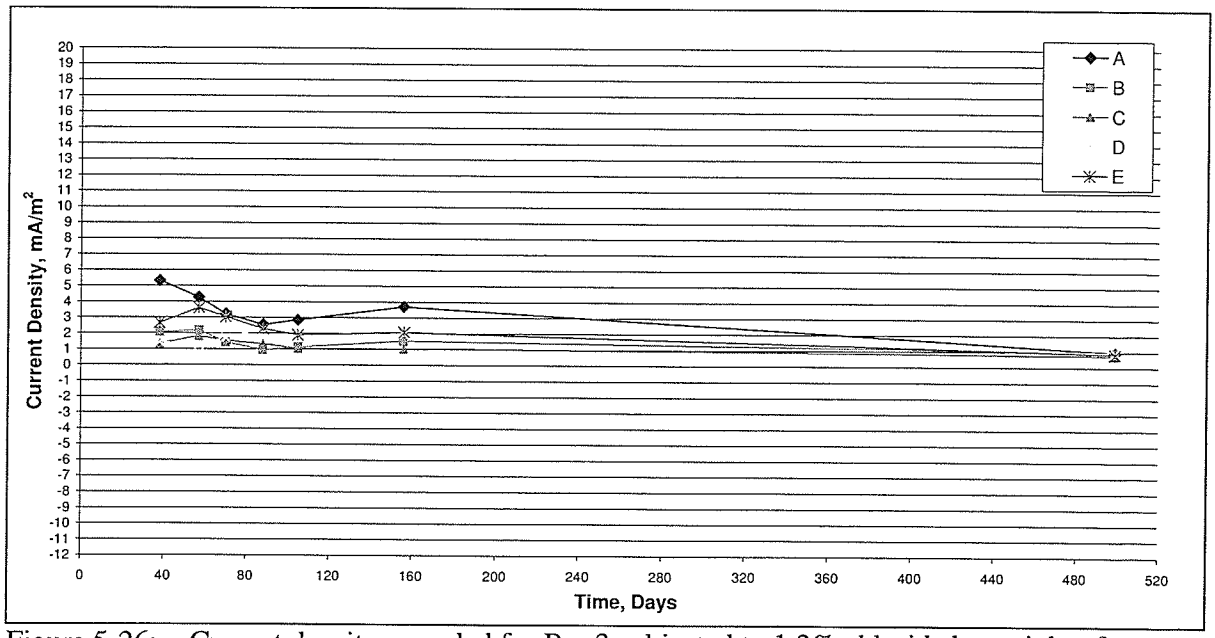

Figure 5-26: Current density recorded for Bar 3 subjected to 1.2% chloride by weight of cement and exposed to the environmental chamber

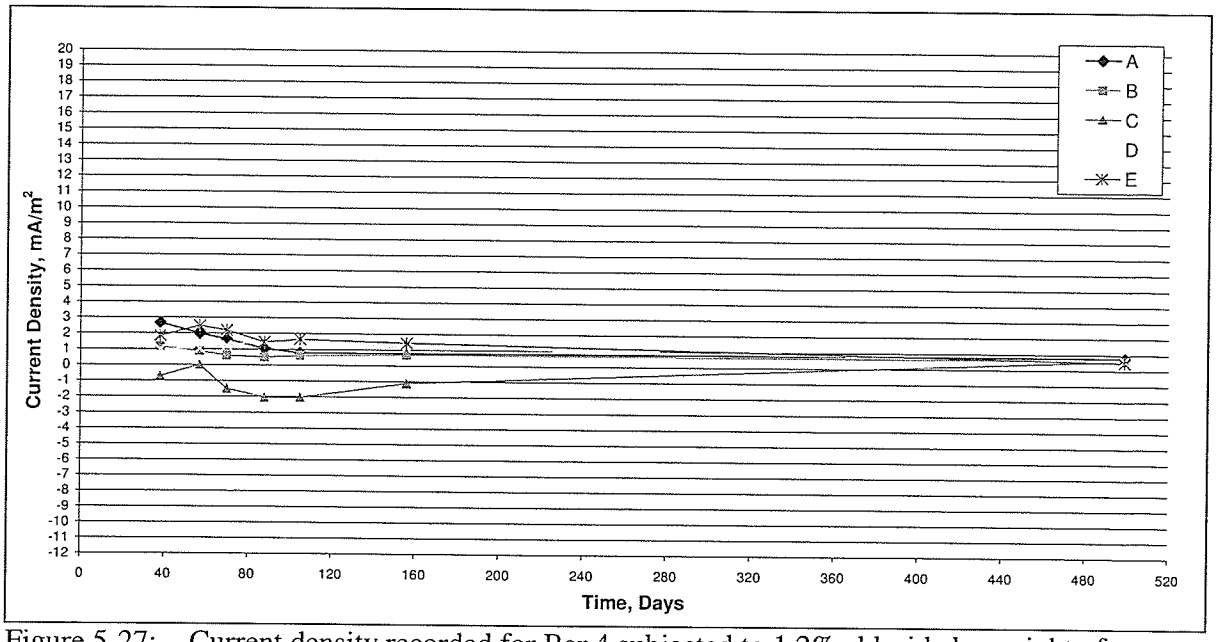

Figure 5-27: Current density recorded for Bar 4 subjected to 1.2% chloride by weight of cement and exposed to the environmental chamber

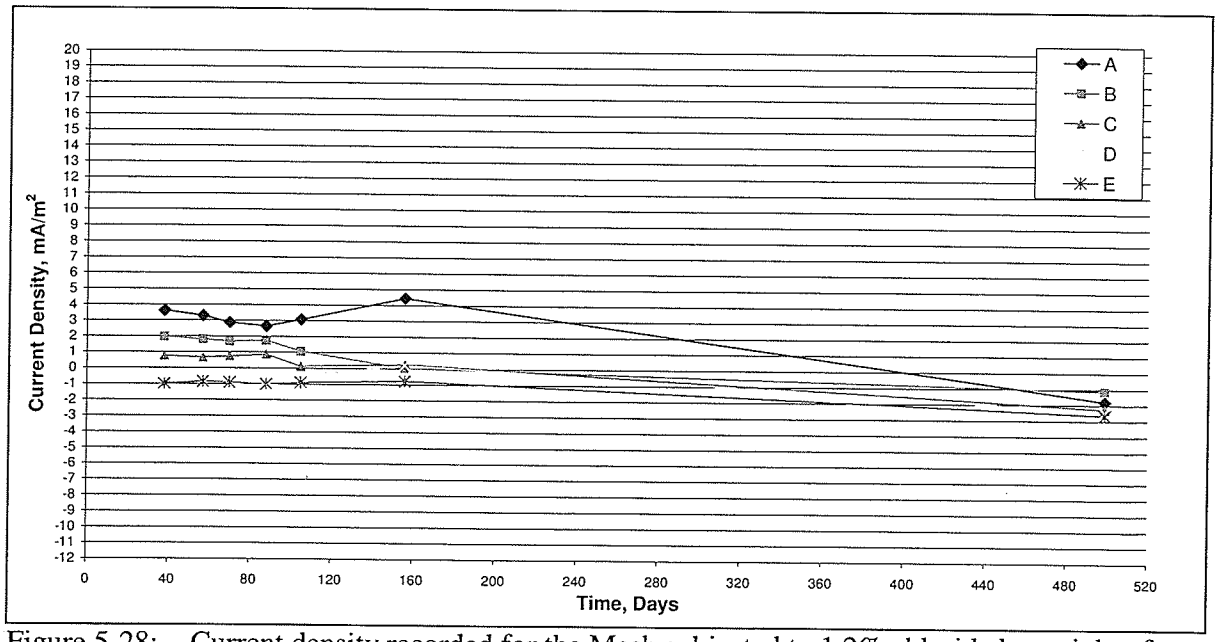

Figure 5-28: Current density recorded for the Mesh subjected to 1.2% chloride by weight of cement and exposed to the environmental chamber

The sacrificial anode was strategically placed in between Bars 1 and 2 for two reasons. The first reason, since sacrificial anodes are generally used for local protection (or prevention), an accurate

reading of the sacrificial anode's capacity to generate current at close proximity to the reinforcement was desired. The average of Bars 1 and 2 could be taken by connecting the exterior of the bars with a wire (Figure 3-1). The bars are placed at an equal distance from the sacrificial anode and so the current distribution to Bars 1 and 2 should be similar. The second reason for placing the sacrificial anode between Bars 1 and 2 is that it skewed the sacrificial anode's position to one side of the slab. This allowed current distribution to be measured to reinforcement located at a further distance (Bar 4). This helps determine the "throwing" power of each sacrificial anode.

At time zero, a surge in initial current output was generally observed. This surge was recorded instantaneously when the system was immediately activated (i.e. switch initially turned "on"), but quickly dissipated. The average initial current density readings for Bars 1 and 2 only, are recorded in Tables 5-5 and 5-6 for the specimens exposed to 3.9% and 1.2% chlorides by weight of cement, respectively. For reasons yet to be discussed, data recorded prior to day 38 for Bars 3, 4 and mesh were not accurate and thus will not be presented. The initial current readings for Bars 1 and 2 were also not included in the Figures 5-21 to 5-28, due to scaling issues. The first reading in Figures 5-21 to 5-28 was taken at 4 hours after the system was activated. The final current output reading taken while the environmental chamber was still functional was recorded at 156 days. The chamber was turned "off" shortly thereafter. A long-term current output reading was taken 499 days after the initial current reading.

Current data prior to day 38 were taken with the assumption that each switch individually controlled the flow of current to its respective bar or mesh. Prior to day 38, the testing sequence was as follows: a multimeter was connected to Switch A (Figure 3-1); the switch was then turned "off", and the current output was recorded. The multimeter was then connected to Switch B; the switch was turned "off", and the current output was recorded. The measurements continued until all readings were taken and then all the switches were turned back "on", until the next set of readings at a later date. This methodology proved to be incorrect since the system is actually a parallel circuit connected by the sacrificial anode; and thereby interrupting the current flow to a particular bar or mesh shifted the current distribution to the remaining connected reinforcements. The first readings taken from Switch A, was not affected because all other circuits were uninterrupted at the time of recording, since Switch A was always the first to be measured. However, as the readings continued on the adjacent switches, current was interrupted since Switch A and possibly other switches were turned "off", depending on which reading was being taken. The testing methodology was corrected immediately upon realization of this problem. The correct methodology is simply to perform the readings one at a time (i.e., connected the multimeter to one particular switch, turn the switch "off", record the output, turn the switch back "on", and move on to the next switch). This ensures that the readings are representative of the current distribution when the system is uninterrupted. Unfortunately, this error proved to be costly in collecting data for the "throwing" power of the sacrificial anodes, in particular affecting the results of the outdoor specimens, as will be discussed later.

Table 5-5: Average initial current density for Bars 1 and 2 subjected to 3.9% chlorides by weight of cement and exposed to environmental chamber conditions

Sacrificial anode	Average initial current density at time zero for bars 1 and 2, mA/m^2
A	50.0
B	12.3
C	47.4
D	1.1
E	46.3

Table 5-6: Average initial current density for Bars 1 and 2 subjected to 1.2% chlorides by weight of cement and exposed to environmental chamber conditions

Sacrificial anode	Average initial current density at time zero for bars 1 and 2, mA/m^2
A	38.9
B	10.7
C	1.3
D	0.2
E	6.25

Prior to activation of the switch, corrosion is free to initiate, with the transfer of electrons occurring from a more negative potential region to a less negative potential region. A very intense, but short burst of current output is generally observed upon activation of the switch (i.e., switch turned "on"). The cause of the burst is primarily due to the difference in potential, which is the driving force of the current. The initial surge in current can be viewed as water building behind a dam that suddenly bursts. The initial surge of water will be very intense. The result would be a sudden surge of water, like a title wave, which would quickly dissipate once it has passed. Afterwards a steady flow of water would flow dictated by the difference in normal water levels upstream and downstream of the dam. However, there are a lot more factors influencing the flow of current in the case of a sacrificial anode system embedded in concrete. One major factor influencing the sacrificial anode's driving force is the presence and properties of the encapsulating mortar, which encases the galvanic metal. This mortar is often used in sacrificial anode designs and is generally composed of a lithanium-based compound. The mortar helps to activate the sacrificial anode and encourages greater, and longer current output. Depending on the mix and design, the mortars can help activate the sacrificial anode and it can generate greater and longer current output. Details regarding the science behind the mortar are not part of the scope of this report.

As shown in Tables 5-5 and 5-6, the initial surge of current density is quite high for certain sacrificial anodes. However, this was not the case throughout. Explanations for this may vary from extremely high resistance between the sacrificial anode and the bar to an initial weak-

driving force due the nature of the sacrificial anode. Another possibility may be due to human error. The initial surge occurs literally instantaneously and the result is merely flashed on the screen of the multi-meter. Unfortunately, only one chance exists to record the initial current surge. On average, the surge was more intense for the specimens containing high chloride levels, as expected. This reflects a greater need for protection of these highly contaminated specimens. In theory, chloride lowers the level of resistivity of concrete, thus permitting an increased flow of current.

Analyzing Figures 5-21 to 5-28, the general trend shows the majority of the current is distributed to the nearest bars. This coincides well with the theoretical analysis, which states current distribution is a function of concrete resistance. Therefore, in general the closest bars should receive the most current and greater protection. This was not always the case, as shown when considering specimens subjected to high levels of chlorides. In the case of Bar 3 for high chloride levels, sacrificial anodes B, C, D, and E all recorded current densities greater than Bar 1 for a sustained period of time. In each case except for specimen E, this was also accompanied by negative current densities recorded at the mesh, as shown in Figure 5-24. This hints at a possible corrosion macro-cell developed between the mesh and Bar 3. The positive and negative symbols in front of the current densities are a conventional sign used to represent the direction of flow. In this context, a positive sign indicates the current is flowing towards the bars or mesh. A negative sign indicates the current is flowing away from the bars or mesh. It is hard to conceive that the current can flow in the opposite direction, but it may be possible if the difference in potential between neighboring bars (or the mesh) becomes so extreme that it overcomes the sacrificial anode's tendency to polarize the steel. This can occur despite of the fact that the sacrificial anode continues to provide current to the bar (or the mesh). Recall, that corrosion rate is proportionally related to the difference in potential (driving force) and inversely related to the surrounding resistivity. Therefore, if the potential difference between two adjacent locations (i.e. bar and the mesh) is sufficiently high, electron transfer may be easier to accomplish due to the low resistance. Although the difference in potential between the sacrificial anode and the steel will almost certainly be higher, the further the steel is to the sacrificial anode, the greater the resistance becomes. If the amount of electrons lost by the steel to a neighboring bar (or the mesh) is greater than the amount of electrons received by the steel from the sacrificial anode, than the net current will be negative. It is important to realize that the corrosion potential and corrosion rates may be different at different locations on the same bar or the mesh. Therefore, it is plausible that certain regions on a bar or mesh are actively receiving electrons, whilst other regions may be corroding. This is the most likely explanation for the negative current densities observed for the mesh for Specimens B, C, and D. If the net current is traveling away from the mesh, this signifies the mesh is losing electrons and in essence the mesh has become an anode. Likewise, this entails that a region of more positive potential must be accepting electrons from the mesh (i.e, a cathode). Since current follows the path of least resistance, the cathode will most likely be in a location near an extreme corrosion cell on the mesh. In all likelihood, the grand majority of these areas of extreme corrosion cells will most likely develop at locations further from the sacrificial anode; reason being, the further away from the sacrificial anode the least amount of protection against corrosion there should be. Therefore, it is very plausible that the electrons from the mesh are being delivered to Bars 3 and 4.

In other words a macro-cell may have developed feeding additional current into these bars. This theory goes well with the result obtained in Table 5-1. The open-circuit potential of the mesh for specimens B, C, and D are all more negative than the corresponding potential for Bar 3, signifying an increased likelihood of corrosion activity in the mesh. It is also interesting to note that the drop in current flow to Bar 3 for Specimen D subjected to high chlorides at time 105 days (Figure 5-22) correlates with a positive jump in current delivered to the mesh (Figure 5-24). Unfortunately, due to extreme corrosion activity on the external wire connecting the anode to the remainder of the bars, testing of the sacrificial System D was not possible at the time of long-term testing (499 days after switch activation).

The general trend for long term testing did not see any great change in current density. For the most part, current density seemed to level off or slightly decrease or slightly increase in intensity. According to basic theory, as current is continuously delivered to the reinforcement, corrosion activity should be minimized and the conditions around the reinforcement should be less aggressive. For example, chlorides should be retracted and the protective film should be re-generated, causing an increase in resistivity. This in turn should lead to a reduction in current density being delivered by the sacrificial anode. In this case, the environmental chamber was turned off shortly after day 156 after initial activation; and therefore, it is expected current distribution would be further reduced, since the demand for current would become less due to improved environment.

In the case of the mesh, all specimens in both chloride level conditions recorded negative current density in the long-term test taken at day 499 (Figure 5-24 and 5-28). These negative currents indicate the net flow of electrons to the mesh is traveling away from the mesh. As discussed previously, this indicates corrosion activity occurring in the mesh, which leads to macro-cell corrosion between the mesh and the other bars. This may explain the slight increase in current density seen for some bars at the time 499 days, despite contradictory common theory.

When comparing the results of the different sacrificial systems by means of a graph, it can often become very difficult to accurately determine the dominant system. This is because of the continuous overlapping in the results. To get a better picture of the performance of the different sacrificial anodes, the average-weighted current density was calculated and presented in tabular form. This enabled the results to be analyzed by a single value representing the average current density generated by each sacrificial anode for a given time frame. The average-weighted current density was calculated for the time period during which the chamber was activated (i.e. initial reading to time day 156). By analyzing the results in tabular form, a simple rating system was also implemented to facilitate the comparison of the performance of the different sacrificial anode systems. The rating of each sacrificial anode is based on a point system, where the maximum amount of points is given to the sacrificial anode that delivers the maximum current density for the particular condition being investigated. For example, the systems with the greatest current density would receive 5 points; the second highest current density would receive 4 points, and so on. By tallying the score for each case, a clear comparison on the overall performance of the different sacrificial anodes can be made. In other words, the sacrificial anode that continuously delivered the highest average-weighted current density for the different conditions would receive the most points and therefore be ranked the better system. Visa versa,

the sacrificial anode that continuously produced the lowest average-weighted current density, would receive the least points and therefore would be deemed the least effective system. The average-weighted current density for high and low chlorides exposed to environmental chamber conditions are presented in Tables 5-7 and 5-8.

Table 5-7: Average-weighted current density subjected to 3.9% chlorides by weight of cement and exposed to 35 C and 95% relative humidity for 156 days

Sacrificial anode system	Average – weighted current density for Bars 1 and 2, mA/m^2		Average – weighted current density for Bar 3, mA/m^2		Average – weighted current density for Bar 4, mA/m^2		Average – weighted current density for Mesh, mA/m^2		Total score, points
A	6.24	V	4.93	III	4.72	IV	1.57	V	17
B	4.44	III	10.59	V	6.26	V	-0.90	III	16
C	2.55	II	3.51	II	2.14	II	-1.35	II	8
D	5.14	IV	6.57	IV	2.46	III	-1.85	I	12
E	2.16	I	4.40	I	1.68	I	0.57	IV	7

Rating system: V – 5 pts; IV – 4 pts; III – 3 pts; II – 2 pts; I – 1 pt

Table 5-8: Average-weighted current density subjected to 1.2% chlorides by weight of cement and exposed to 35 C and 95% relative humidity for 156 days

Sacrificial anode system	Average – weighted current density for Bars 1 and 2, mA/m^2		Average – weighted current density for Bar 3, mA/m^2		Average – weighted current density for Bar 4, mA/m^2		Average – weighted current density for Mesh, mA/m^2		Total score, points
A	9.87	V	3.42	V	1.23	III	3.34	V	18
B	3.38	III	1.45	II	0.66	II	1.19	IV	11
C	1.41	I	1.27	I	-1.42	I	0.46	III	6
D	2.21	II	1.95	III	1.26	IV	-0.59	II	11
E	4.10	IV	2.43	IV	1.75	V	-0.90	I	14

Rating system: V – 5 pts; IV – 4 pts; III – 3 pts; II – 2 pts; I – 1 pt

Comparing the results, Sacrificial Anode System A received the highest score under both levels of chloride contamination when exposed to the environmental chamber conditions. Sacrificial Anode System A was also the only system to achieve a positive average-weighted current density for each reinforcement subjected to both levels of chlorides. Various systems recorded negative average-weighted current densities in particular for the mesh. As discussed previously, this is most likely due to a corrosion macro-cell where the mesh releases electrons, and leads to a surplus in current to the neighboring bars. This explains why Systems B, C, and D subjected to high chloride levels experienced higher average-weighted current densities to Bar 3 instead of the

expected Bars 1 and 2. This occurred despite the fact that Bar 3 is located further from the sacrificial anode; and thus should have a greater resistance, which in turn should lead to less current distribution. The results obtained under low chloride conditions follow closely the expected trend that shows a greater current distribution to nearer bars. The chloride levels mixed with the aggressive environment offered by the chamber and the vast area of the mesh, may have caused unforeseen factors such as the development of macro-cells which produced some unexpected results.

Analyzing Table 5-7, in the case of Bar 1 and Bar 2, the range of average-weighted current density varied from 2.16 to 6.24 mA/m^2 for the different sacrificial systems. According to previous research, corrosion control protection occurs between 1 to 7 mA/m^2 and cathodic protection occurs between 2 to 20 mA/m^2. Therefore, the average-weighted current density recorded in Table 5-7 falls in the level of protection of corrosion control or the lower scale of cathodic protection. The most probable level of protection is corrosion control, which signifies that the corrosion rate is slowed but not stopped. It is difficult to determine the exact level of protection the sacrificial anodes were able to obtain without analyzing the potential decay results. However, the data does indicates the relative "strength" or intensity the sacrificial anodes were able to generate under the given conditions. It is clear however that the average-weighted current density is well above the level of protection given by corrosion prevention. The different levels of protection and the associated range of current densities are given in Table 3-6. Sacrificial anodes are generally used for corrosion prevention or small-scale corrosion control. The only case to clearly register cathodic protection status under high chloride levels according to current density criteria is the Sacrificial Anode System B, which recorded an average-weighted current density of 10.59 mA/m^2 for Bar 3. This is most likely associated with a corrosion macro-cell formation located near Bar 3 as previously discussed, and therefore is misleading.

The lower level chloride contamination specimens behaved more like to the anticipated trends. In all instances, the bars closer to the anode received a higher current distribution than the bars located at further distances. The highest recorded average-weighted current density was recorded for Bar 1 and 2, with a current density of 9.87 mA/m^2 associated with Sacrificial Anode A, as shown in Table 5-8. This was the only current density to clearly fall in the range of cathodic protection. All the other systems generally fell in the lower range of corrosion control.

5.1.4 Current Output: Winnipeg Climate

Specimens left outdoors were exposed to Winnipeg's outdoor conditions throughout the months of April to October. A complete resume of the outdoor conditions can be found in Section 3.4. Figures 5-29 to 5-32 and Figures 5-33 to 5-36 give the current densities recorded by the different specimens throughout the test period, for high chloride and low chloride levels, respectively.

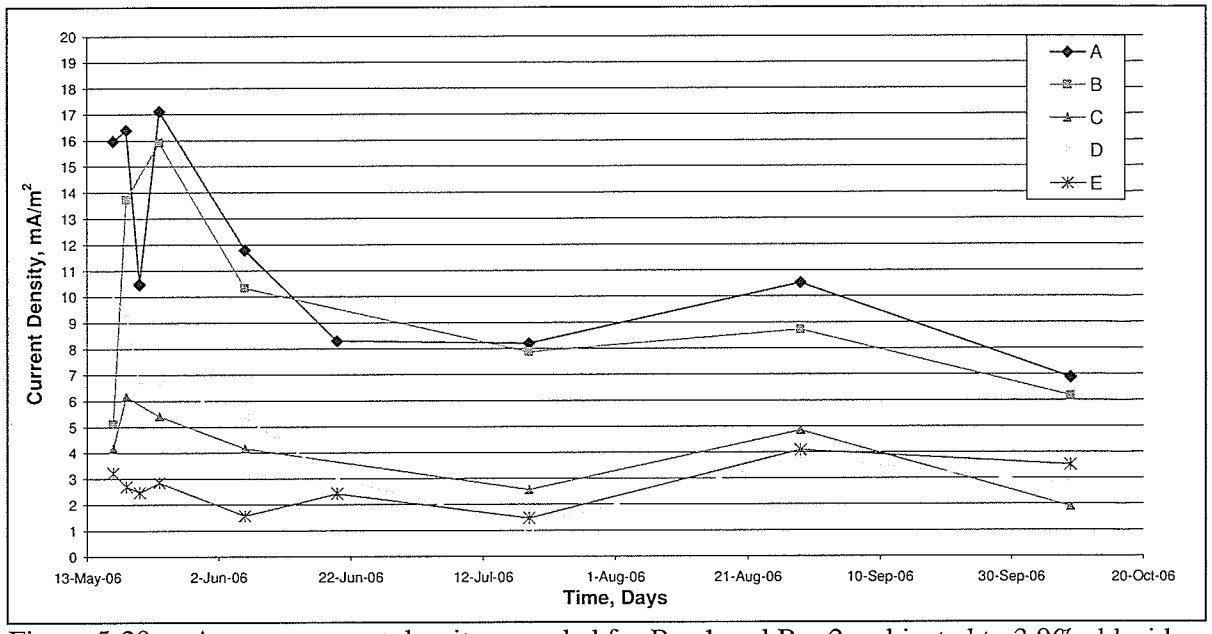

Figure 5-29: Average current density recorded for Bar 1 and Bar 2, subjected to 3.9% chloride by weight of cement and exposed to Winnipeg's climate

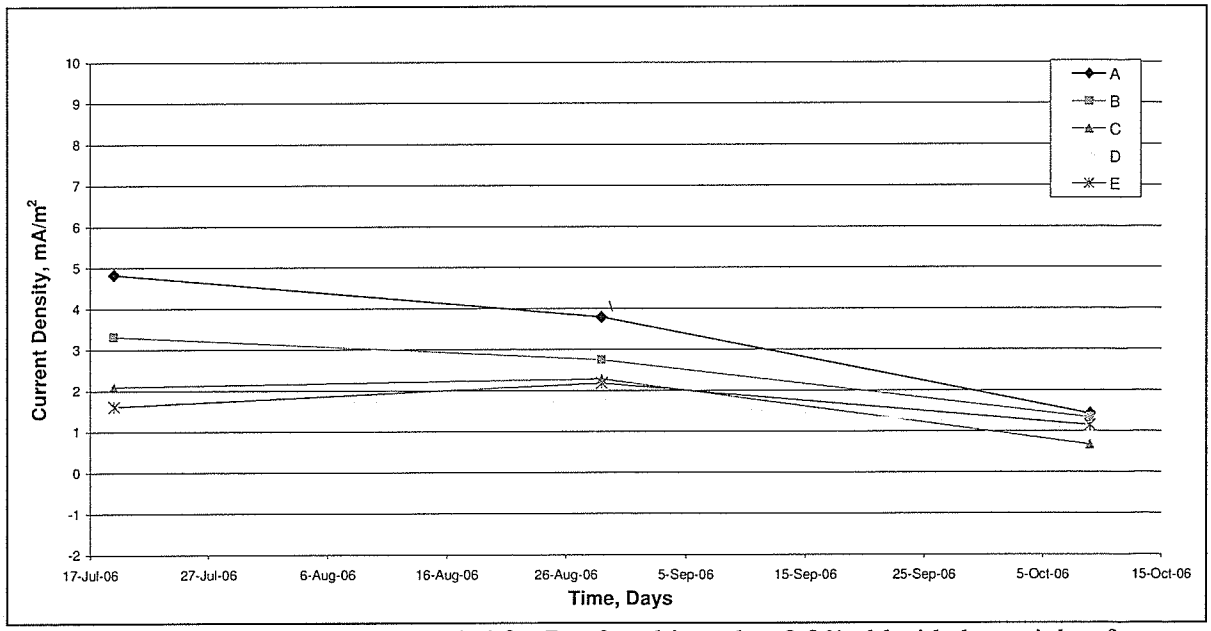

Figure 5-30: Current density recorded for Bar 3, subjected to 3.9% chloride by weight of cement and exposed to Winnipeg's climate

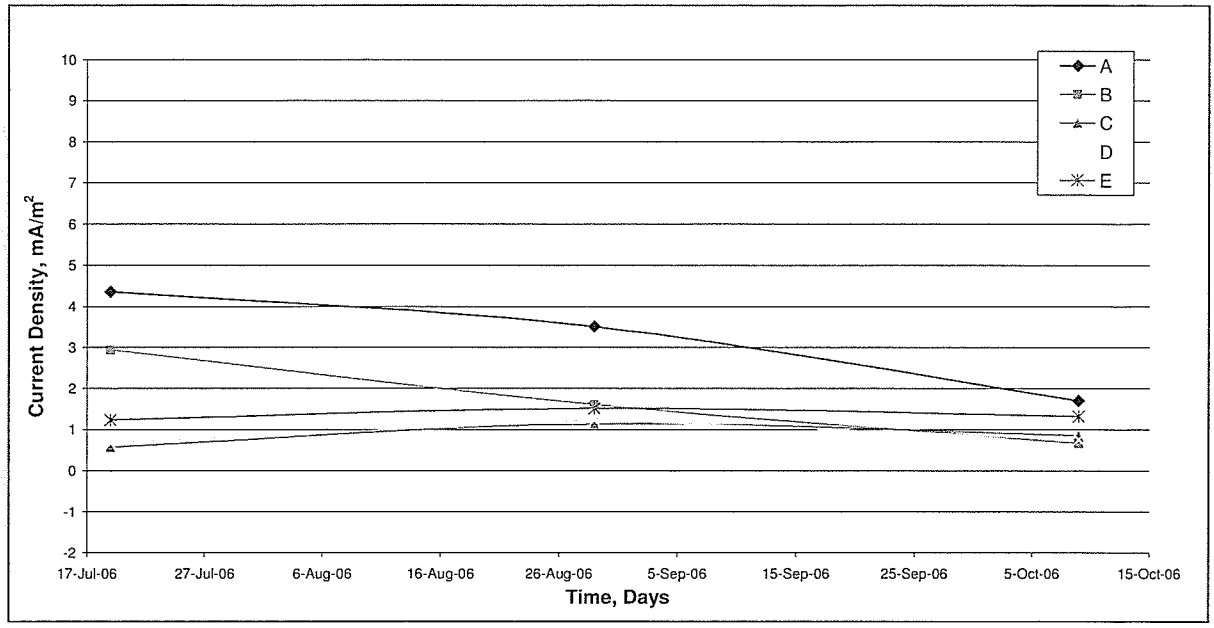

Figure 5-31: Current density recorded for Bar 4, subjected to 3.9% chloride by weight of cement and exposed to Winnipeg's climate

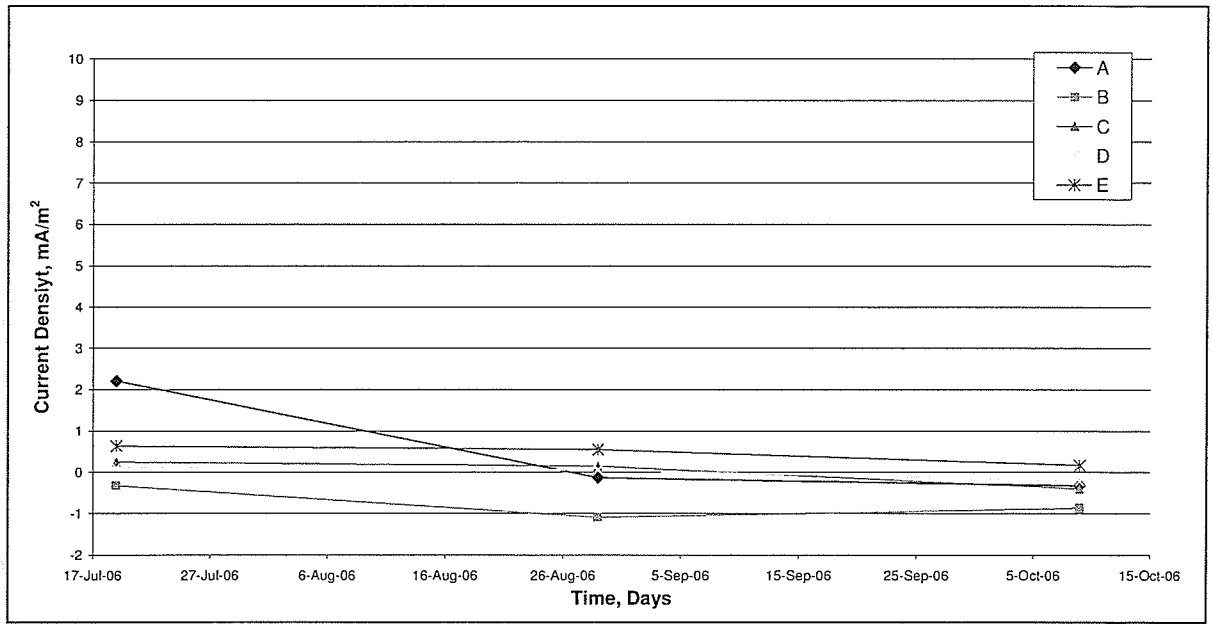

Figure 5-32: Current density recorded for the Mesh, subjected to 3.9% chloride by weight of cement and exposed to Winnipeg's climate

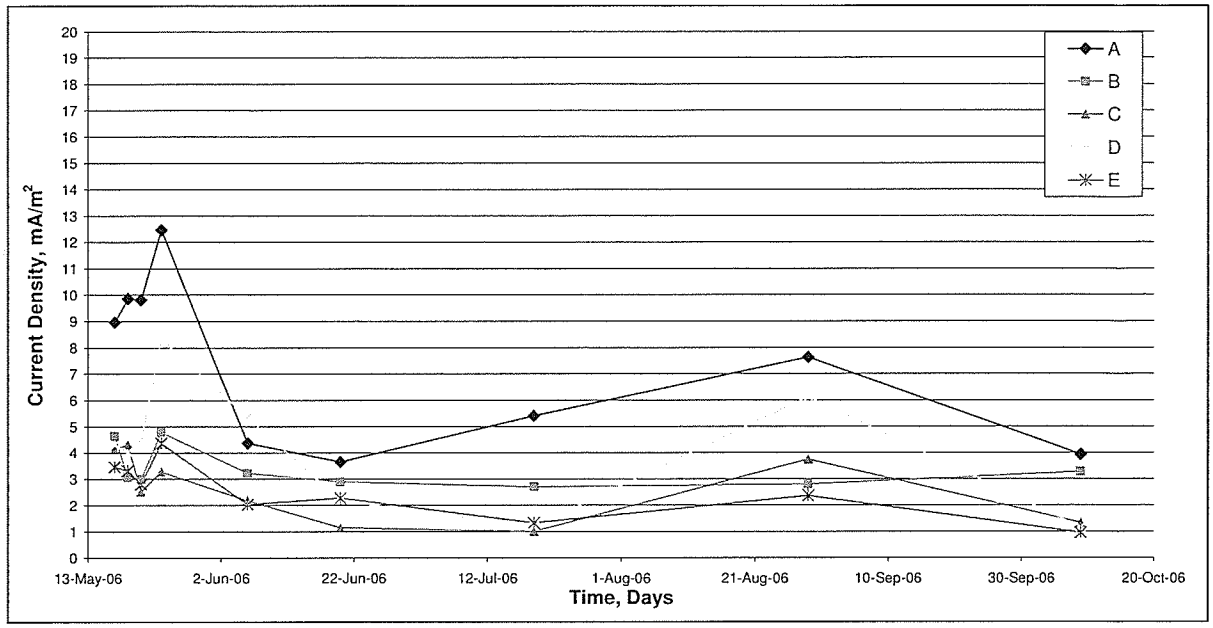

Figure 5-33: Average current density recorded for Bar 1 and Bar 2, subjected to 1.2% chloride by weight of cement and exposed to Winnipeg's climate

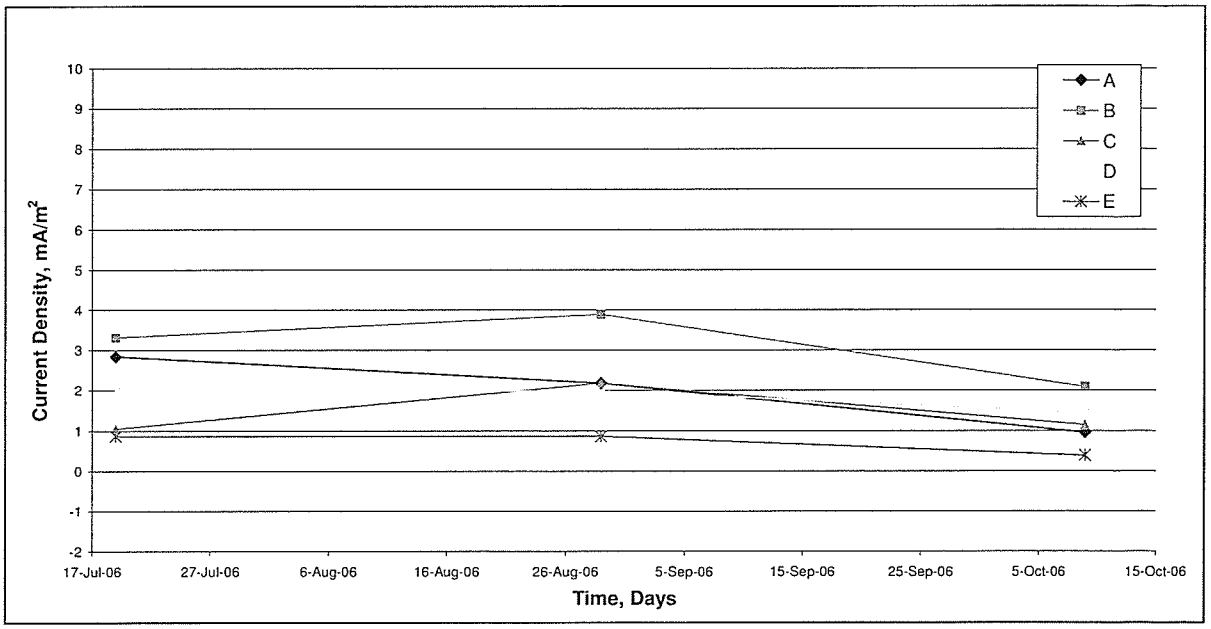

Figure 5-34: Current density recorded for Bar 3, subjected to 1.2% chloride by weight of cement and exposed to Winnipeg's climate

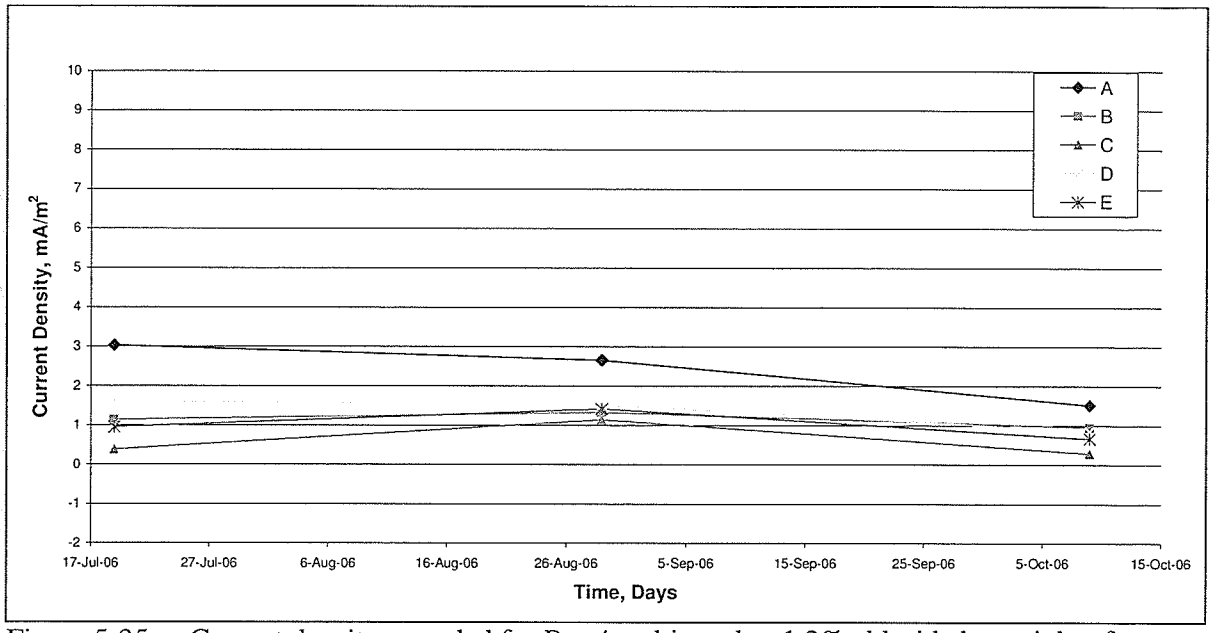

Figure 5-35: Current density recorded for Bar 4, subjected to 1.2% chloride by weight of cement and exposed to Winnipeg's climate

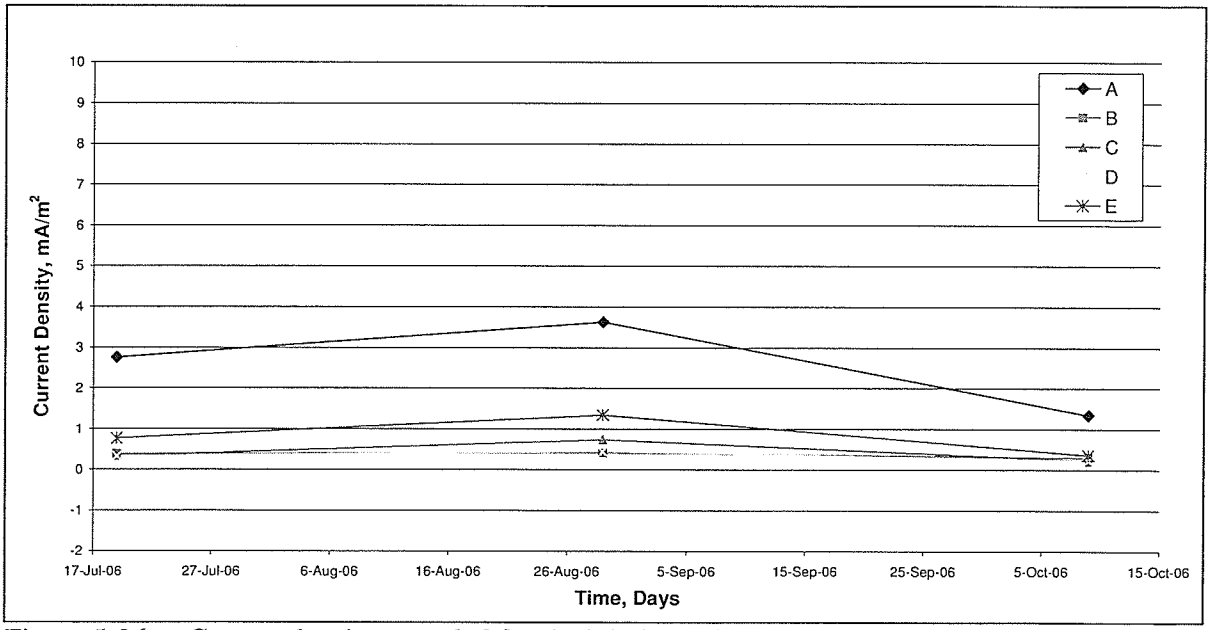

Figure 5-36: Current density recorded for the Mesh, subjected to 1.2% chloride by weight of cement and exposed to Winnipeg's climate

The first readings taken in Figures 5-29 and 5-33 provide the average current density recorded one day after initial activation of the system. The initial surge in current output recorded at time

zero was not plotted in Figures 5-29 and 5-33, due to its great magnitude in comparison with current densities recorded at other dates. By implementing the initial current reading at time zero, it would have been difficult to read the remaining data due to scaling constraints. Therefore, the initial current density reading at time zero for specimens subjected to 3.9% chlorides and 1.2% chlorides and exposed to Winnipeg summer climate are tabulated in the Appendix C, in Tables C-1 and C-2, respectively. Unfortunately, data recorded prior to mid-July for current density relating to Bars 3, 4 and the mesh were conducted improperly and as a result were not presented in the above figures. The reason for this improper testing methodology was discussed in the previous section and is due to involuntarily diverting current readings after turning off the switches during testing.

Analyzing Figure 5-29, it is clear that both Sacrificial Anodes A and B clearly outperformed the remaining sacrificial anodes in terms of current density distributed to Bars 1 and 2. Sacrificial Anodes C, D, and E, all distributed approximately the same current output to Bars 1 and 2 throughout the testing period. Despite the difference in current density magnitude when comparing the performance of each sacrificial anode, a clear trend can be observed when analyzing the current output with time. The first few readings are typically high in magnitude and then drop to lower levels during the month of July. In all cases, current output increases in the month of August, peaking at the reading taken at the end of the month. Current output then decreases once again, as is evident in the final readings taken in October. These fluctuations in current output are directly effected by the continuously changing climate. Unlike the specimens housed in the environmental chambers, which were subjected to constant high temperature and high humidity, the specimens housed outdoors were subjected to changing climate on an almost daily basis. If current data was taken daily, Figure 5-29 would still follow the same trend but there would be much more 'noise' in the data. Despite the changing climate on a daily basis, the climate still follows the traditional patterns historically experienced in Winnipeg's summer months. The sacrificial anode systems were first activated in late April and the beginning of May. Since the specimens were cast 8-months prior with the designated levels of chlorides mixed in with the constituents, corrosion activity was most likely already initiated. As a result, the initial current upon activating the sacrificial systems was high. In addition to the initial surge of current, the months of May and June are generally warm and humid. This climate provides favorable conditions for corrosion activity; and thus, it is expected the sacrificial anodes would generate a high volume of current output. July is traditionally hot and dry, leading to high resistivity in the concrete and therefore low corrosion activity. Low sacrificial current output, as shown in Figure 5-29, are associated with hot and dry conditions. The relatively hot temperatures combined with the high precipitation levels experienced in August is favorable once again for an extremely corrosive environment, and thus greater sacrificial current output is generated.

For comparison purposes, the average-weighted current densities for the different sacrificial systems were tabulated. Using the same rating system as Section 5.1.3. comparisons are facilitated. Tables 5-9 and 5-10 show the average-weighted current densities for the sacrificial systems exposed to an outdoor climate and subjected to 3.9% and 1.2% chlorides per weight of cement, respectively.

Table 5-9: Average-weighted current density subjected to 3.9% chlorides by weight of cement and exposed to Winnipeg's climate

Sacrificial anode system	Average – weighted current density for Bars 1 and 2, mA/m^2		Average – weighted current density for Bar 3, mA/m^2		Average – weighted current density for Bar 4, mA/m^2		Average – weighted current density for Mesh, mA/m^2		Total score, points
A	9.71	V	3.46	V	3.27	V	0.40	IV	19
B	8.96	IV	2.53	IV	1.71	IV	-0.84	I	13
C	3.69	III	1.82	III	0.92	I	0.03	III	10
D	3.35	II	1.54	I	0.97	II	0.00	II	7
E	2.76	I	1.78	II	1.40	III	0.47	V	11

Rating system: V – 5 pts; IV – 4 pts; III – 3 pts; II – 2 pts; I – 1 pt

Table 5-10: Average-weighted current density subjected to 1.2% chlorides by weight of cement and exposed to Winnipeg's climate

Sacrificial anode system	Average – weighted current density for Bars 1 and 2, mA/m^2		Average – weighted current density for Bar 3, mA/m^2		Average – weighted current density for Bar 4, mA/m^2		Average – weighted current density for Mesh, mA/m^2		Total score, points
A	6.02	V	2.04	IV	2.46	V	2.83	V	19
B	3.02	III	3.29	V	1.18	III	0.37	II	13
C	2.17	II	1.63	II	0.73	I	0.50	III	8
D	3.62	IV	1.85	III	1.37	IV	0.35	I	12
E	2.01	I	0.73	I	1.11	II	0.95	IV	8

Rating system: V – 5 pts; IV – 4 pts; III – 3 pts; II – 2 pts; I – 1 pt

Analyzing Table 5-9, the new Sacrificial Anode System A nearly tripled all of the other sacrificial systems except for sacrificial system B, in terms of average current output delivered to Bar 1 and Bar 2. Sacrificial Anode A performed similarly in Table 5-10 when analyzing the average current output to Bar 1 and Bar 2. The fact that the new System A was able to generate so much current should in theory translate into more protection for Bars 1 and 2, under the same conditions. In fact, the average current density of 9.71 mA/m^2 delivered to Bars 1 and 2 subjected to high chlorides (Table 5-9), indicates cathodic protection has been reached in these bars. In Table 5-10, the average current density of 6.02 mA/m^2 for the same bars indicates either corrosion control or cathodic protection has been achieved. Recalling from Table 3-6, corrosion control protection occurs between the range of 1 to 7 mA/m^2, whereas cathodic protection falls within the range of 2 to 20 mA/m^2. It is not as straight forward as stating cathodic protection has or has not been reached simply because the current density is 6.02 mA/m^2. Remember, cathodic

protection is considered to occur only if the steel is polarized at least 100 mV. The amount of current required for this will ultimately depend on the conditions surrounding the steel in question. The amount of current generated specifically by Sacrificial Anode A would definitely be beneficial in a real-life application. Implemented in a new patch repair, the Sacrificial System A would certainly prevent any further corrosion activity on nearby reinforcement spaced directly adjacent to the new repair. If used in an already corroding structure, reinforcement located near the anode (as replicated in Bars 1 and 2) would, at the very least, have its corrosion rate slowed down significantly, if not completely.

It is also noted that, on average, more current is generated in the specimens containing higher chloride content, as shown in Table 5-9 compared to Table 5-10. This is expected since a higher chloride content signifies a harsher environment for corrosion activity and therefore should translate into greater current output from the sacrificial anodes. Although it may appear that the mesh receives the least amount of current with respect to the bars, this is not necessarily the case since current output is being measured as current density. Since the mesh has a much larger area than each of the individual bars, the current density is generally much lower. Negative average-weighted current densities occurred only once in the outdoor conditions as shown by Table 5-9. This is in great contrast to the results obtained for the mesh densities housed in the environmental chamber (Tables 5-7 and 5-8) that saw 50% of the cases recording negative values. This indicates the chamber condition was probably more aggressive in terms of corrosion, since the net flow of current was away from the mesh (negative values). As discussed previously, the current being delivered to the mesh by the sacrificial anode was not enough to prevent extreme corrosion conditions and the formation of macro-cells with neighboring bars.

It is also interesting to note that comparing the performance for the different exposure conditions (environmental chamber and outdoor climate), Sacrificial Anode A was clearly the dominant system achieving the highest score under all conditions. Sacrificial System B performed second best, while the sacrificial System C consistently performed poorly.

5.1.5 Potential Decay: Environmental Chamber

As previously discussed, there exist three principle levels of protection against corrosion: corrosion prevention, corrosion control and cathodic protection. Cathodic protection is deemed the highest level of protection. Under certain conditions, cathodic protection has been known to completely halt corrosion activity. The most common and accepted indicator for achieving cathodic protection is the 100 mV criteria. The 100 mV states that if steel is polarized by a minimum of 100 mV in reference to its corrosion potential (open circuit), cathodic protection is achieved. There are two main methods for determining this phenomenon: potential decay or formation. The potential decay method was used in determining cathodic protection in this project. Figures 5-37 to 5-41 and Figures 5-42 to 5-46 show the potential decay recorded for the specimens housed in the environmental chamber and subjected to 3.9% and 1.2% chlorides by weight of cement respectively. Please note, the figures simply show the amount by which the potential decayed to a stable value. In other words, the results are the potential difference

between the polarized steel at its "instant off" potential and its corrosion potential. The time allowed for depolarization once the system was interrupted (i.e., switches turned off) was at least 24 hours.

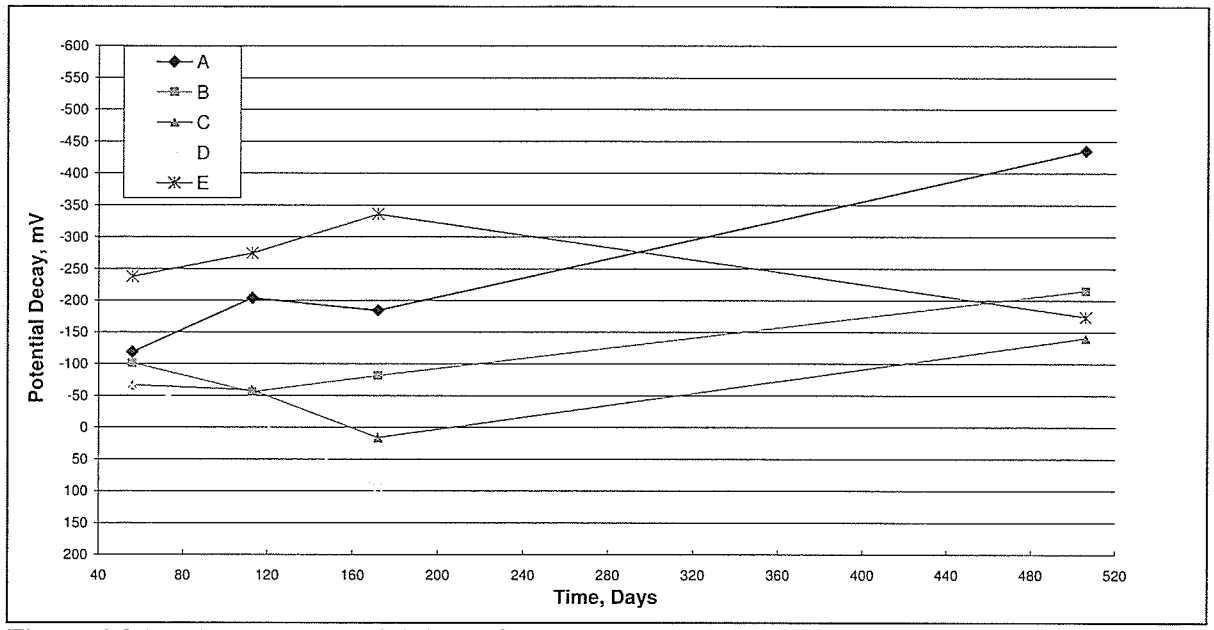

Figure 5-37: Average potential decay for Bar 1, subjected to 3.9% chloride by weight of cement and exposed to the environmental chamber conditions

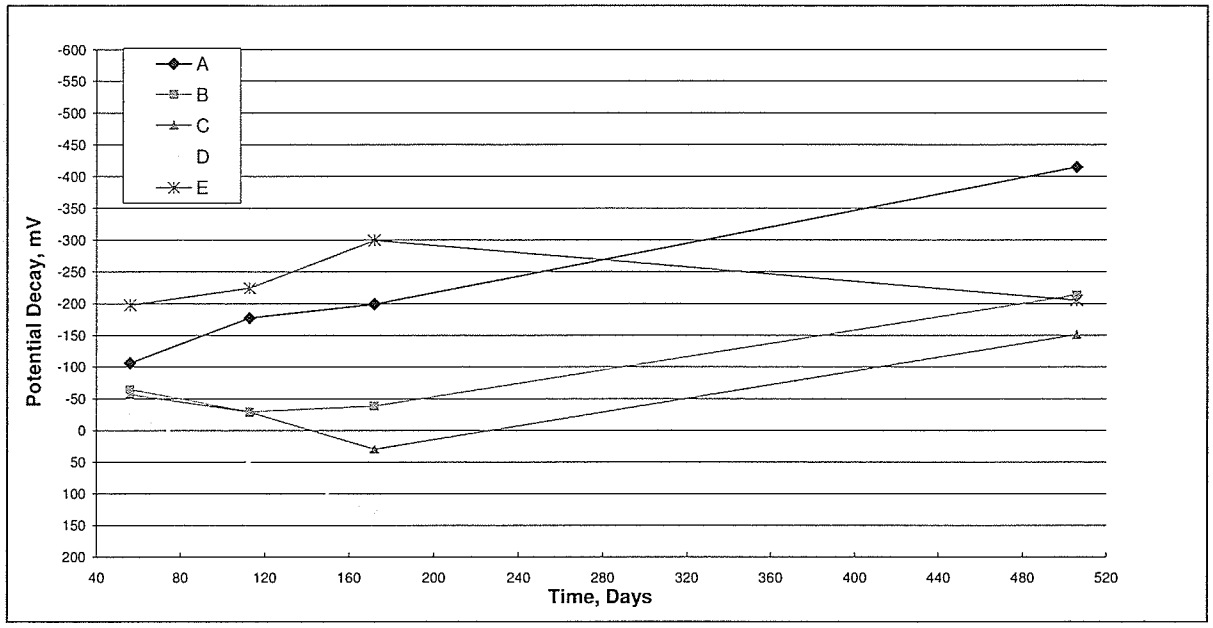

Figure 5-38: Average potential decay for Bar 2, subjected to 3.9% chloride by weight of cement and exposed to the environmental chamber conditions

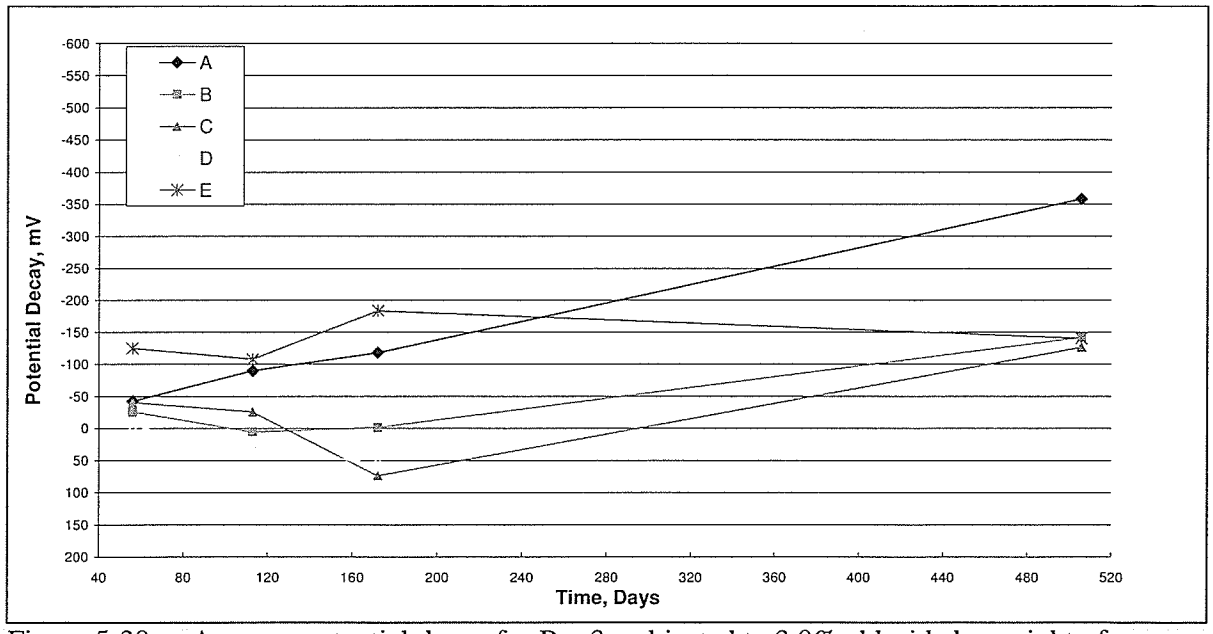

Figure 5-39: Average potential decay for Bar 3, subjected to 3.9% chloride by weight of cement and exposed to the environmental chamber conditions

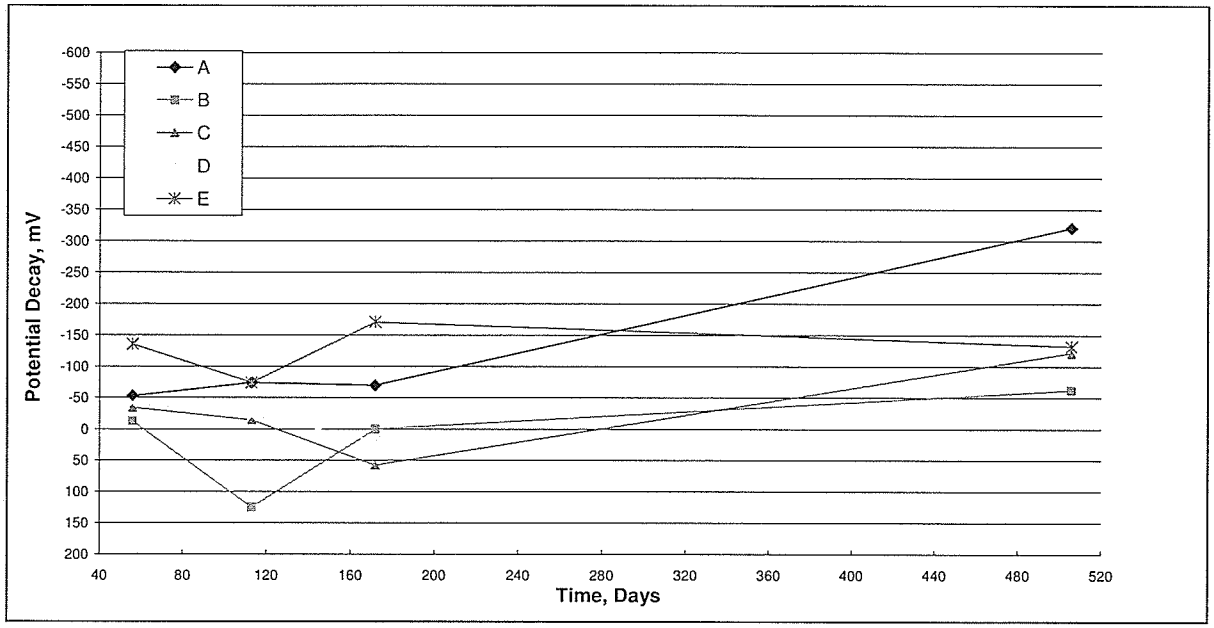

Figure 5-40: Average potential decay for Bar 4, subjected to 3.9% chloride by weight of cement and exposed to the environmental chamber conditions

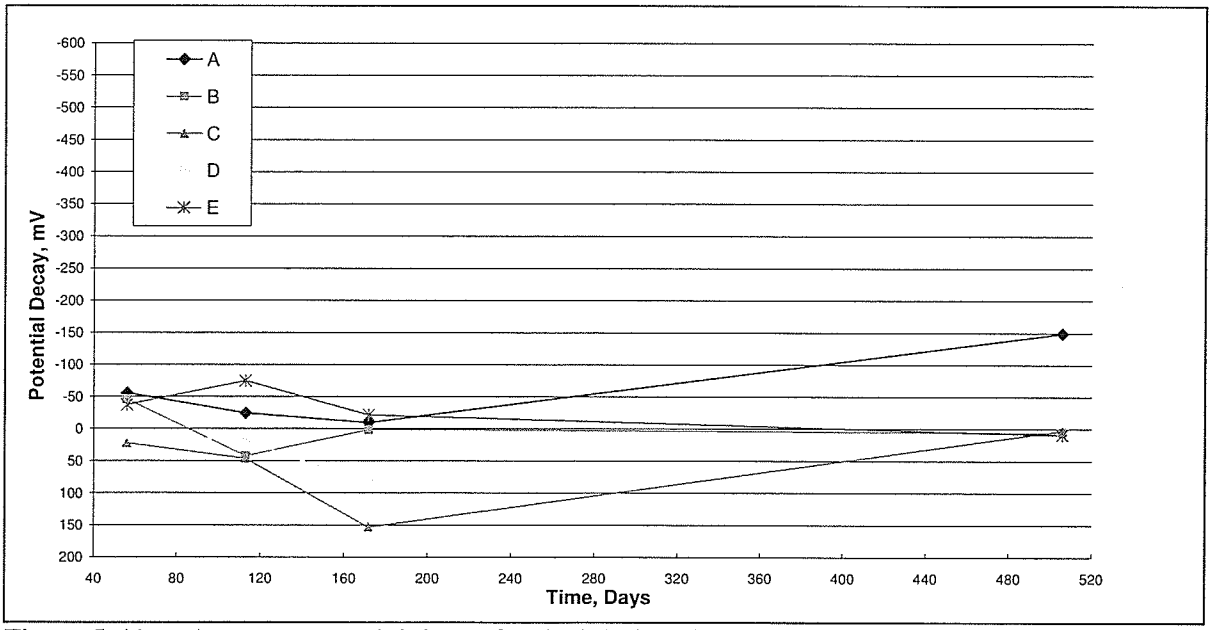

Figure 5-41: Average potential decay for the Mesh, subjected to 3.9% chloride by weight of cement and exposed to the environmental chamber conditions

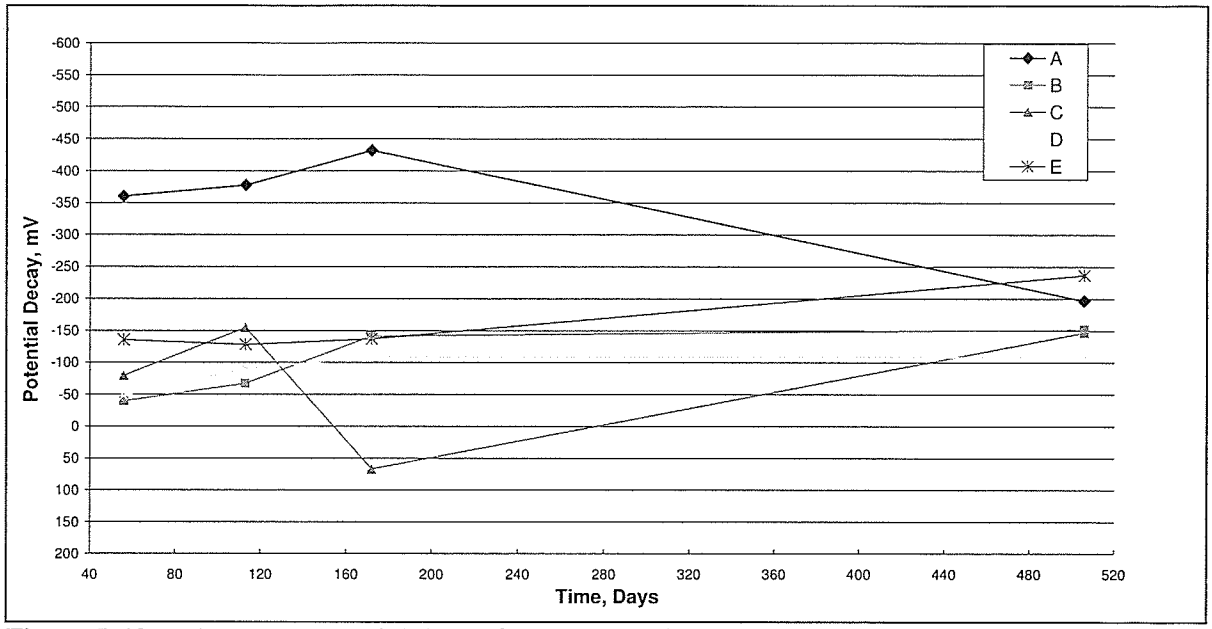

Figure 5-42: Average potential decay for Bar 1, subjected to 1.2% chloride by weight of cement and exposed to the environmental chamber conditions

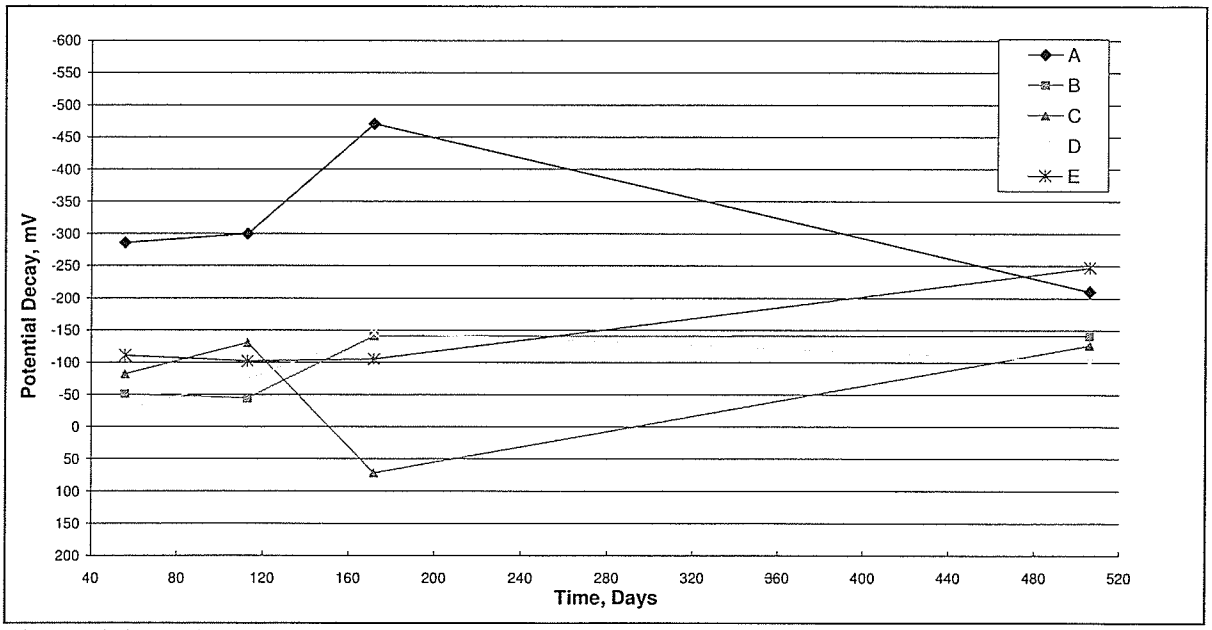

Figure 5-43: Average potential decay for Bar 2, subjected to 1.2% chloride by weight of cement and exposed to the environmental chamber conditions

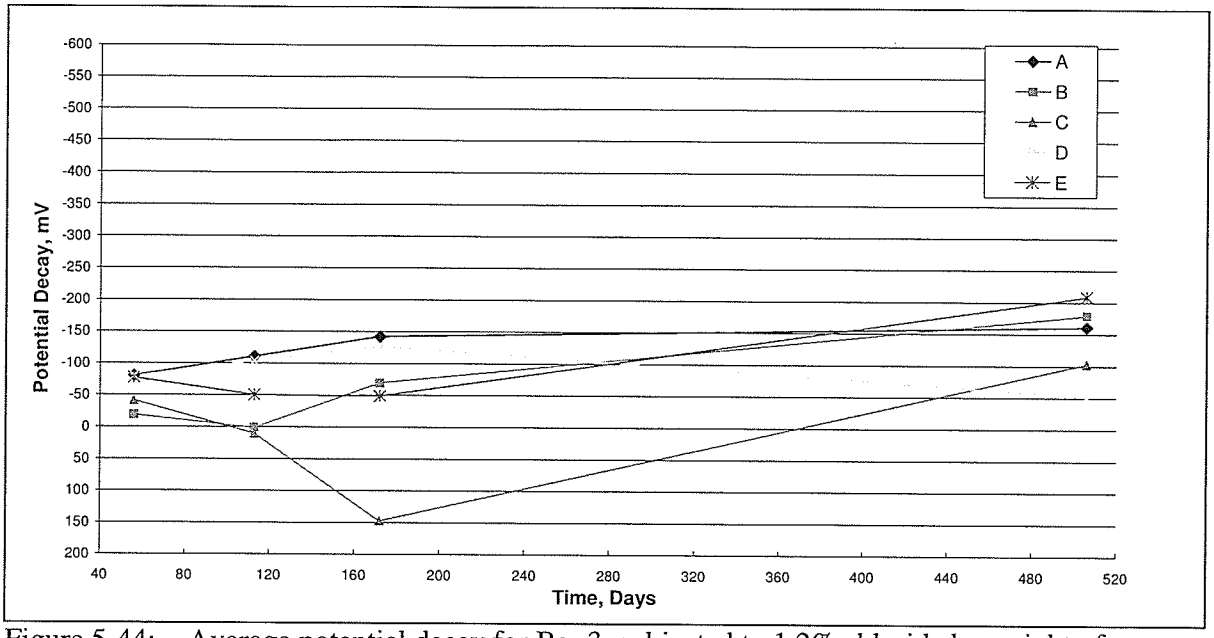

Figure 5-44: Average potential decay for Bar 3, subjected to 1.2% chloride by weight of cement and exposed to the environmental chamber conditions

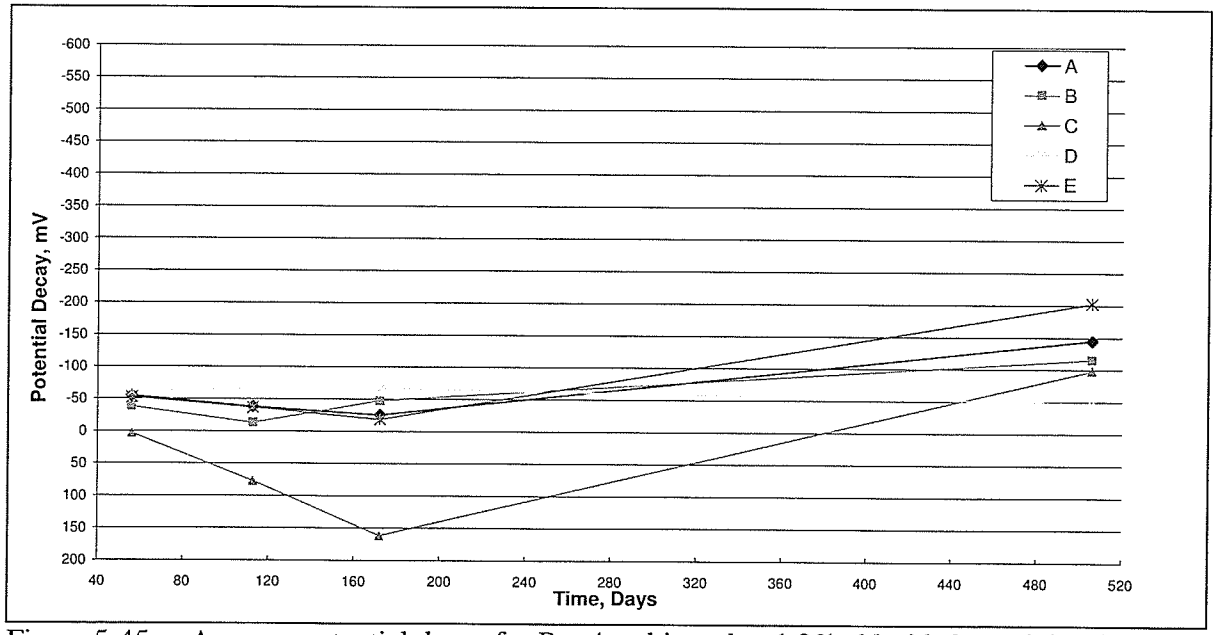

Figure 5-45: Average potential decay for Bar 4, subjected to 1.2% chloride by weight of cement and exposed to the environmental chamber conditions

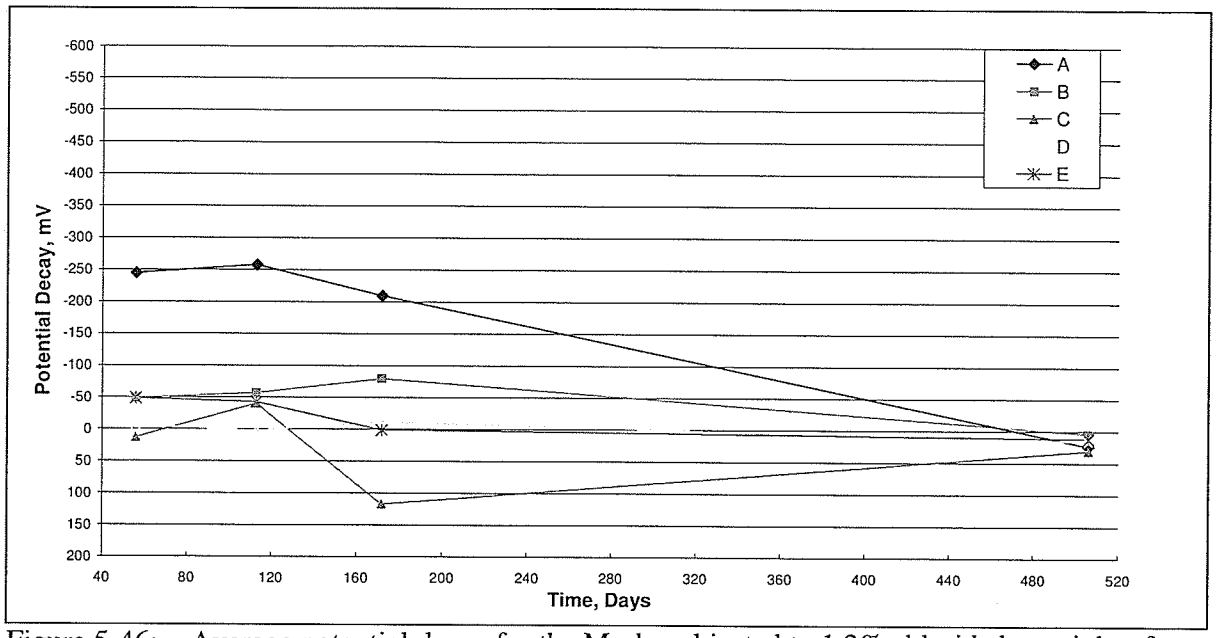

Figure 5-46: Average potential decay for the Mesh, subjected to 1.2% chloride by weight of cement and exposed to the environmental chamber conditions

Before discussion can take place on the results, it is important to point out that due to severe corrosion on the switches and more critically on the wire connecting the sacrificial anode to the other switches, readings after day 172 were not available for Sacrificial System D subjected to high chlorides. Also recall that the environmental chamber was disconnected after day 172; therefore the temperature and relative humidity returned to standard room temperature (approximately 20 C and 70% R.H.). It is also important to understand the sign conventions presented in these figures, keeping in mind that the potential decay is the difference between "instant off" readings and the stabilized potential. Negative potential decay is taken as the amount by which the reinforcement has depolarized once the system is turned "off" from its polarized position. Recall that the potential decay is simply a method of measuring how much the steel has polarized from its half-cell or corrosion potential state. Any polarization of the steel signifies that the distributed current is over-coming the net tendency of the steel to corrode; and so at the very least, minimal protection is provided. Keep in mind, however, polarization of steel does not mean corrosion has halted; it simply refers to a decrease in corrosion rate. A positive potential decay on the other hand is not really "decaying" at all. In fact, it is the opposite. This signifies that the "instant off" potential is less negative than the "corrosion potential"; and therefore, the steel has not polarized. This may occur when the current supply generated from the sacrificial anode is not overcoming the tendency of the steel to corrode. This would suggest that when the system is turned "on", the steel is, in fact, corroding at a faster rate. This is a strange phenomenon and can possibly be explained by the formation of local corrosion macro-cells.

The first potential decay reading was taken at day 56. Time zero is taken from the time the sacrificial systems were first activated (i.e., switches initially turned on). Also, the specimens have been cast with chlorides at least 8 months prior and have already been subjected to the environmental chamber conditions one week prior to activation. This was done in an attempt to ensure corrosion initiation prior to testing. The probability of corrosion activity was confirmed by the potential of the high half-cells taken from the specimens.

Analyzing the results obtained from the specimens subjected to high chlorides (Tables 5-37 to 5-41), Sacrificial Anode E recorded almost consistently the greatest potential decay on all bars and mesh, while the environmental chamber was active (time 0 to 172 days). Sacrificial Anode A recorded the second greatest potential decay throughout the time period the chamber was activated and recorded the greatest potential decay for all bars and mesh for the long-term reading (time 506 days). For the most part the potential decay increased in the long-term reading. This was expected since the harsh humid and hot conditions no longer existed and potential restoration of the protective film may have occurred in some instances. Its interesting to note that Sacrificial Anodes A and E were the only two systems, which had increasing potential decay for Bars 1 and Bars 2 while the chamber was still activated; this is in contrast to the others. This was not so much true for Bars 4 and the mesh. This trend of increasing potential decay with time indicates the level of protection for those individual bars increased. In other words, an adequate current supply is enabling an increase in polarization, thus minimizing the corrosion rate. The reason is most likely due to the current rendering the local environment to less aggression. This is not the case for Sacrificial Anodes C and D, in all cases (Bars 1 to 4 and the mesh). A decrease in potential decay was observed for these two sacrificial systems for the time period in which the environmental chamber was activated. In fact, the first potential decay readings for both of these sacrificial anodes were recorded near –50 mV. At this instance, the current was polarizing the steel, and the corrosion rate would have therefore been decreased. Recognize that the polarized-steel falls short of the minimum -100 mV potential decay required for cathodic protection. The second and third reading revealed a dramatic decrease in the ability for potential decay and even showed potential decay recorded high into the positive values. This, of course, signified that the steel was not polarized; and in fact, an increased corrosion rate while the system was activated may have been occurring.

Analyzing Figure 5-41, which depicts the results for the mesh subjected to high chlorides, it is observed that Sacrificial Anodes B, C and D, all enter into the positive potential "decay" range. Sacrificial Anodes C and D commence in the low positive range and increase in positive potential until day 172. This shows that the current being delivered from the sacrificial anode was not enough to polarize the steel. It should be stated that the potential decay simply records the average net potential difference between the instant off and the depolarized potential (i.e. open-circuit potential). In other words, portions of the mesh may have been polarized, but the net potential of the mesh demonstrates that overall no polarization occurred. This coincides well with the results obtained previously for the mesh subjected to the same conditions (Figure 5-24), which shows that the current densities for Sacrificial Anodes B, C and D were all negative during the time frame of chamber activation. Recall that a negative current density signifies the net flow of current is away from the steel; thus rendering the steel in question into an anode. This means that the current being supplied to the steel from the sacrificial anode was not sufficient to

overcome the anodic state of the steel. A corrosion macro-cell with a nearby bar must have therefore been the cause of the negative current flow.

Analyzing and describing the circumstance of the results for each condition is not straightforward. Despite the fact that all attempts were made to have identical conditions for specimens subjected to the same environment and chloride levels, achieving this was not completely realistic. Although it can safely be assumed that in most cases conditions are relatively the same, there were certainly areas within specimens that had different conditions. There was no way of knowing specifically the conditions surrounding each bar and mesh unless these sites were continuously monitored for influencing factors such as: pH, chloride, moisture, resistivity, corrosion rate, corrosion potential, influencing current from mirco and macro-cell formation and so on. The number of factors able to influence the end result was substantial, despite the special care taken to maintain equal conditions. A perfect example of how different conditions effect the end result was observed when analyzing the average current density and potential decay for Sacrificial Anode E, subjected to high chlorides for Bar 1 shown in Figure 5-21 and 5-37, respectively. In Figure 5-21, Sacrificial Anode E continuously recorded the lowest current density delivered to Bar 1. Despite this low current density, Sacrificial Anode E was able to polarize Bar 1 well above the 100 mV required for cathodic protection. Analyzing Table 5-7 for the average-weighted current density for Bar 1, Sacrificial Anode E recorded 2.16 mA/m^2. This theoretically still falls within the proposed range of 2 to 20 mA/m^2 required to achieve cathodic protection. On the other hand, Sacrificial Anode D, for the same conditions, recorded an average-weighted current density of 5.14 mA/m^2 and was only initially able to slightly to polarize Bar 1 at best. Analyzing Table 5-1, the average-weighted corrosion potential for Bar 1 subjected to the same conditions, Sacrificial Anode D and E, recorded –574 mV and –487 mV, respectively. Although both these corrosion potentials are well within the active corrosion range or 90% corrosion probability, the specimen with Sacrificial Anode D recorded corrosion potential –87 mV more negative than its counterpart. This falls in accordance with the contradicting results. This –87 mV greater corrosion potential would most likely result in an increased current output from the sacrificial anode. Depending on the severity of the corrosion, the increased current output may or may not be able to overcome the corrosion tendency. The corrosion potential recorded for the specimen with Sacrificial Anode E was the lowest for all specimens. This would explain why such a small current density was able to polarize the steel to such an extent. Reasons for these differences in corrosion potential are directly related to a difference in the conditions surrounding Bar 1. Several factors such as higher chlorides, resistivity, or various other factors or a combination of factors can be attributed to this difference. This is why it is not so simple as saying cathodic protection will be reached if a certain current density is met. This also explains the reason why the different levels of protection are categorized by such a wide range in current density, as shown in Table 3-6.

Sacrificial Anode A clearly was able to protect Bars 1 and 2 far more than the other sacrificial anodes subjected to low chlorides and exposed to the environmental chamber as shown in Figures 5-42 and 5-43, respectively. Sacrificial Anode A was able to polarize Bars 1 and 2 upwards of –200 mV throughout the entire testing period and even reached potential decay nearing –500 mV. This extremely high potential decay has clearly reached cathodic protection and it is virtually certain corrosion activity has completely halted. A decrease in potential decay

was visible for Sacrificial Anode A when viewing the results for Bars 3 and 4. When analyzing Figure 5-45 (Bar 4), it is difficult to establish how the sacrificial anodes are performing with respect to one another. Sacrificial Anodes A, B, D and E, are all obtaining potential decays well below the –100 mV criteria needed for cathodic protection during the first 172 days. Sacrificial Anode C on the other hand was the only system that recorded positive "decays" throughout the first 172 days. The results obtained in Figure 5-45 correlate with the results obtained for current densities for the same bar under the same conditions (Figure 5-27). The current density results show all sacrificial anodes recording a positive density of less than 3 mA/m^2, except for Sacrificial Anode C that recorded consistently negative values for the 172-day time frame.

It is important to keep in mind that there are many variables affecting the outcome of the results, some of which cannot be fully controlled. To fully understand each and every result would require continuous monitoring of the influencing factors. This was not within the scope of the project and only a hypothesis based on the results can be made. With that said, it is difficult to explain why the Sacrificial Anodes D and E both recorded negative current density delivered to the mesh subjected to low chlorides in the environmental chamber conditions (Figure 5-28); yet both were able to obtain potential decays (Figure 5-46). This means that despite the fact that the net current was away from the mesh (by definition this is an anode), it was still able to slightly polarize the steel. This is contradictory to theory since it is the current being delivered to steel which would cause polarization and not visa-versa. One possible explanation could be that since potential decays are measured using the half-cell reference electrode, the positioning of where the measurements are taken can perhaps influence the final outcome. The half-cell is intended to be placed directly over the region in which the potential is to be known. This reduces the resistance due to the concrete between the mesh and the reference rod. Although, potential along a steel bar may vary from positions along the bar, the reference electrode reads the corrosion potential of the entire bar. The final reading is no doubt influenced much more by the potential along the steel nearest to the reference electrode. The same can be true for the mesh. The mesh readings were taken directly at the center surface of the slab for each specimen. This was done so as not to have biased results on one side or the other. For example, potential taken near the sacrificial anode would certainly be different from potential taken from the other end of the slab. Since mesh covered the entire area of the slab, corrosion potential would have varied throughout. Therefore, although negative current readings were taken from the mesh for specimens containing Sacrificial Anodes D and E, polarization still may have occurred in certain areas of the mesh; and as a result, a potential decay still may have still possible within these areas. These uncertainties in the results are unfortunate, and it seems the addition of the mesh to the specimens may be the lead cause for all these unexpected and difficult to explain events.

Tables 5-11 and Tables 5-12 show the average-weighted potential decay for the specimens containing the different sacrificial anodes exposed to environmental chamber conditions and subjected to 3.9% and 1.2% chlorides by weight of cement, respectively. The same rating-system was implemented in these tables for comparison purposes. Keep in mind a negative potential decay signifies polarization occurred, whereas a positive value signifies an increase in corrosion activity. Also, the average-weighted potential decays were only calculated until day 172 (i.e. the time period of the chamber activation).

Table 5-11: Average-weighted potential decay subjected to 3.9% chlorides by weight of cement and exposed to the environmental chamber

Galvanic system	Average - weighted potential decay for Bar 1, mV		Average - weighted potential decay for Bar 2, mV		Average - weighted potential decay for Bar 3, mV		Average - weighted potential decay for Bar 4, mV		Average - weighted potential decay for Mesh, mV		Total score, points
A	-178	IV	-165	IV	-85	IV	-67	IV	-28	IV	20
B	-73	III	-40	III	-4	III	59	I	11	III	13
C	-41	II	-21	II	-4	III	-1	II	68	II	11
D	1	I	53	I	30	II	-16	III	34	I	8
E	-281	V	-236	V	-131	V	-113	V	-51	V	25

Rating system: V – 5 pts; IV – 4 pts; III – 3 pts; II – 2 pts; I – 1 pt

Table 5-12: Average-weighted potential decay subjected to 1.2% chlorides by weight of cement and exposed to the environmental chamber

Galvanic system	Average - weighted potential decay for Bar 1, mV		Average - weighted potential decay for Bar 2, mV		Average - weighted potential decay for Bar 3, mV		Average - weighted potential decay for Bar 4, mV		Average - weighted potential decay for Mesh, mV		Total score, points
A	-387	V	-340	V	-111	V	-39	IV	-242	V	24
B	-79	II	-70	II	-21	II	-28	II	-60	IV	12
C	-79	II	-67	I	33	I	81	I	13	I	6
D	-84	III	-80	III	-103	IV	-65	V	-3	II	17
E	-132	IV	-105	IV	-57	III	-36	III	-33	III	17

Rating system: V – 5 pts; IV – 4 pts; III – 3 pts; II – 2 pts; I – 1 pt

Sacrificial Anodes A and E were the only systems able to reach cathodic protection on average for Bars 1 and 2 for specimens with high chloride contents exposed the environmental chamber (Table 5-11). Sacrificial Anode E clearly outperformed all others reaching cathodic protection for all bars and the highest level of protection for the mesh; this in spite of the fact that Sacrificial Anode E recorded very low current density readings. Sacrificial Anode A was able to polarize the steel for the remaining bars and the mesh. One factor that may have slightly affected the overall average-weighted results may have been due to the placement of one of the specimens containing Sacrificial Anode A with high chlorides. Recall that the presented results are the average of two duplicates for every slab under a specific condition. One of these duplicates was placed near the water spray in the environmental chamber, which caused ponding-like conditions. The potential decay for this specimen was well short of the -100 mV mark, and as a result lowered the overall average of the two duplicate specimens. A photograph of the impeding spray on the specimen is shown in Figure 5-47. The specimen with Sacrificial Anode A is labeled "GT #16 High Cl-" in the picture. Ponding is also visible at the far top corner of the slab. The

remaining sacrificial anodes systems did not fair so well, with many of them reaching positive "decay". The positive "decay" hints at extreme corrosion activity and more than likely, formation of corrosion macro-cells throughout this period.

Specimens with Sacrificial Anodes A subjected to low chlorides again did very well in terms of protection offered (Table 5-12). Cathodic protection was achieved for Bars 1, 2, 3 and mesh. Sacrificial Anodes D and E performed equally well, in terms of ranking, followed by System B then C. It is clear that the number of positive potential "decay" seen in the specimens exposed to low chlorides is much less than for the specimens exposed to higher chlorides.

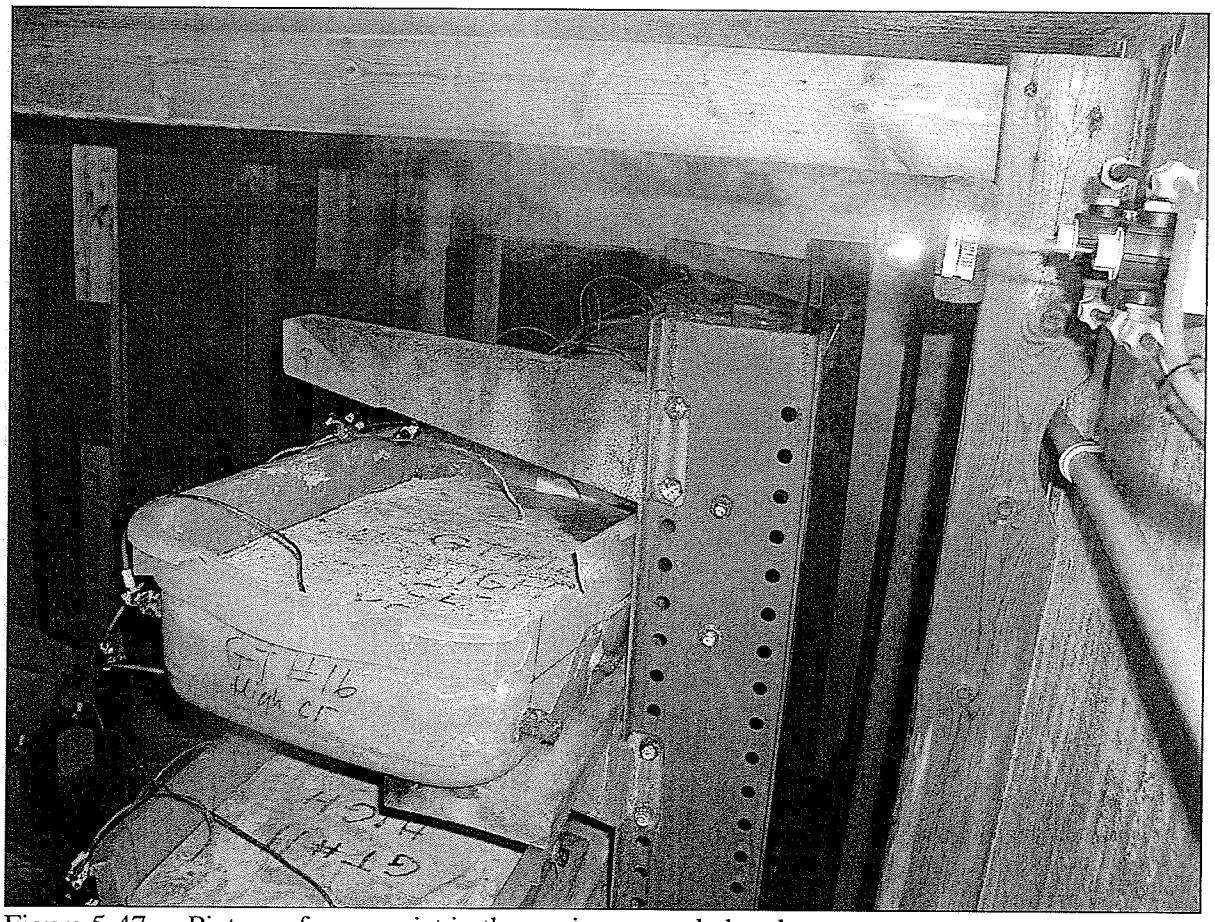

Figure 5-47: Picture of spray mist in the environmental chamber

5.1.6 Potential Decay: Outdoor Climate

Potential decay for the specimens exposed to Winnipeg's outdoor climate and subjected to 3.9% chlorides and 1.2% chlorides is shown in Figures 5-48 to 5-52 and Figures 5-53 to 5-57, respectively. The potential decay was taken between the months of June to October 2006.

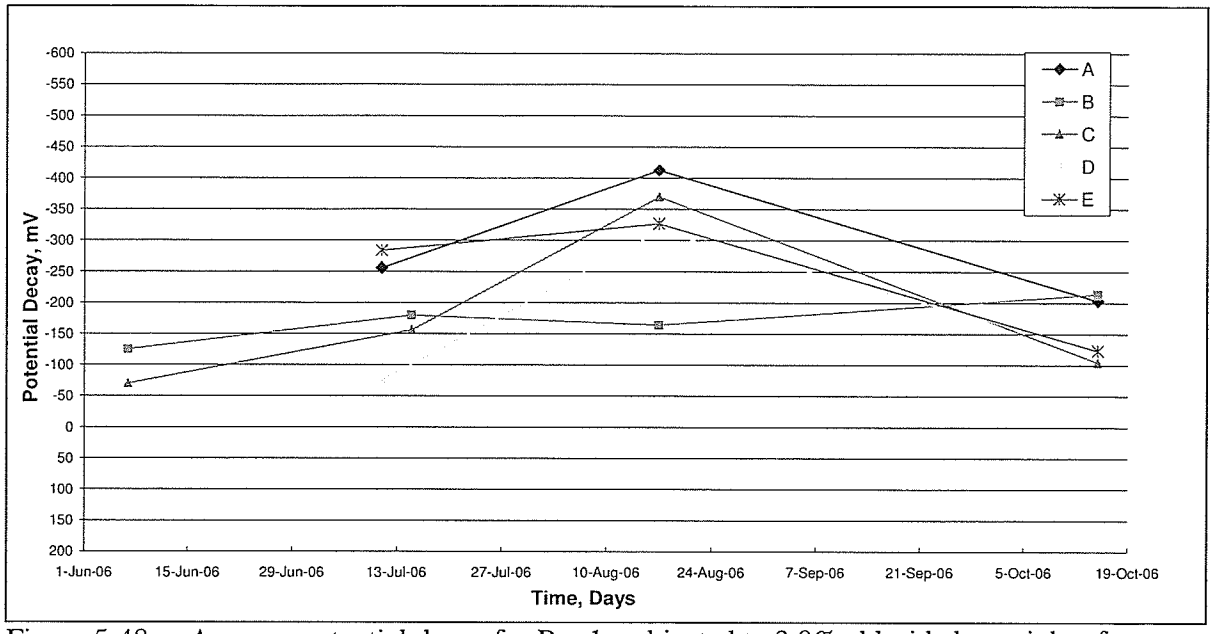

Figure 5-48: Average potential decay for Bar 1, subjected to 3.9% chloride by weight of cement and exposed to Winnipeg's climate

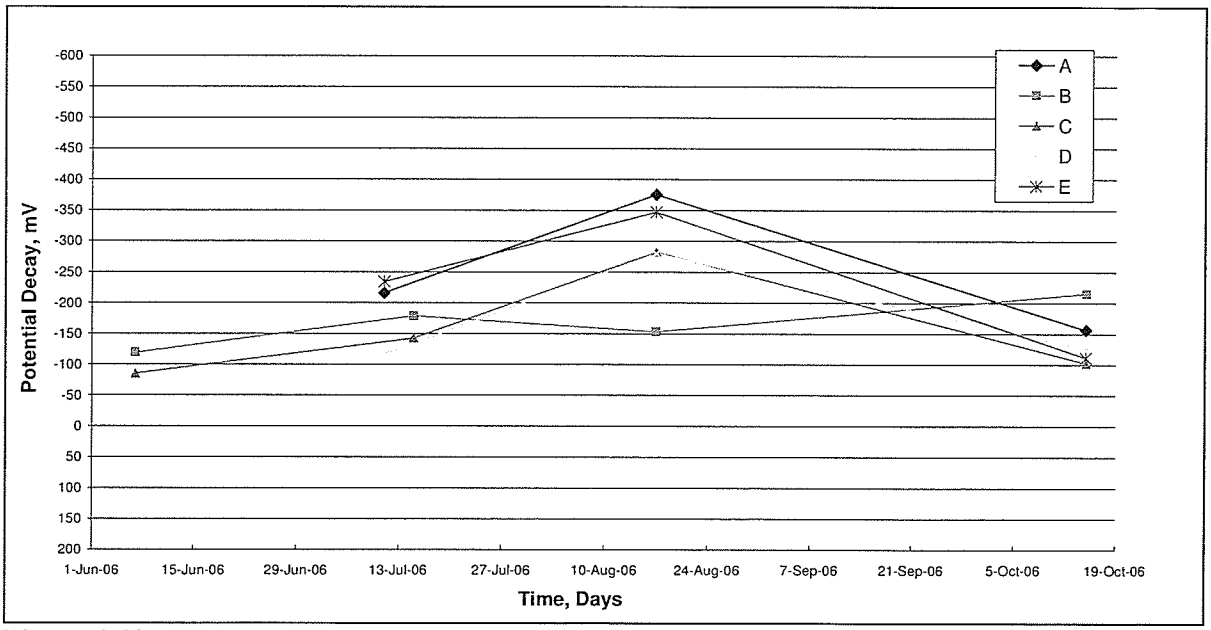

Figure 5-49: Average potential decay for Bar 2, subjected to 3.9% chloride by weight of cement and exposed to Winnipeg's climate

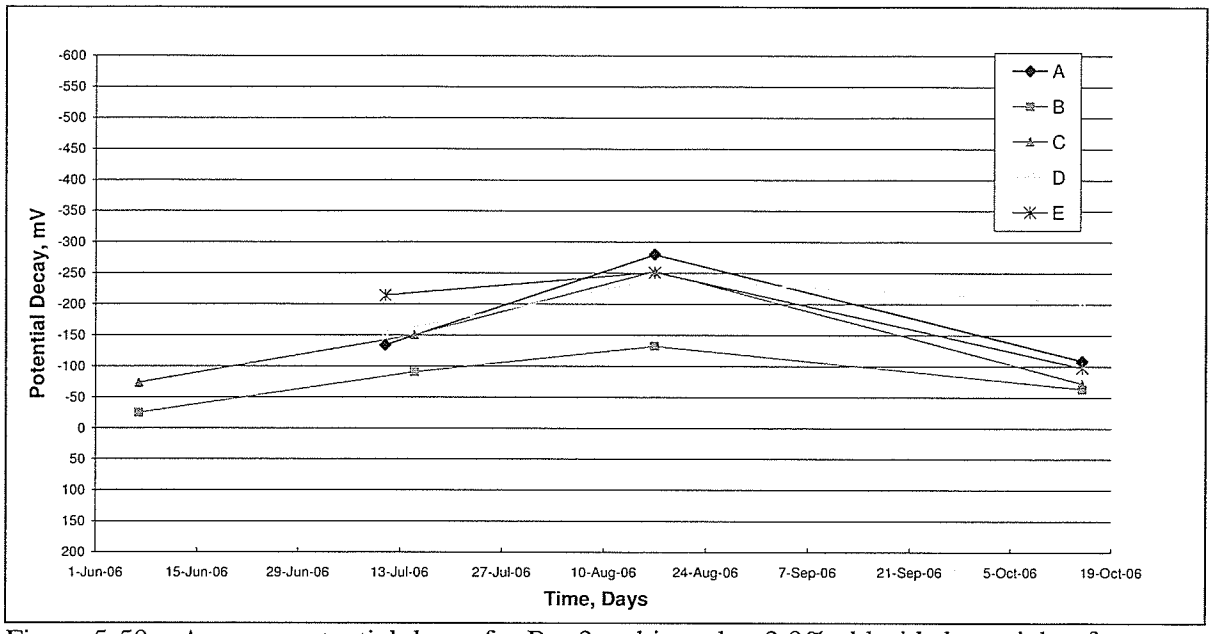

Figure 5-50: Average potential decay for Bar 3, subjected to 3.9% chloride by weight of cement and exposed to Winnipeg's climate

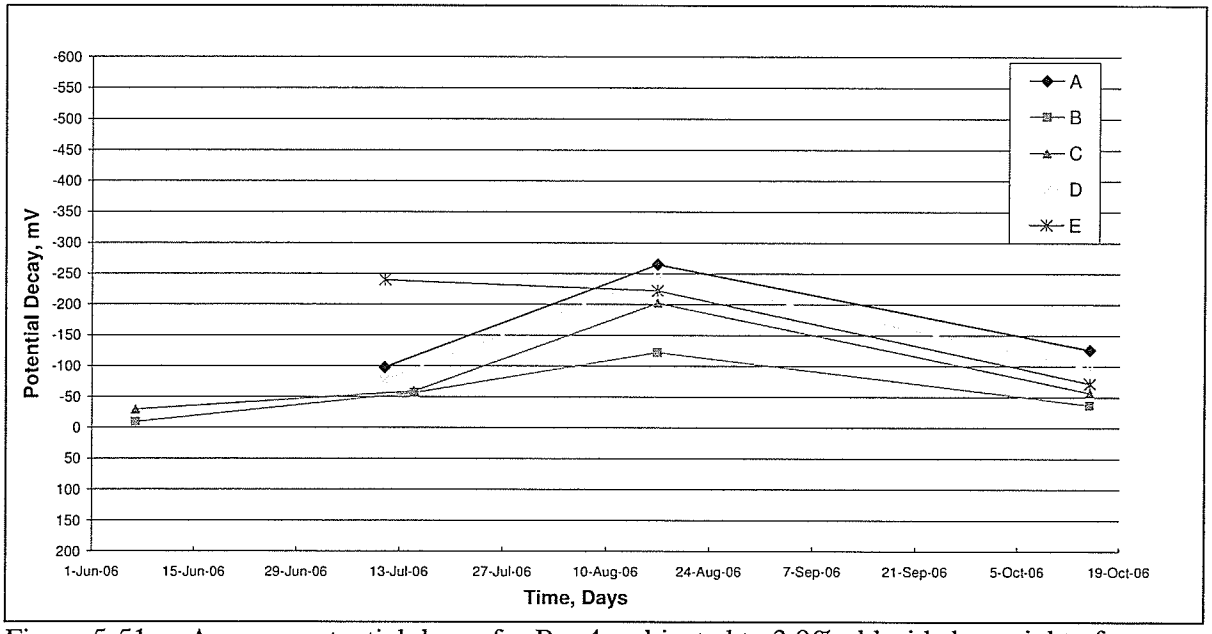

Figure 5-51: Average potential decay for Bar 4, subjected to 3.9% chloride by weight of cement and exposed to Winnipeg's climate

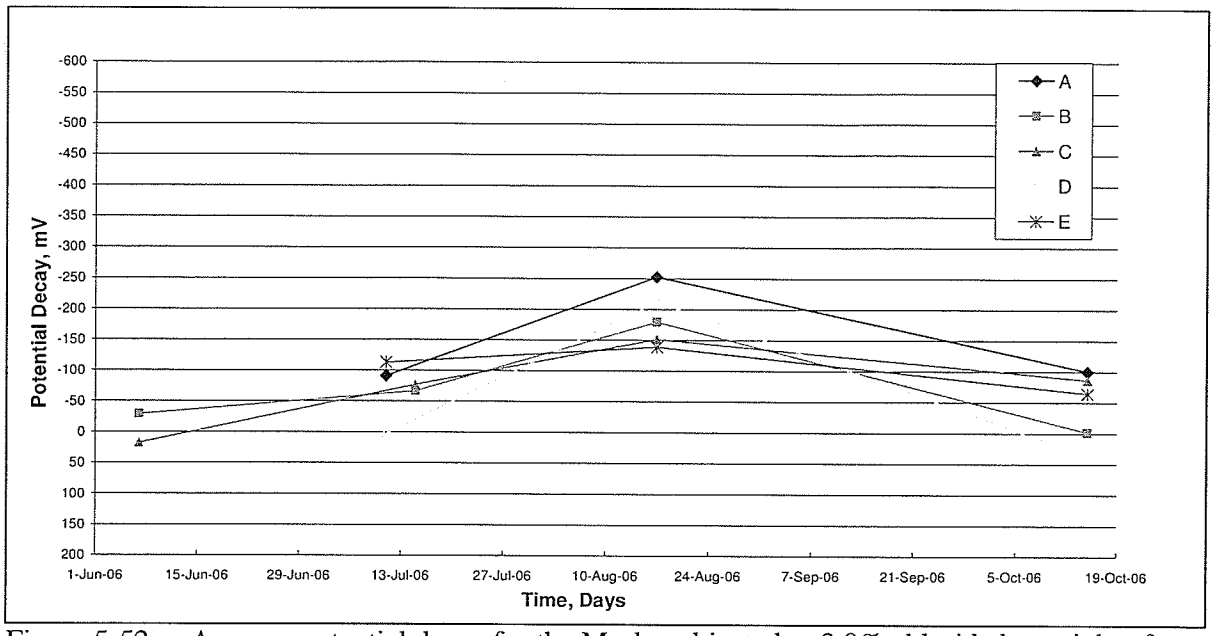

Figure 5-52: Average potential decay for the Mesh, subjected to 3.9% chloride by weight of cement and exposed to Winnipeg's climate

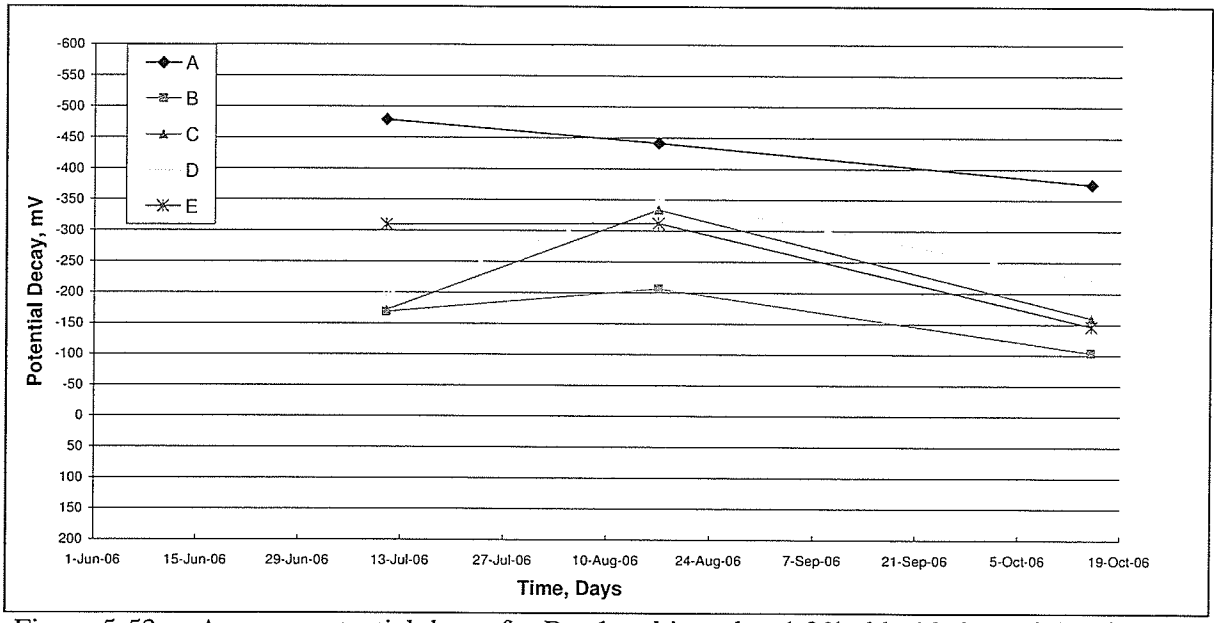

Figure 5-53: Average potential decay for Bar 1, subjected to 1.2% chloride by weight of cement and exposed to Winnipeg's climate

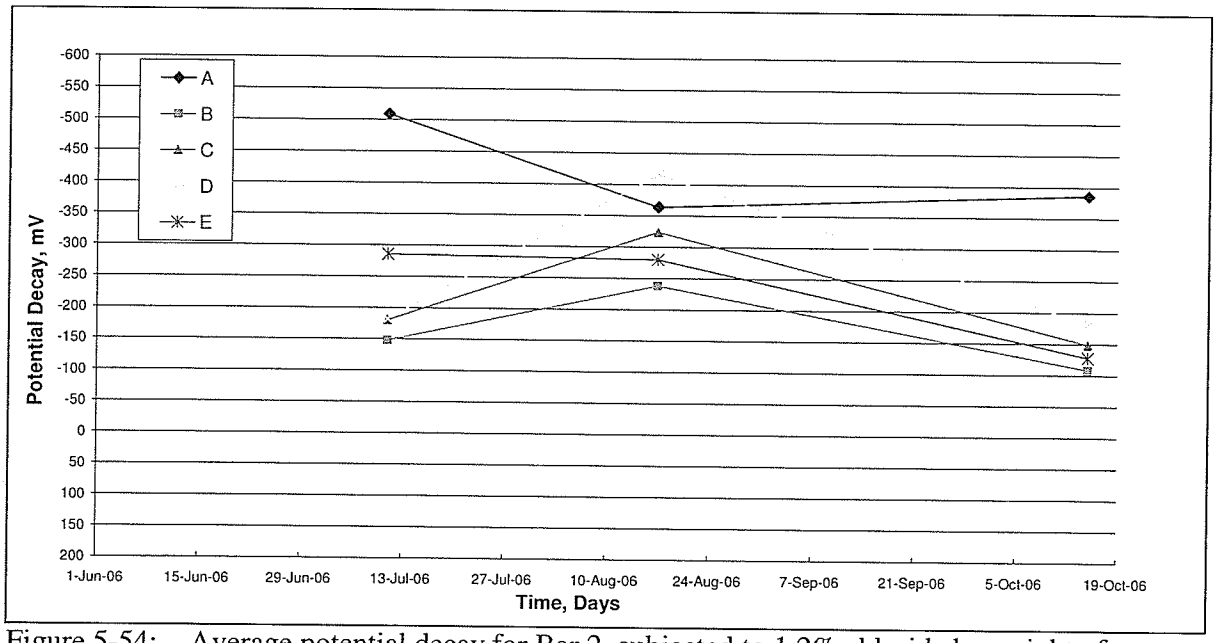

Figure 5-54: Average potential decay for Bar 2, subjected to 1.2% chloride by weight of cement and exposed to Winnipeg's climate

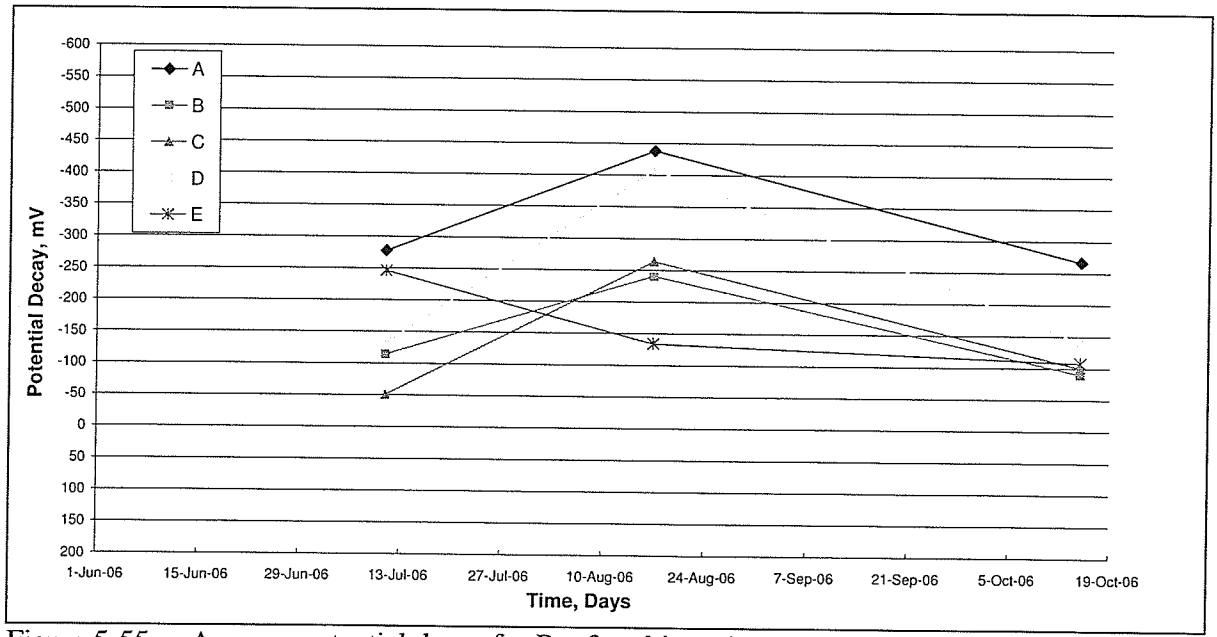

Figure 5-55: Average potential decay for Bar 3, subjected to 1.2% chloride by weight of cement and exposed to Winnipeg's climate

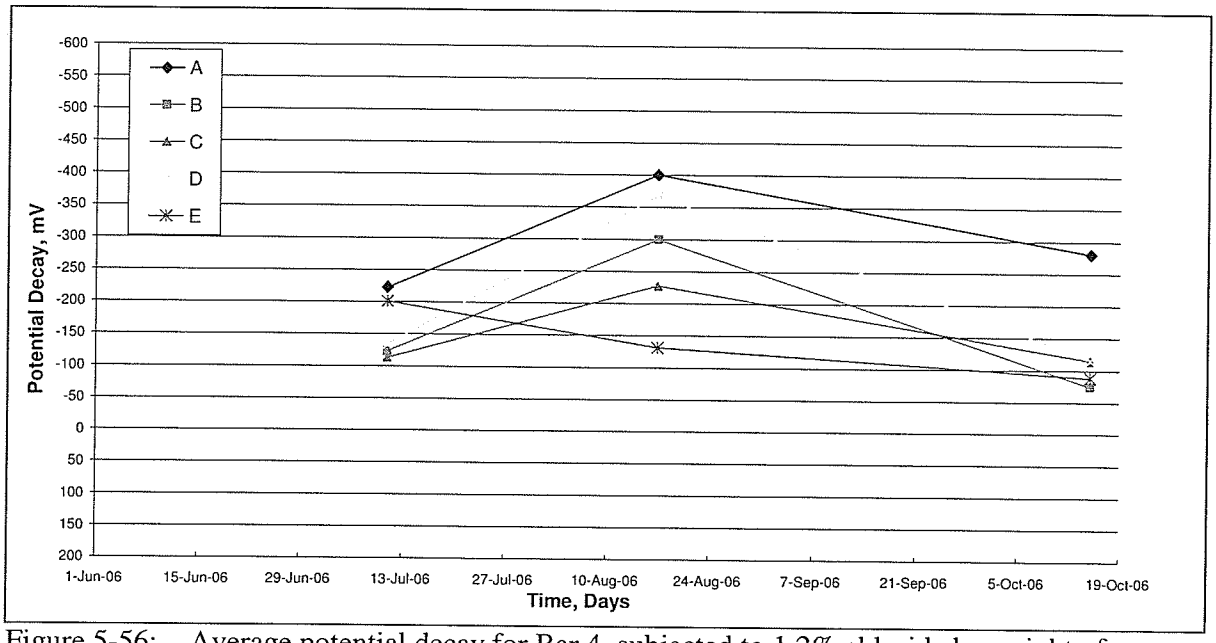

Figure 5-56: Average potential decay for Bar 4, subjected to 1.2% chloride by weight of cement and exposed to Winnipeg's climate

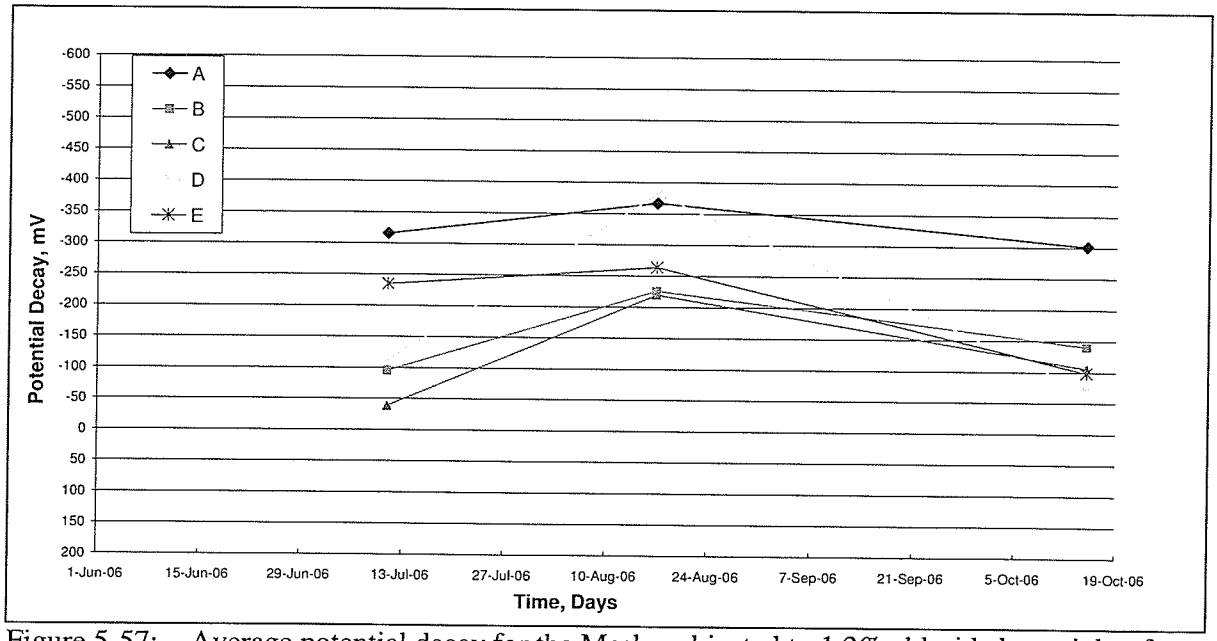

Figure 5-57: Average potential decay for the Mesh, subjected to 1.2% chloride by weight of cement and exposed to Winnipeg's climate

Analyzing the potential decay results for Bar 1 and bar 2 in the specimens containing high chloride content (Figure 5-48 and 5-49) demonstrates that, in most instances, cathodic protection

was achieved. The month of August saw the best results with every sacrificial system achieving cathodic protection for Bars 1 and 2. Sacrificial Anode A recorded the highest potential decay, reaching values near –400 mV. This is four times the required amount required to reach cathodic protection. Under such high polarization, it is certain that the corrosion rate is zero. By shear observation, it is quite clear that the constant, high temperature and high humidity (35 C and 90%, respectively) offered by the environmental chamber proved to be a much more aggressive condition than the outdoor climate. This can be seen by the fact that most specimens reached high polarization or even cathodic protection throughout the testing period when exposed to outdoor conditions as opposed to the environmental chamber.

The most ideal month for corrosion activity to occur was August. Late August was also the period that saw a spike in current density in particular for Bars 1 and 2. This spike corresponded well with the spike recorded for the same bars for potential decay. The reason for such a high level of protection in a favorable climate for corrosion activity is simple. As conditions for corrosion increase, the effectiveness of the sacrificial anode also increases. This is because the sacrificial anode has higher potential and thereby, corrodes preferably to steel. Theory suggests that, if the sacrificial anode is corroding, electrons are released; and thus the steel should be corrosion free. This of course is not always the case. As discussed in a previous section, an anode will form anywhere that the conditions are favorable and also where a potential difference exists. This formation of local anodes will result in the formation of micro- or macro-corrosion cells. Potential differences can arise due to factors as simple as slight variations in chlorides, moisture, resistivity, or even differences in the material property of the steel itself. As shown in the environmental chamber, in extreme corrosion conditions, a sacrificial anode with low driving force (capacity) may have minimal to no effect on the protection of the steel. This is seen by low polarization. In many instances depolarization occurred while the system was active. This signifies that while the system was activated, several bars and particularly the mesh, were losing electrons to other bars due to macro-cell formation. The electron transfer was made possible thanks to the parallel system setup, which linked all bars and the Mesh together. Therefore, while the system was activated some bars or the Mesh actually experienced depolarization and not polarization of the steel. This would render the steel more positive while the system is activated because of lose of electrons.

The month of June and July saw less polarization than August. Since conditions for June and July were less favorable for corrosion, it is conceivable that potential decay was considerably less. This is because the sacrificial anode was corroding at a slower rate and emitted less current. It is important to understand that it is not always necessary to achieve 100 mV polarization in order for the steel to be protected. If corrosion is not taking place, due for example to high resistivity, polarization of the steel is not required. In a dry, desert environment, a sacrificial anode would likely produce no current; and thus, the steel would not be polarized, but the steel would most certainly be corrosion free. In a hot, humid environment, or in coastal regions, a sacrificial anode would be very active, releasing current to the steel. The amount of polarization would ultimately depend on the capability of the sacrificial anode to generate current and the conditions surrounding the rebar. Under these conditions, the rebar may or may not be corrosion free. The effect of the climate can be seen in the trends shown in the results for current density and potential decay. As temperature increased with precipitation, so did current density and

potential decay. This is shown clearly with the peaks in current density and potential decay seen in the month of August.

Analyzing the remaining figures for high chlorides shows that potential decay becomes less with increasing distance from the sacrificial anode. This is expected since less current is generally delivered to these bars and therefore, polarization also tends to be less. However, conditions were such that even in Bar 4, the furthest in distance (located approximately 362 mm from the sacrificial anode), relatively high polarization was achieved as shown in Figure 5-51. The mesh results for high chloride contents exposed to outdoor conditions also showed relatively high potential decay for the most part. All sacrificial systems achieved cathodic protection in the late August reading, with the Sacrificial Anode A recording the greatest potential decay of approximately –250 mV. "Positive" decay on some bars was also recorded in the month of June and October, for some specimens. Recall, "positive decay" is the loss of electrons and thus anodic conditions are the result.

Potential decay results for the specimens containing low chloride contents and exposed to outdoors conditions (Figure 5-53 to 5-57) recorded similar results to the specimens with high chlorides. In the majority of instances for each bar and mesh cathodic protection was achieved. Peak potential decay was also observed in late August as before.

The average-weighted potential decay for specimens exposed to outdoor conditions and subjected to 3.9% and 1.2% chloride content by weight of cement is tabulated in Tables 5-13 and 5-14, respectively. The same rating system as before is also used.

Table 5-13: Average-weighted potential decay subjected to 3.9% chlorides by weight of cement and exposed to Winnipeg's climate

Galvanic system	Average - weighted potential decay for Bar 1, mV		Average - weighted potential decay for Bar 2, mV		Average - weighted potential decay for Bar 3, mV		Average - weighted potential decay for Bar 4, mV		Average - weighted potential decay for Mesh, mV		Total score, points
A	-317	V	-275	V	-199	IV	-190	V	-175	V	24
B	-174	I	-169	I	-90	I	-68	I	-87	I	5
C	-207	II	-174	II	-157	II	-105	II	-91	II	10
D	-210	III	-201	III	-212	V	-167	III	-93	III	17
E	-254	IV	-251	IV	-195	III	-177	IV	-110	IV	19

Rating system: V – 5 pts; IV – 4 pts; III – 3 pts; II – 2 pts; I – 1 pt

Table 5-14: Average-weighted potential decay subjected to 1.2% chlorides by weight of cement and exposed to Winnipeg's climate

Galvanic system	Average - weighted potential decay for Bar 1, mV		Average - weighted potential decay for Bar 2, mV		Average - weighted potential decay for Bar 3, mV		Average - weighted potential decay for Bar 4, mV		Average - weighted potential decay for Mesh, mV		Total score, points
A	-427	V	-397	V	-354	V	-330	V	-336	V	25
B	-166	I	-180	I	-169	II	-196	III	-175	II	9
C	-249	II	-242	III	-173	III	-171	II	-150	I	11
D	-281	IV	-299	IV	-273	IV	-245	IV	-234	IV	20
E	-258	III	-232	III	-146	I	-130	I	-205	III	11

Rating system: V – 5 pts; IV – 4 pts; III – 3 pts; II – 2 pts; I – 1 pt

Analyzing Table 5-13 and 5-14, it is clear that Sacrificial Anode A was dominant in terms of potential decay for the outdoor climate subjected to 3.9% and 1.2% chlorides by weight of cement, respectively. For high chloride content, Sacrificial Anode A achieved 1.25 greater potential decay for Bar 1 than the second leading sacrificial anode system (E) and 1.82 greater potential decay than the lowest sacrificial anode system (B) for the same bar. The amount by which Sacrificial Anode A outperformed the remainder of the systems increased, when analyzing specimens exposed to low chlorides (Table 5-14). Sacrificial Anode A recorded a potential decay 1.52 greater than the second leading sacrificial anode system (D) and 2.58 greater potential decay than the lowest potential decaying system (B). In fact, the average-weighted potential decay for Sacrificial Anode A subjected to low chlorides was not less than –330mV for all bars and the mesh. This high value of potential decay indicates complete protection and a corrosion rate of nearly zero. The fact that all systems recorded such high potential decay for both chloride contents indicates that outdoor conditions were a lot less aggressive than those in the environmental chamber.

5.1.7 Resistivity

Duplicate specimens of Specimen A were created and mixed with 10% of silica fume by weight of cement at the time of casting. The specimens labeled Silica A, represent the specimens containing silica fume and subjected to 3.9% and 1.2% chloride by weight of cement. Although, current output tests were done for Silica A for both the environmental chamber and outdoors conditions, only the results obtained for the environmental chamber will be addressed. The purpose of this test was to simply demonstrate the effect increase resistivity has on corrosion. Table 5-15, shows the resistivity taken by use of a resistivity meter for Specimens A and Silica A, subjected to both chloride levels and exposed to the environmental chamber. The readings were taken 28 days after the first current reading was taken.

Table 5-15: Resistivity of Specimen A and Silica A, exposed to the environmental chamber

	Resistivity of Silica A, subjected to 3.9% chloride by weight of cement, Ohms	Specimen A, average 3.9% chloride by weight of cement	Silica A, average 1.2% chloride by weight of cement	Specimen A, average 1.2% chloride by weight of cement
Bar 1/2	25	16	170	36
Bar 3	49	31	300	72
Bar 4	55	33	250	91
Mesh	14	8	73	18

The results from table 5-15, show the resistivity between the anode and the associated bar or the mesh. As distance increase so does the resistivity as expected. The results also clearly show that Silica A specimens have greater resistivity due to the added silica fume. Another trend that is observed is that resistivity decreases with an increase in chloride content. With an increase in resistivity, the current distribution provided by the sacrificial anode will decrease, signifying a decrease in protection levels. Current output results are shown in Appendix D.

5.1.8 Chloride Content and pH level

Two simple tests were conducted to determine chloride content and pH levels in the control specimen and Sacrificial Anode A, which was subjected to high chloride content and exposed to the environmental chamber. These tests were done to compare the effect the sacrificial system has on the surrounding concrete. The chloride tests were conducted using NDT James Instrument system, and a complete procedure of the test method is shown in Appendix E. The concrete specimens were sawed in half by machine, cutting perpendicular to the bars. By drilling fine holes through the concrete along the bars, concrete dust samples were collected. The dust samples were used in chloride testing and the excess was used in simple pH testing. The pH testing was achieved by mixing 3 gm of the concrete dust sample to 125 ml of distilled water in a beaker. After thoroughly mixing until dissolved, the solution was left to sit covered for 24 hours. The pH level was then measured by means of a pH meter. It is imperative to realize the focus of the pH test is to compare the difference in concrete when protected and not protected by means of a sacrificial anode. The methodology of testing pH was a crude and simple technique and should therefore be considered by way of example only. Chloride content and pH levels of the concrete surrounding the mesh were not tested. The results of chloride content and pH for the control specimens were taken by mixing all the concrete dust extracted from each of the bars. These tests were conducted immediately after day 506 testing was concluded. Tables 5-16 and 5-17 show the results of the chloride content and pH levels respectively.

Table 5-16: Recorded chloride content for Sacrificial Anode A and control specimens initially subjected to 3.9% chloride and exposed to environmental chamber conditions

Specimen	% chloride content by weight of cement at Bar 1	% chloride content by weight of cement at Bar 2	% chloride content by weight of cement at Bar 3	% chloride content by weight of cement at Bar 4
Anode A	0.26	0.24	0.4	0.51
Control	1.12	1.12	1.12	1.12

Table 5-17: Recorded pH level for Sacrificial Anode A and control specimens initially subjected to 3.9% chloride and exposed to environmental chamber conditions

Specimen	pH level, at Bar 1	pH level, at Bar 2	pH level, at Bar 3	pH level, at Bar 4
Anode A	12.5	12.4	12.4	12.4
Control	12.2	12.2	12.2	12.2

It is apparent that the use of the galvanic Anode A, has dramatically reduced the levels of chlorides surrounding the rebar. In fact, there was nearly 5 times less chloride content surrounding bar 2 when using Anode A, compared to the control specimen. The levels of chloride content surrounding the rebar increased, as the distance from the anode increased. There was an average of 0.25% chloride by weight of cement for bars 1 and 2 (which are the nearest to the anode) as opposed to 0.51% chloride by weight of cement for bar 4 (furthest). This is due to current distributions being greater at nearer distances. The end result leads to a lower corrosion rate at the nearer, more protected bars. The same results are obtained when analyzing the pH levels surrounding the rebar. Bars protected by Anode A had a pH levels greater than those bars unprotected in the control specimen. Bar 1 in the protected specimen also had the greatest level of pH measured at 12.5. The pH meter used only had capability to one decimal place.

The results were compatible with what was expected. The lowering of chloride contents and the increase in alkalinity (pH), results in a less aggressive environment and promotes re-passivity of the protecting film, and protects the steel on a long-term basis.

5.1.9 Visual Observations

Visual observations were performed on Specimen A and the control specimen, subjected to 3.9% chloride by weight of cement and exposed to the environmental chamber. After the final set of testing (506 days), both specimens were sawed opened to view the state of the concrete and the steel within the slab. Figures 5-58 (a), and (b) show the cross-section cut and Bar 1 of specimen A, respectively. Figures 5-59 (a), and (b) show a typical bar and the mesh, for the control specimen, respectively.

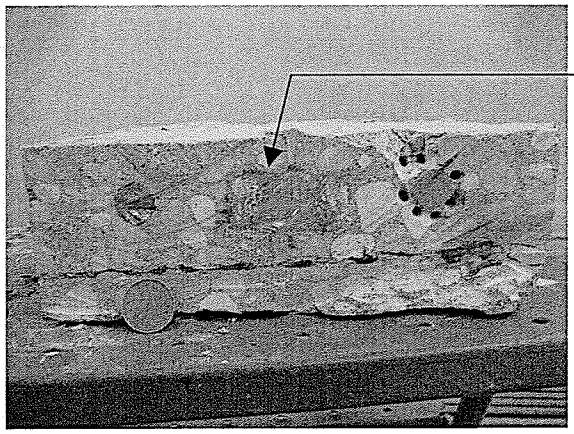

Figure 5-58(a): Saw-cut section of slab with embedded Sacrificial Anode A

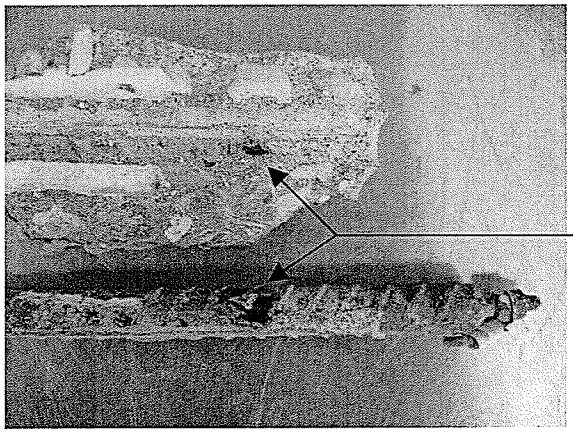

Figure 5-58 (b): Bar taken from slab exposed to high chlorides in environmental chamber and protected by Sacrificial Anode A

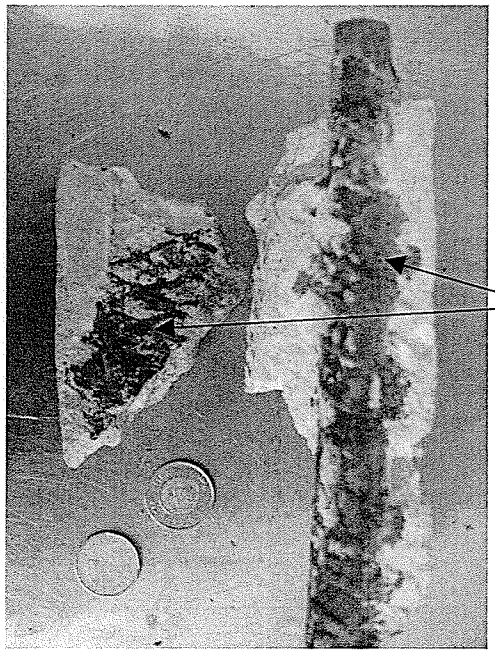

Figure 5-59(a): Typical bar taken from the control slab

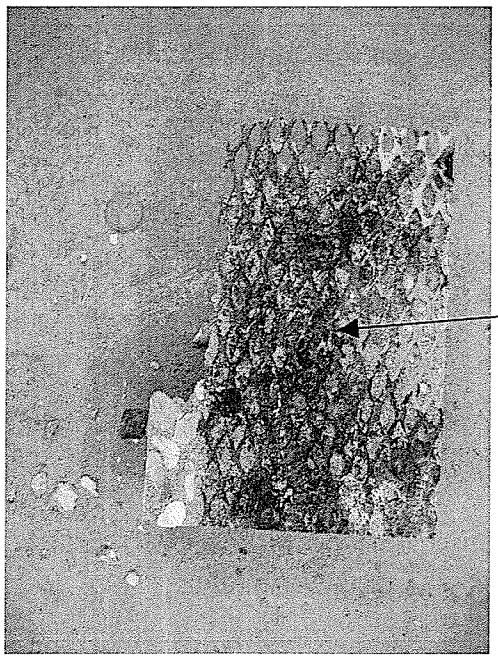

Figure 5-59 (b): Steel Mesh taken from the control slab

5.2 SACRIFICIAL STRIP ANODE ANALYSIS

The objective of the sacrificial "strip" anodes is to provide global protection to structures subjected to corrosion. For the most part, sacrificial anodes are primarily intended to provide corrosion prevention or corrosion control at a moderate level to local corrosion sites. Generally, methods that require external power, such as impressed current systems are used to deal with global corrosion in structures, since the throwing power and magnitude of current generated by these systems is a lot greater than the conventional sacrificial anodes. It was just shown in the results above that the new sacrificial anode system A, was consistently able to reach cathodic protection under almost every circumstance when dealing with bars located approximately 70 mm from the sacrificial anode (bars 1 and 2). As the distance increased, the magnitude of current dropped and therefore, the sacrificial anodes capability in protecting the bars also diminished. In spite of this, the sacrificial anode system A was still able to provide adequate polarization (corrosion control) to even the furthest bar located 363 mm away, under aggressive environments. Many of the commercially available sacrificial anodes were unable to polarize these further bars.

Despite the positive results given by the new sacrificial anode system A, its primary use would most likely still be protection on a local level. In order to utilize this system in a global level, many individual sacrificial anode systems may be required at relatively short spacings, rendering the system impractical for use. Therefore, "strip" anodes were created with the intent of using sacrificial anodes as an economical, and maintenance free way of providing global protection.

In total, three different types of sacrificial strip anode prototypes were tested. For purposes of industry confidentiality the strip anodes will simply be referred to as S, M, and L. It is important to keep in mind that the strip anodes were subjected to all the same conditions as the sacrificial puck anodes, including: concrete mix, specimen geometry, chloride contamination, and exposure conditions. A brief summary and discussion of the results are presented in the following sections.

Table 5-18, shows the average-current density provided by the sacrificial strip anodes along with the sacrificial anode A, subject to 3.9% chloride by weight of cement, and exposed to the environmental chamber. The average is taken only for the time the period the chamber was activated (0-172 days). The factor by which the strip current density is greater or smaller than the Sacrificial Anode A current density is shown in parenthesis.

Table 5-18: Average strip current density

	Average current density, mA/m^2, @ 72.5mm o.c (Bar 1)		Average current density, mA/m^2, @ 72.5mm o.c (Bar 2)		Average current density, mA/m^2, @ 217.5mm o.c (Bar 3)		Average current density, mA/m^2, @ 362.5mm o.c (Bar 4)	
Specimen S	12.08	*(x 1.94)*	12.08	*(x 1.94)*	12.74	*(x 2.58)*	7.09	*(x 1.50)*
Specimen M	4.47	*(x 0.72)*	4.47	*(x 0.99)*	12.74	*(x 2.58)*	8.22	*(x 1.74)*
Specimen L	9.02	*(x 1.45)*	9.02	*(x 2.33)*	10.00	*(x 2.03)*	5.37	*(x 1.14)*
Specimen A	6.24	*(x 1.00)*	6.24	*(x 1.00)*	4.93	*(x 1.00)*	4.72	*(x 1.00)*

Table 5-18, show that the sacrificial strip anodes did remarkably well, providing current density in the cathodic protection region (2-20 mA/m^2) to the Bar 4, located at a distance of 362.5 mm away. Overall, the sacrificial strip anodes where able to provide much greater current to the bars than sacrificial anode A. These results are promising and encourage the use of strip anodes for global protection. The results for half-cell corrosion, current density output, and potential decay are shown in Appendix F.

6.0 CONCLUSION

6.1 SUMMARY

Corrosion in steel reinforced concrete is a crucial ongoing problem affecting modern day infrastructure and costing the economy billions of dollars each year. Corrosion effects can be detrimental to the integrity of a structure and can pose a severe risk to public safety. Corrosion is an electrochemical process that is initiated by the breakdown of the natural protective film, which encases the steel in high alkaline concrete (pH > 12). Chloride is a principal agent in the deterioration of the film and is introduced to the concrete in various ways; the most common is due to deicing salts or structures located in coastal regions.

The objective of this research project was to test a new type of galvanic (sacrificial) anode system for higher current output aimed at providing cathodic protection in harsh environments. Cathodic protection is deemed to be the highest level of protection against corrosion set forth by NACE. Currently, sacrificial anodes available for commercial use only tend to provide minimal protection by means of corrosion prevention or control. The findings in this project revealed the current output limits of this new sacrificial anode A, its range of protection, the degree of protection provided, and its overall comparison to other similar sacrificial anode systems. This project only focused on chloride-induced corrosion.

Galvanic sacrificial anode systems rely on coupling dissimilar metals together. The metal with the higher potential in the electromotive series will have a higher tendency to corrode. This allows the more noble metal (steel) to become the cathode and the less noble metal (i.e. the zinc inside the sacrificial system) to become the anode. By definition the anode is where oxidation occurs and thus where corrosion takes place. The by-product of zinc does not occupy as much volume as the by-product of steel (rust) and therefore, does not cause any serious damage to the concrete. Sacrificial anodes are an attractive tool for combating corrosion since they are relatively inexpensive, require virtually no maintenance, and can extend the service life of a structure by an average of 15 years. The degree of corrosion rate imposed on the steel is influenced by many factors. Primarily, chloride content, temperature and humidity and concrete resistivity are the primary factors influencing corrosion.

The test program was set up to test the different sacrificial systems under various conditions. More specifically, different sacrificial anode was embedded into reinforced concrete slab specimen, and was then subjected to 3.9% or 1.2% chlorides by weight of cement. Studies have shown the chloride threshold varies but is typically taken to by near 1.1 –1.2% chlorides by weight of cement. Half the specimens were tested in the environmental chamber exposed to constant 35C and 90% humidity, while the other half were tested outdoors exposed to the seasonal weather of Winnipeg throughout the months of April to October. Three primary tests were conducted: corrosion potential (or half-cell tests), current output, and potential decay. Corrosion potential indicate the probability of corrosion occurring and gives an indication of the state of the steel. For, instance in high chloride and humid environments the probability of

corrosion is relatively high. Current output was taken to determine the amount of current provided by the sacrificial anodes to the steel reinforcement in the specimens. Corrosion prevention (which is primarily the main use of sacrificial anodes) occurs with current density in the range of 0.25 to 2 mA/m^2. Corrosion control, which is a higher degree of protection, occurs with a current density range of 1 to 7 mA/m^2. Cathodic protection occurs when current density is between 2 to 20 mA/m^2. The wide ranges of current density envelop accounts for the aggressiveness of the environment. Potential decay indicates the amount to which the sacrificial anode was able to polarize the steel from its stable potential. If potential decay reaches 100 mV, the steel becomes cathodically protected.

Polarizing the steel has two main benefits. The primary benefit involves polarizing the cathodic reaction, which therefore, reduces the tendency for the steel to oxidize. This provides immediate protection, but will cease once the flow of current is halted or is insufficient to maintain polarization. The secondary effect, which is often overlooked involves depolarizing the anodic reaction and thereby, generating a less aggressive environment surrounding the steel. Anodic depolarization causes the migration of chlorides away from the anodic region, and raises the alkalinity of the concrete. This in effect promotes the repassivation of the protective film.

The results of the corrosion potential showed a high degree (> 90%) of corrosion initiation at the beginning of the testing period. This was observed in both the chamber and outdoor specimens, subjected to high levels of chlorides. The specimens subjected to low levels of chlorides demonstrated lower potential levels, but still showed high probability of corrosion activity. After the activation of the anodes by use of switches, the trend shows a decrease in potential levels associated with a drop in corrosion probability.

Analysis of the current densities showed Sacrificial Anode A was able to provide almost unanimously higher current levels with respect to the other commercially available sacrificial anodes. Sacrificial anode A was able to sustain an average current density of 6.24 mA/m^2 and 9.87 mA/m^2 for the two nearest bars to the anode in specimens housed in the chamber, subjected to high and low chloride levels, respectively. This current puts the range of protection within the cathodic region. Current density dropped for the bars located at further distances to the anode. Despite the drop, sacrificial anode A, was still able to provide modest protection to the furthest bar located 362 mm off center from the anode, reaching levels as high as 4.72 mA/m^2. Results obtained from the current density for the steel mesh that was placed underneath the bar reinforcements were unusual. Negative current density readings were reported on many anodes systems, signifying a reversal in current direction. This indicated the net flow of current was not to the mesh as would be expected, but instead it was away from the mesh. A possible explanation for this was the creation of several corrosion macro-cells between the mesh and neighboring bars or among the mesh itself. This would have skewed the current readings indicating more current leaving the steel mesh than entering it. Results obtained from the environmental chamber, were comparable to outdoor results. For comparison purposes, a scoring system was implemented based on maximum current density delivered to each bar and the mesh. The system that delivered the highest readings would receive the highest scores. Sacrificial anode A, received in total the highest scores for all the specimens subjected to the different environmental conditions.

Sacrificial anode A was only one of two anode systems capable of sustaining polarization greater than 100 mV for Bars 1 and 2, subjected to high chlorides and exposed to the environmental chamber conditions. This signifies cathodic protection was achieved on these bars. Trends showed protection levels dropped with bars located at further distances as expected. This is due to the decrease in current distribution to the further bars caused by higher resistivity. Protection levels also improved with specimens subjected to lower levels of chlorides. In general, cathodic protection remained elusive for most of the anode systems inside the environmental chamber. In some cases, particularly associated with high chlorides, the sacrificial anode was unable to polarize the corresponding steel and even saw a reduction of potential (or depolarization while the sacrificial was activated). In other terms, while the system was activated (i.e. the circuit was closed), some bars and the mesh was ultimately giving off electrons rather than receiving electrons. This goes against initial expectations, but is associated with the negative current. Once again, the possible explanation for this is the creation of a macro-cell. The bar or the mesh would therefore convert into an anode with respect to a neighboring bar, despite the current being delivered to it from the sacrificial anode. Results from the specimens obtained from the outdoor conditions nearly all achieved cathodic protection. This solidifies the fact that the hot and humid temperature from the environmental chamber was a much more aggressive environment. A scoring system was set up for potential decay based on the maximum potential decay results (polarization), for each condition. The Sacrificial System A scored once again the highest the majority of times.

The presence of chlorides, besides from attacking the passive film, also reduces the resistivity of surrounding concrete. This leads to in increase in electron migration and thus, corrosion rate. Results showed that specimens containing higher levels of chlorides had lower resistivity. If the resistivity is high, this can also affect the capability for the sacrificial anode to protect the reinforcements by providing less current distribution. The results shown in Appendix C show silica fume contaminated concrete slabs (which has a higher resistivity) provided less current to the reinforcement than the slabs not containing any silica fume.

Crude tests to determine the pH levels and chloride content were conducted on specimens with the Sacrificial Anode A and control specimens. These tests were only conducted for the specimens subjected to high chloride levels and exposed the environmental chamber. Findings showed the pH levels increased, and chloride levels dropped substantially when protected with sacrificial system A, as opposed to when no protection was provided (control specimen). Physical observations showed that the bar closest to anode A had very minimal signs of corrosion, while a typical bar embedded in the control specimen had experienced extreme rusting of the steel. Rust was also seen in heavily protruding the surrounding concrete in the control specimen. The steel mesh was also heavily corroded in the control specimen.

Tests were also conducted on a new prototype sacrificial strip anode aimed at providing global protection. Results indicated that current as high as 12.74 mA/m2, and 8.22 mA/m2, was provided to Bars at distance of 217. 5 mm o.c. and 362.5 mm o.c., respectively. These levels are capable of providing cathodic protection at further distances.

Based on the results conducted in this project, Sacrificial Anode A, showed great overall improvement with respect to the existing commercially available anodes. Sacrificial Anode A was able to provide consistently higher levels of current output often reaching levels of cathodic protection. Sacrificial anode A, would therefore be able to be used for corrosion prevention, control or cathodic protection on a local scale. Although, there exist many remedial techniques against corrosion, sacrificial anodes offer a great advantage in localized corrosion problems. It is important to note that the intent of the project is not to support only one certain type of remedial technique, but simply to advance research in corrosion protection of steel in concrete. Sacrificial Anode A and the new strip sacrificial anodes can certainly provide an additional tool for engineers to use in combating the ongoing-crucial corrosion problem.

6.2. RECOMMENDATIONS

To further the understanding and development of sacrificial anodes, continual research should be implemented. Recommendations on the following may be considered:

1) A more focused research can refine the limitations of a particular sacrificial anode under more specific conditions such as: environment, applications, and performance.
2) Frequent monitoring on the environmental conditions, and concrete properties such as pH and chloride content will improve results and understanding
3) Corrosion rate monitoring of steel should also be considered using special instrumentations such as GEO-CORR, would give a better understanding of the performance of the sacrificial anode being tested.
4) Research and development on the mechanics of the sacrificial system and in particular the interaction with the encapsulating mortar.
5) Special precaution should be taken to avoid the development of macro-cells from forming in the setup of a system, as was the case with our project (i.e., the mesh).
6) Also special precautions should be taken to avoid any unwanted corrosion on the exterior connection, such as the switches.

REFERENCES

[1] Whitmore, D. W., and Ball, J. C., "Corrosion Management," ACI, Concrete International, Vol. 26, No. 12, Dec. 2004, pp. 82-84.

[2] NACE International, "Cost of Corrosion Study- Corrosion Costs and Preventive Strategies in the United States," http://www.nae.org/nace/content/publicaffairs/images_cocorr/ccsupp.pdf {last viewed September, 2007}

[3] Dirh, R. K., Dyer, T. D., and Halliday, J. E., "Sustainable Concrete Construction", Thomas Telford Ltd, 2002, pp. 618, London, U.K.

[4] Daily, S. F., "Understanding Corrosion and Cathodic Protection of Reinforced Concrete Structures," Corrpro Companies Inc., http://www.corrpro.com/pdf/CP48.pdf {last viewed October, 2007}

[5] Ahmad, S., "Reinforcement Corrosion in Concrete Structures, its Monitoring and Service Life Prediction – a Review," Elsevier, Cement & Concrete Composites, Vol. 25, Issues 4-5, May-July 2003, pp. 459-471.

[6] Bentur, A., Diamond, S., and Berke, N. S., "Steel Corrosion in Concrete: Fundamentals and Civil Engineering Practice," Taylor & Francis, 1997, pp. 9-10, London, UK.

[7] Isgor, O. B., and Razaqpur, A. G., "Advanced Modelling of Concrete Deterioration Due to Reinforcement Corrosion," Canadian Journal of Civil Engineering, Vol. 33, 2006, pp. 707-718.

[8] Broomfield, J. P., "Corrosion of Steel in Concrete: Understanding, Investigation and Repair," Taylor & Francis, 1997, New York, NY.

[9] Whitmore, D. W., "Impressed Current and Galvanic Discrete Anode Cathodic Protection for Corrosion Protection of Concrete Structures," Corrosion 2002, Paper 02263, http://www.vector-corrosion.com/pdf/SEC_0003/NAC_0007.PDF {last viewed September, 2007}

[10] Khan, M. S., "Detecting Corrosion-Induced Delaminations – An Appraisal of Tools Available," ACI, Concrete International, Vol. 25, No. 7, July 2003, pp. 73-77.

[11] Broomfield, J. P., "Controlling Corrosion of Port Infrastructure," Materials Performance, Vol. 43, No. 10, Oct. 2004, pp. 20-22.

[12] Genesca, J. and Juarez, J., "Development and Testing of Galvanic Anodes for Cathodic Protection," Contributions to Science, 1 (3), 2000, pp. 331-343.

[13] Ball, J. C. and Whitmore, D. W., "Corrosion Mitigation System for Concrete Structures," International Concrete Repair Institute, Concrete Repair Bulletin, July/Aug. 2003, pp. 6-11.

[14] Yunovich, M., and Thompson, N. G., "Corrosion of Highway Bridges: Economic Impact and Control Methodologies," ACI, Concrete International, Vol. 25, No. 1, Jan. 2003, pp.52-57.

[15] Kosmatka, S.H., et al., "Design and Control of Concrete Mixtures," Cement Association of Canada, Seventh Canadian Edition, Ottawa, Cdn, 2002

[16] Bahkt, B., Mufti, A, and Tadros, G., Discussion of "Fibre-Reinforced Polymer Composite Bars for the Concrete Deck Slab of Wotton Bridge," Canadian Journal of Civil Engineering, Vol. 31, 2004, pp. 530-531.

[17] Jordan, L. C. and Page, C. L., "Mortars for Encapsulating Sacrificial Zinc Anodes in Reinforced Concrete," Materials and Corrosion, Vol. 54, Issue 6, 2003, pp. 387-393.

[18] Davison N., Roberts A.C, Taylor J.M., Glass G.K., Aldridge, "Innovative Approaches to Electrochemical Remediation of Concrete," http://www.vector-corrosion.com/pdf/SEC_0003/CON-0001.PDF {last viewed June 2008}

[19] Whiting, D. A., Taylor, P. C., and Nagi, M. A., "Chloride Limits in Reinforced Concrete," Research & Development Information Serial No. 2438, Portland Cement Association, 2002, Illinois.

[20] Montemor, M. F., Simoes, A. M. P., and Ferreira, M. G. S., "Chloride-Induced Corrosion on Reinforcing Steel: From the Fundamentals to the Monitoring Techniques," Elsevier, Cement & Concrete Composites, Vol. 25, Issues 4-5, May-July 2003, pp. 491-502.

[21] Morris, W., Vico, A., and Vazquez, M., "Chloride Induced Corrosion of Reinforcing Steel Evaluated by Concrete Resistivity Measurements," Elsevier, Electrochimica Acta, Vol. 49, Issue 25, October 2004, pp. 4447-4453.

[22] Zivica, V., "Significance and Influence of the Ambient Temperature as a Rate Factor of Steel Reinforcement Corrosion," Bulletin of Material Science, Vol. 25, No. 5, October 2002, pp. 375-379.

[23] Lyons, R., Ing, M., and Austin, S., "Influence of Diurnal and Seasonal Temperature Variations on the Detection of Corrosion in Reinforced Concrete by Acoustic Emission," Elsevier, Corrosion Science, Vol. 47, Issue 2, February 2005, pp. 413-433.

[24] Soroka, I., "Concrete in Hot Environment," Taylor & Francis, 1993, London, UK, pp. 220-221,

[25] Monthly Data Report 2006, Environment Canada, Viewed online. http://www.climate.weatheroffice.ec.gc.ca/climateData/monthlydata_e.html?timeframe=2&Prov=XX&StationID=3698&Year=2006&Month=4&Day=1 {last viewed December, 2008}

[26] Winnipeg climate Livingin-canada, Viewed online. http://www.livingin-canada.com/climate-winnipeg.html {last viewed December, 2008}

[27] ASTM C 876-91 (1999), "Standard Test Method for Half-Cell Potentials of Uncoated Reinforcing Steel in Concrete," ASTM International, West Conshohocken, PA, 1999, DOI: 10.1520/C0876-91R99

[28] Morris, W., Vico, A., Vazquez, M., and de Sanchez, S. R., "Corrosion of Reinforcing Steel Evaluated by Means of Concrete Resistivity Measurements," Elsevier, Corrosion Science, Vol. 44, Issue 1, January 2002, pp. 81-99.

[29] Gu, P., and Beaudoin, J. J., "Obtaining Effective Half-Cell Potential Measurements in Reinforced Concrete Structures," National Research Council Canada, Institute for Research in Construction, Construction Technology Update, No. 18, July 1998, pp. 1-4, Viewed online. http://irc.nrc-cnrc.gc.ca/pubs/ctus/ctu18e.pdf {last viewed November 2007}

[30] Holtsbaum, B., "Application and Misapplication of the 100-mV Criterion for Cathodic Protection," Cathodic and Anodic Protection, Materials Performance, V. 42, No. 1, January 2003, pp. 30-32.

[31] NACE standard TM0497-2002, "Measurement Techniques Related to Criteria for Cathodic Protection on Underground or Submerged Metallic Piping Systems," NACE International the Corrosion Society, Item No. 21231, Houston TX, 2002. Viewed online: http://www.cpsolutionsinc.net/images/NACE_Std._TM0497-2002.pdf {last viewed January 2009}

[32] Pedeferri, P., "Cathodic Protection and Cathodic Prevention," Elsevier, Construction of Building Materials, Vol. 10, No. 5, 1996, pp. 191-402

[33] Polder, R. B. and Peelen, W., "Characterisation of Chloride Transport and Reinforcement Corrosion in Concrete Under Cyclic Wetting and Drying by Electrical Resistivity," Elsevier, Cement & Concrete Composites, Vol. 24, Issue 5, 2002, pp. 427-435.

[34] Gu, P., Beaudoin, J. J., Tumidajski, P. J., and Mailvaganam, N. P., "Electrochemical Incompatibility of Patches in Reinforced Concrete," Concrete International, Vol. 19, No. 8, August 1997, pp. 68-72

[35] Kruger, J., "Electrochemistry Encyclopedia; Electrochemistry of Corrosion," The Johns Hopkins University, Baltimore, USA, April 2001. Viewed online. http://electrochem.cwru.edu/ed/encycl/art-c02-corrosion.htm#diffa {last viewed January 2009}

[36] Glass, G. K., Hassanein, A. M., and Buenfeld, N. R., "Cathodic Protection of Steel in Concrete," Engineering and Physical Science Research Council, Department of Civil and Environmental Engineering, Imperial College, London, http://www.concrete.cv.ic.ac.uk/research/Case/cathodic-protection/cp-main.htm

APPENDIX A

(CONCRETE DESIGN CALCULATIONS)

Concrete Mix Design

- Air entrainer: Wood-resin type, ASTM C260
- Type 10 Cement: rel. dens. 3.15
- Coarse Agg. 20 mm (rounded gravel): rel. dens. 2.68
- Fine Agg. Natural sand: rel. dens = 2.64; F.M. = 2.80; absorption = 0.7%; MC = 6%
- Strength: Design for f'c = 25 Mpa
    - Using Table 9-11 (adjustment for deviations)
    - $f'c_r = 25 + 8.5 = 33.5$ MPa
- w/c ratio
    - Using Table 9-3
        - For $f'c_r = 33.5$, air-entrained = 0.42 (conservative assumption)
    - Target w/c = 0.48 (from table 9-2), f'c = 25 MPa
- Air content
    - For category 2 (not exposed to freeze thaw)
    - Air content btw 4 to 7 %
    - Use 7 %
- Slump
    - Use slump of 75 ± 20 mm
- Water content
    - Using Table 9-5
        - 75 mm slump, air-entrained, 20 mm:
            - 184 kg/m^3
        - However, reduce by 25 kg/m^3 since we are using rounded gravel so water content = 184-25 = 159 kg/m^3
- Cement content
    - w/c = 0.48;
    - Therefore, c = 159/0.48 = 331 kg/m^3 > 320 kg/m^3 min (Table 9-7)
- Coarse Aggregates
    - Bulk density (ovendry) = 1600 kg/m^3
    - Fineness moduli = 2.80
    - Using table 9-4 (20 mm Coarse Agg. & F.M. = 2.8)
        - Bulk volume = 0.62
        - Coarse Agg. = 0.62x 1600 = 992 kg/m^3
- Fine Aggregates
    - Room Temp = 22 C; Density of Water = 997.75 kg/m^3
    - Water = 159/(1 x 997.75) = 0.159 m^3
    - Cement = 331/(3.15 x 997.75) = 0.105 m^3
    - Air = 7/100 = 0.07 m^3
    - Coarse = 992/(2.68 x 997.75) = 0.371 m^3
    - Fine = 1-(0.159 + 0.105 + 0.07 + 0.371) = 0.295 m^3
    - Mass fine agg. = 0.295 x 2.64 x 997.75 = 777 kg/m^3

- Moisture Content Adjustment
  - Coarse Agg (2 % MC) = 992x 1.02 = 1012 kg/m^3
  - Fine Agg (6 % MC) = 777x 1.06 = 824 kg/m^3
  - Water to be added = 159 – (992 x 0.015)-(777 x 0.053) =103 kg/m^3
- Air-entrainer
  - Manufacture recommends 0.5g of entrainer per 1 kg of cement
  - Therefore, 0.5x 331 = 165.5 = 166 g = 0.166 kg air-entrainer

Final Concrete Mix

- Water 103 kg/m^3
- Cement 331 kg/m^3
- C. agg. 1012 kg/m^3
- F. agg. 824 kg/m^3
- Air Content 4 to 7 %
- Slump 75 ± 20 mm
- Air entrainer 0.166 kg/m^3
- w/c 0.48

APPENDIX B

(DAILY WINNIPEG CLIMATE REPORT)

Environment Canada Environnement Canada

[français] [Back]

Daily Data Report for May 2006

Notes on Data Quality.

WINNIPEG RICHARDSON INT'L A
MANITOBA

Latitude: 49° 55.200' N Longitude: 97° 13.800' W Elevation: 238.70 m
Climate ID: 5023222 WMO ID: 71852 TC ID: YWG

Daily Data Report for May 2006

Day	Max Temp °C	Min Temp °C	Mean Temp °C	Heat Deg Days °C	Cool Deg Days °C	Total Rain mm	Total Snow cm	Total Precip mm	Snow on Grnd cm	Dir of Max Gust 10's Deg	Spd of Max Gust km/h
01	14.5	10.3	12.4	5.6	0.0	3.0	0.0	3.0	0		
02	18.0	6.9	12.5	5.5	0.0	8.0	0.0	8.0	0		
03	12.6	2.7	7.7	10.3	0.0	3.0	0.0	3.0	0		
04	4.4	-2.8	0.8	17.2	0.0	0.0	0.0	0.0	0		
05	13.9	-4.8	4.6	13.4	0.0	1.0	0.0	1.0	0		
06	19.3	-2.1	8.6	9.4	0.0	0.0	0.0	0.0	0		
07	27.7	9.9	18.8	0.0	0.8	0.5	0.0	0.5	0		
08	22.3	9.5	15.9	2.1	0.0	0.5	0.0	0.5	0		
09	20.4	7.8	14.1	3.9	0.0	8.5	0.0	8.5	0		
10	12.4	2.5	7.5	10.5	0.0	1.5	0.0	1.5	0		
11	10.5	-1.9	4.3	13.7	0.0	0.0	0.0	0.0	0		
12	15.4	-0.9	7.3	10.7	0.0	0.0	0.0	0.0	0		
13	13.5	6.1	9.8	8.2	0.0	1.5	0.0	1.5	0		
14	14.2	5.3	9.8	8.2	0.0	0.0	0.0	0.0	0		
15	14.9	1.9	8.4	9.6	0.0	0.0	0.0	0.0	0		
16	22.9	-1.2	10.9	7.1	0.0	0.0	0.0	0.0	0		
17	19.1	2.2	10.7	7.3	0.0	0.0	0.0	0.0	0		
18	15.2	0.9	8.1	9.9	0.0	1.0	0.0	1.0	0		
19	20.3	7.9	14.1	3.9	0.0	1.5	0.0	1.5	0		
20	13.1	2.2	7.7	10.3	0.0	2.0	0.0	2.0	0		
21	14.0	-3.2	5.4	12.6	0.0	0.0	0.0	0.0	0		
22	24.1	5.1	14.6	3.4	0.0	0.5	0.0	0.5	0		
23	29.4	13.8	21.6	0.0	3.6	1.0	0.0	1.0	0		
24	27.5	17.0	22.3	0.0	4.3	0.0	0.0	0.0	0		
25	18.2	6.2	12.2	5.8	0.0	0.0	0.0	0.0	0		
26	19.6	4.6	12.1	5.9	0.0	0.0	0.0	0.0	0		
27	23.6	14.6	19.1	0.0	1.1	6.5	0.0	6.5	0		
28	23.6	13.7	18.7	0.0	0.7	1.5	0.0	1.5	0		
29	22.5	12.5	17.5	0.5	0.0	0.0	0.0	0.0	0		
30	22.6	11.5	17.1	0.9	0.0	0.0	0.0	0.0	0		
31	24.9	10.2	17.6	0.4	0.0	3.0	0.0	3.0	0		
Sum				196.3	10.5	44.5	0.0	44.5			
Avg	18.5	5.4	12.0								
Xtrm	29.4	-4.8									

Legend

[empty] = No data available
M = Missing
E = Estimated
A = Accumulated
C = Precipitation occurred, amount uncertain
L = Precipitation may or may not have occurred
F = Accumulated and estimated
N = Temperature missing but known to be > 0
Y = Temperature missing but known to be < 0
S = More than one occurrence
T = Trace
* = The value displayed is based on incomplete data
† = Data for this day has undergone only preliminary quality checking

Navigation Options

Canada Map
Manitoba Map
Customized Search
Nearby Stations with Data
1971-2000 Climate Normals
Customizable Chart
Monthly Data (2006)
Bulk Data (2006) [CSV] [XML]

Environment Canada / Environnement Canada

[français] [Back]

Daily Data Report for June 2006

Notes on Data Quality

WINNIPEG RICHARDSON INT'L A
MANITOBA

Latitude: 49° 55.200' N Longitude: 97° 13.800' W Elevation: 238.70 m
Climate ID: 5023222 WMO ID: 71852 TC ID: YWG

Daily Data Report for June 2006

Day	Max Temp °C	Min Temp °C	Mean Temp °C	Heat Deg Days °C	Cool Deg Days °C	Total Rain mm	Total Snow cm	Total Precip mm	Snow on Grnd cm	Dir of Max Gust 10's Deg	Spd of Max Gust km/h
01	24.7	7.6	16.2	1.8	0.0	0.0	0.0	0.0	0		
02	27.5	7.0	17.5	0.5	0.0	0.0	0.0	0.0	0		
03	29.4	16.4	23.1	0.0	5.1	0.0	0.0	0.0	0		
04	24.1	15.9	20.4	0.0	2.4	0.5	0.0	0.5	0		
05	25.7	13.2	19.5	0.0	1.5	7.5	0.0	7.5	0		
06	25.5	13.1	19.4	0.0	1.4	1.5	0.0	1.5	0		
07	21.3	10.3	16.1	1.9	0.0	0.0	0.0	0.0	0		
08	14.9	6.0	10.5	7.5	0.0	0.0	0.0	0.0	0		
09	18.7	11.8	15.3	2.7	0.0	0.0	0.0	0.0	0		
10	21.4	11.8	16.6	1.4	0.0	0.0	0.0	0.0	0		
11	23.6	9.9	16.8	1.2	0.0	0.0	0.0	0.0	0		
12	24.9	11.4	18.2	0.0	0.2	0.5	0.0	0.5	0		
13	23.9	7.7	15.8	2.2	0.0	0.0	0.0	0.0	0		
14	27.2	9.3	18.3	0.6	0.3	0.0	0.0	0.0	0		
15	27.3	16.8	22.2	0.0	4.2	0.0	0.0	0.0	0		
16	29.3	20.0	24.7	0.0	6.7	1.0	0.0	1.0	0		
17	28.7	16.3	22.5	0.0	4.5	2.6	0.0	2.0	0		
18	21.6	8.8	15.2	2.8	0.0	2.5	0.0	2.5	0		
19	27.6	5.8	16.7	1.3	0.0	0.0	0.0	0.0	0		
20	26.5	15.1	21.0	0.0	3.0	0.5	0.0	0.5	0		
21	23.2	6.7	15.0	3.0	0.0	0.5	0.0	0.5	0		
22	23.6	4.5	14.1	3.9	0.0	0.0	0.0	0.0	0		
23	25.5	10.0	17.8	0.2	0.0	0.0	0.0	0.0	0		
24	24.4	8.2	16.3	1.7	0.0	12.0	0.0	12.0	0		
25	27.3	8.9	18.0	0.0	0.0	0.0	0.0	0.0	0		
26	24.6	9.8	17.2	0.8	0.0	0.5	0.0	0.5	0		
27	24.3	6.7	15.5	2.2	0.0	0.0	0.0	0.0	0		
28	27.2	10.7	19.0	0.0	1.0	0.0	0.0	0.0	0		
29	30.2	14.8	22.5	0.0	4.5	0.0	0.0	0.0	0		
30	29.5	18.1	23.8	0.0	5.8	0.0	0.0	0.0	0		
Sum				35.3	60.6	29.0	0.0	29.0			
Avg	25.2	11.1	18.2								
Xtrm	30.2	4.5									

Legend

[empty] = No data available
M = Missing
E = Estimated
A = Accumulated
C = Precipitation occurred, amount uncertain
L = Precipitation may or may not have occurred
F = Accumulated and estimated
N = Temperature missing but known to be > 0
Y = Temperature missing but known to be < 0
S = More than one occurrence
T = Trace
* = The value displayed is based on incomplete data
† = Data for this day has undergone only preliminary quality checking

Navigation Options

Canada Map
Manitoba Map
Customized Search
Nearby Stations with Data
1971-2000 Climate Normals
Customizable Chart
Monthly Data (2006)
Bulk Data (2006) [CSV] [XML]

Environment Canada Environnement Canada

[français] [Back]

Daily Data Report for July 2006

Notes on Data Quality

WINNIPEG RICHARDSON INT'L A
MANITOBA

Latitude: 49° 55.200' N Longitude: 97° 13.800' W Elevation: 238.70 m
Climate ID: 5023222 WMO ID: 71852 TC ID: YWG

Daily Data Report for July 2006

D a y	Max Temp °C	Min Temp °C	Mean Temp °C	Heat Deg Days °C	Cool Deg Days °C	Total Rain mm	Total Snow cm	Total Precip mm	Snow on Grnd cm	Dir of Max Gust 10's Deg	Spd of Max Gust km/h
01	29.3	16.0	22.7	0.0	4.7	0.0	0.0	0.0	0		
02	28.7	12.5	20.6	0.0	2.6	0.0	0.0	0.0	0		
03	23.1	8.9	16.0	2.0	0.0	0.0	0.0	0.0	0		
04	26.2	6.4	16.3	1.7	0.0	0.0	0.0	0.0	0		
05	28.3	9.7	19.0	0.0	1.0	0.0	0.0	0.0	0		
06	33.3	16.6	24.8	0.0	6.8	0.0	0.0	0.0	0		
07	32.1	19.6	25.9	0.0	7.9	0.0	0.0	0.0	0		
08	29.2	13.2	21.2	0.0	3.2	0.0	0.0	0.0	0		
09	19.1	7.8	13.5	4.5	0.0	0.0	0.0	0.0	0		
10	26.3	6.6	16.6	1.4	0.0	0.0	0.0	0.0	0		
11	32.6	16.6	24.6	0.0	6.6	0.0	0.0	0.0	0		
12	35.9	13.6	24.8	0.0	6.8	0.0	0.0	0.0	0		
13	29.3	19.9	24.6	0.0	6.9	4.5	0.0	4.5	0		
14	32.5	17.0	24.8	0.0	6.8	0.0	0.0	0.0	0		
15	32.1	14.9	23.5	0.0	5.5	0.0	0.0	0.0	0		
16	34.5	13.4	24.0	0.0	6.0	0.0	0.0	0.0	0		
17	27.5	11.8	19.7	0.0	1.7	0.0	0.0	0.0	0		
18	30.3	12.9	21.5	0.0	3.5	0.0	0.0	0.0	0		
19	29.8	12.9	21.4	0.0	3.4	0.0	0.0	0.0	0		
20	27.9	11.3	19.6	0.0	1.6	0.0	0.0	0.0	0		
21	31.2	12.7	22.0	0.0	4.0	0.0	0.0	0.0	0		
22	31.8	12.9	22.4	0.0	4.4	0.0	0.0	0.0	0		
23	35.3	17.2	26.3	0.0	8.3	0.0	0.0	0.0	0		
24	31.0	13.4	22.2	0.0	4.2	0.0	0.0	0.0	0		
25	27.0	15.4	21.2	0.0	3.2	5.5	0.0	5.5	0		
26	30.4	12.2	21.3	0.0	3.3	0.0	0.0	0.0	0		
27	33.1	14.8	24.0	0.0	6.0	0.0	0.0	0.0	0		
28	21.7	12.2	17.0	1.0	0.0	0.5	0.0	0.5	0		
29	24.5	8.2	16.5	1.5	0.0	0.0	0.0	0.0	0		
30	34.3	12.6	23.6	0.0	5.6	0.0	0.0	0.0	0		
31	33.3	14.7	24.0	0.0	6.0	0.0	0.0	0.0	0		
Sum				12.1	120.0	10.5	0.0	10.5			
Avg	29.8	13.2	21.5								
Xtrm	35.9	6.4									

Legend

[empty] = No data available
M = Missing
E = Estimated
A = Accumulated
C = Precipitation occurred, amount uncertain
L = Precipitation may or may not have occurred
F = Accumulated and estimated
N = Temperature missing but known to be > 0
Y = Temperature missing but known to be < 0
S = More than one occurrence
T = Trace
* = The value displayed is based on incomplete data
† = Data for this day has undergone only preliminary quality checking

Navigation Options

Canada Map
Manitoba Map
Customized Search
Nearby Stations with Data
1971-2000 Climate Normals
Customizable Chart
Monthly Data (2006)
Bulk Data (2006) [CSV] [XML]

Important Notices

Created : 2002-06-21
Modified : 2005-04-08
Reviewed : 2005-04-08
Url of this page: http://www.climate.weatheroffice.ec.gc.ca/climateData/dailydata_e.html

The Green Lane™, Environment Canada's World Wide Web Site.

Canada

Environment Canada / Environnement Canada

[français] [Back]

Daily Data Report for August 2006

Notes on Data Quality

WINNIPEG RICHARDSON INT'L A
MANITOBA

Latitude: 49° 55.200' N Longitude: 97° 13.800' W Elevation: 238.70 m
Climate ID: 5023222 WMO ID: 71852 TC ID: YWG

Daily Data Report for August 2006

Day	Max Temp °C	Min Temp °C	Mean Temp °C	Heat Deg Days °C	Cool Deg Days °C	Total Rain mm	Total Snow cm	Total Precip mm	Snow on Grnd cm	Dir of Max Gust 10's Deg	Spd of Max Gust km/h
01	25.2	12.4	20.3	0.0	2.3	0.0	0.0	0.0	0		
02	30.8	13.9	22.4	0.0	4.4	2.0	0.0	2.0	0		
03	27.4	10.9	19.2	0.0	1.2	0.5	0.0	0.5	0		
04	25.7	13.9	19.8	0.0	1.8	5.5	0.0	5.5	0		
05	25.7	16.1	22.9	0.0	4.9	4.0	0.0	4.0	0		
06	24.9	11.3	18.1	0.0	0.1	0.0	0.0	0.0	0		
07	21.7	7.6	17.7	0.3	0.0	0.0	0.0	0.0	0		
08	32.5	16.6	24.6	0.0	6.6	0.0	0.0	0.0	0		
09	31.1	19.9	25.5	0.0	7.5	0.0	0.0	0.0	0		
10	26.2	18.4	22.3	0.0	4.3	20.0	0.0	20.0	0		
11	24.1	17.6	22.9	0.0	4.9	0.0	0.0	0.0	0		
12	24.3	17.4	20.9	0.0	2.9	10.5	0.0	10.5	0		
13	23.5	12.6	18.1	0.0	0.1	0.0	0.0	0.0	0		
14	24.4	11.4	17.9	0.1	0.0	0.0	0.0	0.0	0		
15	27.9	9.3	18.6	0.0	0.6	0.0	0.0	0.0	0		
16	22.8	16.5	20.2	0.0	2.2	0.0	0.0	0.0	0		
17	21.0	13.5	20.3	0.0	2.3	0.0	0.0	0.0	0		
18	24.9	9.9	17.4	0.6	0.0	0.0	0.0	0.0	0		
19	23.7	7.0	17.9	0.1	0.0	0.0	0.0	0.0	0		
20	31.4	13.0	22.2	0.0	4.2	0.5	0.0	0.5	0		
21	23.6	8.9	16.3	1.7	0.0	0.0	0.0	0.0	0		
22	27.3	5.8	16.6	1.4	0.0	0.0	0.0	0.0	0		
23	29.9	15.6	21.8	0.0	3.8	0.0	0.0	0.0	0		
24	28.8	15.4	21.6	0.0	3.6	0.0	0.0	0.0	0		
25	26.0	12.9	19.5	0.0	1.5	4.0	0.0	4.0	0		
26	23.2	10.6	13.9	0.0	0.9	5.0	0.0	5.0	0		
27	30.7	8.1	19.4	0.0	1.4	0.0	0.0	0.0	0		
28	22.7	8.0	15.4	2.6	0.0	0.0	0.0	0.0	0		
29	24.5	6.8	15.7	2.3	0.0	0.0	0.0	0.0	0		
30	27.1	13.1	20.1	0.0	2.1	0.0	0.0	0.0	0		
31	25.8	13.2	19.5	0.0	1.5	0.0	0.0	0.0	0		
Sum				9.1	65.1	52.0	0.0	52.0			
Avg	27.0	12.5	19.8								
Xtrm	32.5	5.8									

Legend

[empty] = No data available
M = Missing
E = Estimated
A = Accumulated
C = Precipitation occurred, amount uncertain
L = Precipitation may or may not have occurred
F = Accumulated and estimated
N = Temperature missing but known to be > 0
Y = Temperature missing but known to be < 0
S = More than one occurrence
T = Trace
* = The value displayed is based on incomplete data
† = Data for this day has undergone only preliminary quality checking

Navigation Options

Canada Map
Manitoba Map
Customized Search
Nearby Stations with Data
1971-2000 Climate Normals
Customizable Chart
Monthly Data (2006)
Bulk Data (2006) [CSV] [XML]

Environment Canada | Environnement Canada

[français] [Back]

Daily Data Report for September 2006

Notes on Data Quality

WINNIPEG RICHARDSON INT'L A
MANITOBA

Latitude: 49° 55.200' N Longitude: 97° 13.800' W Elevation: 238.70 m
Climate ID: 5023222 WMO ID: 71852 TC ID: YWG

Daily Data Report for September 2006

Day	Max Temp °C	Min Temp °C	Mean Temp °C	Heat Deg Days °C	Cool Deg Days °C	Total Rain mm	Total Snow cm	Total Precip mm	Snow on Grnd cm	Dir of Max Gust 10's Deg	Spd of Max Gust km/h
01	22.3	8.1	15.2	2.8	0.0	0.0	0.0	0.0	0		
02	24.4	4.8	14.6	3.4	0.0	0.0	0.0	0.0	0		
03	27.1	7.6	17.4	0.6	0.0	0.0	0.0	0.0	0		
04	29.2	7.2	18.2	0.0	0.2	0.0	0.0	0.0	0		
05	30.7	12.8	21.8	0.0	3.8	0.0	0.0	0.0	0		
06	27.5	9.7	18.6	0.0	0.6	0.0	0.0	0.0	0		
07	23.6	7.0	15.3	2.7	0.0	0.0	0.0	0.0	0		
08	16.4	-1.3	7.6	10.4	0.0	0.0	0.0	0.0	0		
09	19.6	1.1	10.4	7.6	0.0	0.0	0.0	0.0	0		
10	22.3	4.4	13.4	4.6	0.0	0.0	0.0	0.0	0		
11	21.7	6.7	14.2	3.8	0.0	0.0	0.0	0.0	0		
12	27.4	8.5	18.0	0.0	0.0	0.0	0.0	0.0	0		
13	29.5	9.9	19.7	0.0	1.7	0.0	0.0	0.0	0		
14	29.8	17.1	23.5	0.0	5.5	0.0	0.0	0.0	0		
15	31.6	13.9	22.8	0.0	4.8	0.5	0.0	0.5	0		
16	19.9	13.5	16.7	1.3	0.0	3.5	0.0	3.5	0		
17	13.6	9.0	11.3	6.7	0.0	28.0	0.0	28.0	0		
18	9.0	4.6	6.8	11.2	0.0	4.5	0.0	4.5	0		
19	10.8	1.0	5.9	12.1	0.0	0.0	0.0	0.0	0		
20	M	2.0	M	M	M	0.0	0.0	0.0	0		
21	17.2	3.4	10.3	7.7	0.0	0.0	0.0	0.0	0		
22	16.8	5.9	11.4	6.6	0.0	0.0	0.0	0.0	0		
23	16.5	5.1	10.8	7.2	0.0	0.0	0.0	0.0	0		
24	21.2	7.2	14.2	3.8	0.0	1.0	0.0	1.0	0		
25	18.7	5.2	12.0	6.0	0.0	0.5	0.0	0.5	0		
26	15.7	5.8	10.8	7.2	0.0	1.0	0.0	1.0	0		
27	12.9	0.6	6.8	11.2	0.0	0.0	0.0	0.0	0		
28	10.9	-1.4	4.8	13.2	0.0	2.5	0.0	2.5	0		
29	16.1	4.8	10.5	7.5	0.0	0.0	0.0	0.0	0		
30	17.7	4.8	11.3	6.7	0.0	0.0	0.0	0.0	0		
Sum				144.3*	16.6*	41.5	0.0	41.5			
Avg	20.1E	4.3	13.6E								
Xtrm	31.6E	-1.4									

Legend

[empty] = No data available
M = Missing
E = Estimated
A = Accumulated
C = Precipitation occurred, amount uncertain
L = Precipitation may or may not have occurred
F = Accumulated and estimated
N = Temperature missing but known to be > 0
Y = Temperature missing but known to be < 0
S = More than one occurrence
T = Trace
* = The value displayed is based on incomplete data
† = Data for this day has undergone only preliminary quality checking

Navigation Options

Canada Map
Manitoba Map
Customized Search
Nearby Stations with Data
1971-2000 Climate Normals
Customizable Chart
Monthly Data (2006)
Bulk Data (2006) [CSV] [XML]

Environment Canada Environnement Canada

[français] [Back]

Daily Data Report for October 2006

Notes on Data Quality

WINNIPEG RICHARDSON INT'L A
MANITOBA

Latitude: 49° 55.200' N Longitude: 97° 13.800' W Elevation: 238.70 m
Climate ID: 5023222 WMO ID: 71852 TC ID: YWG

Daily Data Report for October 2006

Day	Max Temp °C	Min Temp °C	Mean Temp °C	Heat Deg Days °C	Cool Deg Days °C	Total Rain mm	Total Snow cm	Total Precip mm	Snow on Grnd cm	Dir of Max Gust 10's Deg	Spd of Max Gust km/h
01	26.1	6.7	16.4	1.6	0.0	0.0	0.0	0.0	0		
02	20.0	4.9	12.5	5.5	0.0	0.0	0.0	0.0	0		
03	13.5	-0.6	6.5	11.5	0.0	0.0	0.0	0.0	0		
04	15.0	-2.6	6.2	11.8	0.0	0.0	0.0	0.0	0		
05	13.8	2.7	10.8	7.2	0.0	0.0	0.0	0.0	0		
06	18.6	9.3	14.0	4.0	0.0	0.0	0.0	0.0	0		
07	23.6	11.6	17.6	0.4	0.0	0.0	0.0	0.0	0		
08	14.3	-3.8	5.3	12.7	0.0	0.0	0.0	0.0	0		
09	11.4	-0.8	5.3	12.7	0.0	0.0	0.0	0.0	0		
10	8.5	-4.1	2.1	15.9	0.0	0.0	2.5E	2.5E	0		
11	1.3	-5.7	-2.2	20.2	0.0	M	M	M	M		
12	4.3	-3.1	0.6	17.4	0.0	M	M	M	M		
13	4.9	-1.6	1.7	16.3	0.0	0.0	0.0	0.0	M		
14	7.5	-4.8	1.4	16.6	0.0	0.0	0.0	0.0	M		
15	10.2	-4.8	2.7	15.3	0.0	0.0	0.0	0.0	M		
16	6.5	3.3	5.1	12.9	0.0	8.5	0.0	8.5	M		
17	3.4	0.7	2.1	15.9	0.0	0.0	0.0	0.0	M		
18	2.4	-4.1	-0.9	18.9	0.0	0.0	0.0	0.0	M		
19	4.5	-5.2	-0.4	18.4	0.0	0.0	0.0	0.0	M		
20	3.3	-7.1	-1.9	19.9	0.0	0.0	0.0	0.0	M		
21	2.3	-8.0	-2.9	20.9	0.0	0.0	0.0	0.0	M		
22	1.5	-1.7	-0.1	18.1	0.0	0.0	0.0	0.0	M		
23	2.8	-2.0	0.4	17.6	0.0	0.0	0.0	0.0	M		
24	6.7	-1.6	2.6	15.4	0.0	0.0	0.0	0.0	M		
25	9.7	-4.0	2.9	15.1	0.0	0.0	0.0	0.0	M		
26	13.9	0.7	7.3	10.7	0.0	0.0	0.0	0.0	M		
27	11.2	-2.3	4.5	13.5	0.0	0.0	0.0	0.0	M		
28	7.6	-8.1	-0.3	18.3	0.0	0.0	0.0	0.0	M		
29	0.7	-7.5	-3.4	21.4	0.0	M	M	M	M		
30	-0.5	-4.4	-2.5	20.5	0.0	M	M	M	M		
31	-2.1	-5.3	-4.1	22.1	0.0	M	M	M	M		
Sum				448.7	0.0	8.5*	2.5*	11.0*			
Avg	8.7	-1.7	3.5								
Xtrm	26.1	-8.1									

Legend

[empty] = No data available
M = Missing
E = Estimated
A = Accumulated
C = Precipitation occurred, amount uncertain
L = Precipitation may or may not have occurred
F = Accumulated and estimated
N = Temperature missing but known to be > 0
Y = Temperature missing but known to be < 0
S = More than one occurrence
T = Trace
* = The value displayed is based on incomplete data
† = Data for this day has undergone only preliminary quality checking

Navigation Options

Canada Map
Manitoba Map
Customized Search
Nearby Stations with Data
1971-2000 Climate Normals
Customizable Chart
Monthly Data (2006)
Bulk Data (2006) [CSV] [XML]

▲

Important Notices

Created: 2002-06-21
Modified: 2005-04-08
Reviewed: 2005-04-08
Url of this page: http://www.climate.weatheroffice.ec.gc.ca/climateData/dailydata_e.html

The Green Lane™
Environment Canada's World Wide Web Site.

Canada

APPENDIX C

(PUCK ANODES: INITIAL CURRENT DENSITY RESULTS)

Table C-1: Average initial current density for Bars 1 and 2 subjected to 3.9% chlorides by weight of cement and exposed to Winnipeg climate

Sacrificial anode	Average initial current density at time zero for bars 1 and 2, mA/m^2
A	53.9
B	53.4
C	67.0
D	58.5
E	41.2

Table C-2: Average initial current density for Bars 1 and 2 subjected to 1.2% chlorides by weight of cement and exposed to Winnipeg climate

Sacrificial anode	Average initial current density at time zero for bars 1 and 2, mA/m^2
A	50.0
B	35.5
C	58.5
D	41.9
E	21.7

APPENDIX D

(RESISTIVITY CURRENT DENSITY RESULTS)

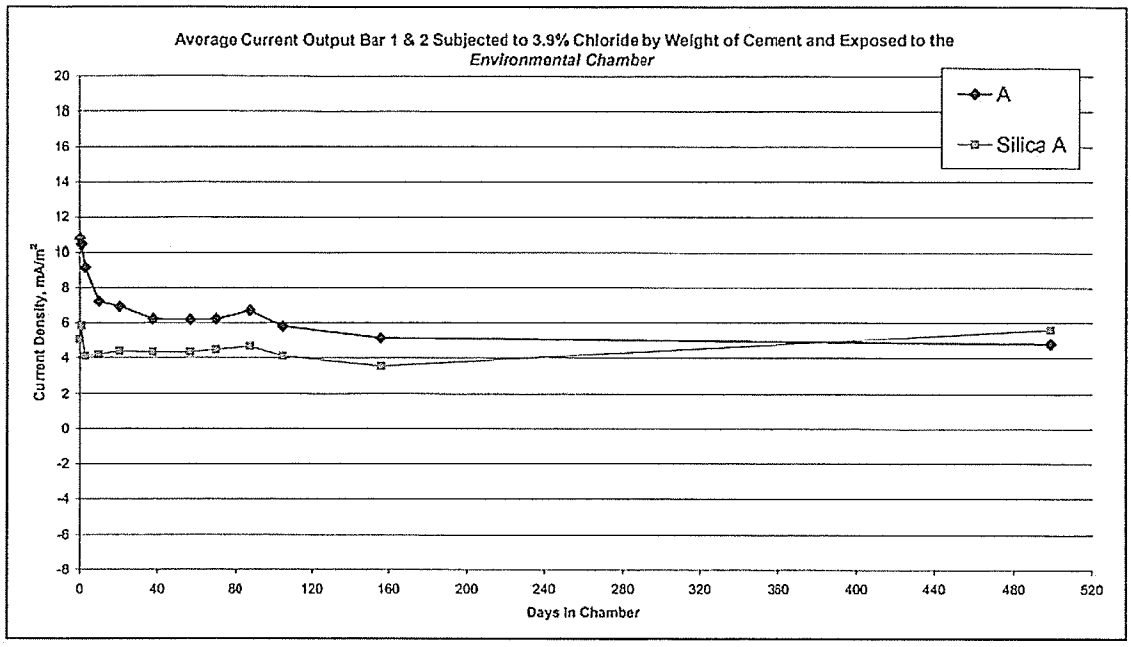
Average Current Output Bar 1 & 2 Subjected to 3.9% Chloride by Weight of Cement and Exposed to the Environmental Chamber
A
Silica A
Current Density, mA/m²
Days in Chamber
20
18
16
14
12
10
8
6
4
2
0
-2
-4
-6
-8
0
40
80
120
160
200
240
280
320
360
400
440
480
520

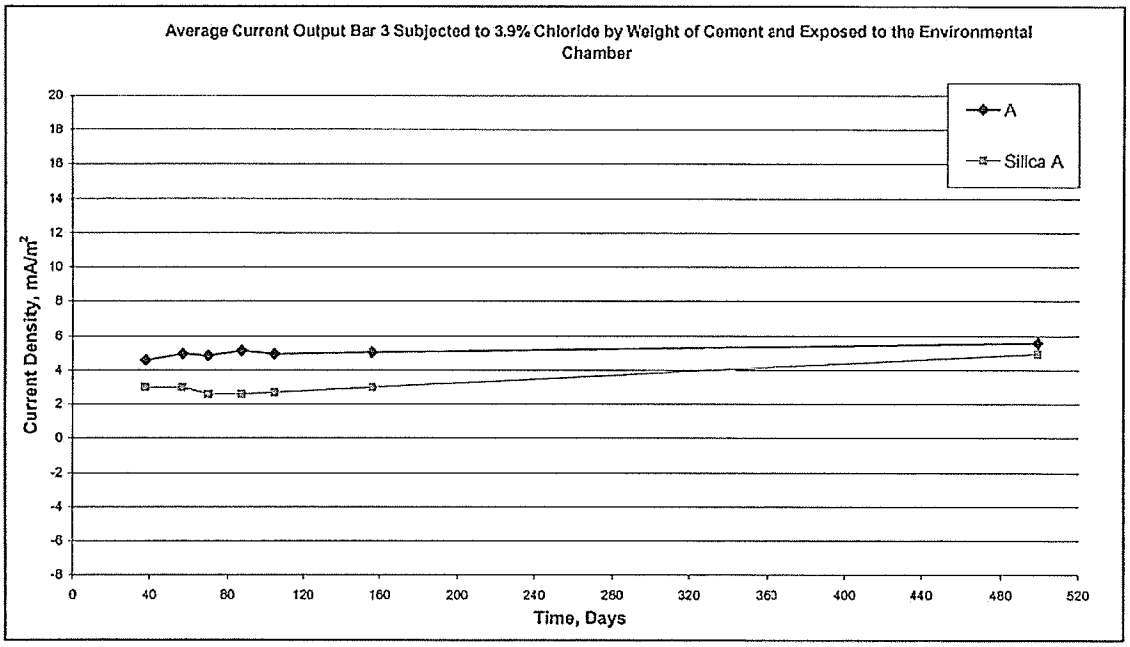
Average Current Output Bar 3 Subjected to 3.9% Chloride by Weight of Cement and Exposed to the Environmental Chamber
A
Silica A
Current Density, mA/m²
Time, Days
20
18
16
14
12
10
8
6
4
2
0
-2
-4
-6
-8
0
40
80
120
160
200
240
280
320
360
400
440
480
520

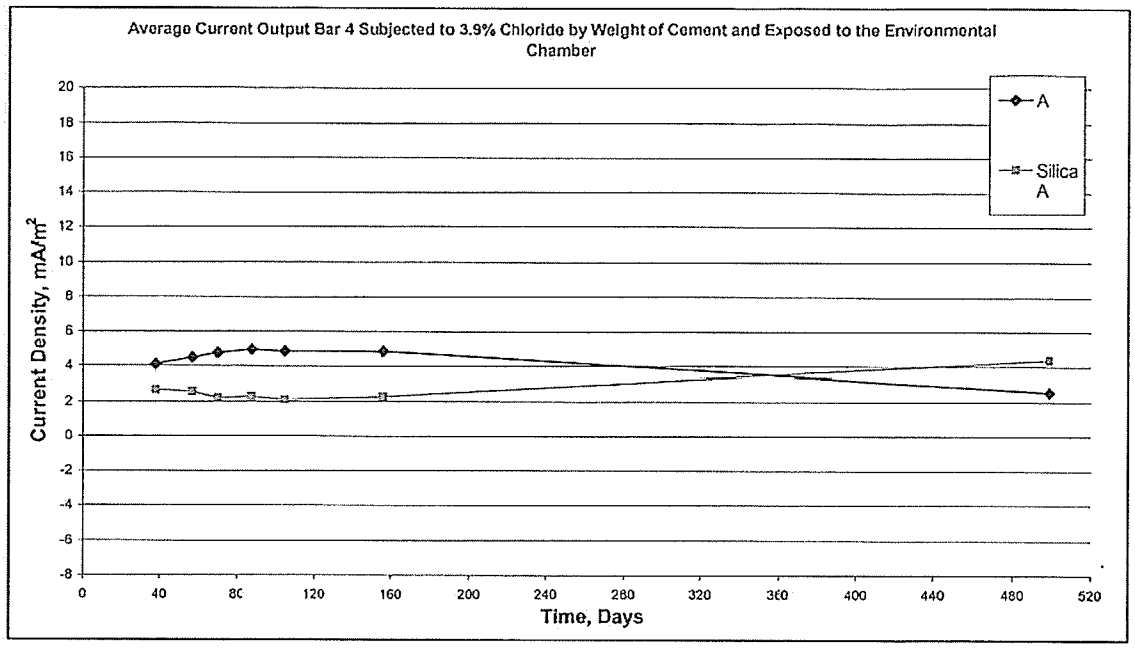
Average Current Output Bar 4 Subjected to 3.9% Chloride by Weight of Cement and Exposed to the Environmental Chamber
Current Density, mA/m2
Time, Days
A
Silica A

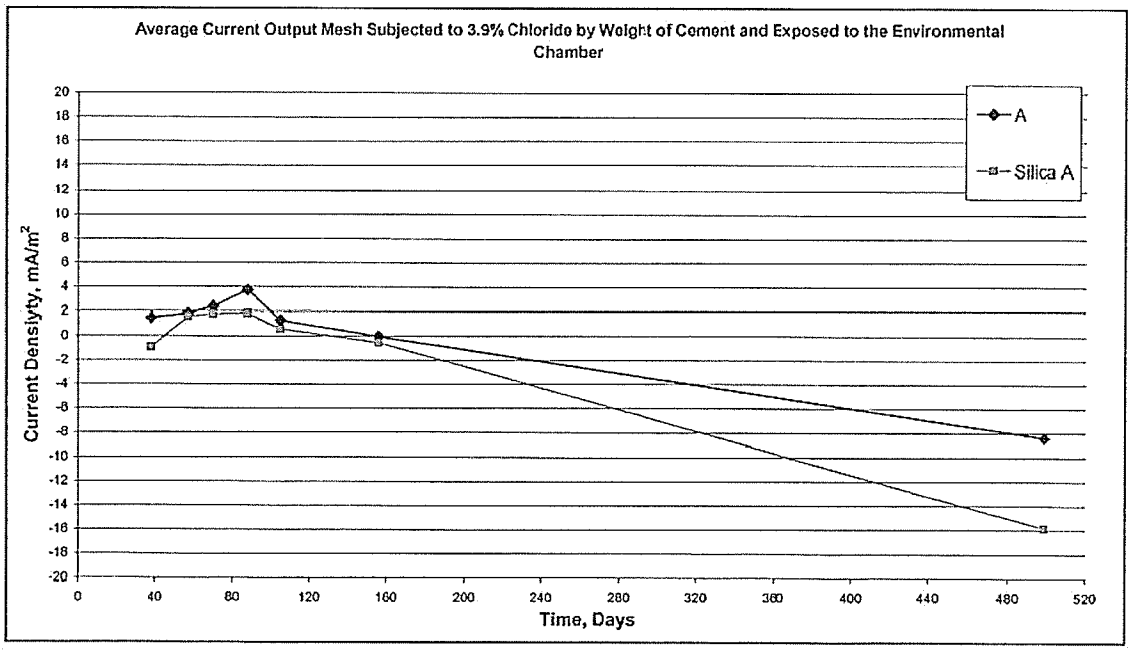
Average Current Output Mesh Subjected to 3.9% Chloride by Weight of Cement and Exposed to the Environmental Chamber
Current Density, mA/m2
Time, Days
A
Silica A

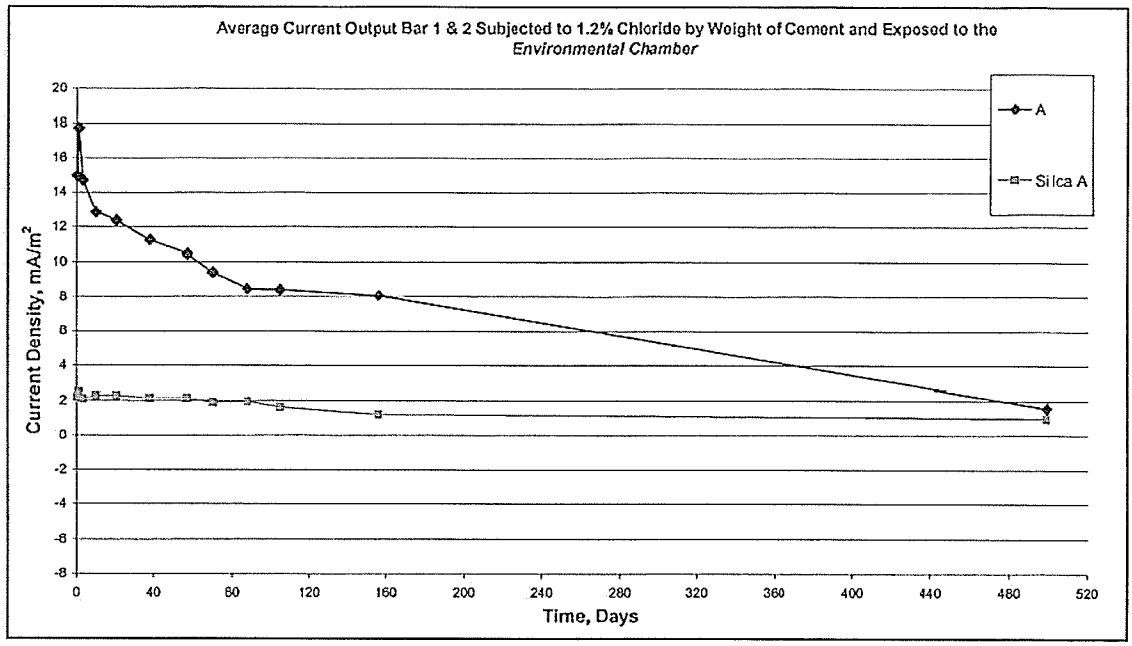
Average Current Output Bar 1 & 2 Subjected to 1.2% Chloride by Weight of Cement and Exposed to the Environmental Chamber
Current Density, mA/m2
Time, Days
A
Silca A
20
18
16
14
12
10
8
6
4
2
0
-2
-4
-6
-8
0
40
80
120
160
200
240
280
320
360
400
440
480
520

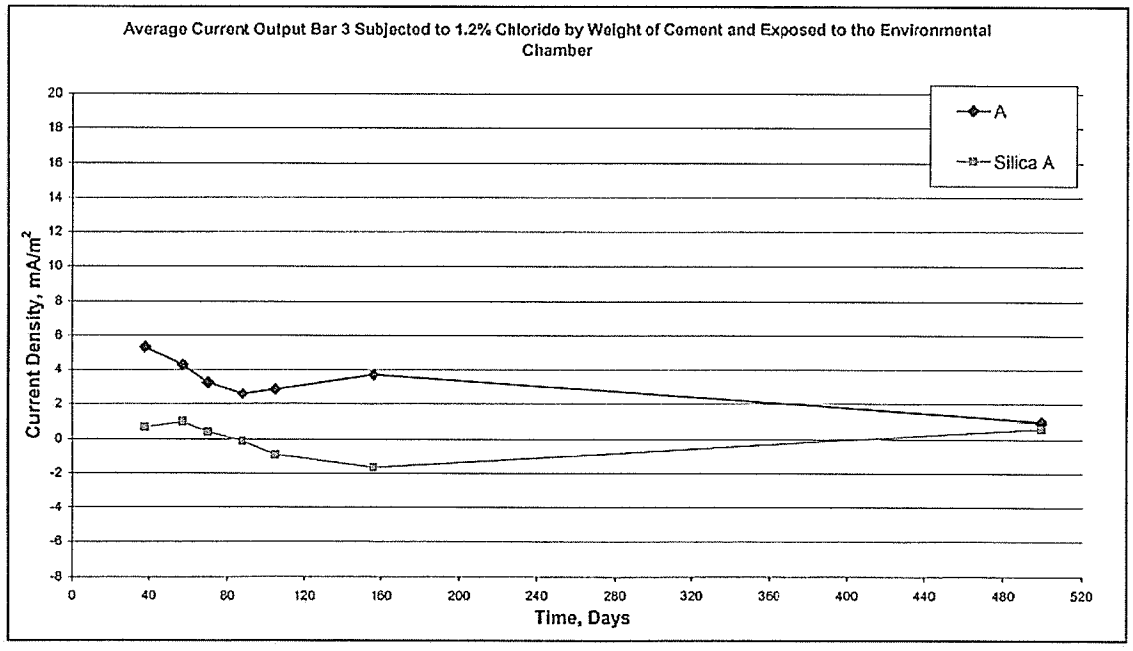
Average Current Output Bar 3 Subjected to 1.2% Chloride by Weight of Cement and Exposed to the Environmental Chamber
Current Density, mA/m2
Time, Days
A
Silica A
20
18
16
14
12
10
8
6
4
2
0
-2
-4
-6
-8
0
40
80
120
160
200
240
280
320
360
400
440
480
520

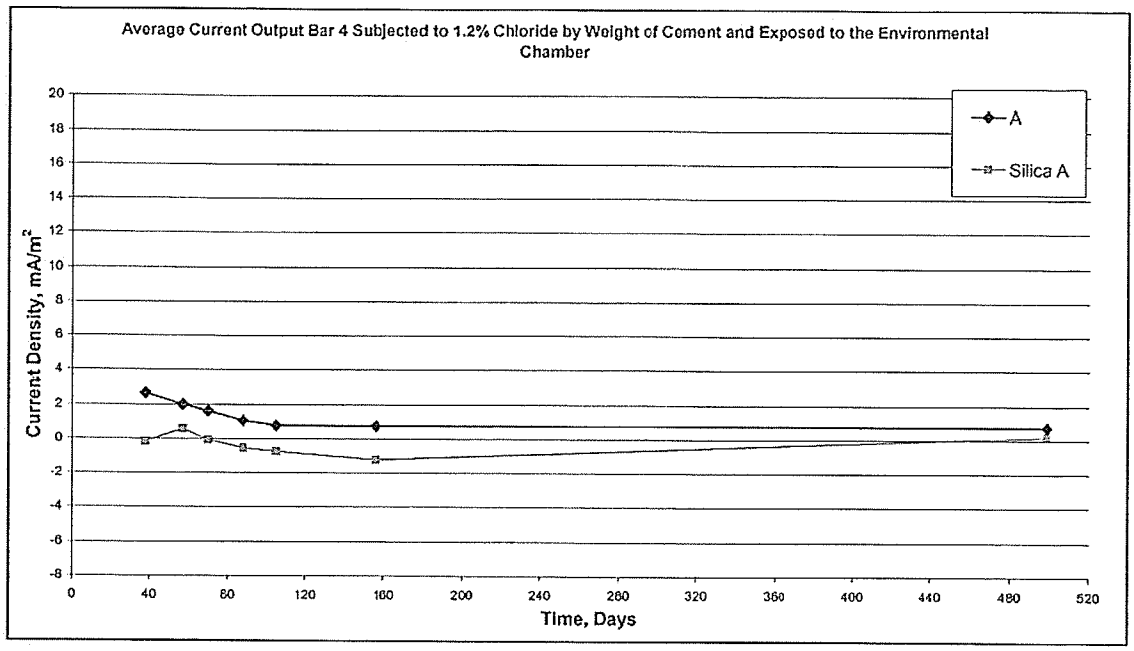
Average Current Output Bar 4 Subjected to 1.2% Chloride by Weight of Cement and Exposed to the Environmental Chamber
Current Density, mA/m²
Time, Days
A
Silica A
20
18
16
14
12
10
8
6
4
2
0
-2
-4
-6
-8
0
40
80
120
160
200
240
280
320
360
400
440
480
520

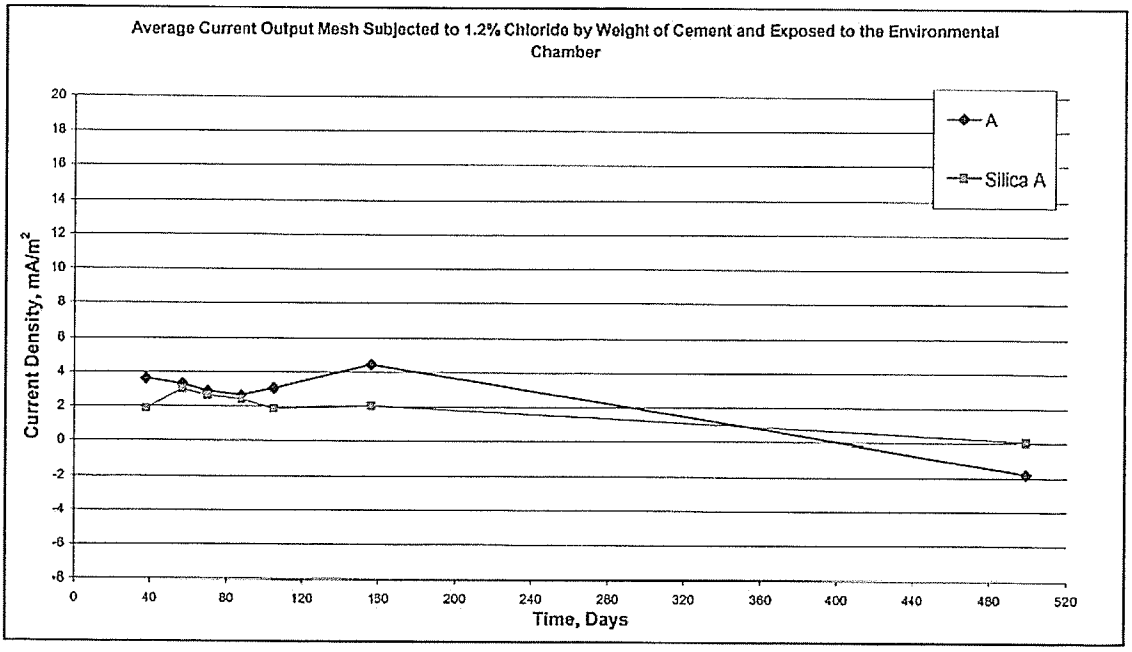
Average Current Output Mesh Subjected to 1.2% Chloride by Weight of Cement and Exposed to the Environmental Chamber
Current Density, mA/m²
Time, Days
A
Silica A
20
18
16
14
12
10
8
6
4
2
0
-2
-4
-6
-8
0
40
80
120
160
200
240
280
320
360
400
440
480
520

APPENDIX E

(NDT JAMES INSTRUMENT METHODOLOGY: CL-2000 CHLORIDE FIELD)

JAMES INSTRUMENTS INC.
NON DESTRUCTIVE TESTING SYSTEMS

CL-2000 Chloride Test System
Operating Instructions

The CL Test System offers a fast, accurate, and in-place determination of the total content (or more precisely the acid soluble content) of chlorides contained in concrete.

The test is easy to perform and requires only the test equipment contained entirely in a small briefcase.

Using a masonry drill bit, the concrete is pulverized at the required sample depth and collected in the dustpan provided. An accurately weighed 3 gram sample is dissolved in 20 ml of extraction liquid consisting of a precise, measured concentration of acid. The chloride ions react with the acid of the liquid in an electrochemical reaction.

An electrode, with an integral temperature sensor, is inserted into the liquid and the electrochemical reaction measured. A uniquely designed instrument converts the voltage generated by the chloride concentration and automatically applies the temperature correction. The percentage of chlorides, or lbs. of chloride per cu yd, is displayed directly on an LCD readout.

Conducted on site, the test gives immediate and direct information regarding the chloride content in critical locations prior to surface repair. In the laboratory the test may be used to measure chloride content of materials which have been pulverized to a fineness equal to that of concrete powder obtained with a masonry drill on a concrete member.

The test may be used on fresh, wet concrete.

Measurement

From main menu: **Select Function:** **CAL MEAS**

Move blinking cursor via the 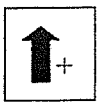 (plus arrow key) or 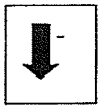 (minus arrow key) in front of the item marked MEAS.

Press  (enter key)

The CL-2020 will now display: **Units**
% Lb/cu. yd.

Move blinking cursor via the key) in front of the unit you wish to display chloride ion concentrations in, either percentage by weight or pounds per cubic yard. (plus arrow key) or (minus arrow

The meter will now display: **Value zz.z °C**
y.yyy

Where zz.z is the temperature display, and y.yyy is the value of the chloride ion content expressed in either percentage by weight or lbs. per cubic yard.

Note: Low battery on the display at any time indicates a battery charge is in order.

SAMPLING

Locate the position and depth of the reinforcement bars with the James Rebar Locator. Set the dust collecting pan over the test area and place clamping pliers in position. Mark the location of the bolt-hole in the base of the clamping pliers. Insert the 3/8 inch masonry bit supplied, into a masonry drill. A rechargeable battery powered masonry drill is available from James – making the whole process independent of an external power source. Drill hole 1" (min.) at the location (fig. 1,1). Place a drop-in anchor and tap anchor flush (fig.1,2). Expand and secure anchor using the set tool supplied (fig. 1,3). Reposition clamping pliers. Prepare clamp bolt by placing on a nut, then a washer; insert bolt into anchor. Drive bolt completely into the anchor using the wrench supplied. The clamping pliers is set to the surface by tightening the hex nut (fig. 2).

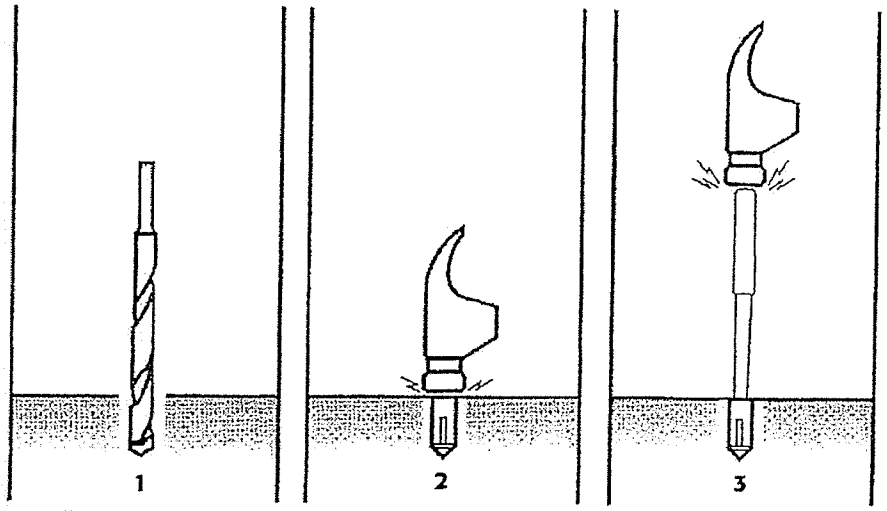

Figure 1

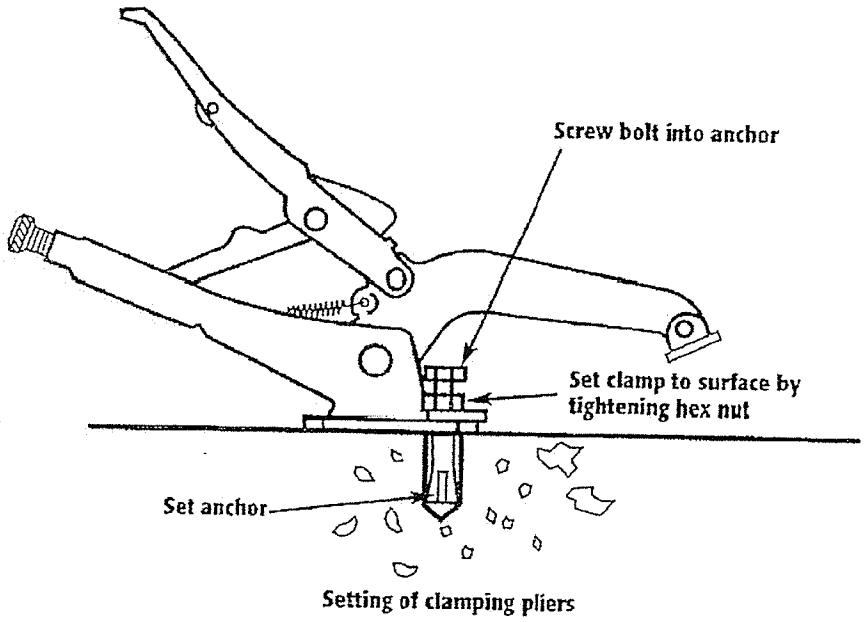

Figure 2

Concrete dust is drilled out to the required depth with the large ¾ inch bit mounted in the masonry drill. The drilling friction removes excessive water from the concrete dust, which should be protected immediately by placing in plastic bags.

It is advisable to select three test locations and drill ¼ inch of concrete for each sample. This will produce approximately 20 grams of dust, which is a common standard sample size. To produce a chloride profile through a concrete slab it is advisable to drill at three levels, e.g., near the top surface, close to the rebar position and 1-1/2 inches below the rebars.

Mix the dust sample on the pan and quarter carefully to ensure the sample's homogeneity, then weigh two separate 3-gram samples, using the scales provided. Keep one sample in a sealed plastic bag with location marked and the other sample for the field test.

Add the 3 gram sample to one of the 12 plastic jars containing 20 ml of chloride extraction liquid. Add the sample dust in stages to avoid excessive fizzing from the limestone present in the dust sample.

Note: Avoid contamination of samples during testing.

Preparation of Electrode for Calibration

The electrode is shipped without filling solution in the reference chamber. To fill the chamber, use the flip-spout bottle marked "electrode wetting agent," proceed as follows:

1. Lift the spout to a vertical position.

2. Insert the spout into the filling hole in the outer sleeve and add a small amount of filling solution to the chamber. Tip the electrode to moisten the O-ring and return it to a vertical position.

3. Holding the electrode by the barrel with one hand, push down on the white electrode cap, allowing the filling solution to wet the inner cone. If needed, the black cover cap may be removed one millimeter to allow sufficient travel of the electrode cones.

4. Release the white electrode cap. If it does not return to its original position immediately, check to see if the O-ring is moist enough; repeat steps 2 through 4 until the white cap has returned to original position. Add filling solution to the chamber, up to the filling hole. To ensure a proper flow rate—add to avoid erratic electrode potentials, this level should be maintained during all testing.

Remove the black cover cap and rinse the electrode thoroughly with distilled water and blot.

Note: *The black cover cap should be on when electrode is not in use. If the electrode is not in use for periods of more than 2 to 3 days, the electrode should be drained, rinsed in distilled water, dried off, polished and protected with the cap. If this is not done, the wetting agent will evaporate leaving crystals. This will render the electrode useless, necessitating its replacement.*

The CL-2000 *Laboratory in a briefcase components:*

CL-3700 Chloride combination electrode with externally mounted temperature sensor, cable, and connectors.

CL-2020 Special battery powered, high impedance, electronic meter—with temperature compensation circuits and microprocessor for direct conversion to percentage of chlorides.

CL-2012 Replaceable pack containing 12 plastic bottles, each with 20 ml of extraction liquid and five plastic jars of different colored calibration liquids.

CL-1030 Spray bottle of electrode wetting agent.
Bottle of distilled water
Dust collecting pan and blower for sampling.
Clamping pliers, drill bit, anchors, wrench, and screwdriver. Scales for weighing 3 gm samples.

Weight of CL-2000 Laboratory, complete in briefcase is 10 lbs.

B-124 A rechargeable battery powered electric drill, complete with battery charger in a metal carrying case (use with CL-2000 *Laboratory in a briefcase*)

Note: *The CL-2000 test correlates to water soluble titration method.*
For the most accurate results the first sample in any test area should be checked every 15 minutes until the last three readings are within about 10 percent of each other. This is because, for safety reasons, a mild acid solution is used and it may take a longer time to completely dissolve chlorides from certain aggregates.

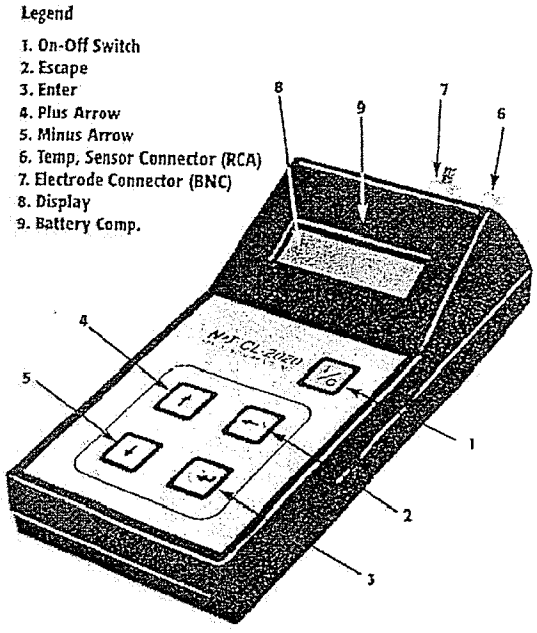

Figure 4

CHLORIDE ASHTO T-260 TEST PROCEDURE

Changing Meter Mode of Operation:

1. From meter main menu press and hold the  (escape key) simultaneously press and hold the 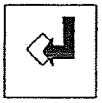 (enter key).

2. Meter will now display: **RESET**

3. Then the alternative menu will be displayed:

Select Function
Cal Meas mV

Measurement Procedure:

1. Use arrow keys to move blinking cursor in front of Meas display.
2. Press  (enter).
3. The meter will now display:

Value zz.z°C
y.yyy

Where zz.z is the temperature reading and y.yyy is the chloride percent concentration.

4. Place 3.0 +/.01g concrete sample in the 125 ml bottle with digestive solution. Shake vigorously to suspend the powder in the solution. Let powder digest for 3 minutes. The bottle may be opened after shaking to relieve pressure from effervescence due to the reaction; then close immediately.

5. Carefully remove the bottle cap and add 80 ml of stabilizing solution.

6. Replace cap and shake vigorously for one minute.

7. Remove bottle cap and place the electrode to a depth of mid-height in the extraction fluid.

8. Wait 3 minutes and record the measurement obtained.

9. After each measurement the electrode should be rinsed in distilled water.

ASHTO Calibration Method

The conversion of the sensors output to a specific chloride ion concentration is normally accomplished via comparison with standardized solutions. ASHTO specifically recommends that the standardized concentrations of 1.25%, 0.60%, 0.30%, 0.03% and 0.01% be used for calibration. It is further specified that this be accomplished by taking millivolt readings from 10 calibration runs, each consisting of the five calibration solutions. Thus, the mV function of the meter (see below for further details of this function). From this procedure a chloride concentration is obtained of the sample. This chloride concentration is further linearly correlated to a standard titration procedure. The values which are recommended by ASHTO for these correlations are currently programmed in the CL-2020. They have been made available to the user if further refinement of the test method is required.

Calibration Menu

1. Using the arrow keys, move the blinking cursor in front of the **Cal.**
2. Press  (enter key)
3. The meter should now display: **Select Constant**
   A B C D

These constants correspond to the following formula,

$$\%Cl = A + By,$$

where y = [(10^(C+DmV))-3](0.00333)

4. Using the arrow keys, move the cursor in front of the constant you wish to change.
5. Press  (enter key)
6. Use arrow keys to change the values of the constant to that which you desire.
7. Press  (enter key)
8. The meter will now display: **saving value**

If you wish to return constants to their original values press and hold the 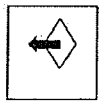 (escape key) while simultaneously pressing the  (down arrow key)

mV Display

1. From the main menu use the arrow keys to move the blinking cursor in front of the **mV** display.

2. Press  enter key)

3. The meter will now display: **mVolts** **zz.z°C**
yyy.y

Tips for successful chloride testing

Exert only moderate pressure on the drill when drilling out the sample dust. This keeps the dust particles fine and they dissolve easily in the extraction liquid.

Do not test wet dust because the weight of the water will be included in the calculations. If the dust is wet, it should be dried. One way of doing this is to place it on blotting paper.

When collecting dust samples at different depths, make sure that the drill bit is always perpendicular to the surface. This ensures that the dust is collected from the bottom of the hole and not from the side of the drilled hole.

Do not drill only one hole to collect the sample, since you may drill through a course aggregate particle and the dust will not be representative of the entire concrete. Drill three holes about four inches apart and mix the dust together.

Make sure the electrode membrane is not scratched or etched. Lower electrode gently, keeping it tilted to keep the electrode tip from touching the dust at the bottom of the extraction liquid bottle. Also, the electrode will suffer etching if the electrode is stored a long time without removing the extraction liquid from the membrane. To avoid this, clean the electrode membrane carefully with distilled water—or place it in distilled water when not in use.

The calibration liquids may become contaminated, especially the weaker ones. This can change the calibration. Always discard the calibration liquid after 12 tests.

Note: *If temperature changes occur, meter and electrodes should be recalibrated. The electrode can be used at temperatures from 0 – 60 °C, provided that temperature equilibrium has occurred. For use at the temperatures substantially different from room temperature, equilibrium times of up to one hour are recommended.*

APPENDIX F

(STRIP ANODES: HALF-CELL RESULTS)

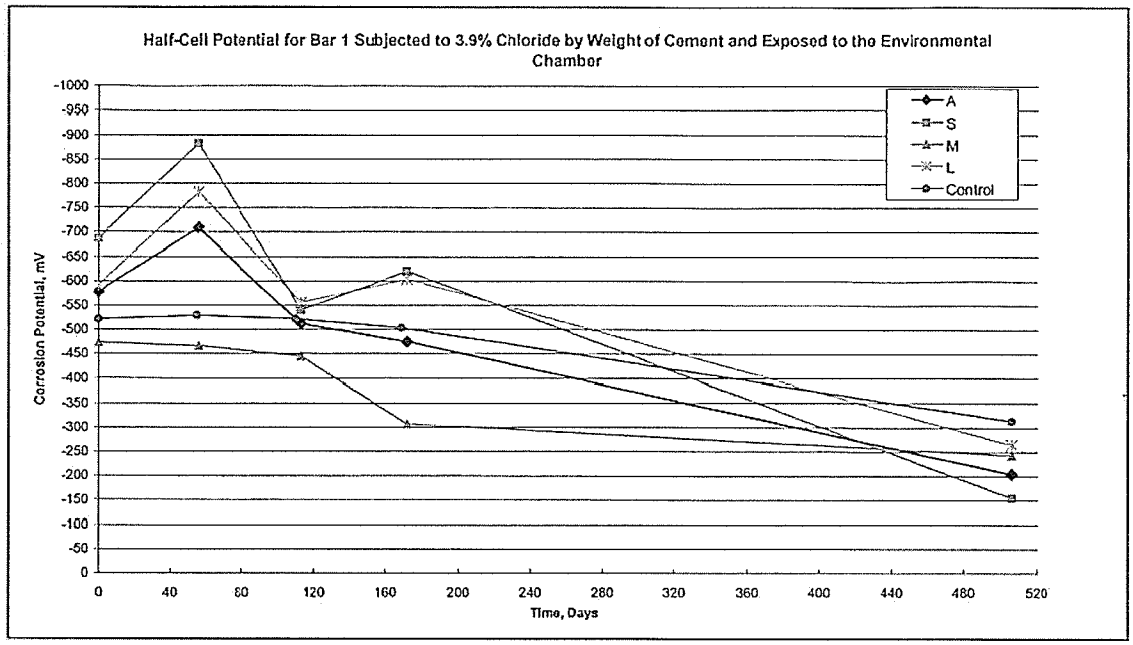
Half-Cell Potential for Bar 1 Subjected to 3.9% Chloride by Weight of Cement and Exposed to the Environmental Chamber
Corrosion Potential, mV
-1000
-950
-900
-850
-800
-750
-700
-650
-600
-550
-500
-450
-400
-350
-300
-250
-200
-150
-100
-50
0
0
40
80
120
160
200
240
280
320
360
400
440
480
520
Time, Days
A
S
M
L
Control

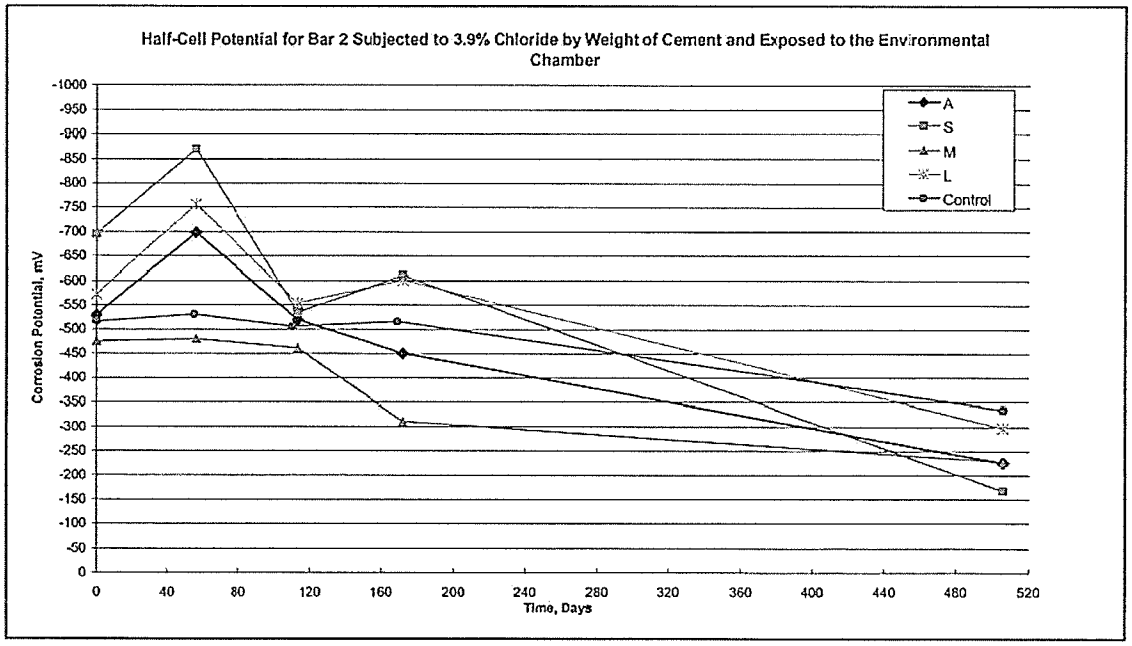
Half-Cell Potential for Bar 2 Subjected to 3.9% Chloride by Weight of Cement and Exposed to the Environmental Chamber
Corrosion Potential, mV
-1000
-950
-900
-850
-800
-750
-700
-650
-600
-550
-500
-450
-400
-350
-300
-250
-200
-150
-100
-50
0
0
40
80
120
160
200
240
280
320
360
400
440
480
520
Time, Days
A
S
M
L
Control

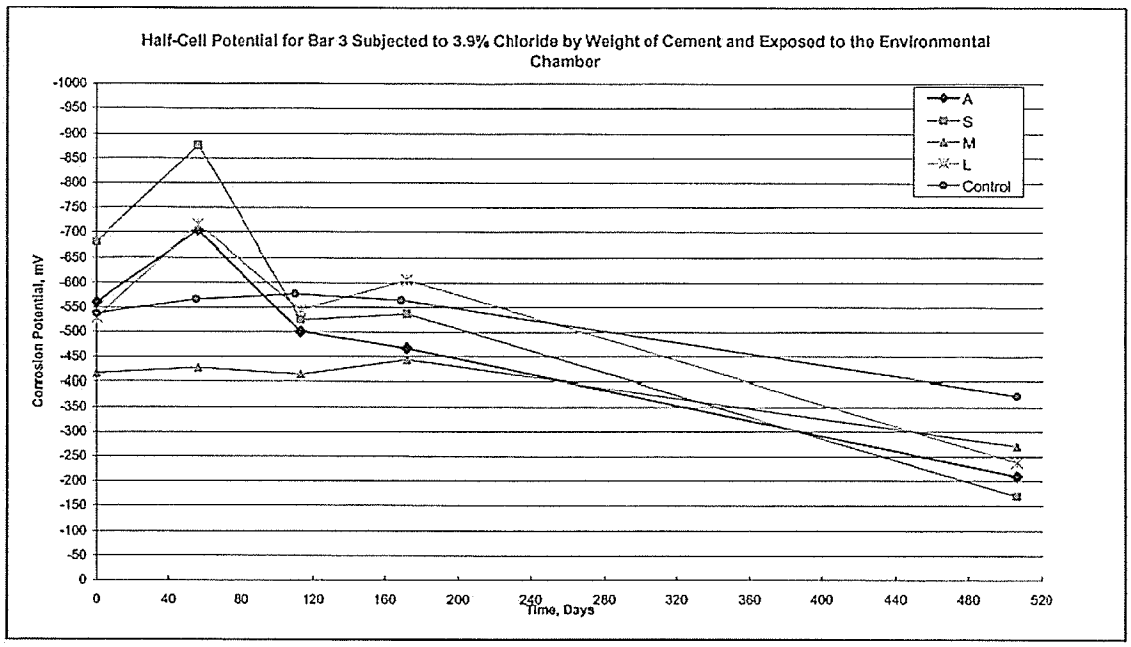
Half-Cell Potential for Bar 3 Subjected to 3.9% Chloride by Weight of Cement and Exposed to the Environmental Chamber
Corrosion Potential, mV
Time, Days
A
S
M
L
Control

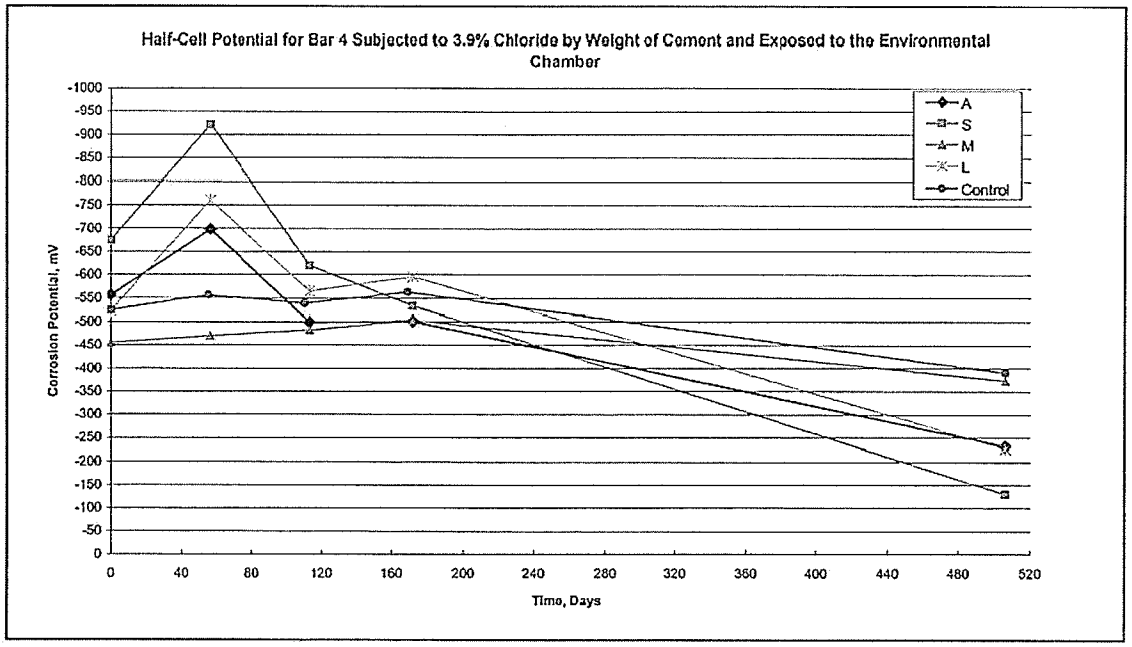
Half-Cell Potential for Bar 4 Subjected to 3.9% Chloride by Weight of Cement and Exposed to the Environmental Chamber
Corrosion Potential, mV
Time, Days
A
S
M
L
Control

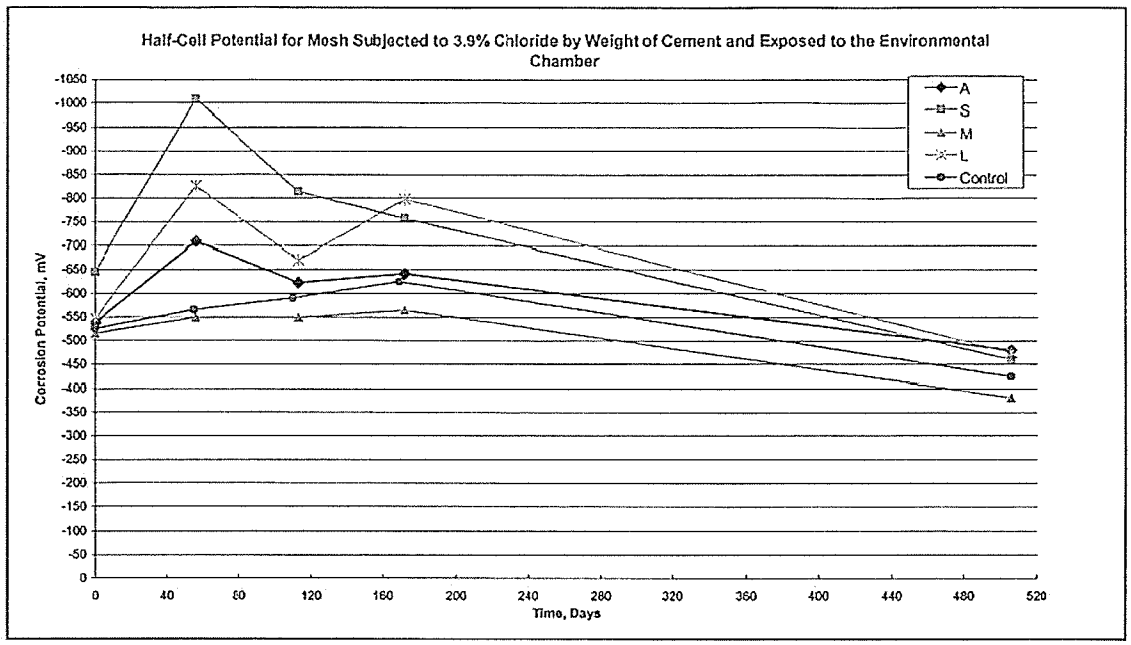
Half-Cell Potential for Mosh Subjected to 3.9% Chloride by Weight of Cement and Exposed to the Environmental Chamber
Corrosion Potential, mV
-1050
-1000
-950
-900
-850
-800
-750
-700
-650
-600
-550
-500
-450
-400
-350
-300
-250
-200
-150
-100
-50
0
0
40
80
120
160
200
240
280
320
360
400
440
480
520
Time, Days
A
S
M
L
Control

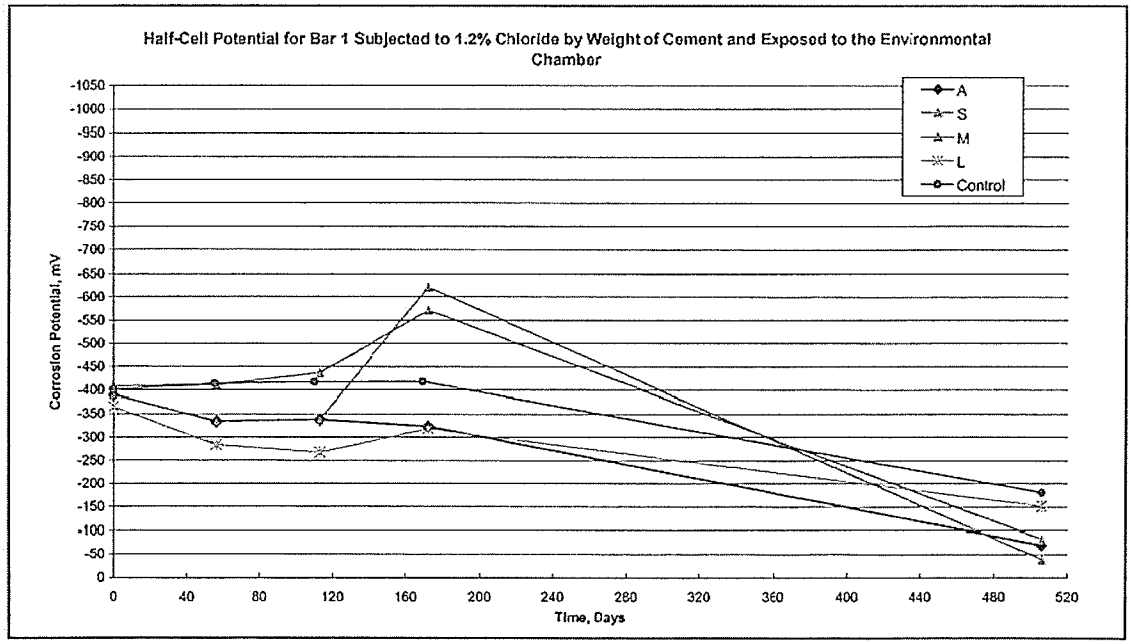
Half-Cell Potential for Bar 1 Subjected to 1.2% Chloride by Weight of Cement and Exposed to the Environmental Chamber
Corrosion Potential, mV
-1050
-1000
-950
-900
-850
-800
-750
-700
-650
-600
-550
-500
-450
-400
-350
-300
-250
-200
-150
-100
-50
0
0
40
80
120
160
200
240
280
320
360
400
440
480
520
Time, Days
A
S
M
L
Control

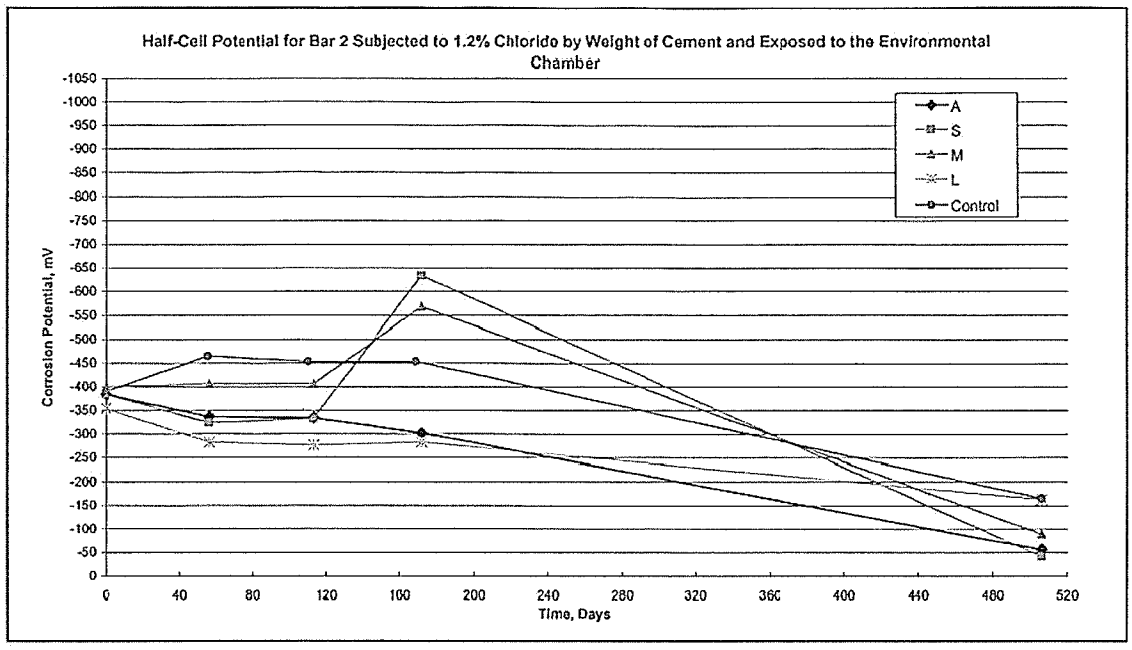
Half-Cell Potential for Bar 2 Subjected to 1.2% Chloride by Weight of Cement and Exposed to the Environmental Chamber
Corrosion Potential, mV
-1050
-1000
-950
-900
-850
-800
-750
-700
-650
-600
-550
-500
-450
-400
-350
-300
-250
-200
-150
-100
-50
0
0
40
80
120
160
200
240
280
320
360
400
440
480
520
Time, Days
A
S
M
L
Control

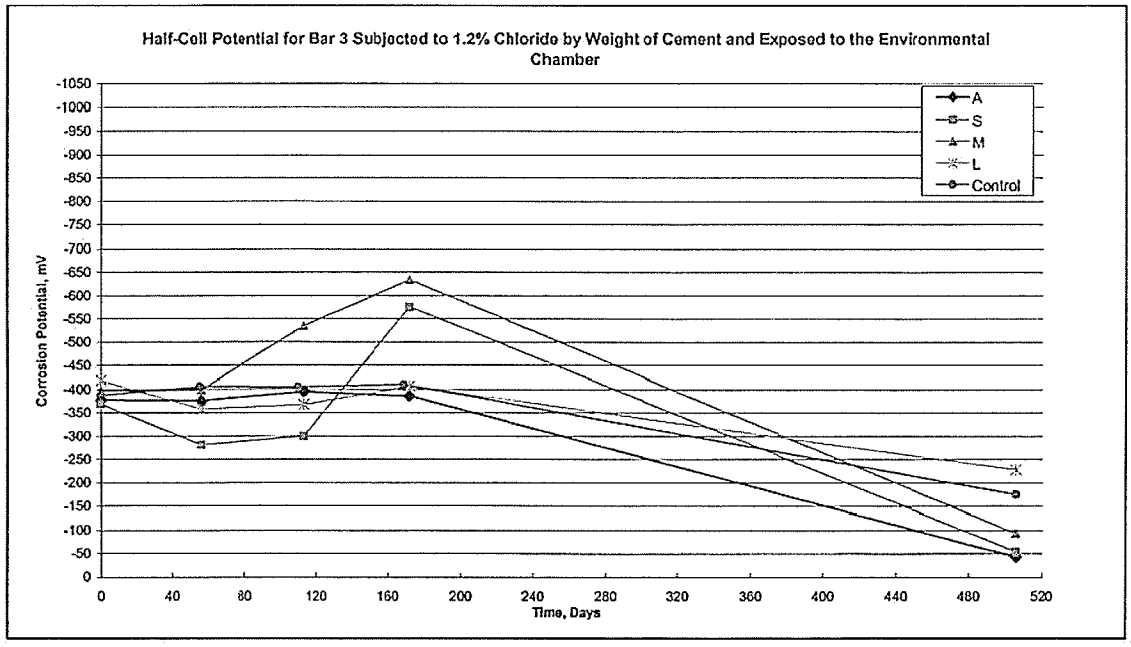
Half-Cell Potential for Bar 3 Subjected to 1.2% Chloride by Weight of Cement and Exposed to the Environmental Chamber
Corrosion Potential, mV
-1050
-1000
-950
-900
-850
-800
-750
-700
-650
-600
-550
-500
-450
-400
-350
-300
-250
-200
-150
-100
-50
0
0
40
80
120
160
200
240
280
320
360
400
440
480
520
Time, Days
A
S
M
L
Control

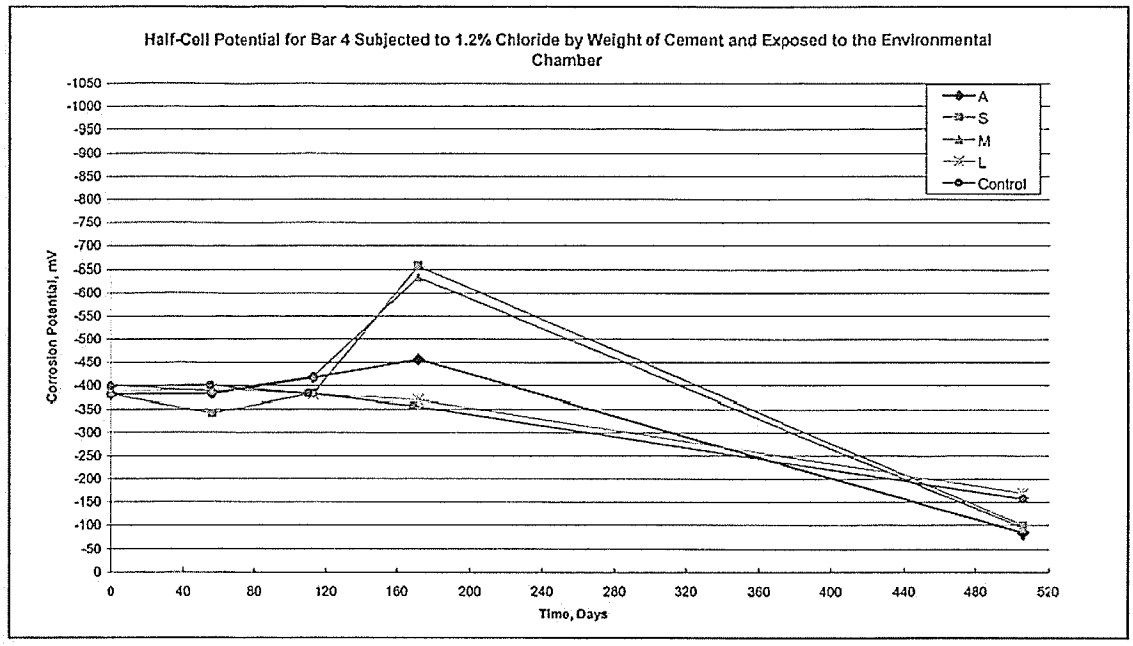
Half-Cell Potential for Bar 4 Subjected to 1.2% Chloride by Weight of Cement and Exposed to the Environmental Chamber
Corrosion Potential, mV
-1050
-1000
-950
-900
-850
-800
-750
-700
-650
-600
-550
-500
-450
-400
-350
-300
-250
-200
-150
-100
-50
0
0
40
80
120
160
200
240
280
320
360
400
440
480
520
Time, Days
A
S
M
L
Control

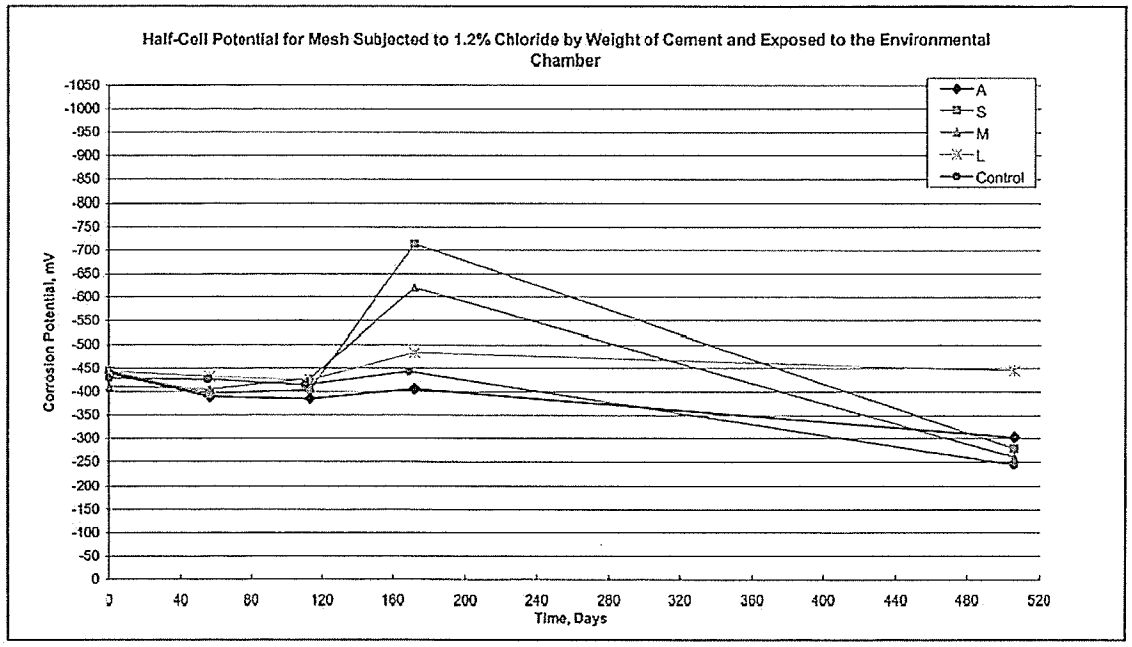
Half-Cell Potential for Mesh Subjected to 1.2% Chloride by Weight of Cement and Exposed to the Environmental Chamber
Corrosion Potential, mV
-1050
-1000
-950
-900
-850
-800
-750
-700
-650
-600
-550
-500
-450
-400
-350
-300
-250
-200
-150
-100
-50
0
0
40
80
120
160
200
240
280
320
360
400
440
480
520
Time, Days
A
S
M
L
Control

APPENDIX G

(STRIP ANODES: CURRENT DENSITY RESULTS)

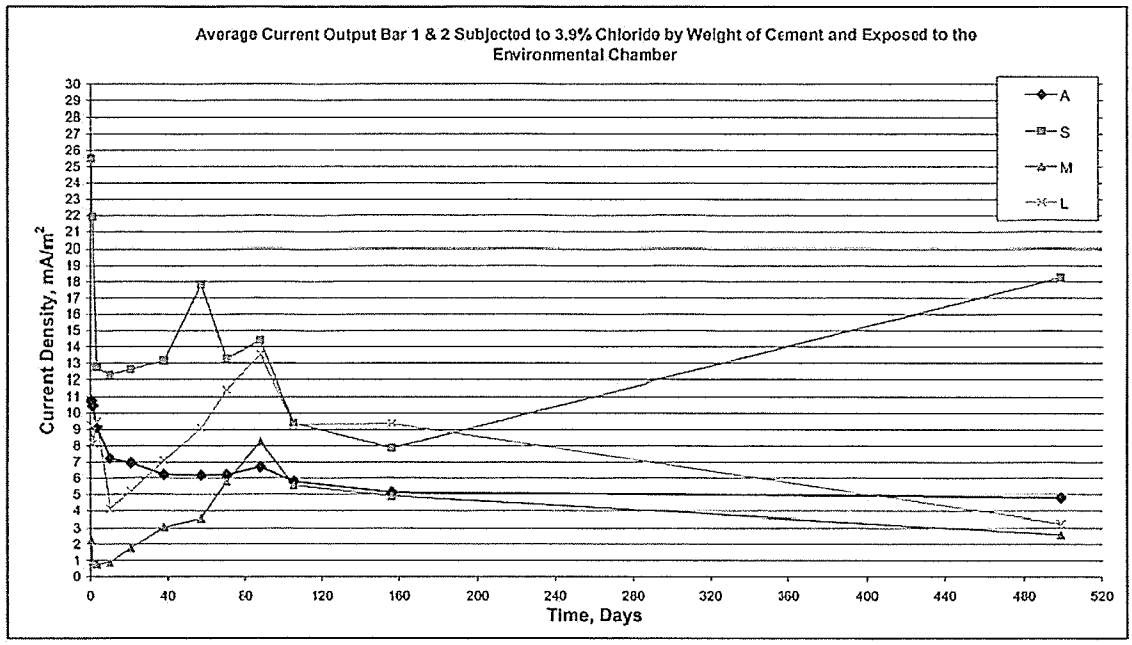
Average Current Output Bar 1 & 2 Subjected to 3.9% Chloride by Weight of Cement and Exposed to the Environmental Chamber
Current Density, mA/m²
Time, Days
A
S
M
L

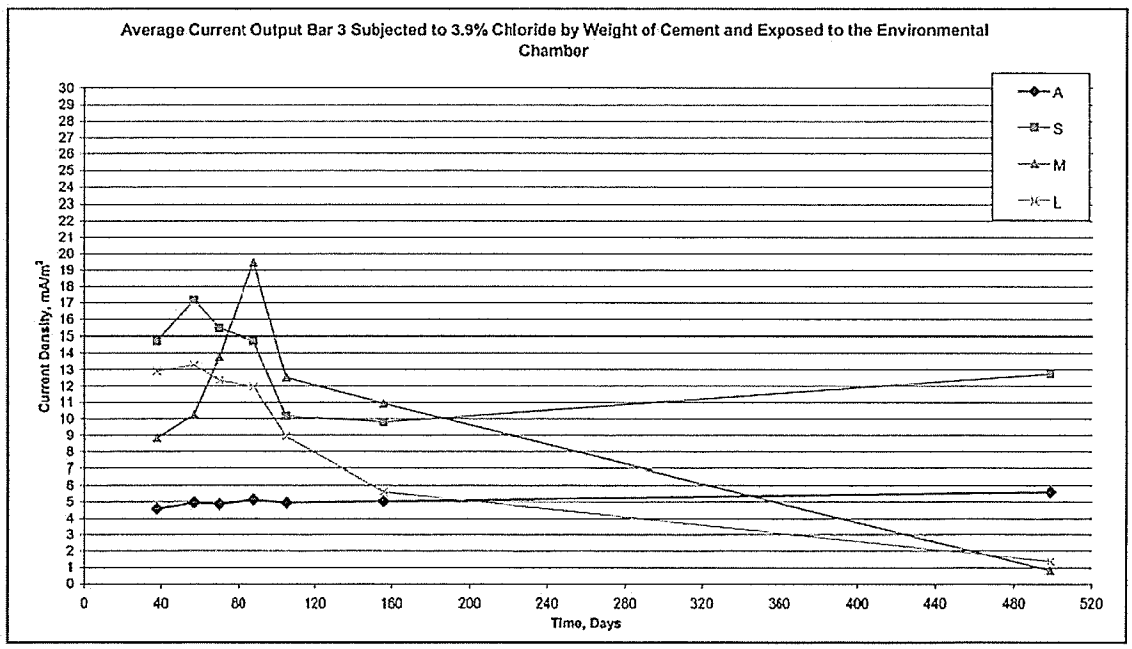
Average Current Output Bar 3 Subjected to 3.9% Chloride by Weight of Cement and Exposed to the Environmental Chamber
Current Density, mA/m²
Time, Days
A
S
M
L

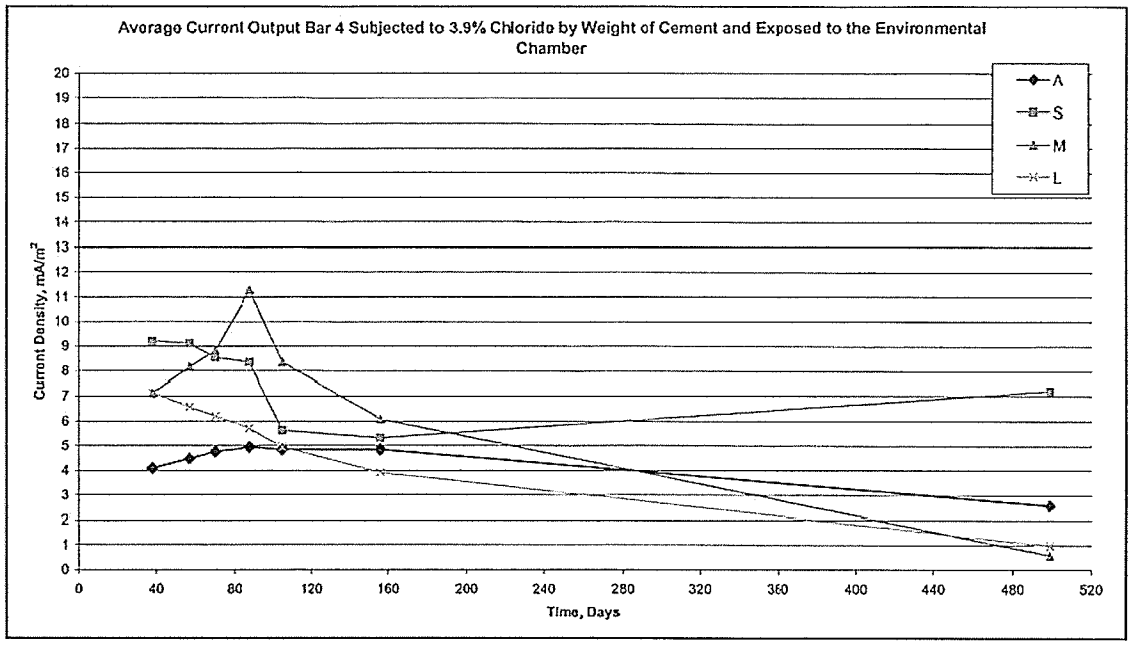
Average Current Output Bar 4 Subjected to 3.9% Chloride by Weight of Cement and Exposed to the Environmental Chamber
Current Density, mA/m²
Time, Days
A
S
M
L

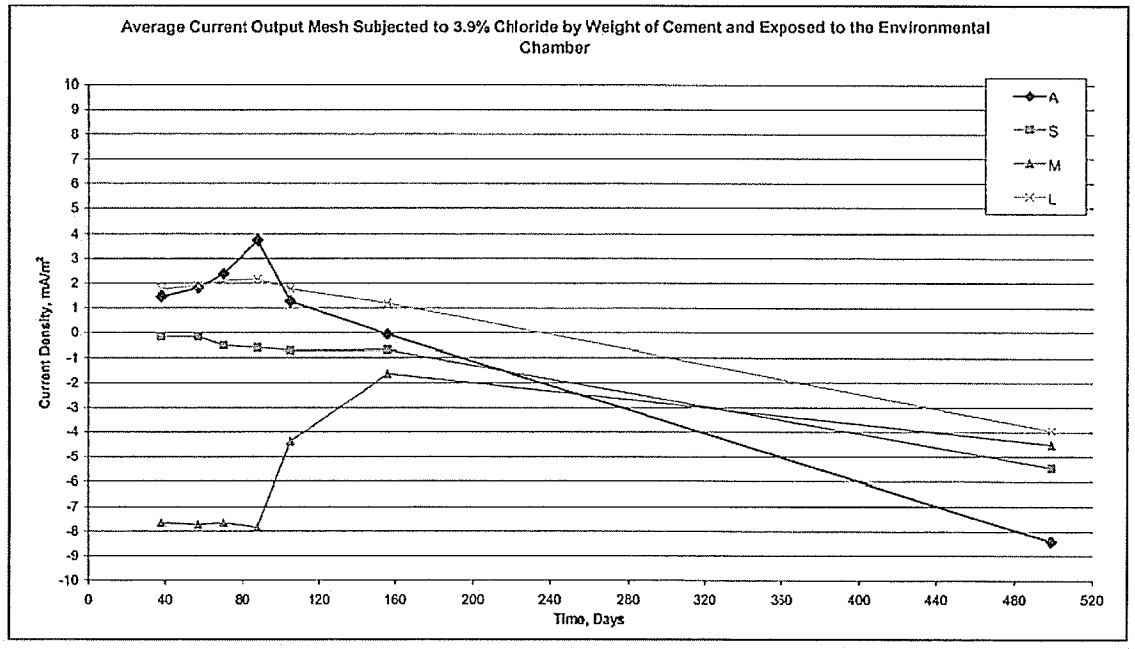
Average Current Output Mesh Subjected to 3.9% Chloride by Weight of Cement and Exposed to the Environmental Chamber
Current Density, mA/m²
Time, Days
A
S
M
L

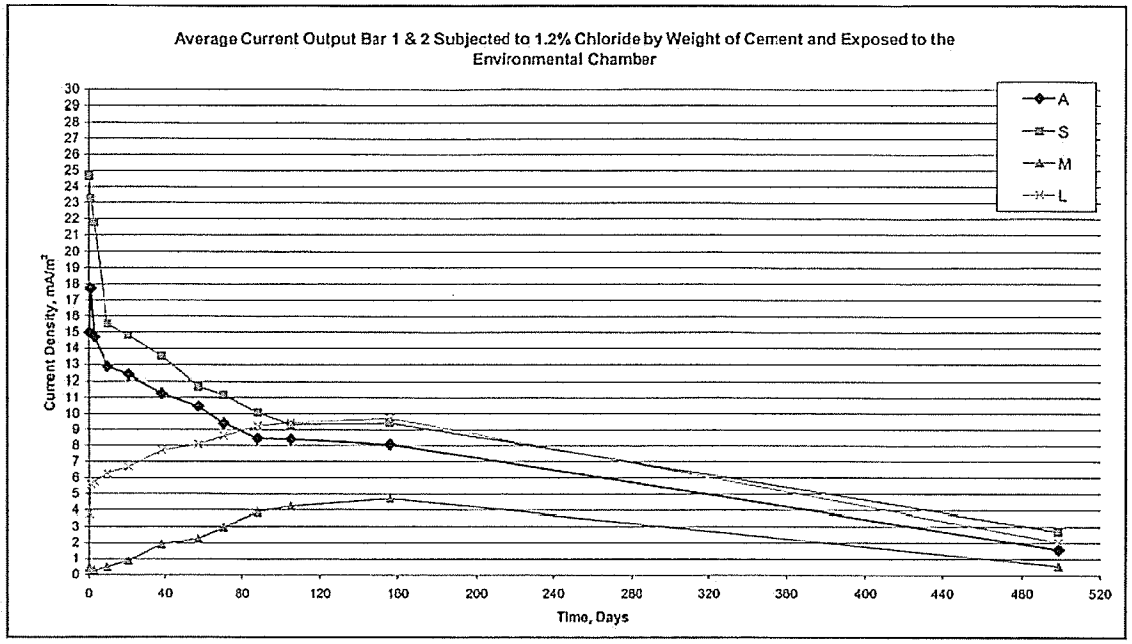
Average Current Output Bar 1 & 2 Subjected to 1.2% Chloride by Weight of Cement and Exposed to the Environmental Chamber
Current Density, mA/m²
Time, Days
A
S
M
L

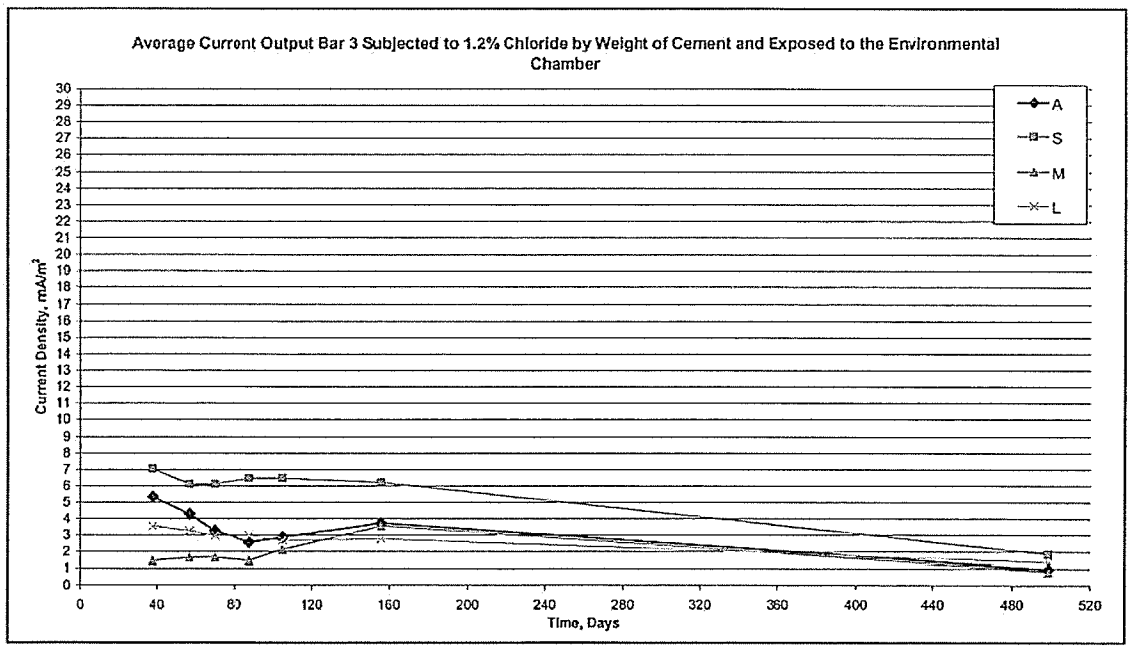
Average Current Output Bar 3 Subjected to 1.2% Chloride by Weight of Cement and Exposed to the Environmental Chamber
Current Density, mA/m²
Time, Days
A
S
M
L

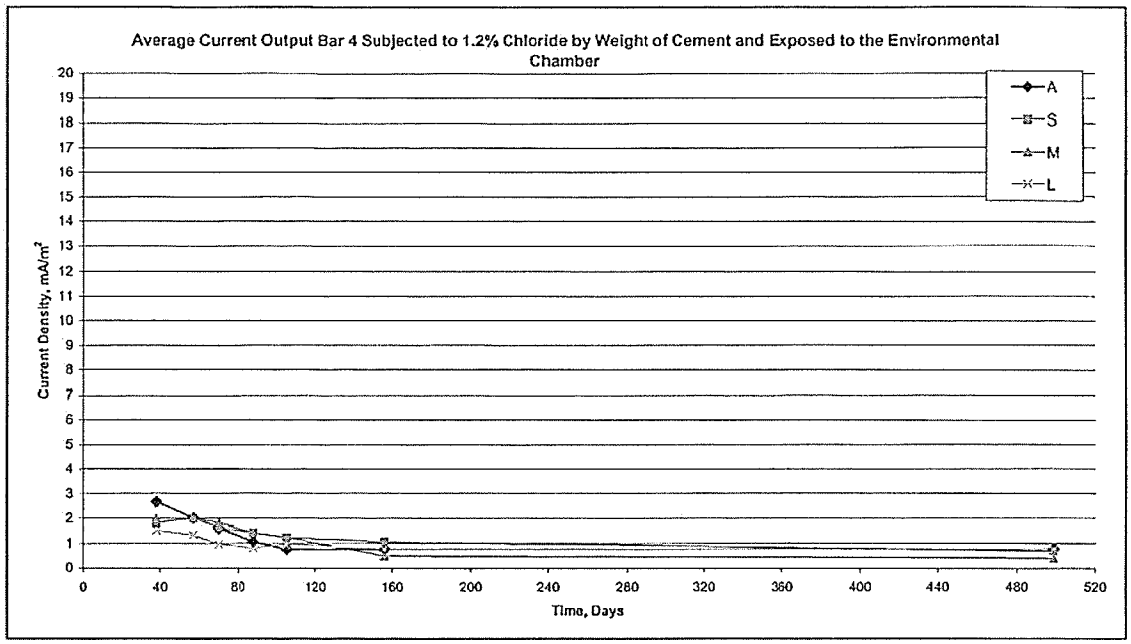
Average Current Output Bar 4 Subjected to 1.2% Chloride by Weight of Cement and Exposed to the Environmental Chamber
Current Density, mA/m²
Time, Days
A
S
M
L

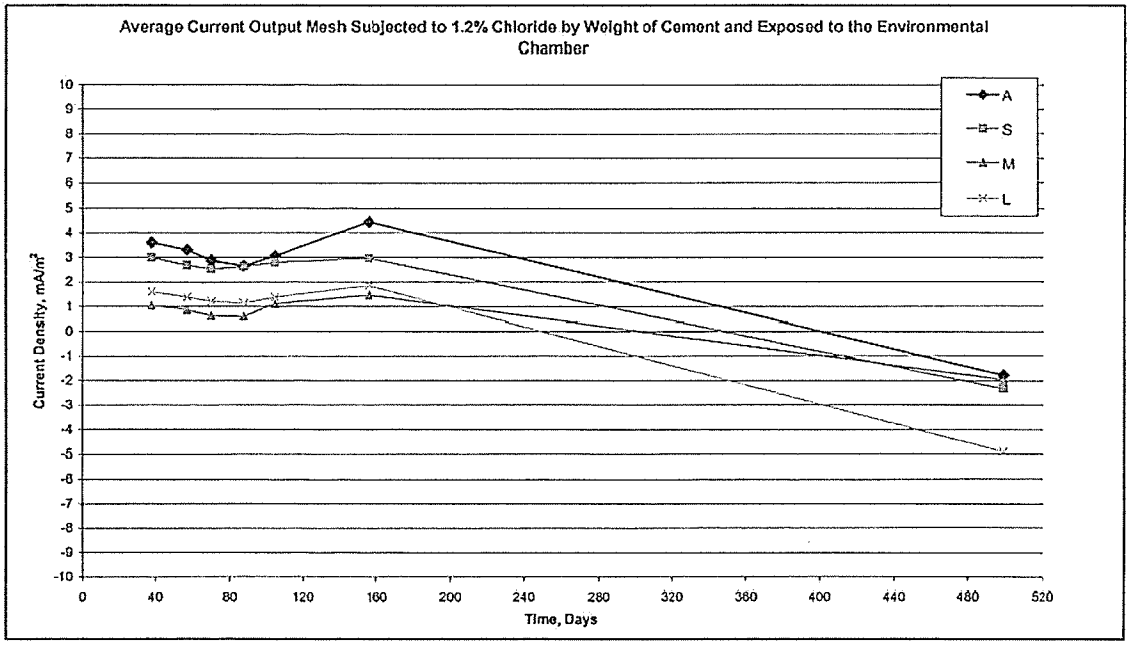
Average Current Output Mesh Subjected to 1.2% Chloride by Weight of Cement and Exposed to the Environmental Chamber
Current Density, mA/m²
Time, Days
A
S
M
L

APPENDIX H

(STRIP ANODES: POTENTIAL DECAY RESULTS)

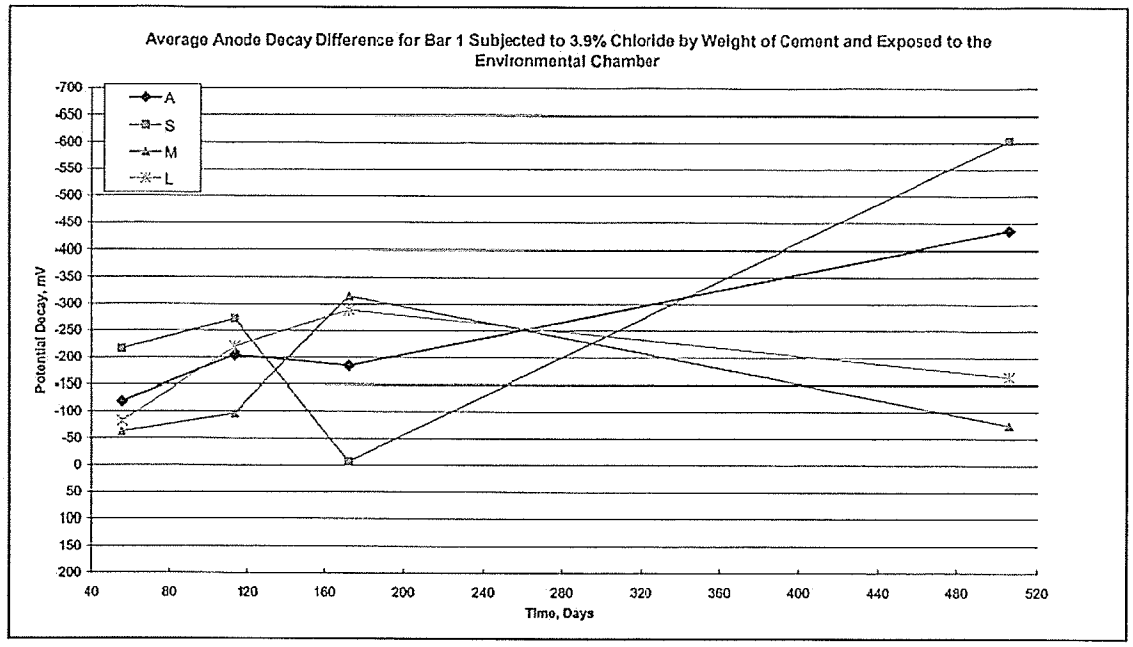
Average Anode Decay Difference for Bar 1 Subjected to 3.9% Chloride by Weight of Cement and Exposed to the Environmental Chamber
A
S
M
L
Potential Decay, mV
-700
-650
-600
-550
-500
-450
-400
-350
-300
-250
-200
-150
-100
-50
0
50
100
150
200
40
80
120
160
200
240
280
320
360
400
440
480
520
Time, Days

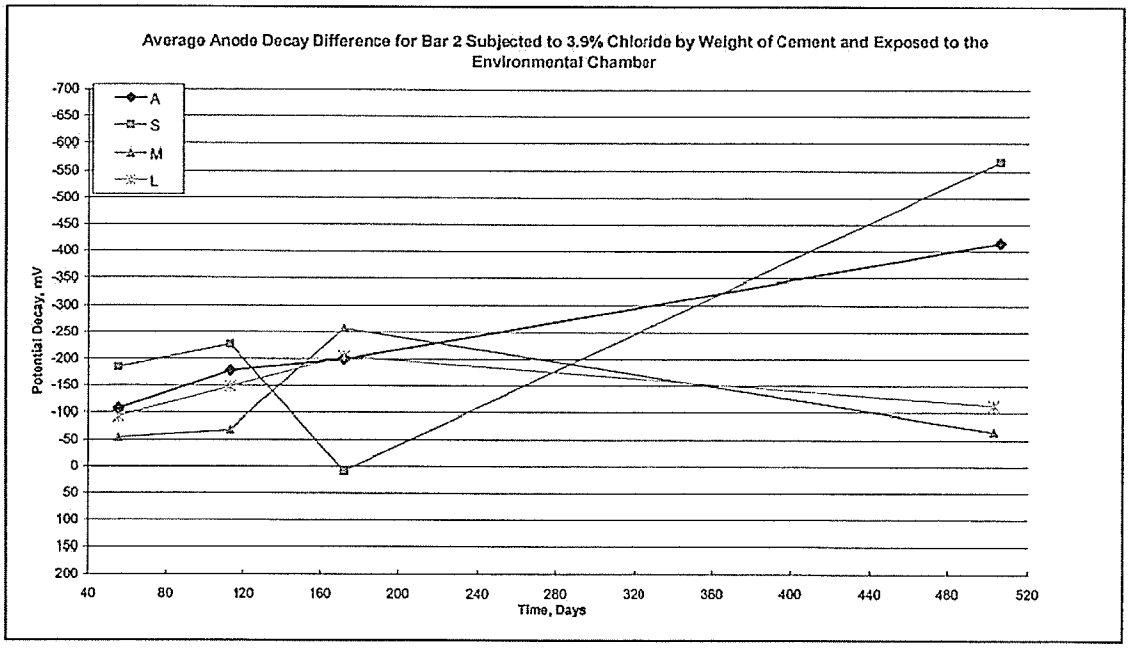
Average Anode Decay Difference for Bar 2 Subjected to 3.9% Chloride by Weight of Cement and Exposed to the Environmental Chamber
A
S
M
L
Potential Decay, mV
-700
-650
-600
-550
-500
-450
-400
-350
-300
-250
-200
-150
-100
-50
0
50
100
150
200
40
80
120
160
200
240
280
320
360
400
440
480
520
Time, Days

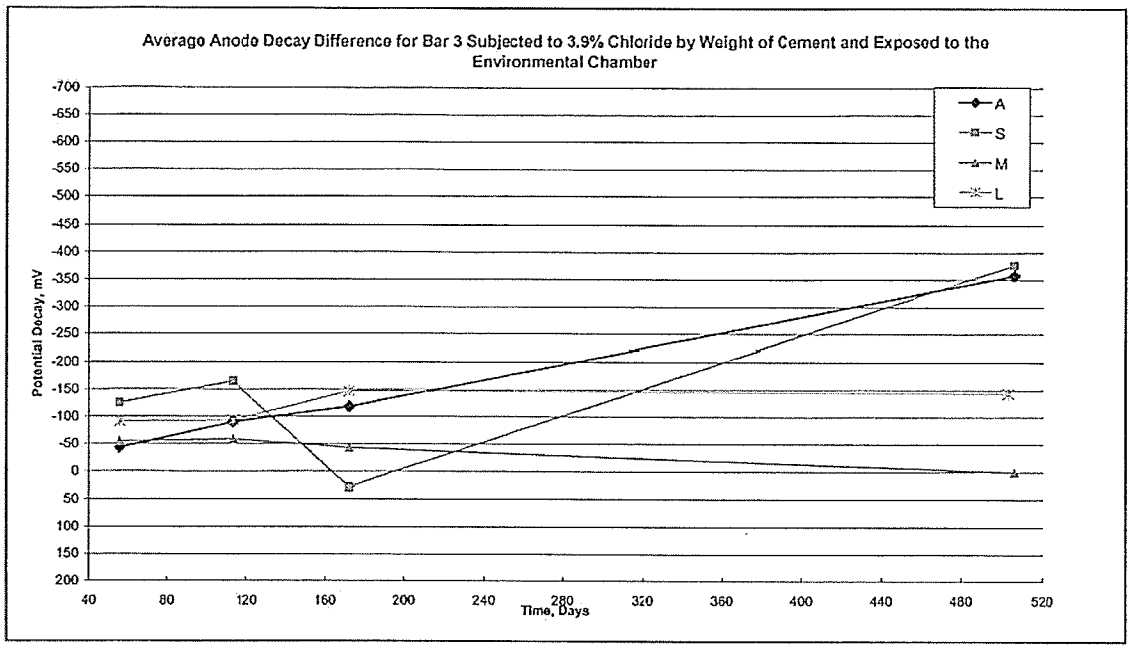
Average Anode Decay Difference for Bar 3 Subjected to 3.9% Chloride by Weight of Cement and Exposed to the Environmental Chamber
Potential Decay, mV
-700
-650
-600
-550
-500
-450
-400
-350
-300
-250
-200
-150
-100
-50
0
50
100
150
200
40
80
120
160
200
240
280
320
360
400
440
480
520
Time, Days
A
S
M
L

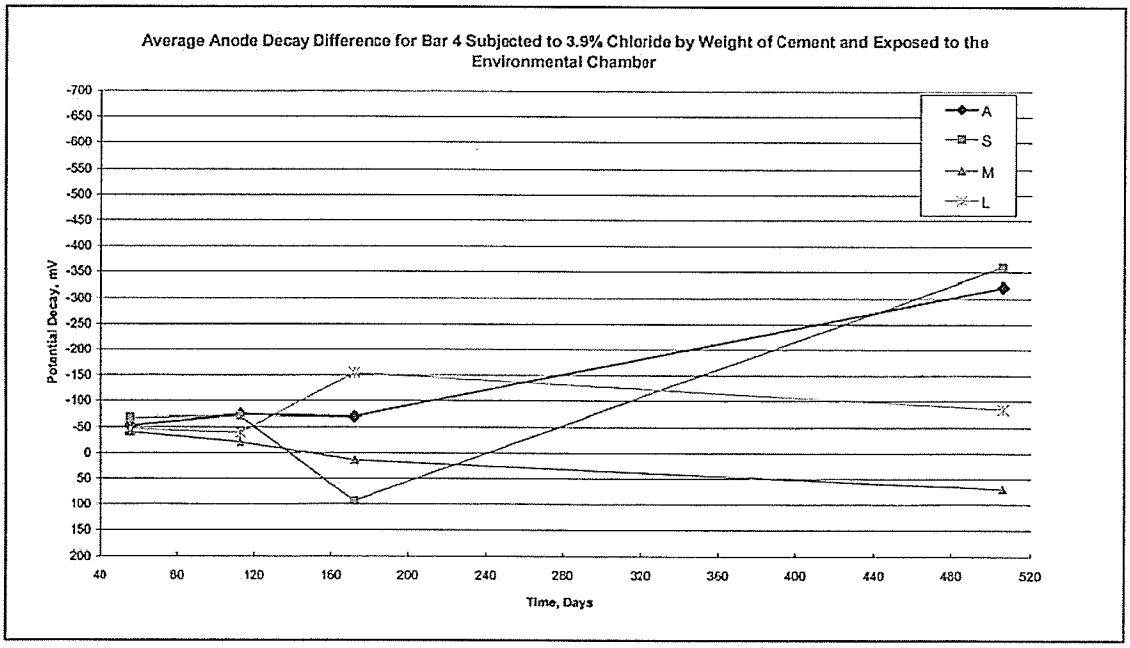
Average Anode Decay Difference for Bar 4 Subjected to 3.9% Chloride by Weight of Cement and Exposed to the Environmental Chamber
Potential Decay, mV
-700
-650
-600
-550
-500
-450
-400
-350
-300
-250
-200
-150
-100
-50
0
50
100
150
200
40
80
120
160
200
240
280
320
360
400
440
480
520
Time, Days
A
S
M
L

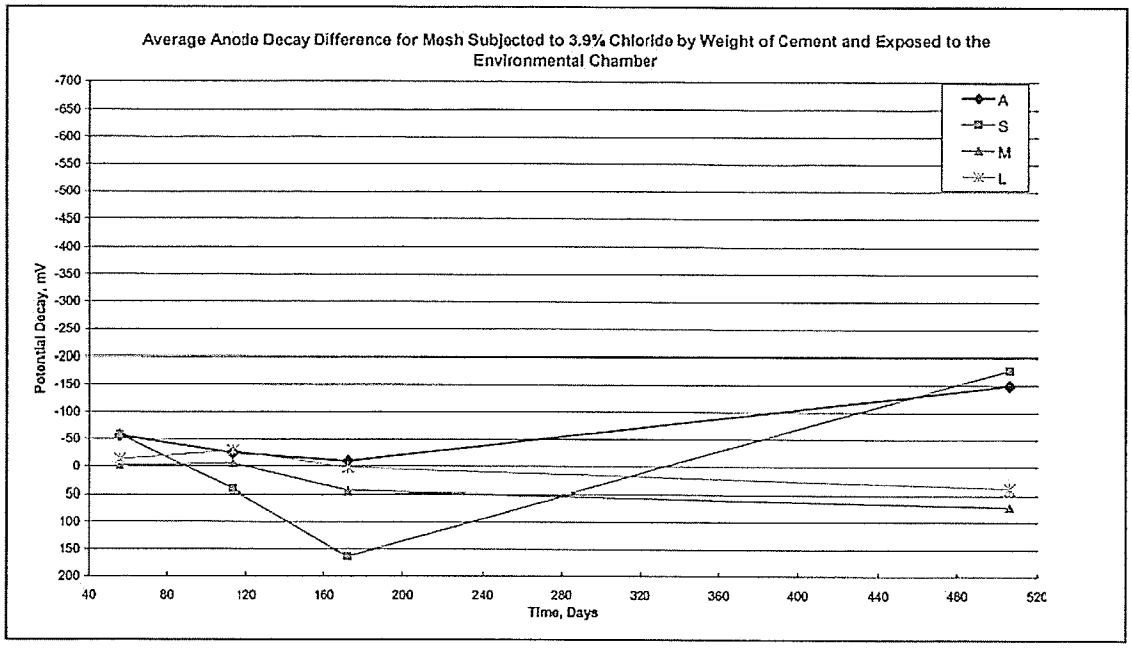
Average Anode Decay Difference for Mesh Subjected to 3.9% Chloride by Weight of Cement and Exposed to the Environmental Chamber
Potential Decay, mV
-700
-650
-600
-550
-500
-450
-400
-350
-300
-250
-200
-150
-100
-50
0
50
100
150
200
40
80
120
160
200
240
280
320
360
400
440
480
520
Time, Days
A
S
M
L

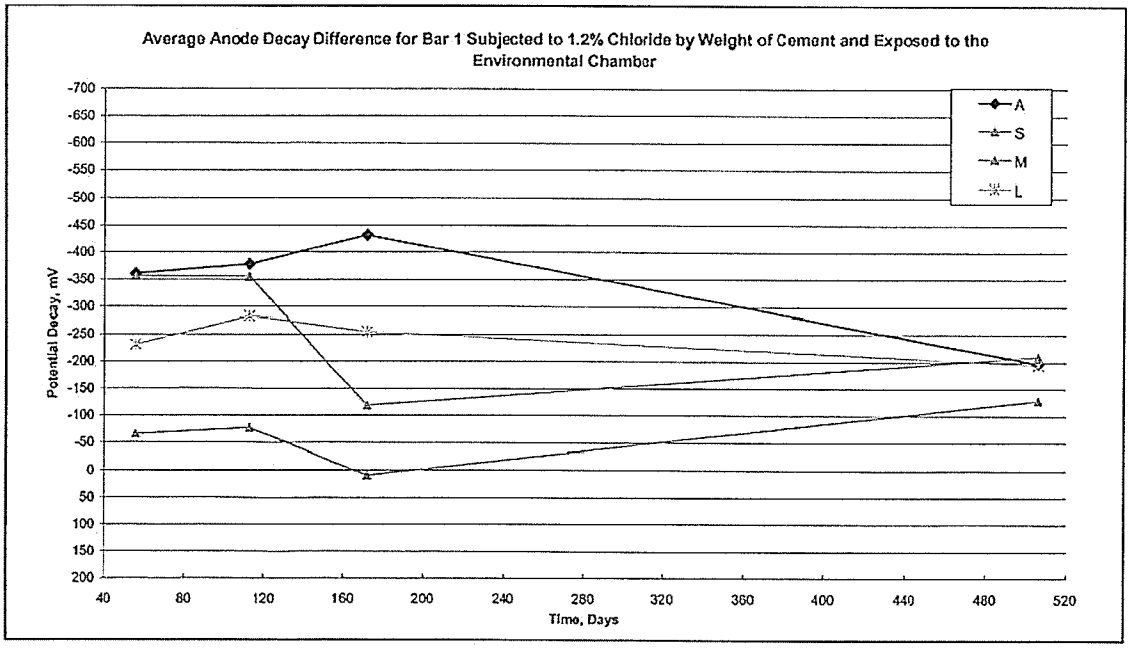
Average Anode Decay Difference for Bar 1 Subjected to 1.2% Chloride by Weight of Cement and Exposed to the Environmental Chamber
Potential Decay, mV
-700
-650
-600
-550
-500
-450
-400
-350
-300
-250
-200
-150
-100
-50
0
50
100
150
200
40
80
120
160
200
240
280
320
360
400
440
480
520
Time, Days
A
S
M
L

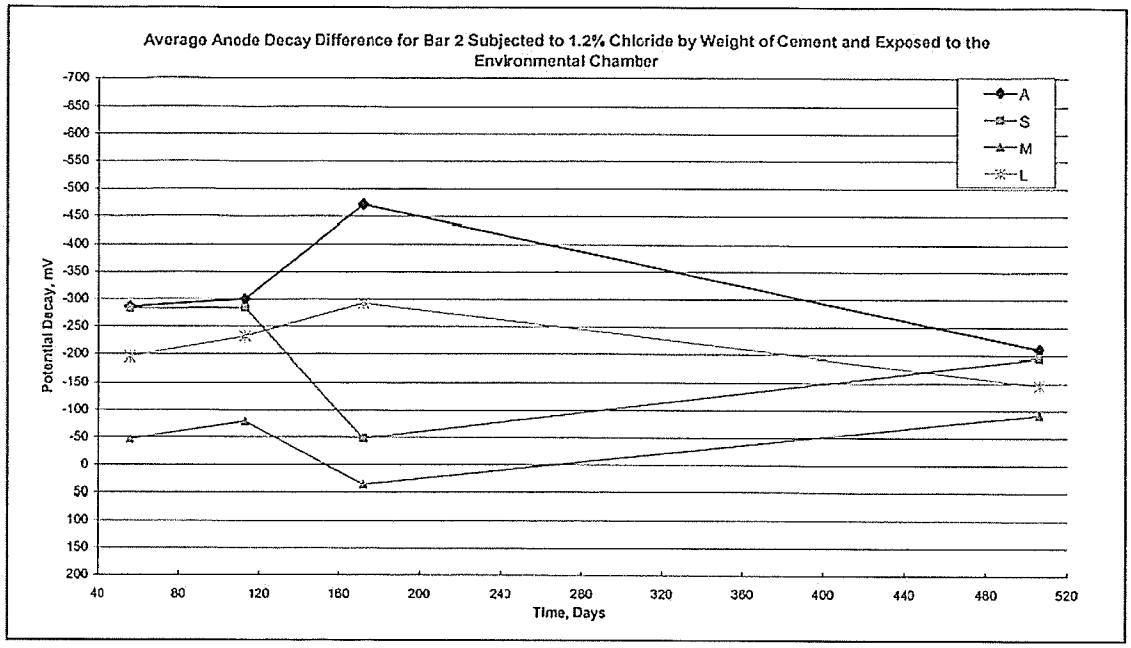
Average Anode Decay Difference for Bar 2 Subjected to 1.2% Chloride by Weight of Cement and Exposed to the Environmental Chamber
Potential Decay, mV
-700
-650
-600
-550
-500
-450
-400
-350
-300
-250
-200
-150
-100
-50
0
50
100
150
200
40
80
120
160
200
240
280
320
360
400
440
480
520
Time, Days
A
S
M
L

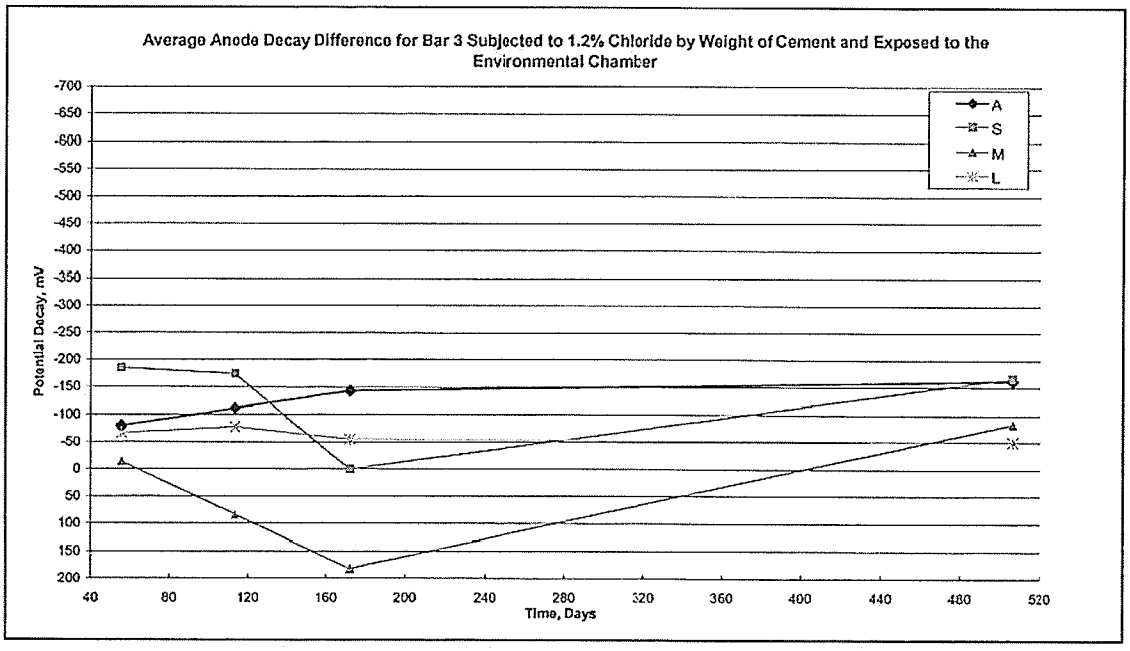
Average Anode Decay Difference for Bar 3 Subjected to 1.2% Chloride by Weight of Cement and Exposed to the Environmental Chamber
Potential Decay, mV
-700
-650
-600
-550
-500
-450
-400
-350
-300
-250
-200
-150
-100
-50
0
50
100
150
200
40
80
120
160
200
240
280
320
360
400
440
480
520
Time, Days
A
S
M
L

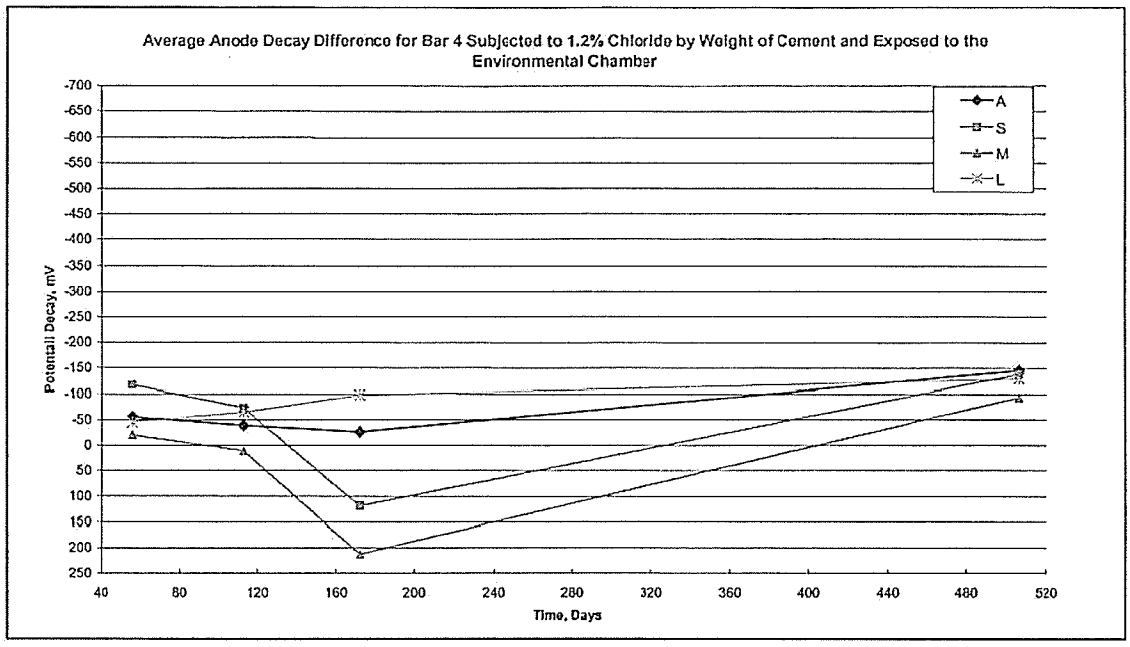
Average Anode Decay Difference for Bar 4 Subjected to 1.2% Chloride by Weight of Cement and Exposed to the Environmental Chamber
Potentail Decay, mV
-700
-650
-600
-550
-500
-450
-400
-350
-300
-250
-200
-150
-100
-50
0
50
100
150
200
250
40
80
120
160
200
240
280
320
360
400
440
480
520
Time, Days
A
S
M
L

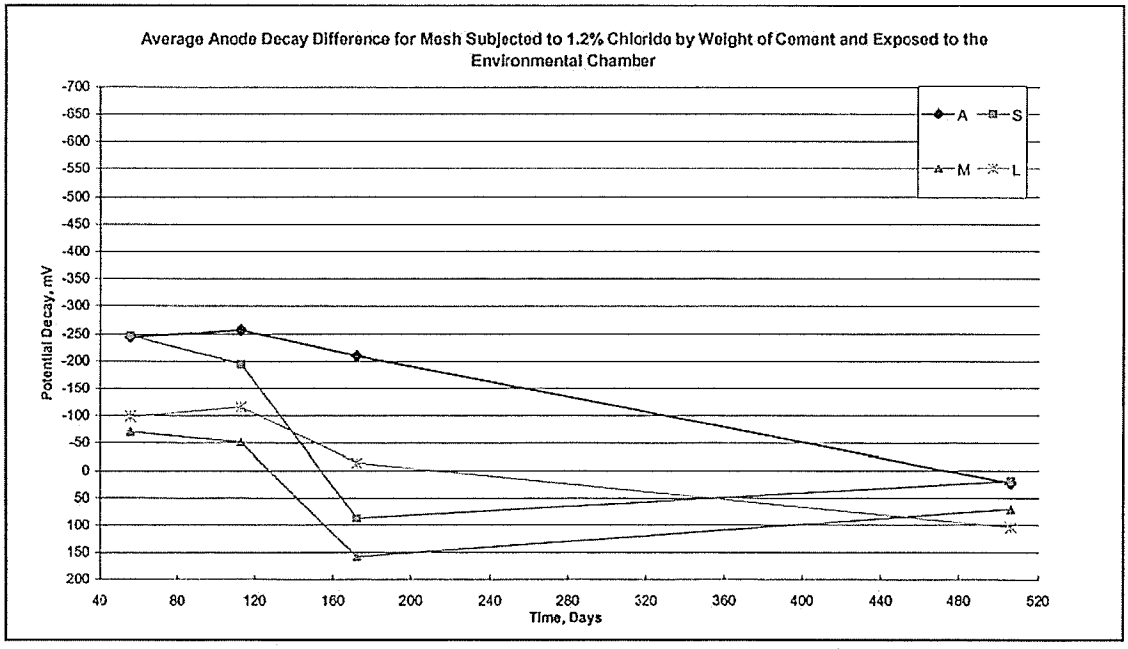
Average Anode Decay Difference for Mesh Subjected to 1.2% Chloride by Weight of Cement and Exposed to the Environmental Chamber
Potential Decay, mV
-700
-650
-600
-550
-500
-450
-400
-350
-300
-250
-200
-150
-100
-50
0
50
100
150
200
40
80
120
160
200
240
280
320
360
400
440
480
520
Time, Days
A
S
M
L